Polymorph Selection with Morphology Control Using Solvents and Additives

By

Manish M. Parmar

Thesis submitted in partial fulfilment of the requirements of Liverpool John Moores University for the degree of Doctor of Philosophy

July 2015

ABSTRACT

Sulphathiazole is a highly polymorphic model system exhibiting at least five polymorphic forms: I, II, III, IV, and V. Polymorph stability is known to be susceptible to solvent environment, and it is established that 1-propanol stabilizes the most metastable form I. This study examines the effect of a range of alcohols on polymorph selection and attempts to elucidate the mechanism. The role of the alcohol functional group in the polymorph selection process is thus investigated and evaluated. Crystals were characterized using optical microscopy, SEM, PXRD, DSC, IR, and single-crystal X-ray diffraction for their polymorphic identity. The role of solvent in the stabilization of polymorphs was investigated by visualizing and calculating energy requirements for the interaction of each solvent molecule with α- and β-dimers of sulphathiazole, using Cerius2 modeling software and GRID based systematic search simulation. These studies showed that solvent had a significant impact on polymorph selection. In common with 1-propanol, 1-butanol was found to stabilize form I by inhibiting the formation of the β-dimer, which is necessary for nucleation of and transformation to forms II-IV. Shorter chain alcohols and branched chain alcohols such as methanol, 2-propanol, and ethanol did not stabilize form I but stabilized forms II, III, and IV, respectively, showing that it is not only the alcohol functionality but also the steric effects of the alkyl chain that contributed to the effect. Sulphathiazole form I normally has a needlelike morphology. Form I with a modified rodlike morphology was produced by crystallization from 1-propanol with the addition of methanol in low concentration, showing that it is possible to control the morphology and selectively isolate polymorphs.

Indomethacin is known to exhibit at least five polymorphs but only the stable γ Form and metastable α Form are reported to be reliably produced by standard methods. The metastable α Form has an undesirable fibrous needle-like morphology. The current study focused on producing crystals of α Indomethacin with a well-defined morphology using additives. Adipic acid, myristic acid, oleic acid and structurally related 3-indoleacetic acid were selected as additives and their impact on the morphology and polymorphism of indomethacin were investigated in this study. Additives did not change the needle-like morphology of α-indomethacin but less fibrous and less aggregated well defined needles were observed in presence of adipic acid, oleic acid and 3-indole-3-acetic acid.

Acknowledgments

I owe a debt of gratitude to my supervisor Dr Linda Seton for giving me an opportunity to work in this exciting and challenging area of crystallization and polymorphism. I am also very grateful to her for providing continuous scientific guidance and sharing her immense knowledge with me. Her guidance helped me in all the time of research and writing of this thesis. I am particularly indebted to her for providing me continuous support, motivation and for her patience while I was going through difficult time due to family commitments during my write up. Without her constant support and motivation, it would have been hard to finish this thesis. I could not have imagined having a better Supervisor and mentor for my Ph.D study.

Besides my Supervisor, I would like to thank Prof J. L. Ford for his insightful comments and suggestions for completing this thesis. I am also very grateful to him for sharing his expert knowledge on DSC with me during my research at LJMU. My sincere thanks also goes to Mr Giles Edward and Mrs Nicola Dempster at LJMU for providing me training and continuous help on DSC, Hot Stage Microscopy and IR Spectroscopy. I am also thankful to my second supervisor Dr Matthew Roberts for his helps and suggestions during my PhD.

I thank to my fellow lab mates Utpal, Aref, and Zahir for the stimulating discussions during coffee and lunch breaks and for all the fun we have had during those three years in the lab. Also I thank to undergraduate project students Farzeen, Omar Khan for their help in this project.

This research would have not been complete without our external collaborators. So, I am also very grateful to Prof. Roger Davey and his group at UMIST for allowing me to use their molecular modelling (Material Studio) facilities at Manchester. I also like to thank Dr Robert Hammond at Leeds University for his help with molecular modelling via Grid based systematic search tools.

I would like to thank my family: my parents, my wife Kinnary, my sons, Aditya and Prahan and my brothers for supporting throughout writing this thesis.

Last but not least, I would like to thank LJMU for providing me scholarship and financial assistance for this research.

Contents

List of Figures

List of Tables

1   Introduction

1.1   Introduction

Most solid drugs can be classified as either crystalline solids, which have regular arrangements of molecules that repeat in three dimensions, or amorphous solids, which lack the long range order present in crystals. These differences in the long-range periodicity of the structures result in substantially different physical and chemical properties of crystals and amorphous solids. Amorphous forms are not marketed as widely as crystalline forms because of their innate tendency to crystallize. Many marketed pharmaceuticals therefore consist of solid molecular crystal forms (Datta et al, 2004).

The arrangement of the molecules in a crystal determines its physical properties and, in certain cases, its chemical properties. These properties of the solid drug can influence its manufacturing process as well as its efficiency. A thorough understanding of the relationships between physical structures and the properties of pharmaceutical solids is therefore important in selecting the most suitable form of an active pharmaceutical ingredient (API) for development into a drug product.

Pharmaceutical materials can show polymorphism, which occurs when the molecule packs in different ways giving rise to two or more crystal structures and is defined as the ability of a substance to exist as two or more crystalline phases that have different arrangements and/or conformations of the molecules in the crystal lattice (Giron, 2001). Polymorphs can exhibit different mechanical, thermal, and physical properties, such as compressibility, filtration, solubility, bioavailability and tableting properties, which can impact on the efficacy of the final drug product (Byrn et al, 2002). So, it is necessary to design a crystallization process where the desired polymorph must be reproducible with consistent morphology.

Control over the generation of polymorphs, morphology, and particle size can be achieved in the final drug product with knowledge of techniques in crystal and nucleation engineering. The ability to engineer nucleation and crystallization behaviour comes from changes to molecule-to-molecule interactions by either

manipulation of solution parameters or by the molecular recognition of structurally related additives (Weissbuch et al, 2001).

In this study, sulphathiazole and indomethacin have been selected as model pharmaceutical solids to observe the effect of solvents, pH and temperature on the polymorphs of these compounds. The study investigates the control over polymorphism and morphology using sulphathiazole and indomethacin as model compounds.

1.2   Crystal structure

An ensemble of randomly organized molecules, ions or atoms in a fluid comes together to form an ordered three-dimensional molecular array, which is termed a crystal (Davey and Garside, 2000). The arrangement of these molecules in a crystal determines its physical and chemical properties (Kitamura, 2002). Therefore, an understanding of the crystalline state would lead to an understanding of the drug properties to some extent.

In the crystal (crystalline state) the constituent molecules are regularly arranged into a fixed and rigid repeating array known as a lattice. A lattice is a set of points arranged so that each point has identical surroundings. The regularity of the internal structure of this crystal lattice results in the crystal having a characteristic shape; smooth surfaces or faces develop as a crystal grows, and the planes of these faces are parallel to atomic planes in the lattice.

The smallest three-dimensional unit of the lattice that contains all the information necessary to replicate the lattice to any size is called the unit cell. When two atoms of the same element in the unit cell have identical atomic environments except for the orientation within the environment, they are said to be related by symmetry (Myerson, 2005). The dimensions of the unit cell are characterized by six quantities; three axial lengths (a, b, c) and three inter axial angles (α, β, γ). Each unit cell contains at least one asymmetric unit. Frankenheim (1842) and Bravais (1850) investigated mathematically the number and types of three dimensional lattices that could exist in space. They found that there are only fourteen possible point lattices that can be

constructed and these are known as the Bravais lattices. This results in the lattices being divided into seven crystal systems known as; regular, tetragonal, orthorhombic, monoclinic, triclinic, trigonal, and hexagonal (Mullin, 2001). Each of these crystal systems has one or more symmetry elements that describe the internal symmetry of the unit cell (Datta et al, 2004).

There are three simple elements of symmetry; a centre, an axes and a plane. A centre of symmetry (symmetry about a point) exists when each point on a crystal surface has an identical point on the opposite side of the centre at equal distance from it, for example a cube (Figure 1.1 a). An axis of symmetry (symmetry about a line) is an imaginary axis placed through the crystal, which if the structure is rotated about this axis then it appears to have reached its original position more than once during a complete rotation (360°). During this complete rotation, if the crystal reaches its original position twice then the axis is called a diad axis (two fold symmetry). Respectively, for three, four and six times, axes are termed triad axes, tetrad axes, and hexad axes. A perfect crystal with a cubic morphology displays 13 axes of symmetry: 6 diad axes, 4 triad axes and 3 tetrad axes as shown respectively in Figures 1.1b, 1.1c and 1.1d. A plane of symmetry (symmetry about a plane) is an imaginary plane, which divides a crystal into two parts such that each reflects the image of the other. Crystals may have more than one plane of symmetry, for example, a cube has nine planes of symmetry; 3 rectangular and six diagonal planes as shown in Figure 1.1e and 1.1f.
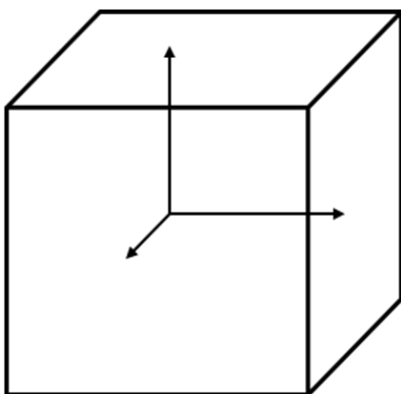
Figure 1.1a   A cubic crystal exhibits a centre of symmetry at its mass centre
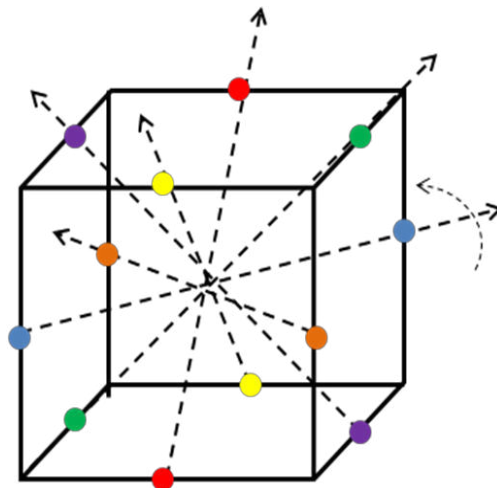
Figure 1.1b   A cubic crystal possesses 6 diad axes of symmetry through opposite edges
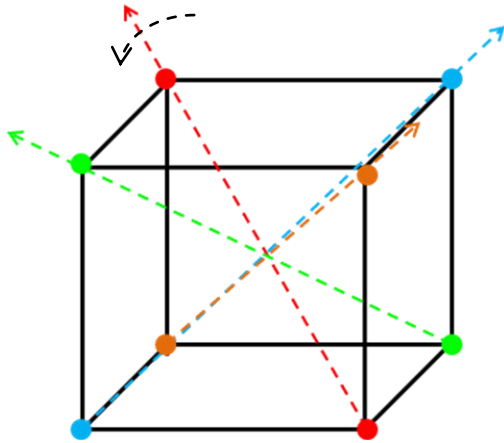
Figure 1.1c A cubic crystal possesses 4 triad axes of symmetry through opposite corner
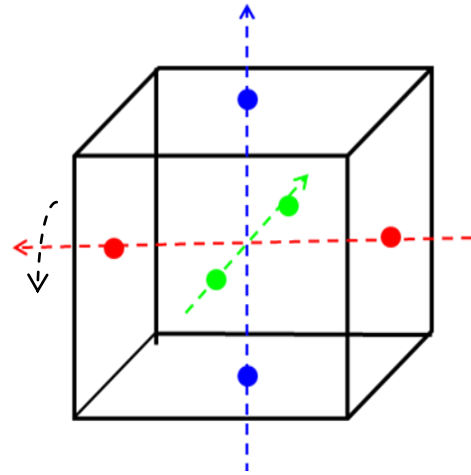
Figure 1.1d A cubic crystal possesses 3 tetrad axes of symmetry through opposite faces
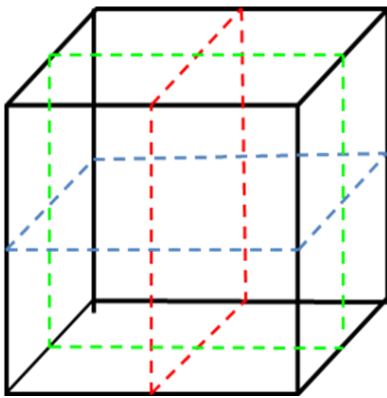
Figure 1.1e A cubic crystal possesses 3 rectangular planes of symmetry, each parallel to two opposite faces of crystal
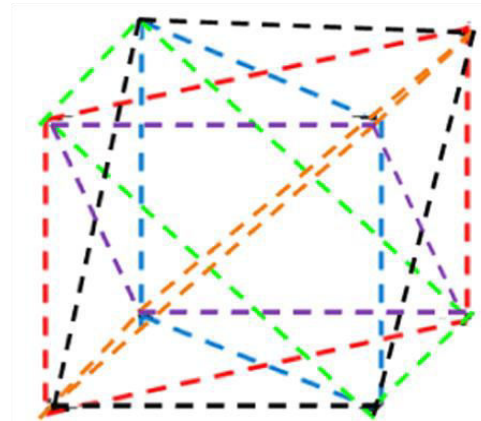
Figure 1.1f A cubic crystal possesses 6 diagonal planes of symmetry, each passing through opposite edges

A fourth element of symmetry which is exhibited by some crystals is the symmetry about a rotation-reflection axis or axis of rotatory inversion (Mullin, 2001). In this type of symmetry, a crystal face can be related to another face by performing two operations; rotation about an axis, followed by reflection in a plane at right angles to the axis. The sum of these two operations is known as inversion about the centre.

There are only 32 possible combinations of the above-mentioned elements of symmetry, which are called the 32 point groups or classes (Aroyo et al, 2006). These 32 classes are grouped into one of the seven crystal systems.

All symmetry operations (elements), when applied to a lattice, result in a return to the initial position. There is also a different type of symmetry operation, which is called translational symmetry. In translational symmetry, simultaneous use of reflection and translation or rotation and translation will result in a displacement of the original position to a new position, corresponding to the next lattice point. The former is called a glide plane and the latter a screw axis. If we add the concept of the screw axis and the glide plane, the number of combinations of symmetry elements that can be derived increases to 230, which are known as the crystallographic space groups (Myerson, 2005). These 230 space groups describe all the possible ways in which identical objects can be arranged in an infinite lattice. Every crystal structure can be assigned to one of the 14 Bravais lattices and to one of the 230 space groups (Bernstein 2002).

1.3   Solubility and supersaturation

At a given temperature there is a maximum amount of solute that can dissolve in a given amount of solvent. When this occurs, the solution is said to be saturated. The amount of solute required to make a saturated solution at a given temperature is the solubility (Myerson, 2005). In thermodynamics, saturation is defined as the state in which equilibrium is established between undissolved and dissolved solute in a dissolution process (Aulton, 2002). The solubility of most materials is a function of temperature, generally increasing with increasing temperature.

A saturated solution is in thermodynamic equilibrium with the solid phase, at a specific temperature. When the concentration of the solute in the solution exceeds its equilibrium concentration (saturated concentration) at the given solution conditions, the solution is said to be in a supersaturated state and the concentration of the solute in the solution, termed the actual or supersaturated concentration (Mullin, 2001). However, a supersaturated solution would not result in spontaneous nucleation, unless the supersaturation level exceeds a certain metastable range, where solute molecules spontaneously form nuclei (Davey and Garside, 2000). Ostwald (1899) first introduced the terms 'labile' and 'metastable' supersaturation to classify supersaturated solutions in which spontaneous nucleation would or would not occur, respectively (Figure 1.2). Mier and Isaac (1906, 1907) represented these relationships

between supersaturation and crystallization using a diagram, which is known as the solubility – supersolubility diagram such as that shown in Figure 1.2.
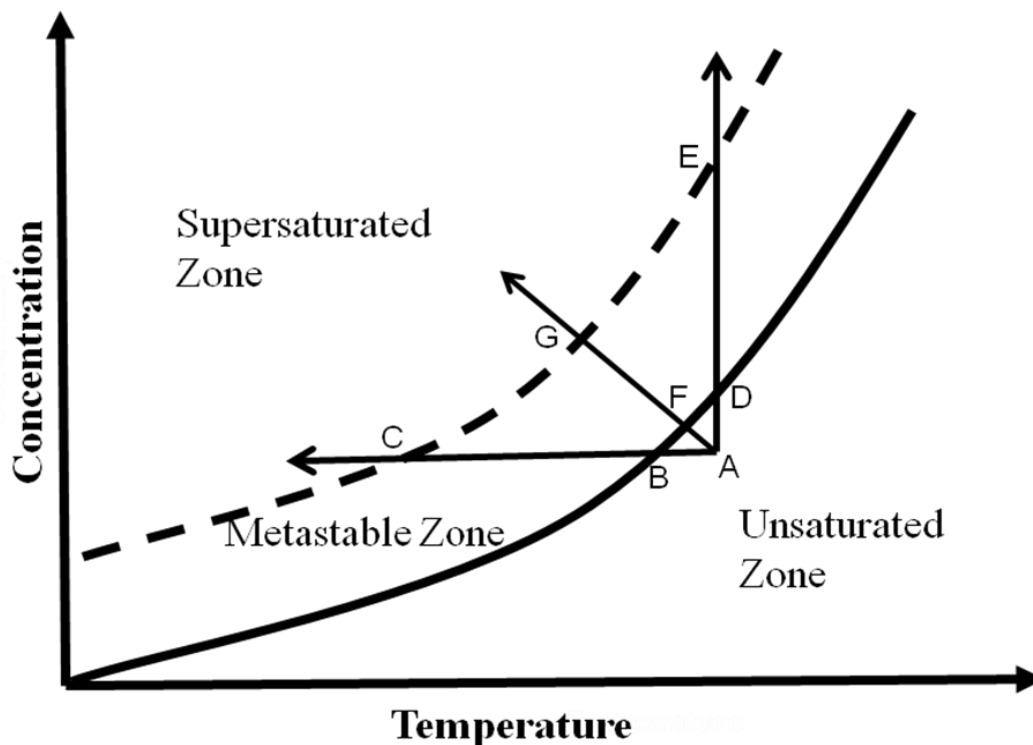
Figure 1.2   The solubility/supersolubility diagram, which classifies the metastable, supersaturated (labile/unstable) and unsaturated (stable) zones).

A solution whose composition lies below the solubility curve is under saturated and existing crystals will dissolve. As shown in Figure 1.2, if cooled, a solution may become saturated and then supersaturated with further cooling. If a solution is continuously cooled down further without losing solvent (i.e. at constant concentration), spontaneous nucleation or crystal formation will take place at a certain temperature at point C (Line ABC, Figure 1.2), designated as the nucleation temperature. Supersaturation can be also achieved by evaporation of solvent (increasing concentration) at constant temperature (Line ADE) or by a combination of cooling and evaporation (Line AFG). The range between the saturation (solubility) temperature and nucleation temperature is designated as the metastable zone. Mier and Isaac (1906; 1907) divided this diagram into three zones; (1) the stable (unsaturated) zone, where crystallization is not favoured, (2) the metastable zone, between the solubility and supersolubility curves, where spontaneous crystallization is

improbable, and (3) the unstable or labile (supersaturated) zone, where spontaneous crystallization is probable.

Mathematically, supersaturation can be defined in a number of ways. The most common expressions are the concentration driving force, Δc, and the absolute or relative supersaturation, σ, as shown in Equations 1.1 and 1.2 (Mullin, 2001),

$$\Delta c = c - c^* \qquad \text{(Equation 1.1)}$$
$$\sigma = \Delta c / c^* \qquad \text{(Equation 1.2)}$$

where c is the solution concentration, and c* is the solubility at a given temperature.

1.4   Crystallization and importance of solubility

Crystallization is used extensively in the manufacture of pharmaceuticals, agrochemicals and fine chemicals as a purification and isolation step (Davey and Garside, 2000). It is the process by which randomly organized atoms or molecules are arranged into an ordered solid state, called a crystal.

The most common type of crystallization is that from solution, in which the component to be crystallized is completely dissolved in a solvent at elevated temperature, where the solubility is relatively high. When the system is cooled down, at some point the concentration of a solute exceeds the solubility at that temperature, i.e., the system is thus supersaturated. In supersaturated conditions, the solute molecules tend to transfer from liquid phase in to solid phase, which is seen as the formation of new crystals (nucleation) or as the growth of existing crystals (Pollenen et al, 2006).

Therefore, the concentration difference between the actual concentration and equilibrium solubility, supersaturation, is the driving force of all crystallization processes. These crystallization processes occur in two steps known as nucleation and growth of crystals (Mullin, 2001).

1.5   Nucleation

Crystallization from a solution involves two steps, nucleation, which is the process of creating a new solid phase from a super saturated homogeneous mother phase (Davey and Garside, 2000), and crystal growth, which is the growth of existing crystals to larger size. The properties of the crystals such as their size distribution, shape and polymorphism depend on these two steps and their relationship with each other (Myerson, 2005).

Nucleation can be classified as primary and secondary. The term primary is reserved for all the cases of nucleation where systems do not contain crystalline matter prior to the formation of nuclei. Secondary nucleation is often generated in the vicinity of the crystals, which are already present in a supersaturated system (Mullin, 2001). Primary nucleation is further classified into homogeneous and heterogeneous primary nucleation.

1.5.1   Primary nucleation: homogeneous nucleation

Homogeneous nucleation occurs as spontaneous nucleation from a supersaturated solution due solely to the supersaturation driving force effect. Classical nucleation theory (Gibbs, 1948; Volmer, 1939) states that when a solution enters the non-equilibrium supersaturated region, the molecules of the solute begin to form aggregates (clusters). If it is assumed that the clusters are spherical, Equation 1.3 can be written that gives the change in Gibbs free energy, ΔG, required to form a cluster of a given radius, r,

$$\Delta G = [4\pi r^2 \gamma] - [(4\pi r^3/3Vm)\ RT\ \ln\ (1+S)] \qquad \text{(Equation 1.3)}$$

where r is the cluster radius, γ is the solid –liquid interfacial tension, Vm is the specific volume of a solute molecule, S is the supersaturation ratio and R is the gas constant. The first term in Equation 1.3 is the change in Gibbs free energy for forming the surface of the cluster, while the second term is the change in Gibbs free energy for forming the bulk of the cluster. It was also reported (Mullin, 2001) that nucleation requires a cluster of a critical size to be formed in the solution. Clusters (aggregates)

less than the critical size with low (or negative change in) Gibbs free energy will be likely to dissolve compared to clusters equal to critical size. Equation 1.3 indicates that clusters with higher surface area and lower volume are likely to achieve critical size radius more easily compared to clusters with lower surface area and higher volume. Equation 1.4 for the critical size, r_c, of the cluster is given below.

$$r_c = 3V_m\sigma/RT \ln(1+S) \hspace{3cm} \text{(Equation 1.4)}$$

As the supersaturation increases, the likelihood of obtaining the critical cluster size in the solution will increase and hence, the possibility of nucleation. The rate of nucleation, J, the number of nuclei formed per unit time per unit volume, can be expressed in the form of the Arrhenius reaction velocity equation commonly used for the rate of a thermally activated process (Volmer, 1939; Nielsen, 1964):

$$J = A \exp(-\Delta G/kT) \hspace{3cm} \text{(Equation 1.5)}$$

where, k is the Boltzman constant, A is the surface area of cluster, ΔG is the change in Gibbs free energy, and T is the temperature (K).

1.5.2 Primary nucleation: heterogeneous nucleation

The rate of nucleation of a solution can be affected considerably by the presence of traces of impurities or a catalytic surface in the system. This type of nucleation induced by the presence of foreign bodies is referred to as heterogeneous nucleation (Davey and Garside, 2000).

As the nucleation is induced by the presence of other foreign particles, the degree of supersaturation will be lower than that required for homogeneous spontaneous nucleation. Therefore, the overall free energy change associated with the formation of a critical nucleus under heterogeneous conditions, $\Delta G'_{crit}$, must be less than the corresponding free energy change, ΔG_{crit}, associated with homogeneous nucleation (Mullin, 2001),

$$\Delta G'_{crit} = \varphi \, \Delta G_{crit} \qquad\qquad\qquad \text{(Equation 1.6)}$$

where, φ is the proportionality constant.

Equation 1.6 indicates that nucleation is easier to achieve because the overall excess free energy required is less than that for a homogeneous nucleation.

1.5.3   Secondary nucleation

The term secondary nucleation is used when the nucleation of new crystals is induced only because of the prior presence of crystals of the material being crystallized. This nucleation mechanism generally occurs at much lower supersaturation than primary homogeneous or even heterogeneous nucleation.

The most important and commonly encountered mechanism of secondary nucleation is contact nucleation, sometimes also referred to as collision nucleation (Davey and Garside, 2000). The existing crystals provide a source of nuclei through collision with each other, the walls of the vessel, and the mixing device used.

1.6   Crystal growth

When a nucleus is formed, it is the smallest stable cluster of molecules that can exist under a given set of conditions (Myerson, 2001). Lui et al (2007) found the critical nucleus size for ice crystallization in a microemulsion.

However, immediately after the formation of nuclei, they begin to grow larger through the addition of solute molecules to the crystal lattice. This part of the crystallization process is known as crystal growth (Myerson, 2005). In this process, at supersaturated conditions, the flux of growth units (atoms, ions, or molecules) to the surface exceeds the equilibrium flux so that the number of growth units joining the surface is greater than the number leaving it (Davey and Garside, 2000). This results in growth of the surface. The ability of a surface to capture arriving growth units and integrate them into the crystal lattice is, among other things, dependent upon the strength and number of interactions that can form between the surface and the growth unit.

The first theoretical model of crystal growth was introduced by Kossel (1934) as shown in Figure 1.3. This model shows three types of sites at which the growth unit can be incorporated into a crystal. A site where the growth unit can bond in only one place is a flat face, F. A site which provides two places (two bonds) for the growth unit to bond to the crystal is a stepped or S face, while a site where three bonds are possible is known as a kink site, K (Hartman and Perdock, 1955).
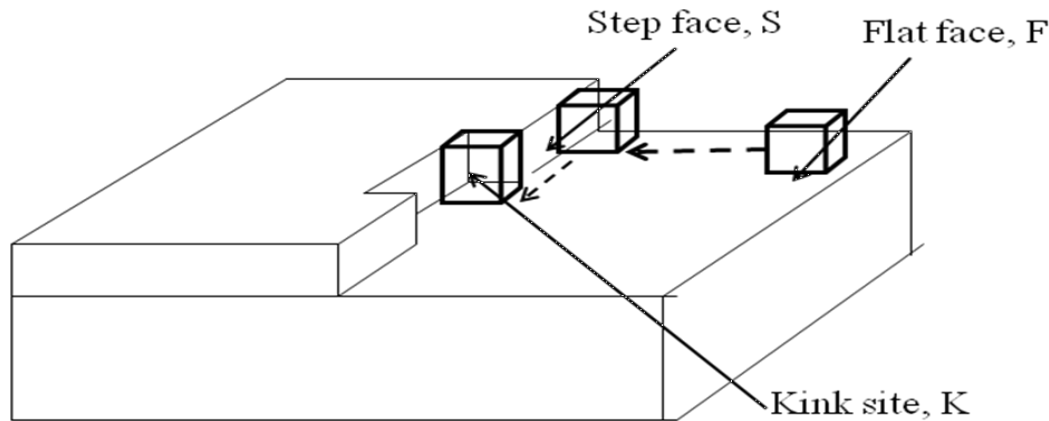
Figure 1.3 The surface of growing cubic shaped crystal shows three types of sites for the attachment of adsorbed atoms; (1) flat face, F, (2) Step face, S, and (3) Kink Site, K (re-drawn from Mulin, Crystallization, 4th edition, Butterworth-Heinemann, 2001)

Kossel (1934) assumed that the strength of binding of an atom to the surface depends on the number of its nearest neighbours. As step or kinked sites display 2 or 3 bonding sites with the growth unit/atom; at these sites atoms would be bound by the maximum number of neighbours. The growth rate, v, of a crystal surface is proportional to the total binding energy of an atom to that surface. Hence, the growth rate at kinked sites is highest followed by growth rate at stepped sites and flat faces (Equation 1.7)

$$v_k > v_s > v_f \hspace{3cm} \text{(Equation 1.7)}$$

This concept of crystal growth is based on thermodynamic reasoning as suggested by Volmer (1939). When an atom of a crystallizing substance arrives at the growing crystal face, it is absorbed on the surface and then diffuses along the surface until it is incorporated into the lattice at a step or kink site where its energy reaches a minimum (Figure 1.3). This stepwise build up will continue until kinked or step sites have

received sufficient atoms to move them to the edge of the crystal. Thereafter, these kinked and step sites can no longer function as low energy nucleation sites. The generation of a new layer/step for further crystal growth requires a launching of a molecule on the crystal surface.

The ease of starting this new layer depends on the surface roughness (kink and step density). One of the earliest attempts to quantify surface roughness was made by Jackson et al (1958) using the dimensionless term, α,

$$\alpha = \Delta E/kT \qquad \text{(Equation 1.8)}$$

where, ΔE is the energy change occurring when a perfectly flat surface is roughened by removing one block from the surface and using it to start a new layer.

The parameter, α, is called the Jackson factor which measures the ease with which a surface/face can form sites with multiple binding interactions. Hence, this parameter reflects the ease with which a surface can grow. If the value of the α-factor is low then growth can proceed easily with many growth sites always present. As the value of α increases, growth becomes more difficult and specific mechanisms have to be envisaged by which necessary growth sites can be created. Depending on the value of α, possible mechanisms of crystal growth are classified, as shown below (Burton, Crabrera and Frank, 1951; Bourne and Davey, 1977).

1.6.1   Continuous growth

When the value of α is less than 3, the surface roughness will be high with many kink and step sites available. All the arriving growth units will find a growth site and will be bound by the maximum number of neighbours. Hence the energy required to form a step is low. The linear growth rate, in supersaturated systems, normal to the surface, v, is expressed as shown in Equation 1.9,

$$v = K_{CG}\sigma \qquad \text{(Equation 1.9)}$$

where, K_{CG} is the rate constant, and σ is supersaturation.

Crystals grow continuously without much effort inside the solution until the supersaturation is reduced and solution concentration is equal to equilibrium concentration.

1.6.2 Surface nucleation

As the value of α increases above 3 (and less than 5), the surface roughness is decreased (Mulin, 2001). The density of steps and kink sites will decrease. Not all the arriving growth units will find growth sites on the crystal surface. The growth units which do not find growth sites or are held loosely only by one neighbour (one bond) and may return to the fluid phase. Whereas the growth units which find available growth sites, will create steps for others, others will join them to create a surface island or nuclei. These islands and nuclei work as the steps and kink sites for other growth units and in this way islands spread across the crystal surface. The linear growth rate normal to the surface, v, is expressed as given in Equations 1.9 and 1.10.

v = f1 (number of critical size nuclei formed per unit time) × f2 (step height) × f3 (step velocity)   (Equation 1.9)

$v = K_{SN}\sigma^{5/6} \exp \{(-\pi/3\sigma) (\gamma_e/kT)^2\}$ (Equation 1.10)

where, K_{SN} is a rate constant, σ is the supersaturation, γ_e is the edge tension, K is Gibbs-Boltzman constant, and T is the temperature (K).

1.6.3 Spiral growth

As the value of α increases above 5, the surface roughness is very low with a nearly flat surface. The surface would no longer contain any low energy nucleation sites (kink and steps). Generation of a new step on the flat surface requires the highest free energy (ΔG), which is energetically most unfavourable. In this case, at an α value above 5, growth can occur only if a step is created by an energetically cheap mechanism. Burton, Carbrera and Frank (1951) proposed that the energetically cheap process that enables a flat surface to grow is mediated by the presence of a screw dislocation lattice defect. A dislocation is the result of the stresses that occur during crystal growth, particularly during the crystal growth taking place on crystal seeds. In

a dislocated crystal, one part of the crystal will be misaligned with respect to the rest of the crystal. Burton, Carbrera and Frank (1951) explained that the emergence points of dislocations with screw components at crystal surfaces act as a continuous generator of surface steps at which further growth can then take place (Figure 1.4). These emergent surface steps extend over only the part of the surface and wind up into a spiral with growth.

Emergence point of screw dislocation
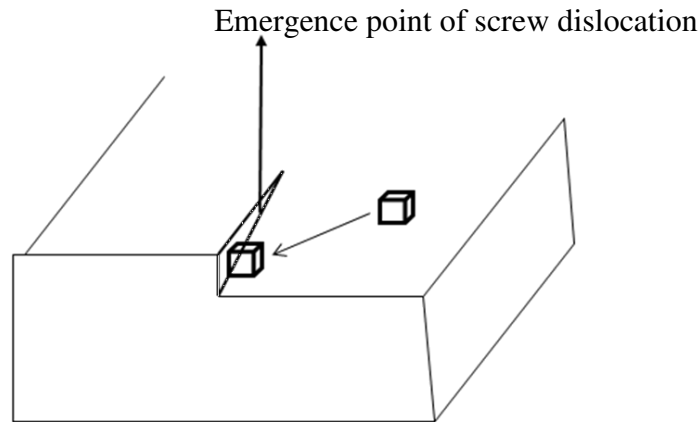
Figure 1.4   A cubic crystal shows emergence point of screw dislocation at the crystal surface, which acts as a step site for the absorbed growth units (re-drawn from Mulin, Crystallization, 4th edition, Butterworth-Heinemann, 2001).

In this system, the growth rate is expressed as shown in Equation 1.11,

v = f1 (step velocity) × f2 (step height) × f3 (step density)   (Equation 1.11)

where, step velocity is the flux of growth units entering at kink sites. According to Burton, Crabera and Frank (1951) the step velocity may be controlled by the diffusion of solute molecules from the solution to the kink sites or by two-dimensional diffusion over the crystal surface. The step density is related to the spiral curvature, which increases with increase in supersaturation, and the height of the steps is dependent on the initial number of defects available in the nucleated crystal. The final form of the Equation 1.11 for growth rate in a supersaturated system is expressed as shown in Equation 1.12,

$v = A\sigma^2 \tanh (B/\sigma)$ (Equation 1.12)

where, A and B are complex temperature dependent constants, and σ is the supersaturation.

1.7 Crystal Habit/Morphology

The morphology/habit of a crystal is an important property of solid crystalline materials that influences a number of other important properties of the material, for instance, dissolution rate, flow, filtering and drying characteristics, compacting, milling, and dust formation. Therefore morphology control of crystals is important in pharmaceutical and fine chemical industry.

As explained in Section 1.1, crystals are formed by the repetition of unit cells in three dimensional space. The extent or limit of building these unit cells in three dimensional space plays a major role in developing crystal faces. Therefore, the shape of a crystal face is in part related to the shape of the unit cell.

Crystal morphology is also dependent upon the growth rate and direction in which the crystal grows as the variable growth rate of crystal faces in different directions defines the faces and shape of crystals. In other words the variable rates, at which molecules or atoms (from the surrounding supersaturated fluid/vapour) attach to different faces/directions of a growing crystal, play a major role in defining the final shape of the mature crystal. Among the faces of a growing crystal, the slowest growing face plays a major role in defining the final shape (morphology).

(c)   (a)   (b)
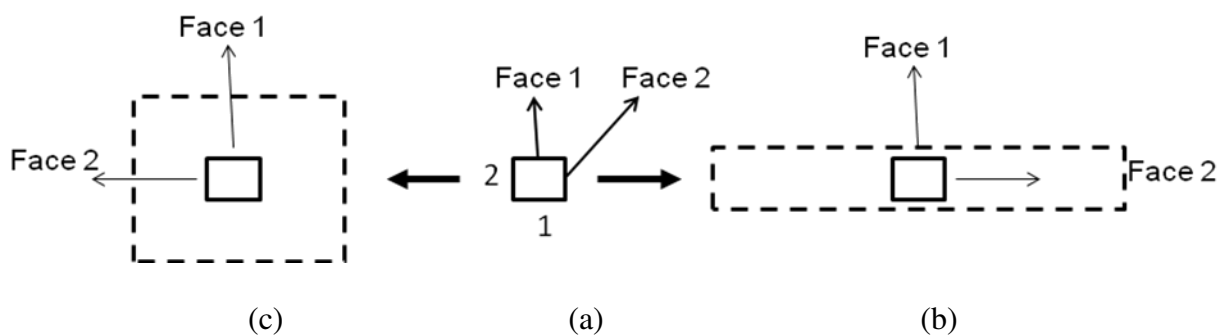
Figure 1.5   Example of a growing crystal to explain the effect of relative growth rates of faces on final morphology; (a) a nucleated rectangular crystal, (b) a nucleated crystal achieves rod-like morphology if Face 1 grows faster than Face 2, (c) a nucleated crystal maintains rectangular morphology if both Face 1 and Face 2 grow at the same rate.

If a crystal nucleates as a rectangle (Figure 1.5a), and exhibits a slower growth rate at Face 1 and a faster growth rate at Face 2, then after a period of growth the crystal would display a rod-like morphology (Figure 1.5b). However, similar growth rates on both Face 1 and Face 2 would maintain a rectangular morphology after a period of growth (Figure 1.5c).

This process of molecule attachment to the surface of a growing crystal can be greatly influenced by external conditions such as level of supersaturation, temperature, pressure, pH, solvent and the presence of impurities or additives within the system. There are a number of studies reported in the literature and a few are described briefly to explain the influence of these factors on morphology.

Finnie et al (1999) studied the crystal growth of paracetamol from aqueous solvent. They measured the growth rate of paracetamol crystals in the [010] and [001] directions, and reported that at low supersaturation, needles elongated along the [001] direction were produced whereas at a high supersaturation, the crystal morphologies were bipyramidal. Cano et al (2001) studied the morphology of ibuprofen crystals grown from ethanol and ethyl acetate. Crystals grown from ethanol were found to have a hexagonal prism morphology, whereas ibuprofen crystallization from ethyl acetate resulted in thin platelet crystals. Pakula (1977) and Rio (2002) reported the crystallization of two different forms of indomethacin (α − needle like morphology and γ − rhombic plate like morphology) with a change in the temperature to which the solutions were cooled, and in the cooling rate. Glycine is a good example to explain the effect of pH on crystallization. There are studies (Yu and Ng, 2002) which report the change in morphology and surface of α and γ glycine crystals with change in pH between 1 and 9.

Foreign impurities can affect the growth rate of one or more faces even at very low concentrations (Grant, 2002). Impurities can become absorbed at the growing surfaces of a crystal to block the growth of certain faces/sites and hence change the morphology. When selected impurities are deliberately added to produce a desired morphological effect, they are referred to as additives or habit modifiers.

1.8   Habit modifying additives

In many cases, crystallization processes result in undesirable crystal morphology in the final crystallized product. Even changes in external process parameters would not be able to change an undesirable morphology into a desirable one. In these circumstances, the crystal habit can be modified using habit modifiers (tailor-made additives) that selectively inhibit or promote growth of certain crystal faces, thereby changing the shape of the final crystal (Deji et al, 2007). Control over the morphology can be achieved in the final product by molecular recognition of tailor-made additives.

The structure of a tailor-made additive molecule is very similar to that of the host molecule. Due to their structural similarity, mechanistically it is thought that they have enough molecular compatibility with the host system (the molecules that are crystallizing) to be able to incorporate onto the surface of the growing crystal and modify energetics, and hence morphology.

A primary feature of most crystal structures is hydrogen bonding. This bonding leads to the formation of hydrogen-bonded chains of molecules, packed in a specific conformation within the crystal structure. Any additive which disrupts the hydrogen bonding network within the crystal has the potential to significantly alter its growth rate and, ultimately, its morphology. According to Hendiksen et al (1998) structurally related additives (tailor-made additives) may influence the nucleation and growth of growing crystals in three principal ways. Additives may: (i) block adsorption of solute molecules and therefore induce morphological changes (ii) dock onto the surface and become incorporated into the crystal lattice; (iii) disrupt the emerging nucleus and thus inhibit the nucleation process.

A variety of important experimental studies for the effect of additives on crystal growth and morphology have been reported in the latter half of the last century. Changes in habit induced in sodium chloride crystals by the presence of α-amino acids are a well known early example being reported by Fenimore and Thraikill (1949).

The presence of structurally related compounds has been shown to alter distinctly the habit of pharmaceutical excipients, such as adipic acid (Fairbrother and Grant, 1978; Chow et al., 1984; Davey et al., 1992; Myerson and Jang, 1995) and α-lactose monohydrate (Garnier et al., 2002). A set of additives were reported to influence the growth of benzamide, each additive in a different growth direction. Benzoic acid blocks growth of benzamide in the *b*-axis direction, transforming the pure plate-like crystals into needles elongated along the a axis, and *p*- and *o*-toluamide block growth in the *a*-axis and the *c*-axis direction, respectively (Berkovitch-Yellin et al. 1982a). Weissbuch et al (1983) reported the crystallization of glycine from water as α-glycine with bipyramid morphology, but similar experiments of glycine in the presence of (R)- α-amino acid additives led to the formation of pyramid crystals of α-glycine with a (010) basal plane, because growth in the +b direction was inhibited. Hendriksen et al. (1998) studied the general effect of a range of molecularly similar additives (acetanilide, *p*-acetoxyacetanilide (PAA), orthocetamol, methylparaben, *p*-acetoxybenzoic acid (PABA), and metacetamol) on the nucleation kinetics and crystallization of paracetamol and observed that the morphology of paracetamol crystals was modified to varying degrees with the presence of each additive. For example, paracetamol crystals grown in the presence of 4 mol % metacetamol attain a columnar habit, distinctly different from the tabular morphology observed in a paracetamol crystal growth in the presence of 4 mol % acetanilide (Clair, 2004).

1.9   Polymorphs and its importance in the pharmaceuticals industry

Polymorphism, a phenomenon of the crystalline solid state, is the ability of a substance to exist as two or more crystalline phases that have different arrangements and/or conformations of the molecules in the crystal lattice (Giron, 2001). Figure 1.6 explains the term 'polymorphs' using the simple example of nine cross shaped units to represent molecules of a solid state substance. It shows three different conformations of nine molecules to result in three different polymorphs of a solid state substance.
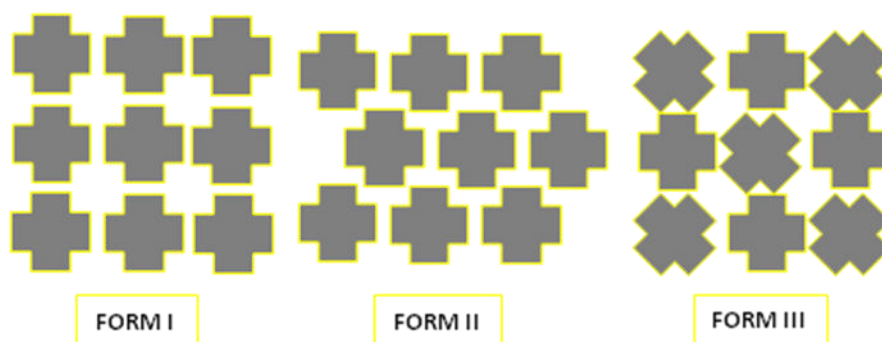
Figure 1.6   Different conformations/arrangements of molecules in a crystalline solid state substance.

A definition of polymorphic forms was first made by Mitscherlich in 1821 in relation to inorganic compounds such as arsenates, phosphates and sulphur (Schutt, 1996). The first example of polymorphism in an organic compound was discovered by Wohler and Liebig (1832) in benzamide. In 1899, Ostwald suggested that every substance could exist in two or more solid phases provided the experimental conditions are suitable. Approximately, one third of organic compounds and 80% of marketed pharmaceutical compounds exhibit polymorphism under assessable experimental conditions (Hilfiker, 2006). According to Haleblian and McCrone (1969) every compound has different polymorphic forms and that, in general, the number of forms known for a given compound is proportional to the time and money spent in research on that compound.

Polymorphs can exhibit different mechanical, thermal and physicochemical properties, such as compressibility, melting point, solubility, and crystal habit, which can have great influence on the bioavailability, filtration, and tableting properties and other performance-related characteristic properties of pharmaceuticals (Ferrari et al., 2003). For example the blockbuster drug Hytrin (terazosin) can exist in various polymorphic forms. The discovery of new polymorphs of Hytrin provides better medicine and more profit to the pharmaceutical company due to better physicochemical properties (Bauer et al, 2006). One famous example is ritonavir (Datta et al, 2004), this drug was crystallized and marketed as Form I but some batches of this drug failed a dissolution test. Investigation revealed that a new polymorph, Form II, had precipitated from the formulation of Form I. Form II was less soluble than Form I, resulting in the precipitation of solid and a decrease in the

dissolution rate of the marketed formulation. The adverse affect of decreased dissolution rate on the bioavailability of ritonavir led to withdrawal of the extant formulated products. Eventually after considerable efforts and expense, a new formulation of ritonavir was developed, submitted to FDA (Food and Drug Administration), approved and launched on to the market (Datta et al, 2004). The differences that could be shown in the physicochemical properties of drugs with different polymorphs (or with changes in polymorphism) are listed in Table 1.1; many of these can influence the drug performance greatly, as explained by the above example.

Table 1.1   Differences in polymorphic properties with changes in polymorphism

	Physicochemical properties that could changes with polymorphism
Packing properties	Molar volume and density, Hygroscopicity, Conductivity
Thermodynamic Properties	Melting point, Internal energy, Enthalpy, Entropy, Solubility, Free energy, Heat capacity
Spectroscopic properties	Electronic transition (UV spectra), Vibrational transitions (IR and Raman spectra), NMR chemical shift
Kinetic properties	Dissolution rate, Physical & chemical stability, etc.
Surface properties	Surface free energy, Interfacial tension, Crystal habit
Mechanical properties	Hardness, Tensile strength, Compactibility, Flowability

Patent rights can also be affected since different polymorphs of the same substance may be associated with separate patent claims as in the high profile litigation surrounding Zantac, in which Glaxo lost the patent claim to Novapharm (Glaxo Inc., 1995). Both of these issues have tremendous financial implication on pharmaceutical companies. Companies realize the importance of early discovery of polymorphism, to determine the most appropriate form to advance for development (lead optimization) and for that they carry out a 'polymorph screen'.

Regulatory bodies, like the Food and Drug Administration (FDA) provide guidelines and specifications that state appropriate analytical procedures should be used to detect polymorphic forms of drug substance. The FDA is an agency of the United States

Department of Health and Human Services and is responsible for regulating and supervising the safety of drugs. Any new drug application (NDA) and abbreviated new drug applications (ANDA) are required to provide enough information to the FDA so that FDA scientists can assure that the drug product possesses acceptable standards of quality to reflect the product's safety and efficacy that was demonstrated in clinical trials. This assessment of product quality also includes the scrutiny of solid state form and polymorph issues in a drug applicant. A thorough study on the occurrences of polymorphs, considering the effect of solvents, temperature and possibly pressure on the stability of drug applicant, would be required by FDA prior to NDA submission (Decamp et al, 1999). FDA has issued regulatory guidelines that outline the specifications and supporting documentation needed for a NDA, which contain several decision trees to guide their selection (Hilfiker et al, 2006). This FDA guideline also states that it is the applicant's responsibility to control the crystal form and its properties (Byrn et al, 2002).

1.9.1 Relative stability and thermodynamics of polymorphs

The relative stability of polymorphs depends on their Gibbs free energy (G). Thermodynamically, the more stable polymorph will have the lower free energy. Under a defined set of experimental conditions (except at transition points) only one polymorph has the lowest free energy. This polymorph is thermodynamically the most stable form and the other polymorph(s) termed metastable form(s). A metastable form is the one that is unstable thermodynamically but has finite existence as a result of a relatively slow rate of transformation. The relative thermodynamic stability between two polymorphs can be determined by the difference in their Gibbs free energy, ΔG:

$$\Delta G = \Delta H - T\Delta S \qquad \qquad \text{(Equation 1.13)}$$

where, the enthalpy term, ΔH, corresponds to the lattice energy difference, the entropy term, ΔS, derives from the difference in lattice vibrations and disorder between the two polymorphs. Difference in Gibbs free energy, ΔG, varies inversely with temperature as the $T\Delta S$ term increases rapidly compared to ΔH with increased temperature.

The equilibrium between stable and metastable forms exists at certain conditions and can be explained using the Gibbs phase rule (Equation 1.14),

F = C – P + 2 (Equation 1.14)

where, F is the degree of freedom, C is the number of components, and P is the number of homogeneous faces.

For example, in a glycine (C =1) system, equilibrium between two polymorphs α and γ (P = 2) can exist at only one degree of freedom (F). Hence, at constant pressure, equilibrium between two polymorphs occurs at a fixed temperature, whereas, at constant temperature equilibrium occurs at one fixed pressure. According to Myerson et al (2003), at constant pressure (ambient pressure) α and γ polymorphs of glycine exhibit equilibrium at 177°C. At this temperature both forms of glycine can co-exist but above and below this temperature only α or γ can exist, respectively. The temperature at which two or more forms are in equilibrium is called the transition temperature and its dependence on the pressure is explained by Clapeyron equation (Equation 1.15).

$dT/dP = T_t\Delta V/\Delta H_t$ (Equation 1.15)

Where, dT/dP is the change in the transition temperature with pressure, T_t is the transition temperature, ΔV is the volume change when one form transforms to the other, and ΔH_t is the enthalpy of transition.

In pharmaceutical and fine chemical industries a metastable form may offer desirable properties over the stable form, such as, better bioavailability, better grinding and compressibility, or lower hygroscopicity. In these cases, metastable forms become desirable (Hilfiker, 2006). However, a metastable form has a themodynamic tendency to reduce its free energy by transforming into the stable form. Such a polymorphic transformation is often detrimental to the efficacy of formulation. Furthermore, process conditions during manufacturing and pharmaceutical processing such as compaction, milling, wet granulation and freeze drying, can also result in polymorphic transition.

1.9.2   Classification of polymorphs

Depending on their thermodynamic behaviour explained in Section 1.11 polymorphs can be divided into two distinct classes, monotropic and enantiotropic (Park et al, 2003). In monotropic systems, only one polymorph is stable below the melting point, the solubility curves do not cross, and there is no reversible transition between the polymorphic forms below the melting point (Figure 1.7a). In enantiotropic systems, a transition point exists below the melting point (above and below this point different polymorphic forms are stable), and this transition is reversible. The solubility curves of an enantiotropic system cross before the melting point (Figure 1.7b) (Park et al, 2003). The polymorphic phase diagrams for monotropic and enantiotropic systems are shown below.
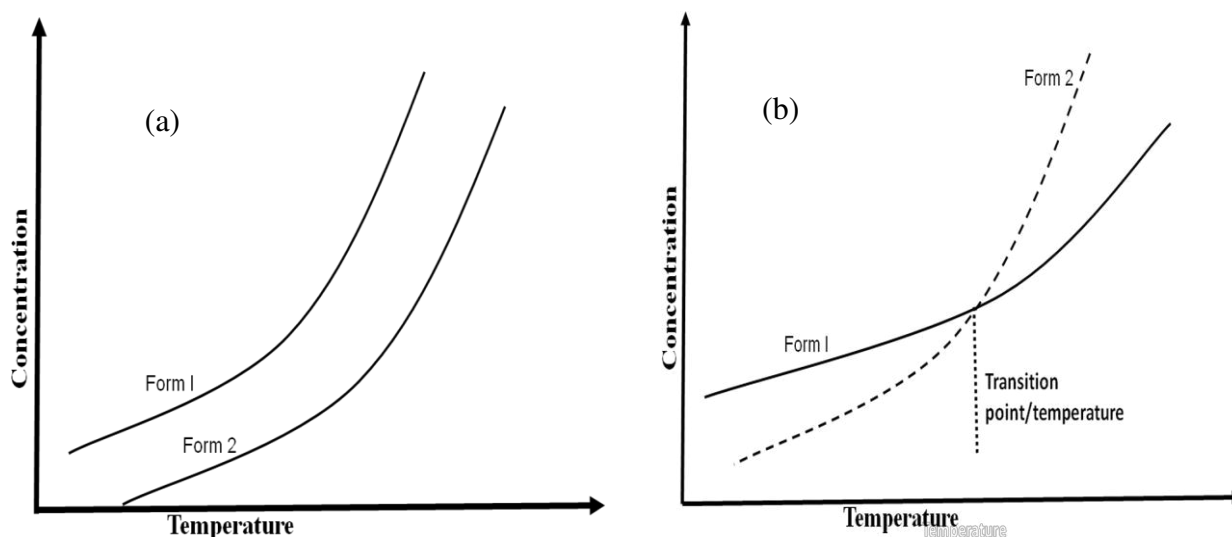
Figure1.7 Solubility curves in (a) monotropic and   (b) enantiomorphic systems.

1.10   Polymorphic transformation

Polymorphic transformation can be categorized by the type of structural changes involved, which can roughly be related to the rate of transformation (McCrone et al, 1965). There are mainly two types of transformation reported in the literature, known as reconstructive and displacive. Reconstructive transformations involve extensive rearrangement of the crystal structure and require breaking of chemical bonds and reassembling the atoms into a different crystal structure. This usually involves a large change in energy of structure, which must occur at the transformation temperature or

pressure. Because of the extensive rearrangement involved, the rate at which this type of transformation occurs may be very slow, metastable polymorphs may exist for long periods of time. Displacive transformations involve only small adjustments to the crystal structure. Generally no bonds are broken, but the angles between the atoms may change slightly. Because there is little rearrangement, displacive transformations involve no change in energy at the transformation temperature and pressure, and the transformations are instantaneous and reversible. Thus, no unstable polymorphs will occur (Park et al, 2000).

1.11   Case studies on model candidates: Sulphathiazole

As mentioned, sulphathiazole and indomethacin have been selected as candidates for this project. The polymorphism, stability, crystallization of these drugs are discussed in detail.

Sulphathiazole is a sulphonamide anti-bacterial drug, well-known for its use as an early antibiotic agent. It is a sulpha drug ($C_9H_9N_3O_2S_2$) derived from thiazole and sulphanilamide. This drug was formerly used in the prevention and treatment of bacterial infections, especially in the treatment of pneumococcus and staphylococcus infections. It has largely been replaced by less toxic sulphonamides, but it has become a useful and well studied model in the investigation of organic polymorphism and crystal growth (Lagas and Lerk, 1981; Anwar et al, 1989; Blagden et al, 1998).
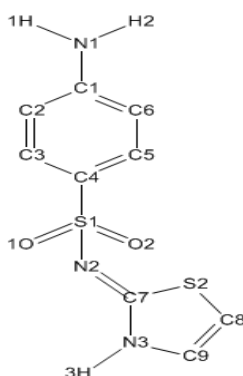
Figure 1.8   The molecule of sulphathiazole with numbering of its atoms

Sulphathiazole is commercially available as a white to yellowish crystalline powder.

1.11.1 Polymorphisms of sulphathiazole

The structure of suphathiazole and its polymorphs has been the subject of investigation for almost 60 years. Sulphathiazole is known to possess at least five polymorphic Forms: I, II and III (Kruger & Gafner, 1971, 1972), IV (Babilev et al, 1987) and V (Anwer et al, 1989; Chan et al, 1999). Of these five polymorphs, four exhibit an enantiotropic relationship, while the fifth is a monotrope (Kordikowski et al, 2001).

The single molecule of sulphathiazole is shown in Figure 1.8. It is known that the hydrogens H1, H2, H3 act as donors and O1, O2, N1 and N2 act as acceptors in the formation of a variety of hydrogen bonded structures, which lead to the formation of different polymorphs (Blagden et al, 1998).

There has been some confusion about the number and naming of different polymorphs of sulphathiazole. The number of Forms reported ranges from two (Grove and Keenan, 1941) to five (Hughes et al, 1999; Chan et al, 1999). It is now commonly accepted that sulphathiazole forms five known crystal structures and their numbers and reference codes are listed in the Cambridge Crystallographic Data Centre (CCDC).

The morphology of sulphathiazole has been widely discussed in the literature since the late 1930s. The morphological habits of sulphathiazole polymorphs reported include hexagonal, plates, rods (needle), and square shapes.

In 1941, Grove and Keenam, obtained two distinct Forms of sulphathiazole; hexagonal prisms, which melted on rapid heating at 173 – 175 °C; and prismatic rods which melted at 200 – 202 °C. Miyazaki (1947) reported evidence for a third polymorph. He used the α, β and α' terms for the three polymorphs. Later on Moustafa and Carless (1969), Shenouda et al (1970) and Mesley et al (1971) confirmed the existence of the two low temperature sulphathiazole polymorphs. Mesley et al (1971) had used the terms IIA and IIB for the two low temperature Forms. They reported a small endotherm peak at 157 °C and at 170 °C for IIA and

IIB, respectively, which transform into Form I upon heating above 180 °C and show melting of Form I at 202 °C.

Kruger and Gafner (1971; 1972) determined the detailed structure of three polymorphs of sulphathiazole, reported by the above authors. They used nomenclatures for Forms as I, II and III corresponding to Forms B, A and C of Mesley (1971).

Later on, Lagas and Lerk (1981) also reported the crystallization of polymorphs I, II and III. Form II (currently recognized as Form V) was prepared by boiling a supersaturated solution of sulphathiazole in water until all the solvent was evaporated while two other polymorphs were prepared by normal crystallization processes using different solvents. Melting points of 201 °C, 196.5 °C and 173.6 °C were obtained for Polymorphs I, II and III respectively. All three polymorphs were characterised by distinct IR spectra.

Burger and Dialer (1983) recognised a fourth form of sulphathiazole. They recorded four different IR spectra for crystals of sulphathiazole, although the IR spectra of Forms III and IV showed very minor differences between them. Later, Babilev et al (1987) described the detailed crystal structure of Form IV. They also explained the close similarities between the crystal structures of Forms III and IV, and the uniqueness of the crystal structure of Form I with respect to the others.

Because of the close similarities in crystal structures, IR spectra, and PXRD patterns of Polymorphs III and IV, there has been confusion about the separate existence of both polymorphs. Anwar et al (1989) re-examined all the four polymorphs of sulphathiazole and confirmed the existences of Form III and IV separately using techniques like Raman spectra and ^{13}C NMR in addition to PXRD, IR and DSC. They prepared Polymorph II using the same technique as Lagas and Lerk (1981). During their study, the isolation of Forms I and II was without problem. In contrast, the isolation of pure samples of Form III and IV proved to be difficult, by the inability of techniques of DSC, PXRD and IR spectroscopy to resolve the separate existence of the two forms. Anwar et al (1989) analysed the individual single crystallite in a Gandolfi X-ray diffraction camera and confirmed the separate existence of

Polymorphs III and IV, which is supported by the results of Raman spectra and ^{13}C NMR techniques.

Blagden et al (1998) carried out an extensive study of crystal structure and hydrogen bonding networks of sulphathiazole Forms I, II, III and IV using graph set analysis, which led to the appreciation of the similarities between structures II, III and IV, and highlighted the uniqueness of Form I.

In 1999, Chan and co-workers carried out a study of sulphathiazole polymorphs and found that, in the previous studies of Anwar et al (1989) and Lagas and Lerk (1981), the form referred as Form II, was actually Form V. They also determined the structure of Form V using Synchrotron high resolution powder X-ray diffraction data. In the same year Hughes et al (1999) carried out a single crystal study of Form V and supported Chan et al (1999) by stating that the form obtained from boiling water which has long been termed Polymorph II in the pharmaceutical literature and which had been assumed to have one of the previously known structures, does in fact have a new structure which therefore identifies a fifth polymorph. Appearly et al (1999) used NMR techniques for the identification of all five polymorphs and results showed that the NMR spectra of all forms were noticeably different, so that solid-state NMR appeared as an excellent technique for monitoring the polymorphic forms of sulphathiazole.

Anderson et al (2001) used an automated platform (reactor) for determining the onset of sulphathiazole crystallization. The power of this technique is its ability to detect the crystallization phenomenon in real time to determine if the desired form is being precipitated. They have presented distinct IR and Raman spectra for all five polymorphs of sulphathiazole. They also confirmed that the range of sulphathiazole crystals was dependent mainly on the crystallization solvent rather than the onset temperature or processing conditions. Kordowski et al (2001) reported a new technique for the control of sulphathiazole polymorphs. They investigated polymorph control in liquid and supercritical CO_2. They obtained crystals of pure Forms of I, II, and IV and their mixtures, at different temperatures and flow ratios of CO_2/methanol. With acetone instead of methanol, Form I or a mixture of Form I and amorphous sulphathiazole was obtained.

1.11.2 The crystal structure and hydrogen bonding of sulphathiazole polymorphs.

The crystal structure and molecular arrangements of the five polymorphs of sulphathiazole are reported in the literature. The unit cell data of these five polymorphs are listed in Table 1.2. The differences between their molecular arrangements and hydrogen bonding are discussed below.

Table 1.2   Unit cell data of Sulphathiazole polymorphs

Unit cell data (CCDC code)	Form I (SUTHAZ01)	Form II (SUTHAZ)	Form III (SUTHAZ02)	Form IV (SUTHAZ04)	Form V (SUTHAZ05)
Transition Point (°C)	none	173-175	160-173	150-173	----
Space group	$P2_1/c$	$P2_1/c$	$P2_1/c$	$P2_1/n$	$P2_1/n$
a (Å)	10.554	8.235	17.570	10.867	14.330
b (Å)	13.220	8.550	8.574	8.543	15.273
c (Å)	17.050	15.558	15.583	11.456	10.443
B (°)	108.06	93.67	112.93	88.13	91.05
Z	8	4	8	4	8

1.11.2.1   Sulphathiazole, Form I

The detailed crystal structure of Form I was first described by Kruger and Gafner (1971). The crystal data for Form I are listed in Table 1.2.

The numbering of atoms in the sulphathiazole single molecule is shown in Figure 1.8. In Form I, two molecules are contained in the asymmetric unit and this situation provided two independent molecular structures in each case. Kruger and Gafner (1972) described those molecular structures as A and B in their discussion. The bond lengths and bond angles were reported in detail in their study.

In Form I, unique centrosymmetric dimers, designated as α (this nomenclature was used by Blagden et al, 1998), are formed by pairs of molecules through symmetrical

hydrogen bonds between the imine nitrogen N(2) and amino hydrogen atom H(3). These separate dimers are bonded together through hydrogen bonds between the amino hydrogen atoms (H1 & H2) and sulfato oxygen atoms (O1 & O2) to make chains of α dimers, which link to form extended layers of α dimer sheets. The hydrogen-bonding of the α-dimer is shown in Figure 1.9.
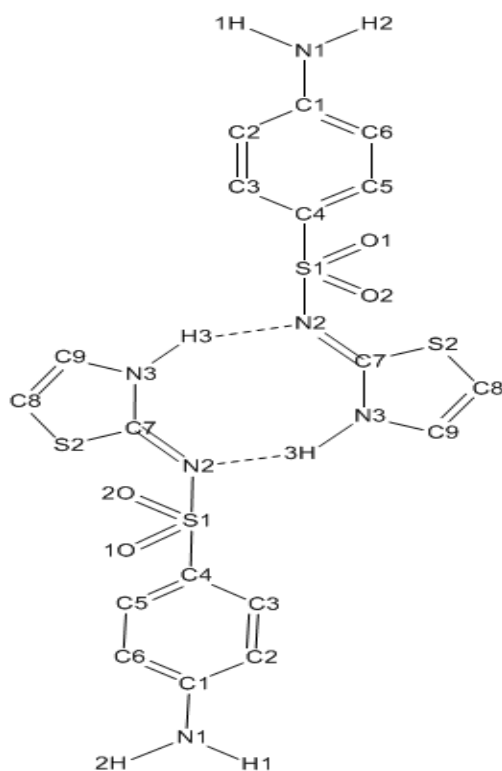
Figure 1.9   Hydrogen bonding in Sulphathiazole Form I, forming the α dimer as a basic unit of crystal structure.

Only symmetry related molecules are bonded, i.e. no hydrogen bonds exist between the independent molecules IA and IB. This means that two intermeshed but independent systems of hydrogen bonded molecules exist in the crystal. These systems are the same except that only one amino hydrogen (H1A) and one sulfato oxygen (O2A) are involved in hydrogen bonding (H1A—O2A). H2A and O1A are not involved in any bonding and remain free in IA. In system IB, both amino hydrogens (H1B & H2B) and sulfato oxygens (O1B & O2B) are involved in hydrogen bonding (H1B—O2B & H2B—O1B).

1.11.2.2 Sulphathiazole, Forms II, III and IV

The crystal structure of Forms II and III were reported first by Kruger and Gafner in 1972 and 1971, respectively, whereas, the crystal structure of Form IV was reported later by Bablidev et al in 1987. The crystallographic data of all three polymorphs are shown in Table 1.2.

The crystals of Forms II and III belong to the monoclinic system and space group $P2_1/c$. Intermolecular bond lengths and angles were calculated and listed in detail by Kruger and Gafner (1972; 1971). Form III crystallised with two molecules in the asymmetric unit. Similar to Form I, Form III also has two sets of enantiomerically related molecules, which are referred to as A (L in Blagden et al, 1998) or B (R in Blagden et al, 1998) depending on the direction of the thiazole -N−H- bond. The intramolecular bond lengths and angles were listed in detail by Kruger and Gafner (1971). The crystals of Form IV belong to the monoclinic system and space group P21/n. Intermolecular bond lengths and angles were calculated and listed in detail by Bablidev et al (1987).

Forms II, III and IV are all based on a common dimer, designated as β (Blagden et al, 1998), which in all three cases is constructed from a sulfato oxygen to aniline hydrogen contact (O2—H1) and an aniline nitrogen to amino hydrogen (N1—H3) contact as shown in Figure 1.10.
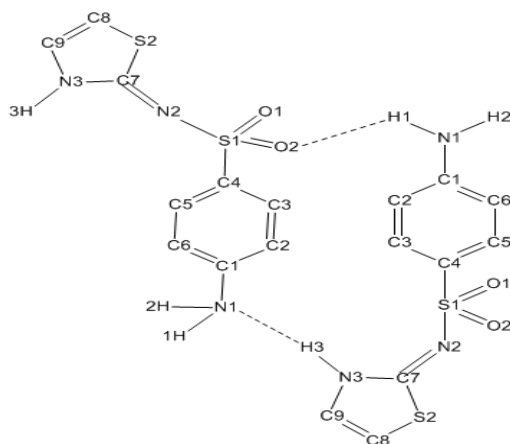
Figure 1.10   Structure of β dimers, which exist in sulphathiazole polymorphs II, III and IV.

These β dimers are linked in an eight membered chain motif of β rings. Therefore the β dimer was considered as the basic molecular packing unit of Forms II, III and IV. In each of the three structures, Forms II, III and IV, β dimer chains are linked with each other into two-dimensional sheets by O2—H2 and/or N2—H2 contacts. The structural differences between these polymorphs arise from the utilisation of the O2—H2 and N2—H2 interaction in forming the interchain linkages between β dimer chains, as shown in Figures 1.11a, b and c.

As shown in Figure 1.11a, in Form II, all the β dimer chains in a sheet are found to be in one direction only, L (left) or R (right) depending on the direction of the thiazole ring, which make two independent sheets of L-β dimer chains and R- β dimer chains in Form II. These β chains are connected with each other via H2—O2 contacts by making a ring formation, which was denoted as ε by Blagden et al (1998).
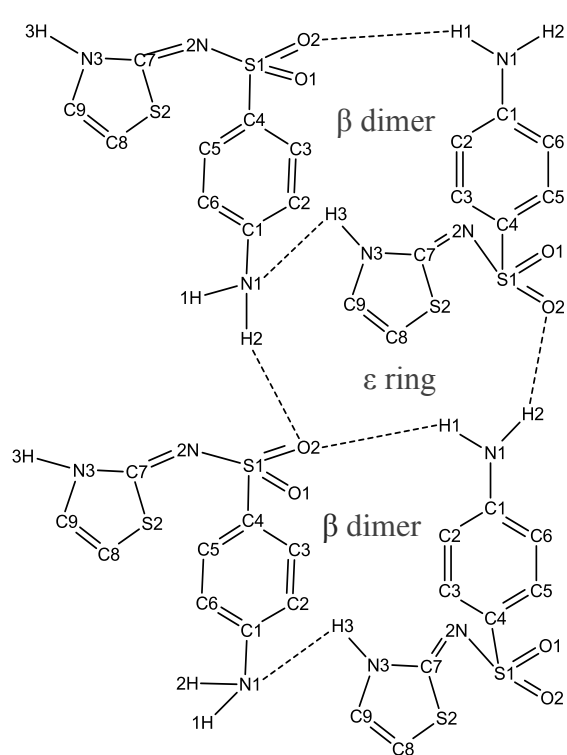
Figure 1.11a   Formation of ε ring in Form II to join β dimer chains
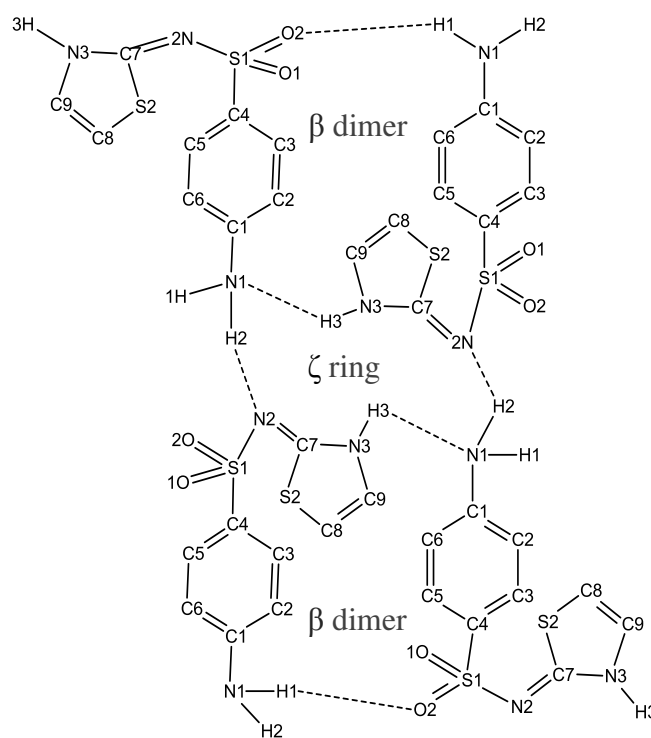
Figure 1.11b   Formation of ζ ring in Form IV to join β dimer chains

In Form IV, all the β dimer chains in a sheet are found to be alternate with each other in a left (L- β dimer chains) and right (R- β dimer chains) direction, which make only one type of β dimer sheets in a structure, as shown in Figure 1.11b. These β chains are

connected with each other via N2—H2 contacts by making a ring, which was denoted as ζ, by Blagden et al (1998).

The hydrogen bonding in sulphathiazole Form III can be thought of as the addition of Form II and IV (Figure 1.11c). In Form III, only one sheet is found, containing configuration of β dimers such that pairs of L- β dimer chains alternate with pairs of R- β dimer chains. The β dimer chains within a left (L) or right (R) sided pairs are connected with each other via H2—O2 contacts, whilst alternate left (L) and right (R) sided β-chain pairs are connected with each other via N2—H2 contacts. Unlike Form II and IV, Form III shows both H2—O2 & N2—H2 contacts between β-chains.
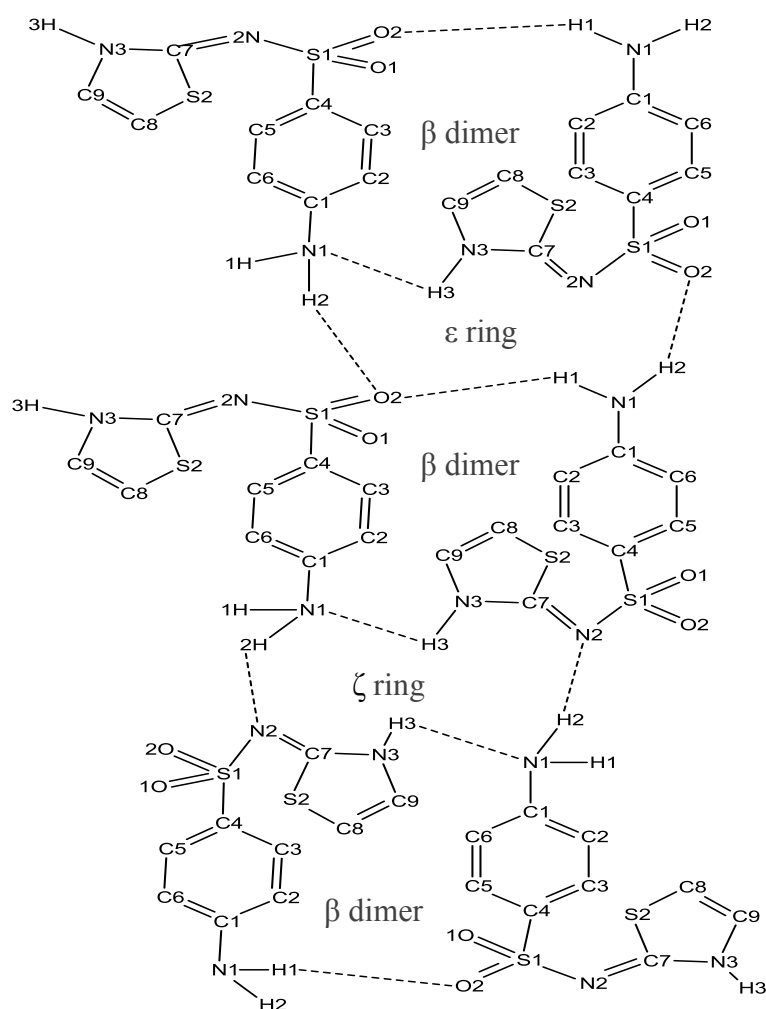
Figure 1.11c   Formation of ε and ζ rings to join stacked chains of β dimers in Form III (re-drawn from Blagden et al, 1998).

Thus the structural differences between these polymorphs arise from the way in which these β chains are arranged with each other to make sheets.

1.11.2.3 Sulphathiazole, Polymorph V

The crystal structure of Form V was reported by Anwar et al (1999) and Hughes et al (1999). The unit cell data of form V are listed in Table 1.2.

The crystal structure contains two independent molecules, termed as A and B, which associate through hydrogen bonds and van der Waals interactions to produce a two dimensional sheet structure. Both of the molecules (A and B) in the asymmetric unit possess the 'L' shape.

The molecular packing is characterized by sheets of molecules lying perpendicular to the **a** axis. A two-dimensional schematic of the hydrogen-bonding network in Form V is shown in Figure 1.12.
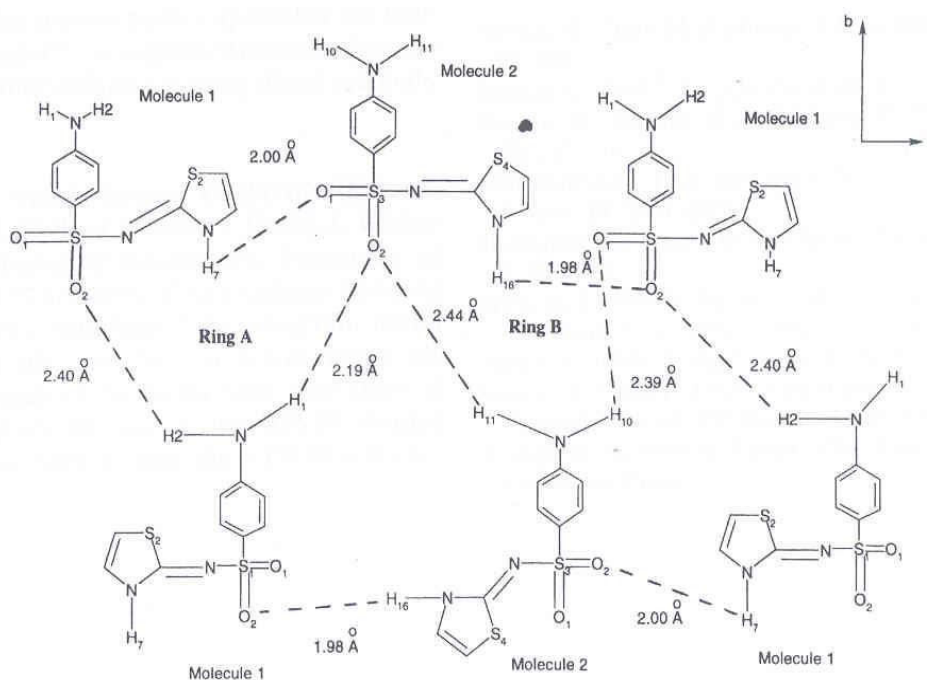
Figure 1.12   The molecular structure and hydrogen bonding of sulphathiazole V (after Anwar et al, 1999)

51

Each sheet is two molecules thick, being integrated by hydrogen bonding. The alignment of the sheets with respect to each other is staggered along the **b** axis. This staggering enables the protruding heterocyclic rings in one sheet to occupy the voids close to the benzene rings in the adjacent sheets and thus optimise the packing. Each sheet consists of chains of molecules that are linked by hydrogen bonding running along the **b** direction. The chains are inter-linked by hydrogen bonds in the **c** direction. Within a sheet, the benzene rings all lie with their respective vertical axis (defined as the vector linking the N atom of the NH_2 group to the S atom of the SO_2 group) pointing along the b axis.

1.11.3 Morphology of crystals

The different shapes of sulphathiazole crystals for different polymorphs are reported in the literature and listed in Table 1.3.

Table 1.3 Summary for the reported morphologies of sulphathiazole Polymorphs

Authors	Form I	Form II	Form III	Form IV	Form V
(Kruger et al, 1971)	elongated needles		Hexagonal Plates		Thin hexagonal platelets
(Kruger et al, 1972)		Hexagonal prisms			
(Blagden et al, 1998)	elongated needles	cuboid	Hexagonal truncated	Hexagonal plates	
(Anwar et al, 1989)	elongated needles	Thin hexagons	Hexagonal Plates	Undefined small plates	
(Groove et al, 1941)	elongated needles				
(Burger et al, 1983)	elongated needles	Thin hexagonal platelets		Hexagonal plates	
(Higuchi et al, 1967)			Hexagonal Plates		
(Miyazaki et al, 1947)	elongated needles		Hexagonal Plates		
(Kordikowski et al, 2001)	elongated needles		Hexagonal Plates	Hexagonal prisms	
Anwar et al (1999)					Thin Hexagonal platelets

In all previous studies, the morphology of Form I is consistently reported as a rod-like needle shape morphology. The morphology of crystals mainly depends on the way crystals grow after nucleation (Section 1.8). Different phases of crystals grow at different rates. Blagden et al (1998) investigated the fastest growing faces of Form I to IV, where Form I possesses a needle-like morphology with (010) faces as the fastest growing face. Form II possesses a cuboid morphology in which (110) faces are identified as the fastest growing faces, Form III possesses a truncated hexagon morphology with (110) as the fastest growing face, while Form IV possesses a plate-like hexagonal morphology with (111) being the fastest growing face.

From Table 1.3, it is clear that Form I is easy to identify with unique morphological shape. However, analytical analysis (e.g. DSC, PXRD, IR, Solid state NMR) accompanied with morphological analysis would be needed for the unambiguous characterization of sulphathiazole polymorphs.

1.11.4   Properties of sulphathiazole polymorphs

(a)   Stability

Ostwald's (1893) rule of stages suggests that crystallization of a compound from any solvent at a given temperature should crystallize initially to the least stable form in the solution followed by its stepwise conversion to the thermodynamically most stable form. It has been established that sulphathiazole follows the rule of stages (Blagden, 1998). The subsequent appearance of the stable form was observed to occur in a stepwise manner in water; the system proceeded from the most metastable Form I, followed by other metastable Forms II and III to the thermodynamically most stable Form IV. Any of the pure forms of sulphathiazole were observed to remain unchanged for several months once separated and preserved in dry ambient conditions.

After the recognition of Form V, Chan et al (1999) made a few comments about the thermodynamic stability of the five forms. Assuming that the lattice energies are directly related to unit cell densities, the rank of order of thermodynamic stability at 0 K was III ≈ IV > II > I > V. Form III and IV were both found to be kinetically stable and did not show any conversion at ambient conditions.

(b)   Dissolution rate/ solubility

Various studies have examined the dissolution rate of sulphathiazole. For example Lagas and Lerk (1981) reported dissolution rates of polymorphs in the order of V > I > III, while Burger and Diler (1983) reported that order as I > II > III. Polymorph IV was revealed by Bablidev et al (1987); thereafter Anwar et al (1989) measured the solubilities of four polymorphs that ranked as I > V > IV > III.

Generally high energy or metastable polymorphs show higher dissolution rates than the stable form (Niazi, 1976), which is also true in the case of sulphathiazole as most studies report that the most metastable Form I has the highest dissolution rate.

However, in some instances, where the conversion of the metastable to a stable form is extremely rapid in the solvent medium, the differences between the dissolution rates of metastable and stable forms are indistinguishable as the transformation occurs very rapidly (Niazi, 1976). This kind of rapid conversion was reported for sulphathiazole (Anderson et al, 1976). Niazi (1976) observed the dissolution rates of Forms I and III to be indistinguishable in water and in a water-ethanol mixture due to rapid conversion of Form I into Form III. Lagas and Lerk (1981) performed dissolution studies in water at 37°C. They reported that only the dissolution rate of Form III was constant during entire run, whilst dissolution rates of Polymorphs I and V were constant for only a few minutes and started to decrease after four minutes to approach those for Form III. These studies suggested that metastable Polymorphs I and V must be converted rapidly into the more stable Form III under the experimental conditions.

The use of additives has been also reported to enhance the solubilities of sulphathiazole. Niazi (1976) and Boldyrev et al (2005) reported the use of polyethylene glycol 4000 and calcium carbonate respectively to enhance the overall solubilities of sulphathiazole polymorphs.

(c)   Compressibility

The compaction behaviour of crystalline powder is critically dependent on the mechanical properties of the compound and hence on the arrangements of molecules

in the crystal form, and consequently on the polymorphic form (Roberts and Rowe, 2000).

The critical properties for powder compaction are the Young's modulus (which describes the elasticity or stiffness of the material) and yield stress (Roberts and Rowe, 1996). These properties vary between polymorphic pairs depending on the structural differences in the packing motif. The most stable form would have the higher Young's Modulus and yield stress, which make it the most difficult to compact amongst all the forms of the compound. Conversely, the most metastable form would be easy to compact/deform due to its lower Young's Modulus and yield stress (Sheth et al, 2004). However, according to Roberts and Rowe (1996) and Summers et al (1976), Sulphathizole Forms I and III showed very close values of Young's modulus and yield stress. Roberts and Rowe (1996) explained that, although both polymorphs show different hydrogen bonding, the number of hydrogen bonds and their strength are very similar in both polymorphs and these similarities are reflected in the closeness of both Young's modulus and yield stress of Forms I and III.

Roberts and Rowe (1996) also reported that Forms I and III did not show any transformation due to compaction. However, 100% conversion of Form I into Form III was reported at very high pressure (1052 MPa) (Kala et al, 1982). Aaltonen et al (2003) observed the transformation of Form I into Form III during compression.

(d)   Surface energy and roughness

The surface energy of a substance is defined as the amount of work required to increase the surface area of a substance by 1 m^2 (Buckton et al, 1955). The surface energy of a system is of importance in many pharmaceutical dosage forms, such as suspensions and pressurised metered dose inhaler formulations (Traini et al, 2005; Parsons et al, 1992). Surface energy is also a very important factor during pharmaceutical processing, such as granulation, in the prediction of granule strength, morphology, failure process and film formation with binders. It is known that positive values of surface energy can lead to strong granules, whereas negative values of surface energy leads to weaker granules (Rowe et al, 1989a). Hence, prior knowledge of surface energy can be used to select the best binders for a particular drug substance.

For a crystalline substance changes in surface chemistry/energy can occur as a result of shift in a polymorphic form and crystal habit.

Hooten et al (2001) measured the roughness and surface energy of sulphathiazole Form I, III and IV crystals using Atomic Force Microscopy. At a sample size less than 1µm × 1µm the polymorphs rank in terms of roughness as I > IV > III, whereas at larger scale the polymorphs rank in terms of roughness as I > III > IV. The surface energy of polymorphs was ranked in order of IV > III ≈ I. The similarities of surface energies between Form I and III could be explained by the similarities in the number and strength of hydrogen bonds in these polymorphs (Section 1.11.2.2).

1.11.5 The role of solvent on crystallization of polymorphs

The ability to select the desired polymorph during crystallization can be achieved by either manipulation of solution parameters or by the molecular recognition of structurally related additives (Weissbuch et al, 2001).

From previous studies (Blagden et al, 1998), it was established that 1-propanol stabilised the metastable Form I. In case of Form II to IV (Table 1.4), for example: Form II was observed to crystallize from nitromethane, ethanol, and n-propanol; Form III crystallized from water, dilute ammonia, or chloroform-acetone mixture, and ethanol; and Form IV crystallized from water, n-propanol and a chloroform-acetone mixture. Clearly, in most solvents, sulphathiazole showed polymorph selection with the use of different solvents. However, apart from 1-propanol for Form I, no other solvents were repetitive or consistent for the selection of a particular polymorph.

Blagden et al. (1998) investigated the differences and similarities between the structures of sulphathiazole polymorphs using graph set analysis and used these to explain the observed solvent dependence of polymorph appearance. The study reported the crystallisation of Forms I, II, III and IV from n-propanol, nitromethane, aqueous ammonia and water, respectively. In agreement with other studies, this study also reported that n-propanol stabilised Form I and did not show conversion of Form I into the thermodynamically more stable Forms II to IV for a long period of time when

slurried in n-propanol. Blagden et al (1998) observed from the graph set analysis that one bond, H3—N1, which was required for the β dimer (basic unit of Form II, III and IV; Section 1.11.2.2) was absent from the Form I structure. They suggested that the interference of n-propanol could be responsible for the non-appearance of this bonding required to complete β dimer and conversion of Form I into the more stable polymorphs II to IV. Similarly, for Forms II, III and IV, the effect of the other solvents on the ring to ring contact between β chain motifs could relate to the solvent's ability to stabilize a particular mode of ring association and then desolvate without disrupting the overall ring to ring association process. However, Blagden et al (1998) concluded that, on the basis of these qualitative considerations, it was hard to predict any sure solvent dependence of polymorph appearance in the system.

1.11.6 Effect of other factors on sulphathiazole polymorphs.

Apart from the solvent, there are several other factors that can also affect the polymorph appearance and structure of crystals.

(a)   By product and additives

Blagden et al (1998) explored the role of additives in controlling sulphathiazole polymorphs. They observed the effect of the ethamido group on the crystallisation behaviour of sulphathiazole. From the results of this study, it was clear that while water yields only Form IV after 24 h, in a solution containing 10 mol % of additive only Form I crystallises. Within the range of 1 – 0.5 mol % of impurity a mixture of Form I (40%), II (20%), III (20%) and IV (40%) was obtained. The 0.01 mol % sample was identical to the pure system, yielding 100 % Form IV. In this context the effect of the ethamido derivative is to inhibit the nucleation and growth of Forms II, III and IV, thus kinetically stabilising Form I. The ethamido group is found to be one of the main by-products during synthesis of sulphathiazole. According to Blagden (1998), an increase in the level of ethamido by-product, during the manufacturing process would result in the stabilisation of Form I. This selectivity of ethamido to crystallise/stabilise Form I was shown to be possible through the differences in hydrogen bonding contacts along the fastest growing faces of Form I compared to Forms II, III and IV.

(b)   Cooling rates

Helenski et al (2003) reported that a very high cooling rate could also affect the crystal form of sulphathiazole. The polymorph obtained with slow cooling rates was Form III and, with the same solvent system, the polymorph formed with fast cooling rate was Form I. Theoretically, differences in polymorphic form were more likely due to the polymorphic conversions that happen according to Oswald's rule of stages than dependent on the cooling rate.

(c)   Grinding

The effect of grinding on sulphathizole Form III was examined by Anwar et al (1989). Samples of Form III were ground in a pestle and mortar for 1, 3 or 5 min. They observed the PXRD pattern of all the samples and compared it with the theoretical pattern of Form III. The agreement between the observed and the theoretical pattern was seen to improve with increased grinding for Form III.

(d)   Effect of heating/temperature

The effect of heating was checked on sulphathiazole polymorphs using DSC. Form I did not show any change on heating and was observed to melt at 202 °C. Forms II, III and IV show transformation into Form I in the temperature range of 148° − 177°C followed by melting at 202 °C. So, it can be said that Forms II − IV are not stable at temperatures higher than 140°C and show the transformation to Form I (Table 1.2).

1.11.7 Crystallization of sulphathiazole polymorphs

The crystallization technique and its conditions are very important for achieving a particular polymorph and for the isolation of a particular form. In the case of sulphathiazole polymorphs, the literature is dominated by cooling and evaporation methods using various solvents.

Nevertheless, there are consistent reports of crystallising Form I from n-propanol. Kruger and Gafner (1971) and Lagas and Lerk (1981) obtained crystals of Form I by evaporation or cooling of a saturated n-propanol solution from 80 °C to room temperature. Anwar et al (1989) and Blagden et al (1998) also obtained Form I using

a saturated solution of n-propanol by cooling from 90 °C or above to room temperature. Apperley (1999) reported the heating of commercial sulphathiazole at 180°C to obtain Form I.

Kruger and Gafner (1971) and Burger et al (1983) obtained crystals of Form II from a saturated n-propanol solution at room temperature by evaporation. Anderson et al (2001) reported the preparation of Form II by slow cooling of a saturated aqueous solution. Blagden et al (1998) obtained crystals of Form II by cooling from saturated nitromethane or ethanol solution, while Apperley et al (1999) used a supersaturated aqueous solution and evaporated it to dryness to obtain Form II.

Form III was crystallized by slow evaporation from dilute ammonium hydroxide solution at room temperature (Kruger and Gafner, 1971). Lagas and Lerk (1981) obtained Form III by very slow cooling/evaporation from water, ethanol and water-ethanol or chloroform-acetone mixtures. Anwar et al (1989) recrystallized Form III from saturated aqueous solution by cooling at 5-10 °C/h. Blagden et al (1998) crystallized Form III by cooling a saturated aqueous ammonia solution at 40 °C to room temperature.

Form IV was crystallized mainly by cooling or evaporation from saturated solutions of acetone-chloroform mixtures, boiling water and n-propanol. Burger et al (1983) reported the crystallization of hexagonal crystals of Form IV by evaporation using n-propanol as a solvent. Anwar et al (1989) recrystallized Form IV from a 50:50 mixture of acetone and chloroform by cooling to room temperature. Blagden et al (1998) prepared a saturated solution of sulphathiazole in water (25 g/l) and obtained Form IV by cooling the solution from 40 °C to room temperature. Apperely et al (1999) crystallized a sample of Form IV by cooling from acetonitrile.

Form V was prepared by boiling a supersaturated solution of sulphathiazole in water until all the solvent evaporated (Lagas and Lerk, 1981; Anwar et al, 1989; Chan et al, 1999; Hughes et al, 1999). Appearly et al (1999) purified Form V by dissolution in alkali followed by neutralization.

There were also some unique techniques reported for the crystallization of sulphathiazole polymorphs. Anderson et al (2001) used a HEL-Auto-MATE (HEL, Hertfordshire, UK) laboratory reactor for the crystallization of sulphathiazole with different solvents. Their objective of using the automated reactor system was to determine if the proper form was being precipitated, and real time onset of crystallization. Kordikowski (2001) used the SEDS^{TM} process (Solution Enhanced Dispersion using Supercritical fluids) to separate the enantiotropic forms of sulphathiazole. Variation of temperature and flow rate of CO_2 and solvent proved that thermodynamic and kinetic control could be applied to generate certain forms. Three Forms (I, II and IV) could be crystallized with methanol only by choosing the appropriate temperature and flow rate conditions (Kordikowski et al, 2001).

1.12   Indomethacin

Indomethacin is a non Steroid Anti-Inflammatory drug (NSAID) used primarily to relieve pain and inflammation caused by conditions such as gout and arthritis, and works by blocking cyclooxygenase. The structure of indomethacin is shown in Figure 1.13. The main features are the benzoyl ring, the benzoyl chlorine atom, an indole ring and a carboxylate group.
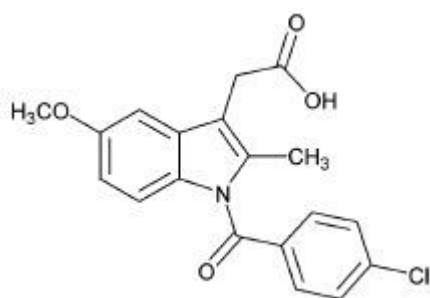
Figure 1.13   A molecule of indomethacin

Indomethacin was first approved by the FDA in 1965 (Yamamoto, 1968). It is available in three dosage forms; capsules, suspension and suppositories with the first two dosage forms containing the drug as a solid. A good understanding of the properties of its solid state is therefore essential in designing dosage forms with optimum drug delivery characteristics and stability.

1.12.1 Polymorphs of indomethacin

Indomethacin is known to exhibit at least five polymorphs and has a tendency to form solvates with a wide range of solvents under super-saturation conditions (Slavin et al, 2002). The γ Form (Form I) is the most thermodynamically stable and forms at low supersaturation conditions. It has a plate-like morphology, largely unchanged by solvent of crystallization. The α Form (Form II) is observed under high supersaturation conditions, is metastable, but can be isolated and stored for up to 18 months without transformation (Slavin et al, 2002). Only these two forms are produced reliably. The remaining polymorphs, Forms III, IV and V (β), exist only in thin films grown from the melt and in the presence of co-solutes (Yamamoto, 1968; Borka et al, 1974, Slavin et al, 2002). All of these Forms, III, IV and V (β), are metastable and readily transform to Forms I or II on standing or heating. The relative appearance of the two principle Polymorphs α (II) and γ (I) is consistent with Ostwald's rule (1893) which would predict that the α phase should form under rapid precipitation conditions followed by its transformation to the stable γ Form on long periods of standing or lengthy growth periods.

The polymorphism of indomethacin has been discussed extensively, particularly, after FDA approval for use as a medicine in 1965. First of all, Yamamoto (1968) stated that indomethacin can be found in different crystalline forms determined as α (Form II), β (Form V) and γ (Form I) and also presented distinct PXRD patterns of these three forms. However, later reports reported only two of these forms. Allen and Kwan (1969) reported Form I and Form II with melting points respectively at 160 and 154 °C. Monkhouse and Lach (1972) identified Forms I and II, with melting points respectively at 158 and 152 °C, and presented IR spectra. Borka (1974) identified another two Forms, III and IV and a solvent containing (solvate) Form V. Borka stated that Form V may contain various amounts of different solvents without any stoichiometry. Form I (160 °C) and Form II (154 °C) can easily be isolated in pure form both from the melt and from solvents. Form III (148 °C) can only be observed by its appearance and melting point in microscopic preparations. Form IV (134 °C) can be isolated in pure form from the melt and from warm methanol (Borka, 1974). Borka (1974) also interpreted that Yamamoto's (1968) Form β was a solvate of Form

V, which melted at low temperature, lost the solvent, recrystallized into Form I and gave the high melting point of 160 °C.

Polymorphic forms of indomethacin show different therapeutic properties as well as side effects (Singhal et al, 2003). Thus, the preparation of polymorphic forms of indomethacin was an important technological problem. Pakula et al (1977) defined the technologically useful methods of preparing α (II), β (V), and γ (I) Forms of indomethacin, and also defined the influence of various parameters, such as solvent, heating and cooling rate, concentration and temperature, on the formation of individual forms of indomethacin during crystallization. Kaneniwa et al (1985) also established the methods for the preparation of the pure α (II) and γ (I) Forms of indomethacin, and also re-examined the physico-chemical properties of these polymorphs.

Lin et al (1992) reported that a new polymorph of indomethacin was precipitated from an aqueous solution of indomethacin and β-cyclodextrin by a titration method. The DSC analysis of crystals that precipitated from the solution of indomethacin without β-cyclodextrin was the same as that of the α Form (II), which suggested that the formation of the new polymorph of indomethacin depended on the absence or presence of β-cyclodextrin (Lin et al, 1992). However, the occurrence of this new polymorph could be considered as a complex of indomethacin and β-cyclodextrin rather than Form VI. Bratu et al (2001) reported the α (II) and γ (I) Forms and solvate of indomethacin from various solvents and presented X-ray diffraction and FTIR spectra.

Also there are many reports available on the crystallization of indomethacin polymorphs from the amorphous state. Andronis and Zografi (2000) determined the effect of temperature on the overall crystallization, and the crystal nucleation of indomethacin polymorphs from the amorphous state. They reported that crystallization of amorphous indomethacin at close to or below its glass transition temperature, Tg, (42 °C), favours the formation of the stable γ Form, while crystallization at higher temperature favours the formation of α Form. Wu and Yu (2006) concluded that the liquid dynamics of indomethacin control its crystal growth kinetics over a wide range of temperatures but changes of growth morphologies near

Tg also lead to apparent acceleration of growth of certain polymorphs.

Indomethacin is used in many pharmaceutical preparations (Yamamoto, 1968, Rio et al, 2002). Despite its utility and the need to understand the morphological properties of its crystals for the purpose of formulation, little has been published on the morphologies of the polymorphic forms. Slavin et al (2002) described the morphological variation of α, γ, and solvates grown from a range of solvents, and particularly defined the morphologies of the γ Form and compared the results with modelling calculations of the predicted morphology of the γ Form. Also Rio et al (2002) developed the recrystallization method of the desired α and γ Forms, using specified solvent ratios and cooling parameters, at a satisfactory level of efficiency. Moreover, they also defined the pre-formulation properties of both forms, such as dissolution, flowability, and compressibility for the production of pharmaceutical tablet forms.

Often metastable forms have desirable properties, and are preferable to the stable form. The stability to transformation of the metastable α Form of indomethacin makes commercial usage viable. Both α and γ Forms are monotropic polymorphs and they did not report inter conversion in the solid-state without a solvent such as ethanol (Andronis et al, 1997; Okumura et al, 2006). However, the α Form has an undesirable morphology consisting of fibrous structures. For this reason, its properties are uninvestigated and its potential for exploitation remains untapped. This project will examine the morphological expression of the α and γ Forms of indomethacin with the aims of producing crystals of the α Form with a well defined morphology, and producing γ crystals with modified morphology.

1.12.2 Crystal structure of indomethacin forms

The crystal structures of both α and γ Forms were reported in detail in the previous literature. They will be referred to briefly here in order to understand differences, particularly, in their hydrogen bonding.

(a)   γ Indomethacin (Form I)

Kistenmacher et al (1972) were the first to report the solid-state structure of γ-indomethacin by single crystal x-ray diffraction methods. There are three chemical groups present in the structure of indomethacin; a benzene ring, indole ring and carbonyl group. γ-indomethacin crystallizes in the centro-symmetric triclinic space group P1 (triclinic) with Z = 2, and unit cell a = 9.295 Å, b = 10.969 Å, c = 9.742 Å, α = 69.38°, β = 110.79°, and γ = 92.78°. Also, Galdecki et al (1976) solved the structure of γ indomethacin using three dimensional photographic data. They also compared their data with x-ray data of γ indomethacin found by Kistnemacher et al. (1972).
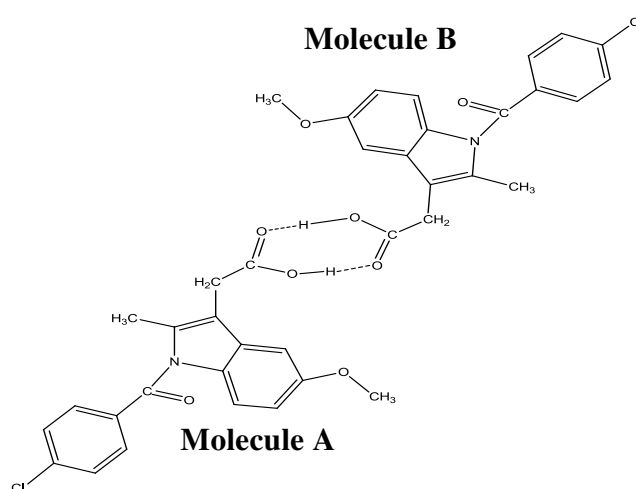
Figure 1.14   Dimer formation in γ indomethacin structure via hydrogen bonding between carboxylic functional groups (re-drawn from Kistemnmacher et al, 1972)

Two features dominate the crystal packing. The first is the expected hydrogen bonding of the carboxylic acid group about centres of inversion to form molecular dimers as shown in Figure 1.14. The second important feature of the crystal packing is the overlapping of the indole ring with the acetic acid group of another molecule.

Chen et al (2001) reported that these hydrogen bond dimers are caged inside a hydrophobic shield. In one direction, the bulky indol and phenyl rings of the molecule protect the dimers. Two indol rings from neighbouring unit cells block the second direction. In the third direction, two phenyl rings provide protection. Recently, Carpentier et al (2006) characterized the crystalline γ phase by the existence of rotational dynamics related to the chlorobenzyl group motion using solid state NMR.

(b)   α Indomethacin (Form II)

The crystal structure of the metastable α Form was not published until 2001 due to the small size of α crystals, which were not large enough for single crystal x-ray diffraction. In 2001, Chen et al developed large single crystals of the α Form by diffusion of water vapour into a solution of glacial acetic acid, and reported the crystal structure of α indomethacin using single crystal X ray diffraction. α indomethacin crystallized in the non centrosymmetric monoclinic space group $P2_1$ with $Z = 6$. The unit cell constants were $a = 5.462$ Å, $b = 25.310$ Å, $c = 18.152$ Å, $\alpha = 90.00°$, $\beta = 94.38°$, $\gamma = 90.00°$, with $V = 2501$ Å^3 (Chen et al, 2001). The calculated density, obtained from single crystal data, was measured as 1.43 g/cm^3, which agrees well with the experimentally determined value of 1.40 g/cm^3 (Andronis et al, 2001).

The asymmetric unit of α indomethacin consists of three molecules with very different conformations. These three molecules exist as trimers in which two of the molecules form mutually hydrogen bonded carboxylic acid dimers and the third molecule forms a hydrogen bond between the carboxylic acid and an amide carbonyl in the dimer (Figure 1.15). Furthermore, the hydrogen bond between the carboxylic acid of molecule C and the amide carbonyl of molecule B in the α-Form is the longest in the two modifications, and the hydrogen bond of the A-B carboxylic acid dimer is considerably longer than the B-A hydrogen bond of the A-B dimer and the hydrogen bond of the γ-Form dimer
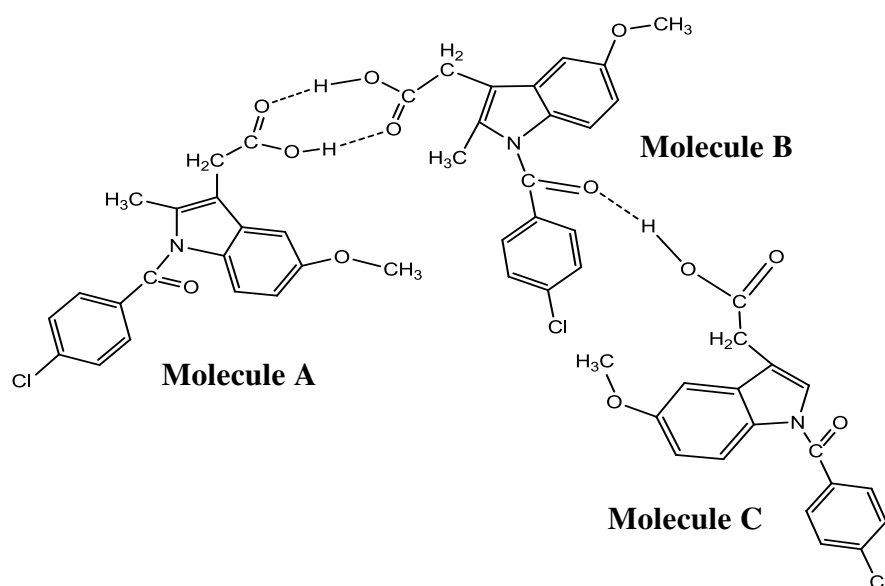
Figure 1.15 A trimer formation in α-indomethacin (re-drawn from Chen et al, 2001)

The determination of the crystal structure of the α Form gave confirmatory evidence that this metastable form has a greater density as compared to that of the γ Form (Chen et al, 2001). Typically, in comparing two polymorphs, the form having a lower density than the other is assumed to be less stable at 0 K, which is known as the density rule (Burger et al, 1979). In indomethacin, however, the metastable α Form has a greater density than the more stable γ Form. There are some exceptional cases to the density rule reported in the literature (Burger et al, 1979), which involve strong hydrogen bonding or conformational changes along with hydrogen bonding. Thus, the greater density of the α Form may be related to the additional hydrogen bonding present (between a carboxylic acid hydroxyl group and the carbonyl oxygen of an amide group) and the three conformations that indomethacin adopts in the α Form as compared to the single conformation in the γ Form. The additional conformations of the α Form provide a closer packed crystal and hence a greater density than that possible in the γ Form (Chen et al, 2001).

Recently, Carpentier et al (2006) used solid state NMR to characterize the molecular mobility of indomethacin in its different forms below its Tg. They reported that no molecular mobility exists in the α phase, except methyl group rotations. In a similar study, Masuda et al (2006) analyzed the difference in the molecular conformation packed in the crystal lattice between the metastable α Form and stable γ Form of indomethacin on the basis of solid state ^{13}C NMR spectral pattern. The chemical shifts of each resonance of the α Form were distinctly different from the γ Form. Carbon nuclei of the α Form showed a complicated set of resonances for each carbon.

1.12.3 Properties of Indomethacin Polymorphs

The significance of polymorphism to the pharmaceutical industry lies in the different properties of various polymorphs, which affect the efficiency of the active substance (Brutu et al 2001). Many of these physico-chemical properties of indomethacin polymorphs were already reported in the literature and are discussed briefly here.

(a)   Toxicity
There are few studies in the literature, concerning indomethacin toxicity or the influence of its crystalline forms on toxicity and absorption. Naciazek-Wieniawska et

al (1975) found that α indomethacin was more toxic than the γ Form. This study reported that α indomethacin was 1.3-2.2 times more toxic than γ indomethacin in mice.

(b)   Solubility and bioavailability

Many drugs are poorly soluble or insoluble in water, which results in poor bioavailability because the solubility of a drug is an important factor in determining the rate and extent of its absorption. Hence, this property is of a great importance in developing pharmaceuticals. Indomethacin is a hydrophobic drug and both forms show poor solubility in water. However, α indomethacin has been reported to have a better dissolution rate compared to γ indomethacin (Andonis et al, 2000). Rectal absorption rate of the metastable α Form (dissolution rate) in the rat was greater than the stable γ Form (Yokoyama, 1979). According to Rio et al (2002), the higher solubility of the α Form is not only due to its crystal state, but also to its higher original specific surface.

(c)   Stability

The γ Form is the most thermodynamically stable as implied by melting point. melting/fusion of all the polymorphs are reported in the literature (section 1.12.1). From this Slavin et al (2001) suggested that indomethacin polymorphs follow the rank of stability in order of I (γ) > II (α) > III > IV > V > amorphous. The α Form (II) can be prepared by direct crystallization, however and although metastable, has been shown to persist at room temperature for periods of longer than 18 months without transformation (Slavin et al, 2002).

Forms III, IV, V and the amorphous form are not kinetically stable and therefore not of interest for pharmaceutical use.

(d)   Compressibility and Flow ability

Rio et al (2002) reported the compressibility and flowability of γ and α Forms. They measured the compression ratio, which showed that the α Form had a better capacity for compressibility compared to the γ Form. This was further confirmed by α Form tablets offering greater resistance to fracturing due to their higher hardness indices

(Rio et al, 2002). The flowability was also expressed as good for the α Form (Rio et al, 2002).

(e) Chemical stability

Chen et al (2001) showed that the distinct crystal packing of the α and γ Forms of indomethacin has a profound impact on the chemical stability of the forms. They demonstrated this by exposing both forms to the presence of ammonia gas. The α Form single crystals became opaque within 8 minutes, which indicates that there was a rapid interaction between α -indomethacin and ammonia gas. Chen et al (2001) suggested that the development of opacity in α indomethacin is due to an acid-base reaction with ammonia to make the ammonium salt. Conversely, γ indomethacin showed inertness to ammonia gas and did not show any changes even after 24 hours of exposure. Additionally, Chen et al (2001) supported this result by weight gain measurements of the α and γ Forms, when exposed to ammonia for 1 hour. The results showed that α-indomethacin crystals gained significant weight, 3.81 %, by reacting with (absorbing) ammonia gas, whereas the weight gain for the γ Form was nearly zero, which further confirms the inertness of the γ Form and reactivity of α Form to ammonia gas.

1.12.4 Crystallization methods of indomethacin

As shown in Table 1.4, there are three types of crystallization techniques reported in the literature for indomethacin; (1) evaporation, (2) cooling and (3) precipitation.

Table 1.4   Summary of the crystallization techniques reported in literature for Indomethacin polymorphs.

Solvent	Crystallization technique used	Polymorphs	Literatrure
Acetonitrile	Cooling/evaporation	γ	A, E, K
		α	E,
Ethyl ether	Cooling/evaporation	γ	B, E, K, L, P
		α /solvates	E
Ethanol	Water precipitation, cooling/evaporation	α	D, E, F, G, J, K, L, M, P, Q, R
		γ	D, E, M
Range of alcohols	Cooling at room temperature	α /solvates	E
		γ	E

Ethyl acetate	Cooling at room temperature	γ	E, G,
		α /solvates	E
	Evaporation	α	K
Toluene	Cooling	γ	E, H
		α /solvates	E
Acetone	Evaporation/cooling	α /solvates	E, F
	Water precipitation /fast cooling	α	F, G,
	Cooling	γ	E, F
	Cooling (3 hour)	γ	G
		β	G
Acetic acid: water	Fast cooling /evaporation/water vapor diffusion	α	G, K, M
	Slow cooling to 45°C	γ	G,
Benzene	Cooling	β	G, J, P
CHCl₃, CCl₃	Cooling	β	G

Key used in Table 1.4   **A** – Kistenmacher et al (1972); **B** –Galdecki et al (1976); **C** – Kim et al (2003); **D** – Andronis et al (2000); **E** – Slavin et al (2002); **F** – Rio et al (2002); **G** – Pakula et al (1977); **H** – Brutu et al (2001); **J** – Yamamoto et al (1968); **K** – Borka et al (1974); **L** – Otsuka et al (2001); **M** – Chen et al (2001); **P** – Lin et al (1999); **Q** – Masuda et al (2006); **R** – Okumura et al (2006)

According to the literature (Table 1.4) the γ Form is normally crystallized from diethyl ether and acetonitrile as plates and prisms; whereas the α Form is mainly crystallized from ethanolic solutions. However the choice of solvent is not the only parameter responsible for the polymorphic outcome. It is clear from the data presented in Table 1.4 that attention should be given to experimental techniques and conditions such as concentration, cooling rate or temperature.

For example, Pakula et al (1977) reported that the crystallization of indomethacin from aqueous ethanol by cooling from elevated temperature to 40-45 °C gives reproducibly pure α Form, whereas cooling below 40 °C caused, in the majority of cases, the precipitation of a mixture of α and β Forms. For the majority of alcohols low super-saturation conditions yielded the γ Form alone and high supersaturation yielded a mixture of the α Form and solvates (Table 1.4). In the same way, acetonitrile generally resulted in the crystallization of γ Form. However, Slavin et al (2002) reported that acetonitrile gave the pure α Form at high supersaturation and

pure γ Form at low supersaturation conditions. They studied a range of solvents and observed a similar effect of supersaturation on the polymorphic outcome of indomethacin (Table 1.4).

In addition to temperature and concentration, cooling rate is also reported as one of the deciding parameters for the crystallization of indomethacin. Rio et al (2002) studied the recrystallization of γ Form from aqueous acetone solution at a cooling rate of 0.17 °C/min. If the rate was increased to 0.4 °C/min, α Form crystals were obtained. Previously, Pakula et al (1977) also observed the effect of cooling rate and solvent ratio on the crystallization of polymorphs. They reported that fast cooling of an acetic acid and water solution (2:1.5) within 10 min, resulted in the formation of the α Form; whereas, slow cooling to 45 °C of an acetic acid and water solution (2:1), resulted the crystallization of the γ Form.

The β Form occurs during crystallization from a range of solvents such as acetone, benzene, chloroform, carbon tetrachloride by cooling (Table 1.4). The β Form is, however, unstable and storage at room temperature as well as drying or any other operation causes its transformation into the α- or γ-Form.

Apart from solvent crystallization, melt crystallization was also studied for indomethacin at higher temperatures. By preparing a crystal film and placing it on a Kofler hot stage, most forms were observed within the melt with increase in temperature (Borka et al, 1974). Form IV grows readily between 70 and 90 °C in a crystal film. By raising to the higher temperature of 110-115 °C, Form III grew as spherulites, but always together with α Form (II) and Form IV. Form III was not obtained in its pure form. At a few degrees higher, α Form (II) dominated with γ Form (I). They grew side by side up to 150 °C, then α Form (II) melted at 154 °C and γ Form (I) crystals grew and remained in the melt below 156 °C as plates and prisms until they melted finally at 160-161 °C.

1.12.5 Morphological studies of indomethacin polymorphs

Despite its utility and the need to understand the morphological properties of product crystals for the purpose of formulation, surprisingly little has been published on the morphologies of the predominant polymorphic forms of indomethacin.

Transparent yellowish crystals of γ-indomethacin were obtained by Galdecki et al (1976). γ-indomethacin showed a well defined large, prismatic and plate-like morphology in most previous studies (Table 1.4). The α-Form grew as a fibrous/spherulitic micronized needle/columnar like morphology (Slavin et al, 2002), white in colour (Rio et al, 2002). These micronized needles of the α Form were observed to be clustered into bundles.

Of particular note was the close similarity of the morphologies of the γ-species precipitated under similar conditions from a wide range of solvent types. This implies that there is little or no solvent direction of the morphology or polymorphic type. This assumption was confirmed by the observation of similar morphologies following growth from the melt where no solvent direction or mediation can be envisaged (Slavin et al, 2002).

A full analysis of the morphology of the γ Form has been carried out for crystals grown from acetonitrile, at both high and low super saturation. Morphological modelling calculation based on the Attachment Energy (Slavin et al, 2002) model was also carried out on the γ Form, which showed good agreement with the γ-indomethacin crystals grown at low super-saturation from acetonitrile.

1.12.6 Effect of various factors on indomethacin polymorphs

(a) Humidity

Absorbed water vapour lowers the Tg of amorphous indomethacin and enhances the overall crystallization rates, favouring the γ-Form at low water content and the α-Form at higher water content of the amorphous form (Andronis et al, 2000).

(b)   Grinding with controlled temperature

Otsuka et al (1986) investigated the effect of grinding on the polymorphs of indomethacin at various temperatures. The results suggested that the α -and γ-Forms of indomethacin were converted to a non-crystalline solid during grinding at 4 °C by mechanical stress. However, it seems that the γ Form was more stable than the α Form during grinding at 4 °C since the γ-Form was converted to non-crystalline solid after grinding for 4 h, but the α-Form was converted in only 2 h. At 30 °C, the α-Form of indomethacin was more stable than the γ-Form during grinding since the latter was transformed to the metastable α-Form on grinding, whereas the α-Form did not change and finally converted to a non-crystalline solid after intensive grinding.

(c)   Pressure

Indomethacin powder was examined under a hydrostatic pressure of 400 Mpa to determine the effect of pressure on the powder. Under high pressure, the γ -Form of indomethacin showed the transformation into α-Form. However the α-Form showed traces of amorphousness at higher pressure but did not show transformation into other polymorphic forms (Okumura et al, 2006).

1.12.7 Effect of additives

No relevant studies were found in the literature for the effect of additives on the morphology of indomethacin. However, there are some reports which describe the complex of indomethacin with carriers and excipients. Also amorphous indomethacin is reported to complex with polymers. Hamza et al (1994) studied the enhanced aqueous solubility of indomethacin in the form of physical mixtures, with nicotinamide as a carrier. The authors reported the formation of an indomethacin/nicotinamide complex. This complex is formed in the molten state or in solution. H bonding and π- electron donor- acceptor links are probably the main contributions to the interaction mechanism between indomethacin and nicotinamide. (Bogdanova et al, 1998; Truelove et al, 1984; Fawzi et al, 1980).

In solution, PVP (Poly Vinyl Pyrrolidone) has been found to interact with numerous organic molecules and it has been suggested that the mechanism of crystallization inhibition is related to the extent of interaction between drug and polymer (Zograffi et

al, 1998). The addition of PVP to amorphous indomethacin to form a miscible binary amorphous phase, results in the disruption of the indomethacin dimers. This is brought about by a hydrogen bond formed between the PVP amide carbonyl group and the indomethacin hydroxyl group. The formation of a hydrogen bond between indomethacin and PVP offers an explanation as to how PVP is able to inhibit crystallization from the amorphous phase at levels where the antiplasticising effect is minimal (Zograffi et al, 1998).

1.13   The scope of the thesis

As discussed in Sections 1.8 and 1.10, polymorphs and their morphology can have great influence on the final product/drug efficacy. The control over the appearance of polymorphs and morphology can be achieved in the final product with a knowledge of techniques in crystal and nucleation engineering. Understanding of the supramolecular processes that take place when polymorphic materials nucleate is expanding and can be applied to a variety of systems to control the polymorphic outcome of nucleation.

Sulphathiazole is a highly polymorphic model system (five polymorphs, I to V), which is used to demonstrate the ability to isolate polymorphs from different solvents. Already the subject of extensive study, the sensitivity of this material (for polymorph selection) to solvent environment is well established (Anwar et al, 1989; Blagden et al, 1999). The crystal structures of five polymorphs are already reported in the literature. It is also established that 1-propanol stabilizes the most metastable Form I. The current project aims to examine the effect of a range of alcohols on polymorph selection of sulphathiazole and attempts to elucidate the mechanism of alcohols in polymorph selection process.   The role of the alcohol functional group in the polymorph selection process will be thus investigated and evaluated. Various experimental crystallization and analytical techniques will be employed for the crystallization and polymorphic identification of sulphathiazole polymorphs. Based on an experimental study, the role of solvent in the stabilization/selection of polymorphs will be also investigated by visualizing and performing thermodynamic calculations using Cerius^2 molecular modelling software.

Another model system, Indomethacin is known to exhibit at least five polymorphs. However, only γ Form (I, the most stable form) and α Form (II, metastable form) are produced reliably. The remaining polymorphs, Forms III, IV and β (V), are metastable and readily transform to Forms γ (I) or α (II) on standing or heating. The α Form (II) is metastable, but can be isolated and stored for up to 18 months without transformation, which makes commercial usage of the metastable form viable. However, the α-Form has an undesirable morphology consisting of fibrous structures. For this reason, its properties have not been investigated and the potential for exploitation untapped. The project will examine the morphological expression of the α- and γ Forms of indomethacin with the aims of producing crystals of the α polymorph with a well defined morphology using structurally related additives. Various experimental techniques will be employed for the crystallization of indomethacin with structurally related additives.

Chapter 2   Materials and Methods

In this study, sulphathiazole and indomethacin were crystallized using various methods and conditions. The crystallization of sulphathiazole using different solvents with an alcohol (-OH-) functional group, was studied for effects on polymorphic and morphological behavior. Indomethacin was crystallized using various crystallization techniques/conditions to study the effect on crystal morphology. In addition, additives were also used with indomethacin to improve the fibrous morphology of the α-Form. Crystal samples were characterized using analytical techniques such as optical microscopy, hot stage microscopy, powder X-ray diffraction, differential scanning calorimetry, and infra-red spectroscopy to study the morphological and polymorphic behavior of the samples. The effect of solvents (alcohols) on polymorph selection of sulphathiazole was predicted using 'Cerius2' (Accelrys, Cambridge, UK) and 'GRID' based molecular modelling software (Roberts et al, 2007).

2.1 Materials

All the materials used in this study are listed in Table 2.1.

2.1.1   Sulphathiazole

Sulphathiazole (98%) was used as a model drug to study the role of solvents on polymorph selection.

2.1.2   Indomethacin

Indomethacin (99.5%) was used to study the effect of additives and various crystallization conditions on crystal morphology.

2.1.3   Solvents and Additives

A number of solvents and additives were used in the experimental studies. A list of all these solvents and additives is given in Table 2.1

Table 2.1 List of all chemical compounds used in experimental studies

Reagents	Supplier	appearance	Boiling point (BP) or melting point (MP)
Sulphathiazole	Sigma-Aldrich, Dorset, UK	White crystalline powder	MP 200-202°C
Indomethacin	Sigma-Aldrich, Dorset UK	White powder	MP155°C
Adipic acid	Sigma-Aldrich, Dorset UK	white crystalline powder	MP 151-154°C
Myristic acid	Sigma-Aldrich, Dorset, UK	White powder	MP 52-54°C
Oleic acid	Sigma-Aldrich, Dorset, UK	Colourless liquid	MP 13-14°C, BP 194-195°
Capric acid	Sigma-Aldrich, Dorset, UK	Crystalline white powder	MP 27-32°C, BP 268-270°C
1-indole 3-acetic acid	Sigma-Aldrich, Dorset, UK	White crystalline powder	MP 168-170°C
Tetramethylsilane	Sigma-Aldrich, Dorset, UK	Colourless liquid	BP 28 °C
1-propanol	VWR International Ltd, Lutterworth, UK	Clear colorless liquid	BP 97°C
2-propanol	VWR International Ltd, Lutterworth, UK	Clear colorless liquid	BP 82°C
Ethanol	BDH, Poole, UK	Clear colorless liquid	BP 78°C
Methanol	BDH, Poole UK	Clear colorless liquid	BP 64.7°C
Butanol	BDH, Poole, UK	Clear colorless liquid	BP 116-118°C
Deionised water	Inhouse	Clear colorless liquid	BP 100°C
Acetonitrile	VWR International Ltd, Lutterworth, UK	Clear colorless liquid	BP 81-82°C
Ethyl acetate	VWR International Ltd, Lutterworth, UK	Clear colorless liquid	BP 76.5-77.5°C
Acetic acid	VWR International Ltd, Lutterworth, UK	Clear colorless liquid	BP 117-118°C

2.2 Methods

The experimental techniques employed in this study are discussed in detail in this Section.

2.2.1 Solubility experiments

The solubility data for sulphathiazole and indomethacin were determined experimentally in each of the solvents used in the crystallization studies. The solubilities were determined at various temperatures ranging from 25° to 65 °C.

A 400 ml jacketed beaker, a magnetic stirrer and a waterbath (Thermo Haake, Dieselstr.4.D-76227 Karlsruhe, Germany) with temperature control were used for the solubility measurement experiments. 100 ml pure solvent was added to the jacketed beaker. The beaker was enclosed with a glass lid to prevent evaporation. The beaker was equipped with a water bath for the control of temperature and placed on a magnetic stirrer. The experimental set up is shown in Figure 2.1. Initially, the temperature of the water bath was set at 25 °C. Very small quantities of solid were added gradually into the solvent with constant stirring, until no more solid drug was observed to dissolve at 25 °C in the solvent. At this point the solvent is said to be saturated with dissolved material.
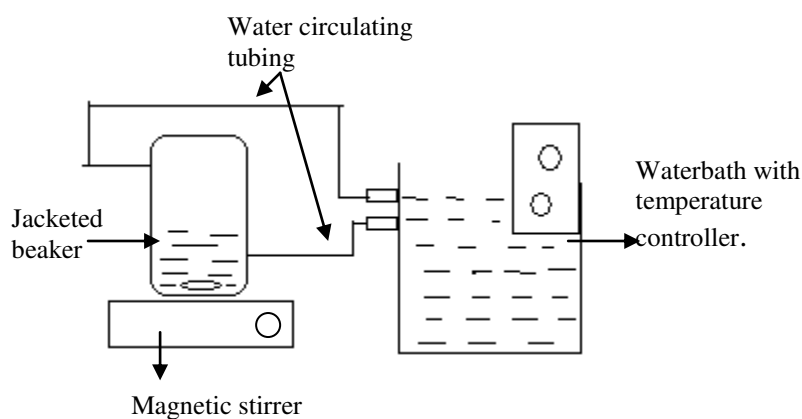
Figure 2.1   Generic set up used for solubility and crystallization experiments

Thereafter, the temperature of the waterbath was raised by 10 °C to 35 °C. The increase in temperature made the solution undersaturated (Section 1.2). Therefore, again, very small quantities of solid were added gradually into the solution with constant stirring, until the solution became saturated at 35 °C. The total weight of solid added to the solvent was noted as the solubility at 35 °C. Similarly, the solubility was measured at 45 °, 55 °, and 65 °C using the same method. The solubility for sulphathiazole and indomethacin is reported in Table 3.1 and Table 6.1.

2.2.2 Crystallization methods

Different crystallization techniques were used for the crystallization of sulphathiazole and indomethacin.

2.2.2.1 Crystallization by cooling

Crystallization experiments of sulphathiazole and indomethacin were performed by cooling supersaturated solutions. Batch experiments were conducted in thermostated, jacketed beakers with magnetic stirrer and water bath as shown in Figure 2.1. Known quantities of sulphathiazole or indomethacin (see Tables 2.2, 2.3, 2.4 and 2.5 for the quantity of drug dissolved in experiments) were dissolved in 100 ml of selected solvent at 60 °C with stirring (250 rpm) for 40-60 minutes to allow complete dissolution of solid material. Thereafter the solution was cooled to 26 °C at 1 °C/min for crystallization. Finally, the resultant crystals were filtered and dried in a vacuum oven at 30 °C overnight to remove solvent.

The quantity of model drug to be dissolved in 100 ml of solvent at 60 °C to make a supersaturated solution was determined from the solubility data. Any additive, where appropriate, was added as 2% or 10% of dissolved drug by weight (see quantities of additives in particular experiments in Table 2.6) to the hot solution prior to cooling. Any seeds, where appropriate (Table 2.3), were added (0.1g) to the solution once cooling started, prior to the nucleation of crystals. In the case of adding seeds to the solution, it was also ensured that seeds remained in the solution without any dissolution prior to nucleation. All the crystallization experiments performed by cooling with sulphathiazole and indomethacin are listed in Tables 2.2 to 2.6.

Table 2.2 Cooling crystallization experiments of sulphathiazole in various solvents

Experiment	Solvent used	Sulphathiazole dissolved (g)
1	1-Propanol	1.1
2	1-Butanol	0.9
3	2-propanol	1
4	Ethanol	1.15
5	Methanol	1.3

Table 2.3   Cooling crystallization experiments of sulphathiazole with seeding of stable polymorphs of sulphathiazole

Experiment	Solvent used	Sulphathiazole dissolved (g)	Seeds used	Quantity of seeds added (g)
1	1-Propanol	1.1	Form II	0.1
2	1- Propanol	1.1	Form III	0.1
3	1-propanol	1.1	Form IV	0.1

Table 2.4   Cooling crystallization experiments of sulphathiazole using various ratios of 1-propanol and methanol as solvents

Experiment	Ratio of 1-propanol:methanol used as Solvent	Sulphathiazole dissolved (g)
1	0:100	1.35
2	20:80	1.29
3	40:60	1.24
4	50:50	1.21
5	60:40	1.2
6	80:20	1.15
7	90:10	1.08
8	100:0	0.99

Table 2.5   Cooling crystallization experiments of indomethacin in various solvents

Experiment	Solvent used	Indomethacin dissolved (g)
1	Ethanol	1.40
2	Acetonitrile	1.45
3	Ethyl acetate	1.48
4	Aqueous Acetic acid	1.1
5	Butanol	1
6	Acetone	1.25

Table 2.6   Cooling crystallization experiments of indomethacin in ethanol in the presence of additives

Experiment	Indomethacin dissolved (g)	Additive used	Quantity of additive added (g)	% w/w of additive to Indomethacin
1	1.40	Myristic acid	0.028	2
2	1.40	Myristic acid	0.14	10
3	1.40	Adipic acid	0.028	2
4	1.40	Adipic acid	0.14	10
5	1.40	oleic acid	0.028	2
6	1.40	oleic acid	0.14	10
7	1.40	3-Indoleacetic acid	0.028	2
8	1.40	3-Indoleacetic acid	0.14	10

2.2.2.2   Crystallization by slow evaporation.

Saturated solutions were prepared by dissolving sulphathiazole (see Table 2.7 for the amount of drug dissolved in solvents) in 100 ml of solvent at 25 °C with stirring (250 rpm) for 40-60 minutes to allow complete dissolution of solid material.

The saturated solution was transferred to two glass petri dishes in equal amount (50ml in each petri dish) at ambient conditions. The petri dishes were covered with parafilm (Bemis, USA), which was pierced to make eight small holes to promote slow evaporation. Nucleation and crystal growth occurred with evaporation of solvent. In the first petri dish, sulphathiazole crystals crystallized immediately after nucleation (within 5 minutes of nucleation) and were isolated by filtration and dried in the vacuum oven prior to solid state characterization. The second petri dish was left undisturbed on the bench until the complete evaporation of solvent was observed. Finally, crystals were collected from this second petri dish and dried in the vacuum oven at 30°C prior to further use. Experiments performed using this technique are listed in Table 2.7.

Table 2.7   List of crystallization experiments of sulphathiazole by evaporation in various solvents

Experiment	Solvent used (100 ml)	Sulphathiazole dissolved (g)
1	1-Propanol	0.4
2	1-Butanol	0.25
3	2-propanol	0.3
4	Ethanol	0.45
5	Methanol	0.5

2.2.2.3   Crystallization by liquid precipitation (drown out method)

Crystallization by liquid precipitation requires two solvents, a solvent in which the solute compound shows good solubility and an anti-solvent in which the solute compound has low solubility (Uusi-Penttilä and Berglund, 1996).

A solution of 1.40g of indomethacin in 100 ml ethanol was prepared at 60°C as described in Section 2.2.2.1. The solution was kept at 60 °C with stirring for 20 minutes and during this period 400 ml of water as the anti-solvent was added drop-wise into the solution, which caused the precipitation of crystals in the solution. Slavin et al (2002) suggested the use of 1:4 solvent: anti-solvent ratio for liquid precipitation experiments. Thereafter, the solution was further cooled to 26 °C at 1 °C/min. Finally, the precipitated crystals were separated by filtration and dried overnight in a vacuum oven at 30 °C.

2.3   Analytical analysis of crystal samples

2.3.1   Optical microscopy

Morphology of crystals was observed using an Olympus BH2 Optical Microscope (London, UK) under a magnification of X 10. Pictures and video were taken using a digital video camera (JVC TK-C1381, colour video camera, Japan) fitted to the microscope and linked to a computer. The studio capture software (version 1.3.4 for FP80 controller) was used to display the captured image on a computer screen.

Crystal samples were placed on microscopic slides and covered with cover slips and then observed. Also crystals were observed from solution (crystal slurry) by taking a drop of liquid on a microscopic slide, covered with a cover slip, to observe the morphology whilst the crystals were growing.

2.3.2 Scanning Electron Microscopy (SEM)

Scanning electron microscopy is widely used to study the morphological and surface features of chemical and biological samples (Goldstein et al, 1981). In a scanning electron microscope, an electron beam is induced from an electron gun, which contains a tungsten filament as an anode (Figure 2.2). The electrons then pass through the condenser lens (magnetic lens) to focus into a very fine spot of 0.4 nm to 5 nm diameter. The beam then travels through the scanning coils in the electron column to the specimen surface. The incident beam emits radiation from the specimen, which is detected and amplified using a detector and a video amplifier. SEM is able to measure particle sizes less than 5 µm and particles can be magnified from 25X up to 250,000X magnitude. Unlike the optical microscope, the magnifying power of the SEM is controlled by the current supplied to the scanning coils, and not by the objective lens.
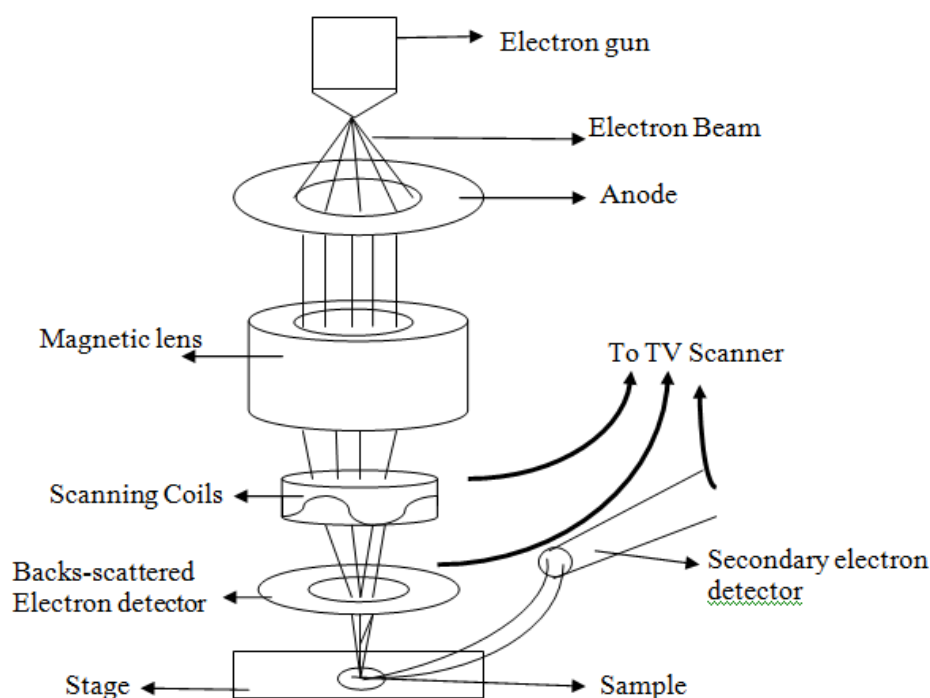
Figure 2.2   Schematic diagram of Scanning Electron Microscope (re-drawn from Perdue university's module http://www.purdue.edu/rem/rs/sem.htm)

2.3.2.1   Methodology

A Scanning Electron Microscope (Jeol Electron Microscope, JSM 840 Rontec Scanvision, Image Capture) was used to study the morphology of crystals. A small sample of crystals was mounted onto aluminium stubs using 13 mm aluminium pin stubs with double-sided carbon conductive adhesive tab and a sputter coater was used to apply a thin layer of gold at 10 Torr vacuum before examination. Samples were scanned with an electron beam of acceleration potential of 1.2 KV and the images were collected using an image capture software (Spirit, UK).

2.3.3   X-Ray Diffraction method

Powder x-ray diffraction (PXRD) is a powerful tool for identifying different crystalline phases by their unique diffraction patterns. Typical applications of powder x-ray diffraction methodology include the evaluation of polymorphism and solvates, evaluation of degree of crystallinity, and the study of phase/polymorph transitions (Pecharsky and Zavalij, 2003). Even small changes in the x-ray powder patterns of a crystalline compound due to the appearance of new peaks, additional shoulders or shifts in the peak position can imply the presence or occurrence of new polymorphs in that compound.

As explained in Section 1.1, crystalline solids consist of atoms and atomic groupings that are regularly arranged in space in three dimensions. In a crystal, all planes with identical sets of Miller indices (Section 1.1) are parallel to one another and they are equally spaced (Pecharsky & Zavalij, 2003). Thus each plane in a set (hkl) (Figure 2.3) may be considered as a separate scattering object. The set is periodical in the direction perpendicular to the planes and the repeat distance in this direction is equal to the interplaner distance d_{hkl} (Figure 2.3).

In x-ray diffraction, x-rays are generated by a cathode ray tube, filtered to produce monochromatic radiation, collimated to concentrate, and directed toward the sample. When x-rays interact with the random orientation of a crystal lattice in a powder sample, the scattering centres arranged in a plane act like a mirror to incident x-rays, so that diffraction patterns at specific angles (θ) occur when conditions satisfy

Bragg's law (Bragg et al, 1913) (Equation 2.1) for a series of crystallographic planes. Bragg's law relates the wavelength of electromagnetic radiation (λ) to the angle of diffraction (2θ) and the lattice spacing (d) in a crystalline sample. The specific angle θ, is established from Braggs law, as explained in Figure 2.3.
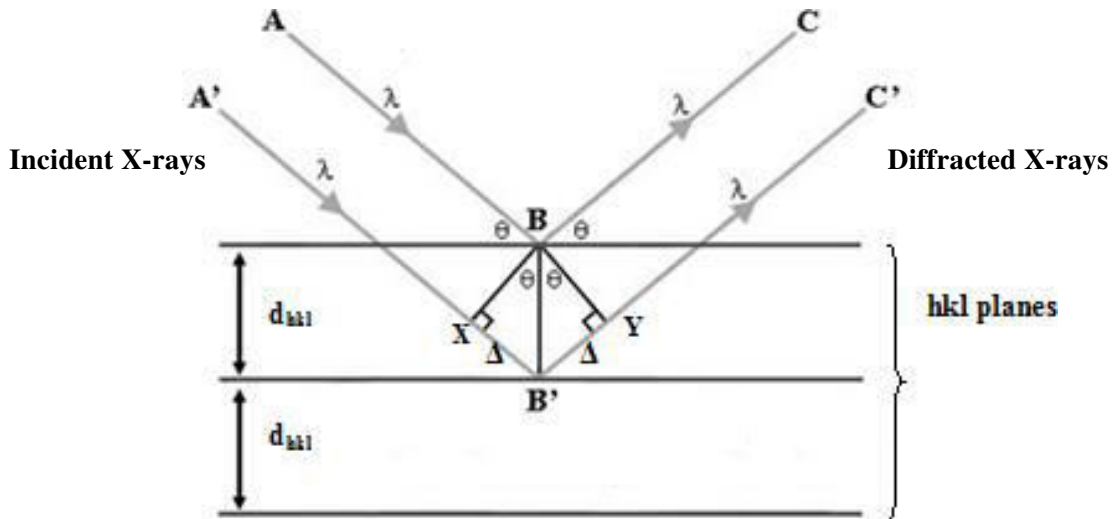
Figure 2.3 Diffraction of x-rays explained by Bragg's law

Consider an incident front of waves with parallel propagation vectors, which forms an angle θ with the planes (hkl). In a mirror reflection, the reflected/diffracted wavefront will also consist of parallel waves, which form the same angle θ with all planes. The path differences introduced between a pair of waves both before and after they are reflected by the neighbouring planes, Δ (XB' or YB'), are determined by the interplaner distance as $\Delta = d_{hkl}Sin\theta$. The total path difference is 2Δ, and constructive interference is observed when $2\Delta = n\lambda$, where n is an integer and λ is the wavelength of the incident wavefront. This simple geometrical analysis results in Bragg's law (Equation 2.1).

$$n\lambda = 2d_{hkl}Sin\theta_{hkl}. \qquad \text{(Equation 2.1)}$$

Diffraction occurs only when Bragg's law is satisfied. By scanning the sample through a range of 2θ angles, all possible diffraction directions of the lattice should be attained due to the random orientation of the powdered material. The diffracted x-rays are then detected and processed by the detector and recorded electronically.

2.3.3.1 Methodology for Powder X-ray Diffraction

A Miniflex PXRD Instrument (Rigaku Corporation, Japan) was used for generating PXRD patterns of the samples. Dried crystals were ground in a mortar and pestle. The cavity of the metal sample holder was filled with the ground powder of the sample and pressed with a glass slide to make the surface of the powder flat and smooth. The samples were scanned at a scanning rate of 10 ° 2θ/min over a range of 5 – 50 ° 2θ values. The sample was irradiated with x-rays of wavelength of 1.54059Å.

The resulting patterns were compared against the reference patterns of the samples for polymorphic identity. The reference patterns were obtained from literature and the Cambridge crystallographic database (Mercury 2.1, CCDC, Cambridge, UK).

2.3.3.2 Methodology for single crystal X-ray Diffraction

In some cases, PXRD patterns for polymorphs of the same substance are very similar and very hard to distinguish from their fingerprint PXRD pattern. In that case, single crystal -xray diffraction can be used. Every solid crystalline compound has its own particular unit cell, which should be unique in its dimensions (Section 1.1). Different polymorphs of the same compound also differ from each other in their unit cell dimensions (a, b, c and α, β, γ - Section 1.1). An understanding of a unit cell simplifies the understanding of a crystal as a whole and this is the basis of single crystal x-ray studies.

Single crystal x-ray diffractometers consist of three basic elements, an x-ray tube, a sample holder, and an x-ray detector. x-rays are generated in a cathode ray tube by heating a filament to produce electrons. The incident x-ray beam strikes a mounted single crystal, which diffracts the x-ray beam and generates the diffraction patterns through the planes of a crystal to provide detailed information of the crystal structure including unit cell dimensions.

In this study, unit cells of a single crystal samples were measured for polymorphic identification using a Stoe IPDS area detector (Stoe, Germany) and calculated by least

squares refinement using the setting angles of 25 reflections. Crystals in excess of 200 micron size were selected and mounted in the diffractrometer for single crystal x-ray diffraction analysis.

2.3.4 Infra Red (IR) Spectroscopy

Spectroscopy is the study of the interaction between electromagnetic radiation and matter. All molecules are capable of vibrating when they absorb infrared radiation energy (Stuart, 2004). According to the Beer-Lambert law the fraction of light absorbed by a sample is proportional to the number of molecules in the light path. Mathematically it can be expressed by Equation 2.2.

$$\log_{10}(I_0/I) = A = \varepsilon cl \qquad \text{(Equation 2.2)}$$

Where, I_0 and I are the incident and transmitted intensity (i.e. the light entering the sample and the light coming out from the sample, respectively)

l, is the thickness of the absorbing medium,

$\log_{10}(I_0/I)$ is defined as the absorbance A,

ε, is the molar absorption coefficient,

and c, is molar concentration of the sample.

In Equation 2.2 transmittance, T, is defined as I/I_0 (the fraction of radiation transmitted). Hence, Equation 2.2 could be rewritten to Equation 2.3.

$$A = \log_{10} 1/T \qquad \text{(Equation 2.3)}$$

According to quantum mechanics, no vibration can be excited unless the molecule is provided with a certain minimum energy absorbed by electromagnetic radiation. The frequency at which these absorptions occur gives valuable structural information of molecules. Even certain fragments within a molecule adsorb at different wavelengths. An IR spectrum is generally displayed as a plot of the energy of the infrared radiation (expressed in wave numbers, cm^{-1}) versus the percentage of radiation intensity transmitted or absorbed through the sample. Therefore within a particular energy range, the spectrum of a molecule will appear as a series of broad absorption bands of

variable intensity, each of which corresponds to a bend or stretch within a bond. Absorption bands in the range of 4000-1500 cm^{-1} are typically due to functional groups, such as –OH, C=O, N-H, CH$_3$, etc. The regions between 1500-400 cm^{-1} are generally due to intra-molecular phenomena, and are highly specific for each compound (Beckett & Stenlake, 2001). So, for any molecule, there will be a unique spectrum.

As explained in Section 1.9, different polymorphs have different structural configurations and due to that the appearance of shoulders, shifts or new adsorption bands would be observed in their IR spectrum. The resulting spectrum of each sample was compared against the reference spectrum (Anderson et al, 2001; Burger et al, 1983; Anwar et al, 1989) of the polymorph of the model compound for polymorphic identity.

2.3.4.1   Methodology for Infra Red spectroscopy

In this study, a Perkin Elmer FT-IR (Spectrum BX, USA) was used for the infra-red analysis of samples. A small amount (2-5 mg) of sample was placed on the 1.8 mm diamond window and compressed with a pressure clamp. Samples were irradiated with infra-red radiation and absorption measured in the range of 600-4000 cm^{-1}.

2.3.5   Differential Scanning Calorimetry

Differential Scanning Calorimetry (DSC) monitors heat flow differences associated with phase transitions and chemical reactions as a function of temperature. In DSC, the equipment involves two parallel temperature measurement systems, a sample and a reference. The reference is an inert material such as alumina, or just an empty aluminum pan, and the sample pan usually contains 2 to 10 mg of sample. Each pan is placed over separate heaters (Figure 2.4). The temperature of pans, the sample and the reference, are controlled. The differences in heat flow needed to maintain the sample and a reference at the same temperature ($\Delta T = 0$) is recorded as a function of temperature. This information is sent to an output device, a computer, to plot the

difference in heat flow as a function of temperature. Since the DSC is at constant pressure, heat flow is equivalent to the enthalpy changes (Equation 2.4).

$$(dq/dt)p = dH/dt \qquad \text{(Equation 2.4)}$$

Where, dq/dt is the differences in heat flow per unit time, p is the pressure, and dH/dt is the difference in enthalpy per unit time.

Therefore, the heat flow difference between the sample and reference pan is,

$$\Delta\, dH/dt = (dH/dt) \text{ of sample} - (dH/dt) \text{ of reference} \qquad \text{(Equation 2.5)}$$

This heat flow difference can be positive or negative, which can depend on the changes that occur in the sample material with heating, such as endothermic (melting and phase transition) or exothermic (crystallization) changes. In DSC graphs of temperature increases (x-axis) verses the difference in heat flow between the sample and reference pan (y-axis) are produced. If a sample shows any phase changes with heating (melting, sublimation of vapour, crystallization, glass transition, polymorphic transition) then the heat flow curves shows those changes as peaks in the graph relevant to that temperature. Hence, DSC is commonly used to measure melting points, polymorphic stability and polymorphic transformation, glass transition, presence of hydrate/solvates, purity, and crystallinity of the samples (Ferrero et al, 1999; Leitão et al, 2002).
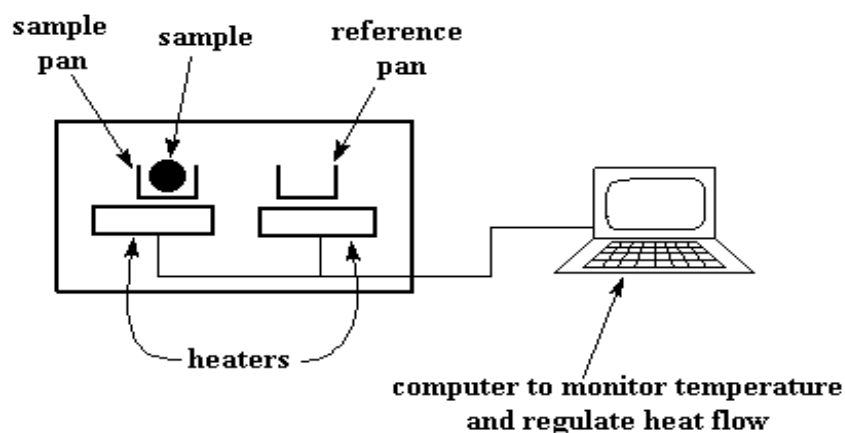
Figure 2.4   Schematic diagram of Differential Scanning Calorimeter

2.3.5.1   Methodology for DSC

In this study, a DSC (DSC7, Perkin Elmer, USA) was used to determine the polymorphic identity of the sample from the melting points and the phase transformation peaks for each polymorph. Perkin Elmer pans and lids were used for sample preparation. A small quantity of each sample (2 to 8 mg) was weighed accurately into the pan and the lid was crimped with the press. The samples were scanned at 10 °C/min from 40° to 250 °C. Onsets, offsets of the melting peaks and enthalpies of fusion were calculated using Perkin Elmer software (Pyris version 7).

2.3.6   Hot Stage Microscopy

Hot-stage microscopy (HSM) is used for the visual observation of a sample whilst it is heated. The microscope is fitted with the stage (an aluminium block), on which a sample is placed and can be heated from room temperature to the specified temperature at a controlled rate. HSM allows visual characterization of phase transitions occurring in a sample with increase in temperature such as, melting, glass transition, polymorphic transformation, crystallization. These observations aid interpretation of data obtained by other thermo-analytical methods, such as DSC.

2.3.6.1   Methodology for Hot Stage Microscopy

A Mettler FP82 Hot Stage and a Mettler FP80 central processor were used with an Optical Microscope (Olympus, BH2 microscope) for HSM analysis. A small amount of sample (1-5 mg) was spread on a microscopic slide and covered with a cover slip. The samples were heated from room temperature to 250 °C at 10 °C/minute. Observations were recorded using Studio Capture (version 1.3.4 for FP80 controller) and a camera (JVC TK-C1381, Japan) connected to the microscope.

2.3.7   Liquid ^{1}H NMR studies

Liquid ^{1}H NMR allows identification of hydrogen atoms and their position in compounds. This technique is useful in analyzing hydrogen bonds and the role of hydrogen in the structure of any compound. The technique can help to identify the

different types of hydrogen present in a molecule and the electronic environment of the different types of hydrogen (Silverstein et al, 1991).

Hydrogen atoms, within a sample, absorb energy of different wavelengths depending on their bonding environment. For example, the hydrogen of the hydroxyl group in propanol is different from the hydrogens of its carbon skeleton. ^{1}H NMR can easily distinguish between these two sorts of hydrogen. It is known that the use of different solvents can led to the formation of different pre-nucleation clusters of solute (sulphathiazole), which led to different polymorphs (Blagden et al, 1998). The electronic environment surrounding the hydrogen atoms of the solute also changes with the formation of different pre-nucleation clusters in different solvents, which can result in variation in chemical shifts in the ^{1}H NMR spectrum. Therefore in the current study ^{1}H NMR was used to investigate the role of different alcohol solvents in the formation of pre-nucleation clusters of sulphathiazole.
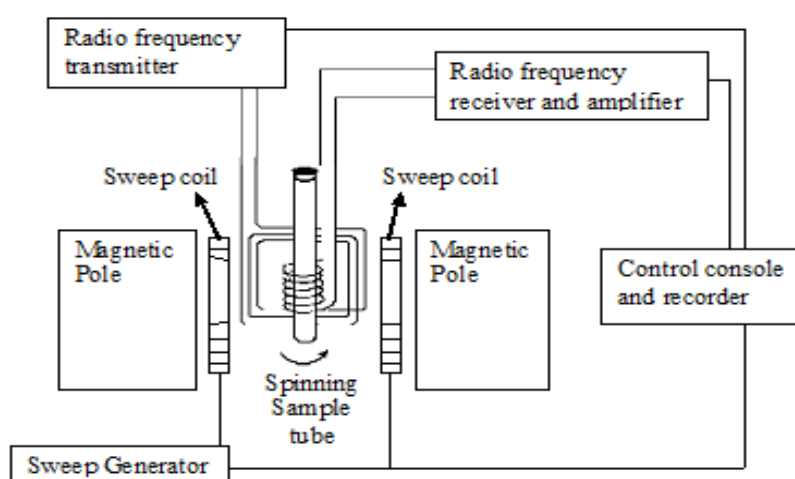
Figure 2.5   Schematic diagram of nuclear magnetic resonance spectroscopy (re-drawn from Michigan State University module for ^{1}H NMR www2.chemistry.msu.edu/faculty/reusch/VirtTxtJml/Spectrpy/nmr/nmr1.htm)

The nuclei of hydrogen, as an elemental isotope, have a characteristic spin, I = 1/2. The spinning charge of nuclei generates the magnetic field and that results in a spinning magnet (spinning nuclei) with a magnetic moment, μ. This magnetic moment is proportional to the spin (I) of the nuclei (Clayden et al, 2001). In the presence of an external magnetic field, nuclei of hydrogen can show two states of spin, +1/2 (lower energy state) and -1/2 (higher energy state). The magnetic moment

of the lower energy spin state, +1/2, is aligned with the external field, whereas the higher energy spin state, -1/2, is opposed to the external field. In ^{1}H NMR, when the sample is irradiated with a short pulse of radio frequency energy, r_f, the equilibrium balance between the two energy levels is disturbed and causes the excitation of a low energy spin state, +1/2, ^{1}H nuclei to the higher energy spin state, -1/2 (Clayden et al, 2001). When ^{1}H nuclei fall back down to the lower energy level, they emit the absorbed r_f energy, which will be detected using a sophisticated radio receiver and computer as shown in Figure 2.5.

2.3.7.1 Methodology of ^{1}H NMR

The 1H NMR study was performed on a Bruker Avance 300 MHz Spectrometer (Germany) operating via XWIN-NMR software (version 3.5) and locked using the deuterium signal from deuterated methanol, ethanol and 1-butanol solvents.

5-8 mg of samples powder were dissolved in 1 ml deuterated methanol, ethanol or 1-butanol at room temperature. 0.2 ml of the reference solvent (Tetramethylsilane) was also added to the sample solution. 400-600 microlitres of this solution were placed in a thin-walled NMR glass tube. Thereafter, the NMR glass tube was oriented between the poles of a powerful magnet and irradiated with the appropriate energy of radio waves. The results are displayed in the form of intensity against frequency, r_f.

Each nucleus/atom in a molecule is shielded from the applied external magnetic field to a greater or lesser extent by the other atoms in the vicinity and their electrons. The less the shielding experienced, the higher the chemical shift; whereas the more heavily shielded hydrogen atoms display lower chemical shift. Even, similar hydrogen atoms of different polymorphs would absorb energy of different wavelengths and represent variation in chemical shifts due to different bonding and electron environment surrounding these hydrogen atoms. Based on this principle, in a NMR spectrum, peaks are assigned to each hydrogen atom in a molecule. The area under each NMR peak/resonance is proportional to the number of hydrogens which that resonance represents. By integrating the different NMR resonances, information regarding the relative numbers of chemically distinct hydrogens can be evaluated.

2.4. Molecular modelling

2.4.1 Molecular modelling using Cerius2

Cerius2 (Accelrys, Cambridge, UK) is a comprehensive molecular modelling and simulation package used for the visualization and thermodynamic calculation of crystal structures. The package runs on a Silicon Graphics workstation (Silicon Graphics Inc., USA) and provides a three dimensional graphic of the molecules which make up a crystal.

The Cerius2 program offers a broad range of application modules for various molecular environments, such as, visualizer, crystal builder, force field editor, mopac, etc. The energy of α- and β-dimers of sulphathiazole and proposed clusters (pre nucleation clusters of sulphathiazole molecules with solvent molecule) of α- and β-type dimers in the presence of each of the solvents was investigated using Cerius2. Detail of this molecular modelling study is presented in Chapter 4.

2.4.2 Molecular modelling via Grid based systematic search

The systematic search approach uses a grid based search system of translations and rotations to assess all the possible intermolecular packing arrangements or interactions in direct space (Hammond et al, 2003). The systematic search approach has been successfully applied to predict the crystal structures of various materials from knowledge of unit cell parameters and space group alone, and to solve the crystal structures of various materials from the powder diffraction data (Kutzke et al, 2000; Smith et al 2001; Hammond et al, 2003). In the current study, the systematic search approach has been applied to calculate the interaction energies between sulphathiazole dimers and solvent molecules. Further details of this method are described in Chapter 4.

Chapter 3   Crystallizations of sulphathiazole and characterization of experimental samples

3   Introduction

It has been established that the polymorphic outcome of the crystallization of sulphathiazole is susceptible to the solvent environment and that the metastable form, Form I, can be selectively stabilized by 1-propanol (Anwar et al, 1998, Blagden et al, 2001). In this study, the mechanism of the selection of the metastable and stable polymorphs by solvent change was probed by investigating the influence of a range of alcohols on the polymorphic outcome of sulphathiazole crystallization. The role of the alcohol functional group in the polymorph selection process was thus investigated and evaluated.

Methanol, ethanol, 1-propanol, 2-propanol, and n-butanol were selected as solvents for the crystallization of sulphathiazole by cooling and slow evaporation. Crystal samples were characterised using optical microscopy, PXRD, DSC, IR, and single crystal x-ray diffraction to identify their polymorphic form. Details of experimental methods are described in Sections 2.2 to 2.4 (Chapter 2).

3.1 Solubility of sulphathiazole in alcohols

The solubility of sulphathiazole was determined over the temperature range of 25 – 70 $^\circ$C. Amounts of sulphathiazole were added gradually into the solvent to determine its solubility, as described in Chapter 2. The solubilities in the various alcohols are shown in Table 3.1.

Table 3.1 Solubility data of sulphathiazole in various alcohol solvents

Temp (^{0}C)	Methanol	Ethanol	1-Propanol	2-Propanol	1-Butanol
	Sulphathiazole concentration (g/100 ml)				
28	0.42	0.37	0.3	0.21	0.17
35	0.5	0.45	0.38	0.30	0.24
55	0.88	0.81	0.73	0.62	0.57
70	1.23	1.12	1.05	0.92	0.88
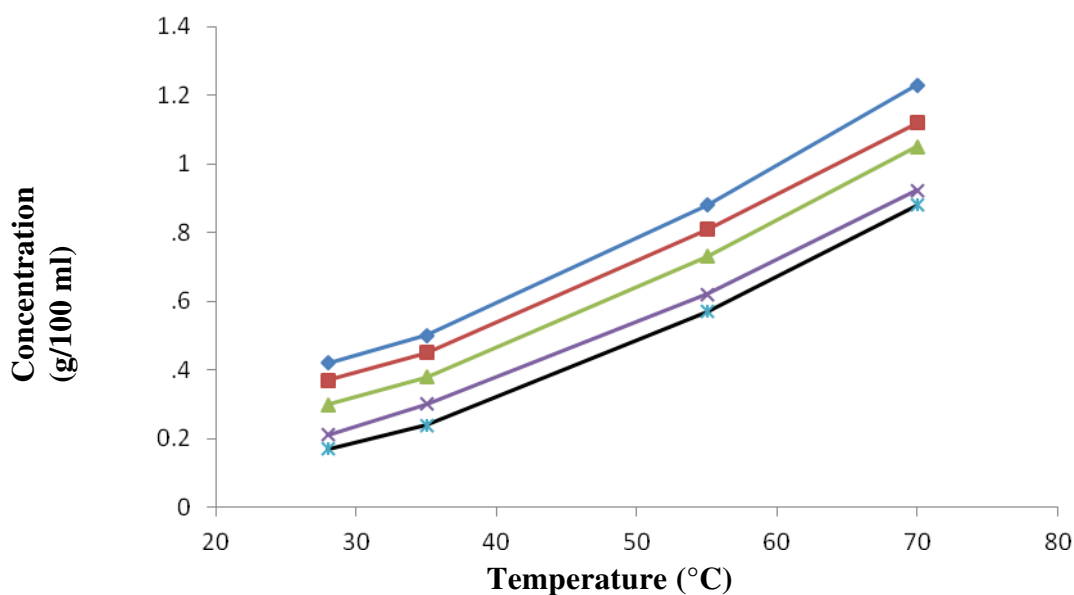
Figure 3.1 Solubility of sulphathiazole in the chosen solvents at different temperatures.
Key – Solubility in methanol, Solubility in ethanol, Solubility in 1-propanol, Solubility in 2-propanol, and solubility in 1-butanol

The solubility of sulphathiazole showed a near linear relationship in all solvents with increase in temperature (Fig 3.1). These data were also used to determine the amount of sulphathiazole to be added to obtain supersaturation in the crystallization experiments. The solubility of sulphathiazole was higher in the lower carbon chain alcohols (methanol and ethanol) but it decreased in long chain alcohols (1-propanol, 2-propanol, and 1-butanol).

3.2   Characterization of sulphathiazole crystals obtained from cooling crystallization

The experimental method of crystallization of sulphathiazole by cooling with five different alcohols is described in Section 2.3.1.1. A list of these experiments is also indicated in Table 2.2

Samples obtained from cooling crystallization, were analyzed using optical microscopy, powder x-ray diffraction, infrared spectroscopy, differential scanning calorimetry, and hot stage microscopy (methods are described in Section 2.3) to determine polymorphic identity.

3.2.1 Morphological analysis of crystallized samples

Samples were taken periodically from each cooling experiments and analysed under the optical microscope to observe the growth and changes in morphologies. Time resolved morphologies of crystals are shown in Figures 3.2 to 3.6.
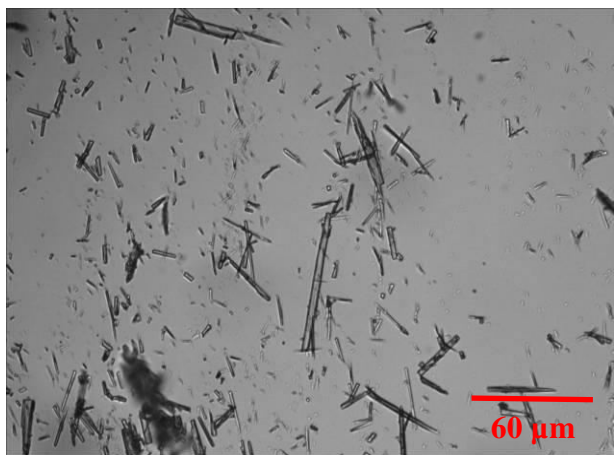
Figure 3.2 (a) sample from 1-propanol within 5 minutes of nucleation
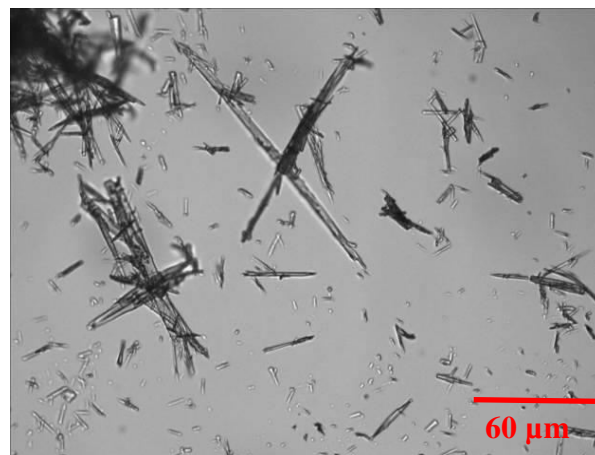
Figure 3.2 (b) sample from 1-propanol 1 hour after nucleation observed
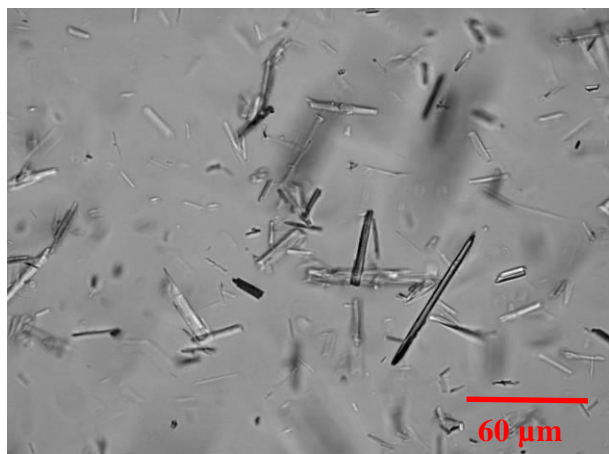
Figure 3.3 (a) Sample from n-butanol within 5 minutes of nucleation
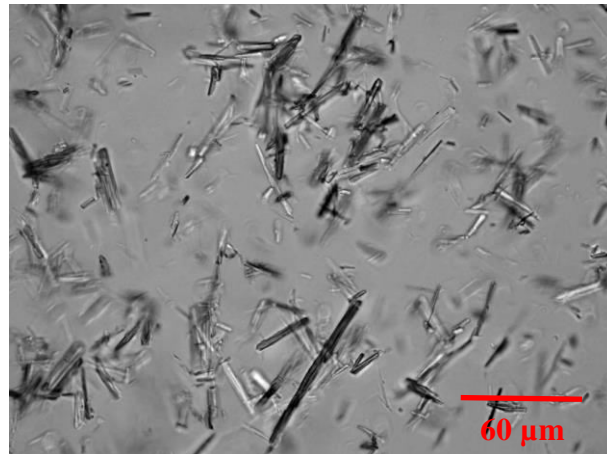
Figure 3.3 (b) sample from n-butanol 1 hour after nucleation observed
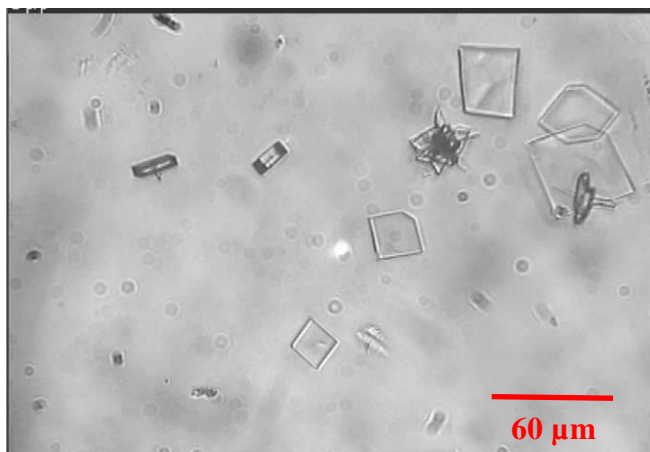
**Figure 3.4 (a) Sample from 2-propanol
5 min after nucleation observed**
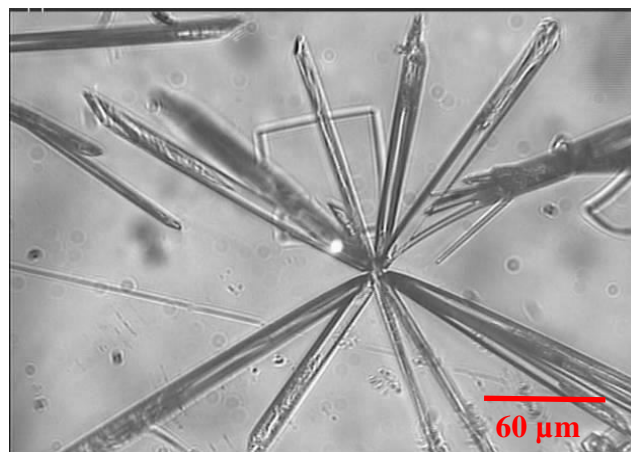
**Figure 3.4 (b) Second sample from
2-propanol 5 min after nucleation**
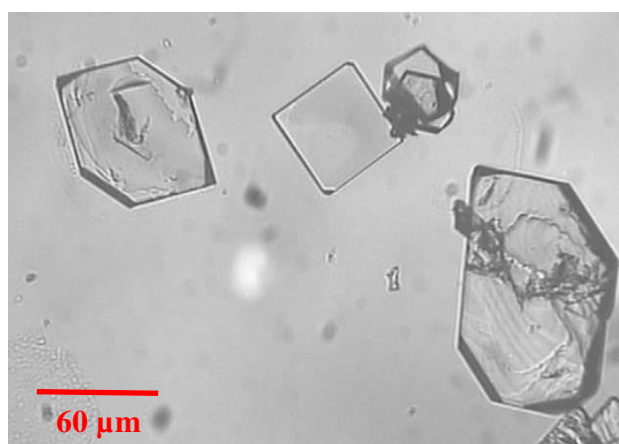
**Figure 3.4 (c) Sample from 2-propanol 4 h
after nucleation observed**
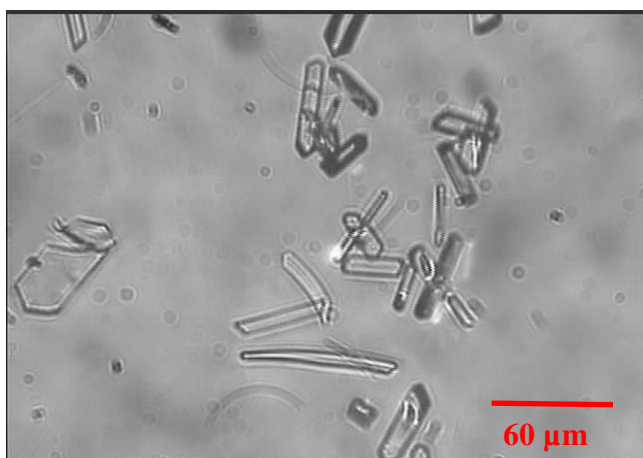
**Figure 3.5 (a) Sample from ethanol
5 minutes after nucleation observed**
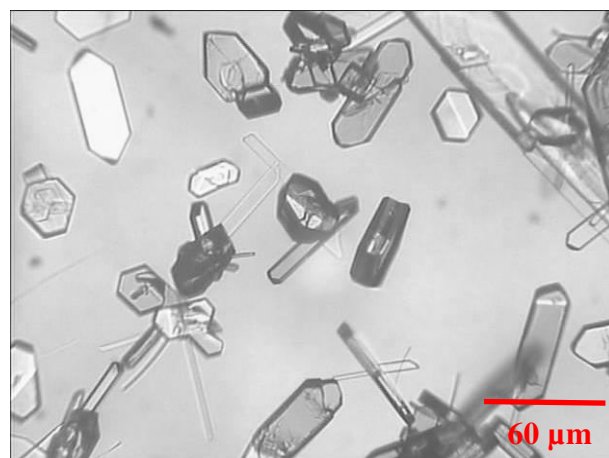
**Figure 3.5 (b) Sample from ethanol
30 minutes after nucleation observed**

96
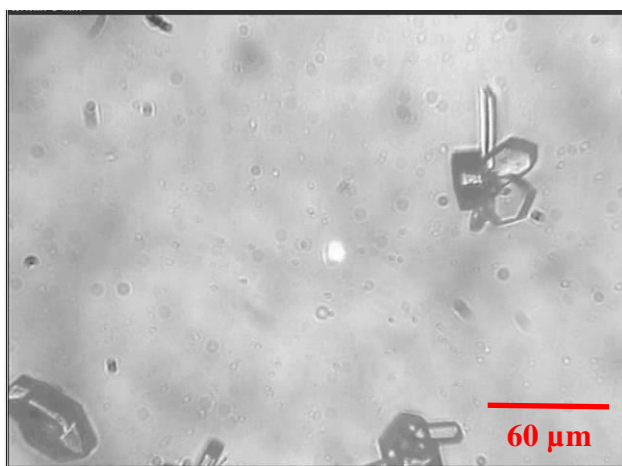
Figure 3.6 (a) Sample from methanol 5 min after nucleation observed
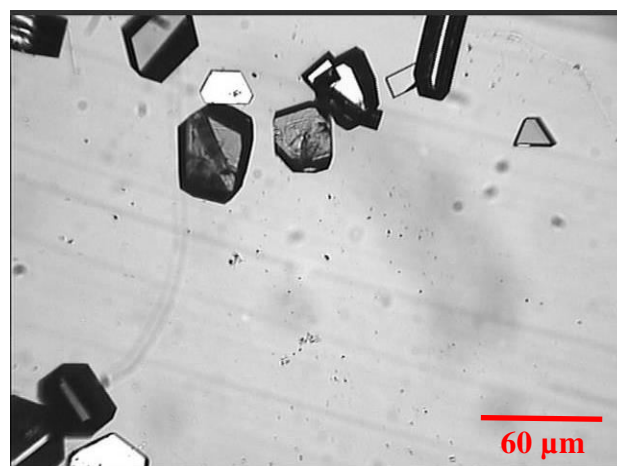
Figure 3.6 (b) Sample from methanol 30 min after nucleation observed

All samples initially crystallised as elongated, or needle particles. This is established in the literature as the morphology of Form I, (Anwar et al, 1989, Blagden et al, 1998) and predicted by Ostwald's Rule to crystallise first (Section 1.11.3).

When methanol or ethanol was the solvent, needles nucleated initially followed by small hexagonal plates which appeared within 5 minutes of nucleation (figure 3.5 a and 3.6 a). The needle-shaped particles dissolved very quickly, within a few minutes of nucleation and hexagons grew in size and thickness resulting in hexagonal prisms in the case of methanol (figure 3.6b), and thin plates in the case of ethanol (figure 3.5b). This change in morphology may indicate polymorphic changes from the needle-like metastable Form I to the more stable Forms II, III, or IV as growth progressed. Once mature crystals were obtained, there was no further change in the morphology.

When 2-propanol was the solvent, sulphathiazole initially nucleated as needles and very small square plates (Figure 3.4a). Initially needles were present predominantly. Figure 3.4b shows the prompt nucleation of needles when a droplet as a sample was taken on microscopic slide from the 2-propanol solution. However, with time, square plates grew slowly in size and numbers, and the needles disappeared from the slurry/solution when left for 4 hours as shown in Figure 3.4c. Square plates also converted into hexagonal plates by developing faces on the angles of the square plates (Figure 3.4c). The rate of growth was slower than for those crystals grown from the straight chain alcohols, with growth continuing for more than 4 hours after nucleation. There was no further change to the morphology during growth. As with

samples grown from methanol and ethanol, changes in morphology during the crystal growth process indicate the polymorphic transformation from metastable to more stable forms.

For 1-propanol and 1-butanol, nucleation of needle-shaped crystals was very prompt, within a minute of reaching temperature, with maximum growth having occurred within 17-20 min of nucleation. No further growth was observed and the particles remained without transformation for the length of the experiment (1 hour) as shown in Figures 3.2a to 3.3b. No platey or prismatic crystals were observed.

3.2.2   Powder X-ray analysis of sulphathiazole crystals samples

Powder X-ray diffraction studies were carried out for polymorphic identification of samples obtained from cooling crystallization. The results of the PXRD patterns were compared with previous PXRD studies for the identification of sulphathiazole polymorphs.

Only a few reports have previously mentioned clear PXRD patterns of sulphathizole polymorphs. Anwar et al (1989) have reported the PXRD patterns of sulphathiazole Form I to IV. Kordikowski (2001) obtained polymorphs I, III and IV and performed PXRD analysis for each polymorph. Blagden et al (2001) and Appearly et al (1999) have reported identification peaks for Form I (Table 3.2). In addition, PXRD spectra were also obtained from the Cambridge Crystallographic Database and used as reference for polymorphic identification (Figure 3.8). These studies reported very similar spectra for Forms II, III and IV, which make it very difficult to differentiate between these polymorphs from their PXRD results. The similarities in their spectral behaviour were reported due to the structural and molecular similarities of these three polymorphs as all of them contain β dimers as their basic unit (Section 1.14.1.2). Many previous studies, such as Anwar et al (1989) and Appearly et al (1999) confirmed the identity of each polymorphic sample by combining PXRD results with various solid state analytical techniques such as Solid state NMR, single crystal XRD, and Raman spectra.

Table 3.2   Characteristic peaks for each of the reported polymorphs

Study	Identification peaks reported at 2θ values in the diffraction patterns of each polymorph				
	Form I	Form II	Form III	Form IV	Form V
Anwar et al (1989)	11, 16, 18, 19, 21, 22.2, 24.5		15.1, 15.4, 16.2, 18.5, 19.2, 20, 21.7, 21.8, 25.3, 26.9	15.1, 15.5, 16.3, 18.5, 19.3, 20, 21.6, 25.3, 26.9	16, 16.2, 18, 18.7, 20.1, 21.4, 21.6, 23.5, 25.1, 26, 26.8
Appearly et al (1999)	21.9		21.9	21.7	22.1
Blagden et al (2001)	11 {010}				
Kordikowski et al (2001)	11, 16, 17.8, 18.9, 21, 22, 22.3, 24.6		15.32, 15.56, 18.4, 18.5, 19.3, 20.1, 20.7, 21.6, 22, 25.4, 26.8, 26.9	15.1, 15.5, 18.4, 19.25, 19.9, 20.3, 20.5, 21.6, 22, 21.8, 24.9, 25, 25.4, 26.7, 26.8, 26.9	

In the current study, the resultant crystals, obtained from crystallization from each of the solvents by cooling as described in Section 2.3.2.1, were analysed by powder x-ray diffraction for polymorphic identification. The powder diffraction data of each sample were collected using a Miniflex (Rigaku Corporation) laboratory powder x-ray diffractometer at ambient conditions as described in Section 2.4.3. The PXRD spectra obtained for crystallization of sulphathiazole by cooling are shown in Figure 3.7.
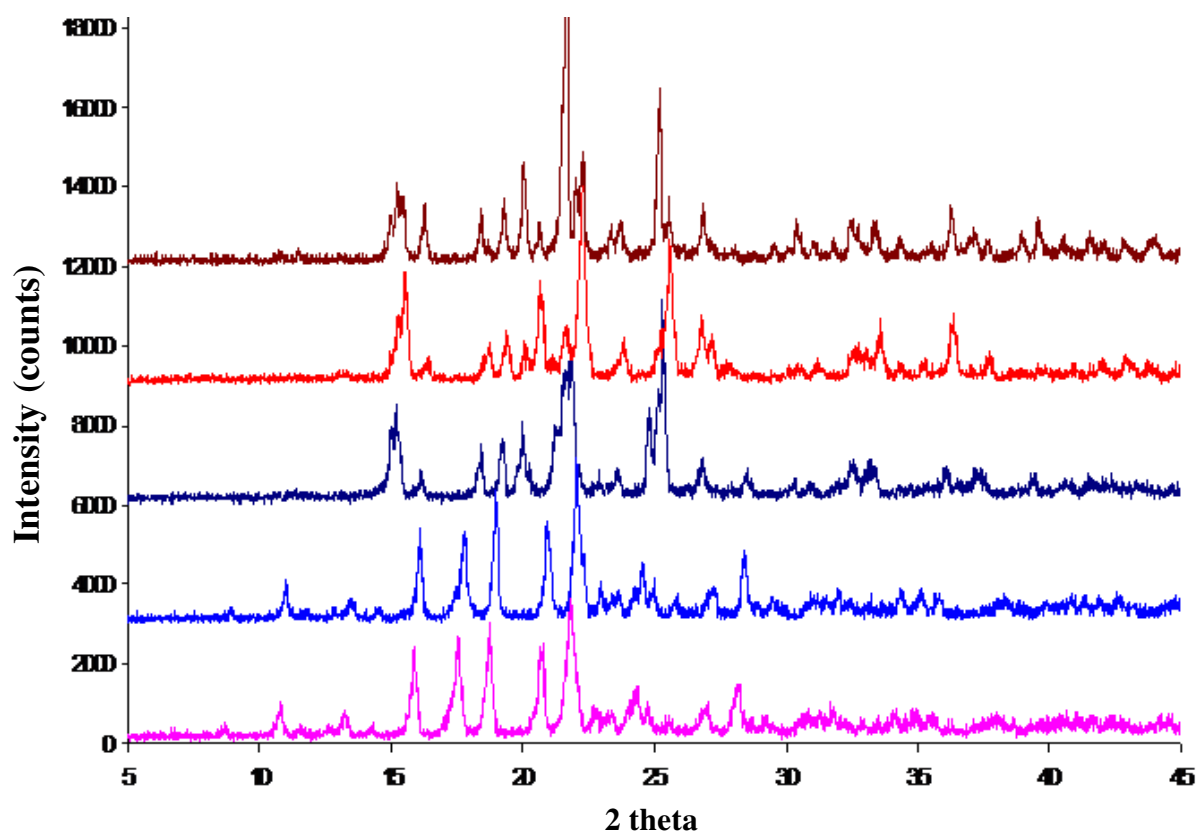
Figure 3.7 Powder –X-Ray Patterns of sulphathiazole samples obtained from alcohols. Samples from 1-propanol, n-butanol, methanol, 2-propanol and ethanol,
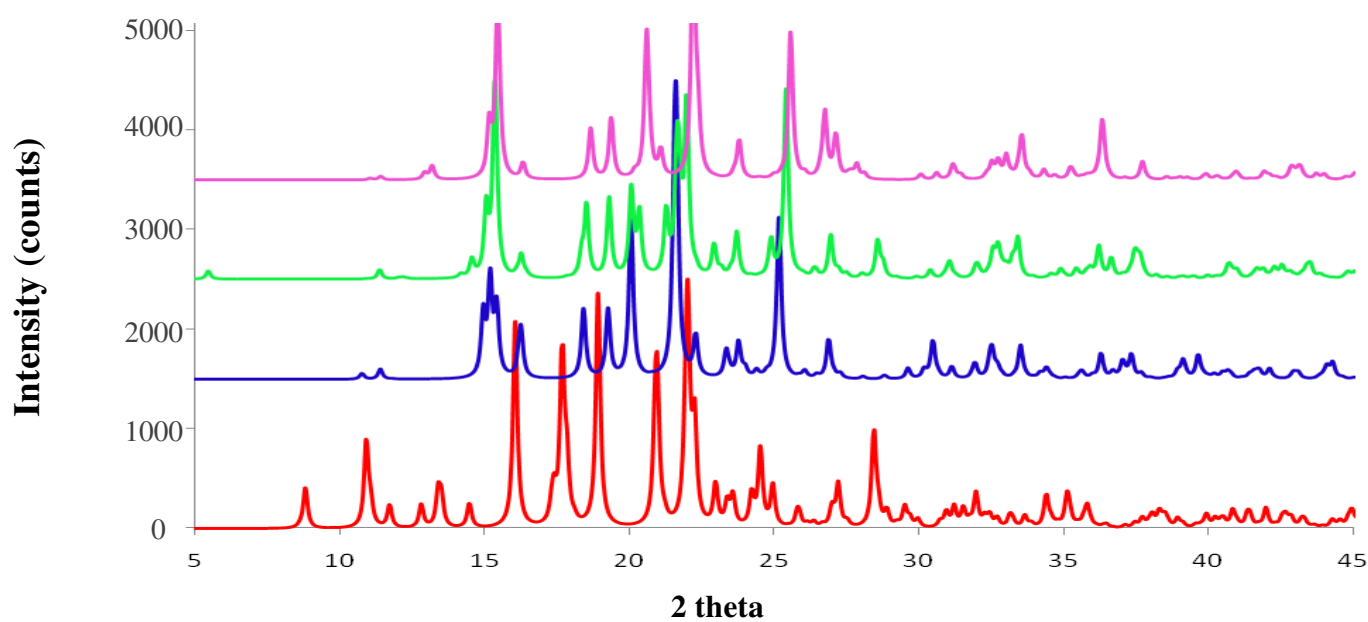
Figure 3.8 Reference powder X-ray pattern of Sulphathiazole polymorphs obtained from CCDC. Form I, Form II, Form III, and Form IV

A detailed comparison was carried out to investigate the polymorphic identity of the sulphathiazole samples obtained from the different solvents. It was easy to identify sulphathiazole samples crystallized from 1-propanol and butanol as Form I. These samples were identified by the peak with a 2θ value of 11, which is a characteristic peak for Form I (Blagden et al, 1998 & Appearly et al, 2001). In addition, the intense peak at 21.9 in both samples also stands as one of the identification peaks for Form I (Appearly et al, 1999). Furthermore, PXRD patterns of these two samples also showed an exact match with the PXRD pattern of Form I obtained from CCDC (Figure 3.8). This evaluation of PXRD patterns leads to the conclusion that the sample crystallized from 1-propanol and n-butanol were each sulphathiazole Form I.

In contrast, samples crystallized from methanol, ethanol and 2-propanol did not show a peak at 2θ value of 11, so the possibility of the presence of polymorph I in these samples could be eliminated. By comparing the PXRD patterns of these samples with reference values in Table 4 and CCDC patterns (Figure 3.8), it was clear that these three patterns contain most of the peaks found in the reference PXRD patterns of Forms II, III and IV. Therefore it is likely that sulphathiazole samples crystallized by cooling from methanol, ethanol and 2-propanol may contain Form II, III or IV, or a mixture of these polymorphs.

Due to structural and molecular similarities, Forms II, III and IV show very similar PXRD patterns and their peak values coincide with each other. So, it was possible to identify samples crystallized from 1-propanol and butanol as Form I, but not to positively identify the other three polymorphs.

3.2.3   Infrared (IR) analysis of sulphathiazole samples

Each of the samples of crystals, obtained from the crystallization of sulphathiazole by cooling from each solvent as described in Section 2.3.2.1, were analysed by IR spectroscopy (Perkin Elmer) for polymorphic analysis in the sample.

The IR spectrum of each of the samples was compared with the previous IR studies of sluphathiazole polymorphs for polymorphic identification. In the early 1980s Lagas and Lerk

(1981) reported the IR spectra of polymorphs I, III and II. Thereafter Burger et al (1983) presented the detailed IR spectra of sulphathiazole polymorphs I to IV. Anwar (1989) studied polymorphs of sulphathiazole and reported IR spectra similar to Burger et al. (1983). Anderson et al (2001) presented the IR spectra for all the five polymorphs of sulphathiazole with a list of the characteristic peaks for all the five polymorphs. A brief description of previous IR studies for each polymorph is listed in Table 3.3. It is clear from the previous studies mentioned in Table 3.3 that the IR spectra of sulphathiazole polymorphs II to IV have similar peak values (wavelength, cm^{-1}) and similar spectral patterns. Thus, it would be difficult to distinguish polymorphs II to IV from the results of the IR spectra only.

Table 3.3   Characteristic peaks of IR spectrums for each of the polymorphs reported

Study	Identification peaks reported at different wavelengths (cm^{-1}) in the spectra of each Polymorph.				
	Form I	Form II	Form III	Form IV	Form V
Anderson et al (2001)	3464, 3354, 1627, 1672, 1418, 1278, 929, 856, 830, 733, 703	3442, 3417, 3346, 1643, 1565, 1408, 1290, 1264, 935, 732, 710	3351, 3318, 3278, 1627, 1590, 1572, 1424, 1280, 1294, 1265, 920, 886, 730, 702	3347, 3287, 1627, 1592, 1575, 1428, 1265, 937, 887, 730, 703	3320, 3279, 1625, 1596, 1574, 1428, 1281, 1267, 927, 732, 700
Burger et al (1983)	3460, 3356, 1671, 1415, 1280, 930, 854, 831, 730, 701	3442, 3417, 3346, 1643, 1565, 1408, 1290, 1264, 935, 732, 710	3350, 3320, 1630, 1595, 1575, 1425, 1298, 1280, 1269, 924, 732, 705	3350, 3322, 3285, 1628, 1595, 1575, 1430, 1269, 935, 885, 729, 701	
Anwar et al (1989)	Values found to be similar to Burger et al (1983)				

The IR spectra, obtained in the current study for sulphathiazole crystallized from each solvent by cooling, are presented in Figure 3.9. The identification of polymorphs was carried out by comparing the above IR spectra with previous studies reported in Table 3.3.
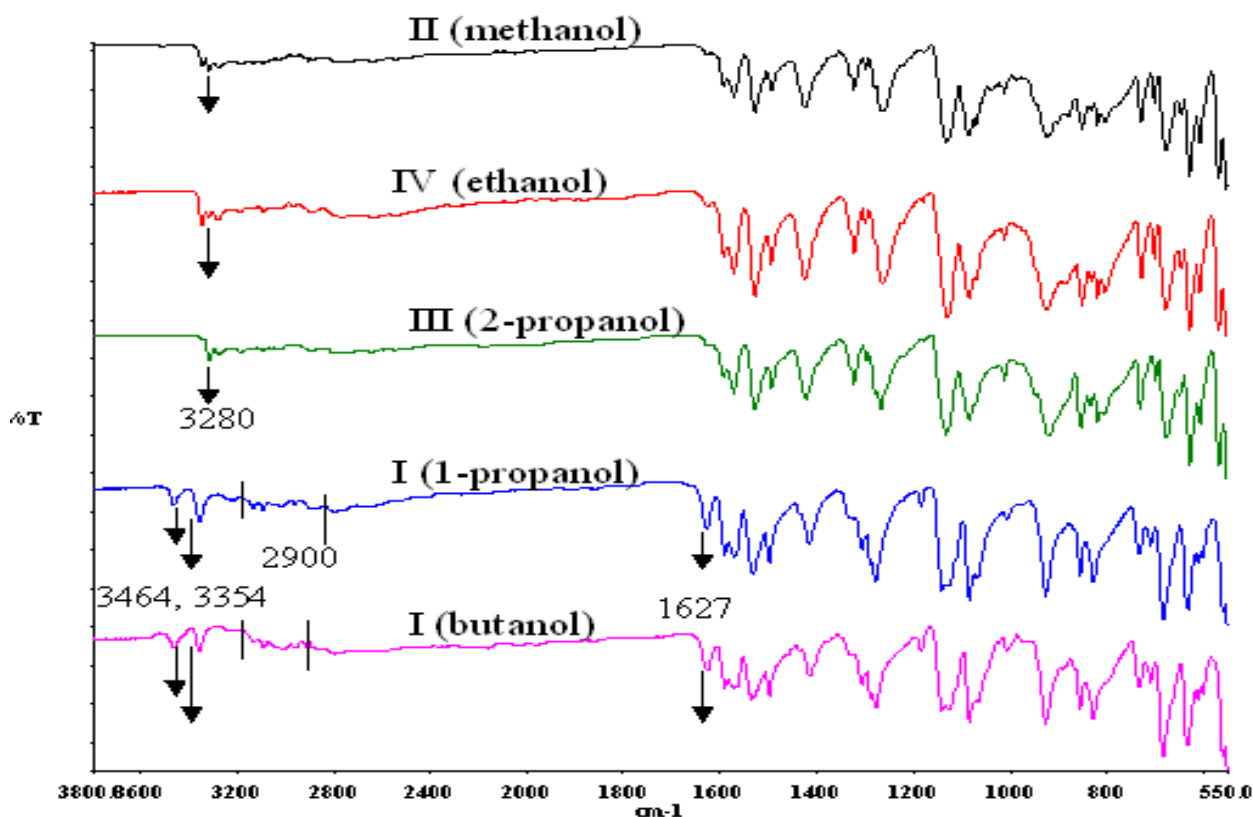
Figure 3.9   IR   analyses   of   sulphathiazole   samples   obtained   from   cooling crystallization

The samples from the crystallization by cooling in propanol-1 and butanol were analysed by IR for the identification of polymorphs. The IR spectra for both experiments are shown in Figure 3.9. In agreement with PXRD patterns, samples crystallized from 1-propanol and n-butanol also showed similar IR spectra and peak values, which suggest that both experiments result in a similar polymorph. These samples, obtained from n-butanol and 1-propanol, produced the spectra which exactly matched with the absorption bands of polymorph I previously reported by Anderson et al (2001) and Anwar et al (1989), Burger et al (1983) and Lagas and Lerk (1981) (Table 3.3). According to Anderson et al (2001) (Table 3.3), the diagnostic peaks for Form I, are 3355, 3462, 1627, 1418, 1499 and 633 cm^{-1} which were also found in the spectra of above samples. The IR spectra of Form I is distinct and unique compared to the IR spectra of other sulphathiazole polymorphs. So, samples crystallized using 1-propanol and n-butanol are easily identified as polymorph I. In both samples, a very

broad absorption centred near 2900 cm^{-1} appeared for the sulphonamide NH group in polymorph I (Anderson et al, 2001). This broad feature is attributed to strong hydrogen bonding to a second nitrogen atom, probably that in the thiazole ring. The NH_2 bands in Form I occur at 3460 and 3555 cm^{-1}, corresponding to some degree of hydrogen bonding, probably to the oxygen atoms of the SO_2 group. The identification of each of these samples as Form I by IR also agrees with the result obtained by PXRD.

The infra-red spectra of the samples, obtained from the crystallization of sulphathiazole by cooling using 2-propanol, ethanol, and methanol as solvents, are very similar to each other. The IR spectra of these samples are shown in Figure 3.9. IR spectroscopy of the samples did not yield any distinct spectra; the minor sample-to-sample variations in the spectra were insufficient to categorize any sample as being different. However, these spectra were compared with the reference spectra of sulphathiazole polymorphs, reported by Anwar et al (1989), Anderson et al (2001), Burger et al (1983), and Lagas and Lerk (1983) (Table 3.3). None of the spectra of samples crystallized from 2-propanol, ethanol and methanol, contain the characteristic peaks of polymorph I (3464, 3354) and polymorph V (3442, 3417) (Table 3.3), so, polymorphs I and V were absent in these samples. However, the IR spectra of samples crystallized from 2-propanol, ethanol, and methanol, follow the similar pattern as shown in Figure 3.9 and match with the reference IR spectra of Forms II to IV (Table 3.3) which showed the appearance of very similar and repetitive peaks with minor differences. The use of the data in Table 3.3, to distinguish each spectrum for the remaining sulphathiazole polymorphs (II, III and IV), did not seem to be practically possible due to the high occurrence of duplicated and overlapping bands among the spectra of these polymorphs. For example, one of the characteristic bands of polymorph III at 730 is also apparent in the spectra of polymorph II and IV. Therefore, from this IR study, it was not easy to distinguish any of these samples as a separate existence of polymorph II, III or IV. However, it could be said that they may contain Form II, III, IV or a mixture of them, but do not contain Forms I or V.

As shown in the IR results, the spectrum for polymorph I is undoubtedly distinct from the IR spectra of polymorphs II to IV. The difference between the IR spectrum of polymorph I on the one hand and polymorphs II to IV on the other, lie in the hydrogen bonding variation involving the NH_2 group (Appearly et al, 1999). In polymorphs II to IV, the amino nitrogen acts as a hydrogen bond acceptor (the donor atom being the ring NH nitrogen of another

molecule), and leading to a partial positive charge on the amino nitrogen. This H-bonding occurs as part of a dimeric ring structure referred to by Blagden et al (1998) as the β-dimer. Hydrogen bonding of this type also causes a low frequency shift in the IR for these three polymorphs, giving a band at 3280 cm^{-1}, which is shown in the spectra of polymorphs II to IV (Figure 3.9). This close relationship between the structures of polymorphs II to IV is responsible for the similarities in their IR spectra and PXRD patterns (Section 1.11.2.2).

3.2.4 Thermal characterization of sulphathiazole samples

The thermal properties of sulphathiazole using Differential Scanning Calorimetry (DSC) have been known from previously reported studies. The DSC data were not definitive in distinguishing different polymorphic forms. Anderson et al (2001), Kordikowski et al (2001), Anwar et al (1989), Lagas and Lerk (1981) and Kruger and Gafner (1972), consistently reported that Form I melts around 201-203 °C without any transformation. The remaining polymorphs of sulphathiazole can undergo multiple transformations when heated in the DSC above 140°C, and ultimately convert to the most stable Form I, which melts at 201 °C.

In the current study, the effect of heating on all samples obtained by cooling crystallization of sulphathiazole, were analysed using DSC to observe any polymorphic transformations and to identify the polymorphic identity of the samples. All the samples were scanned at 10 °C/min on DSC. Samples were also examined by Hot Stage Microscopy (HSM) to complement the results obtained from DSC.

The DSC results of the sulphathiazole samples obtained by cooling crystallization using 1-propanol and n-butanol as solvents, are presented in Figure 3.10 and 3.12, respectively. Photographs from HSM for these samples are also presented in Figures 3.11 and 3.13.
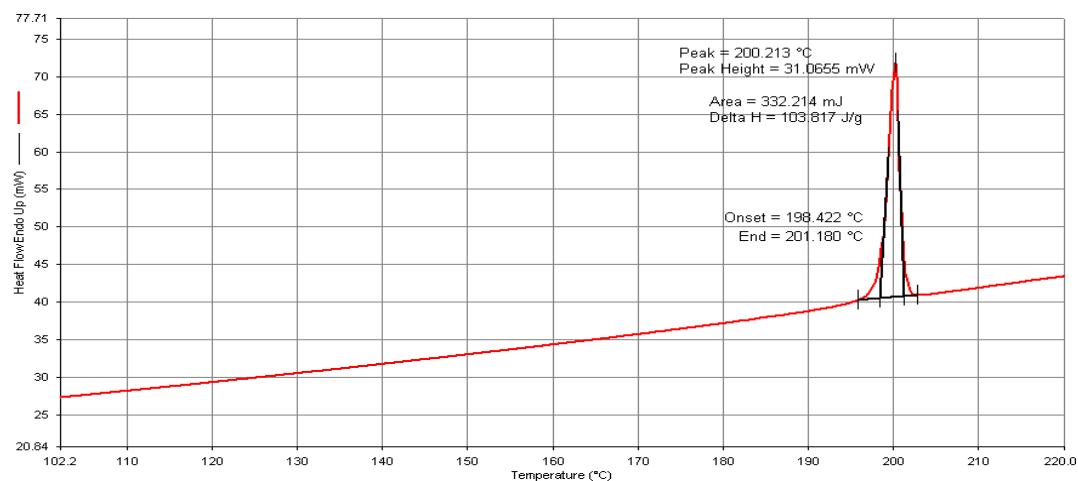
Figure 3.10   DSC scan at 10ºC/min of sulphathizole sample, obtained by cooling from 1-propanol
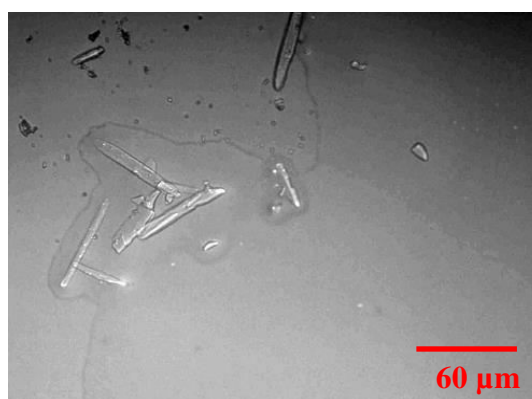
<center>(a)</center>

<center>(b)</center>

Figure 3.11   Sulphathiazole crystal sample, obtained by cooling from 1-propanol, analysed under Hot Stage Microscope to observe the thermal events (a) Crystal sample before melting at 197 °C (b) Crystal sample after melting at 204 °C
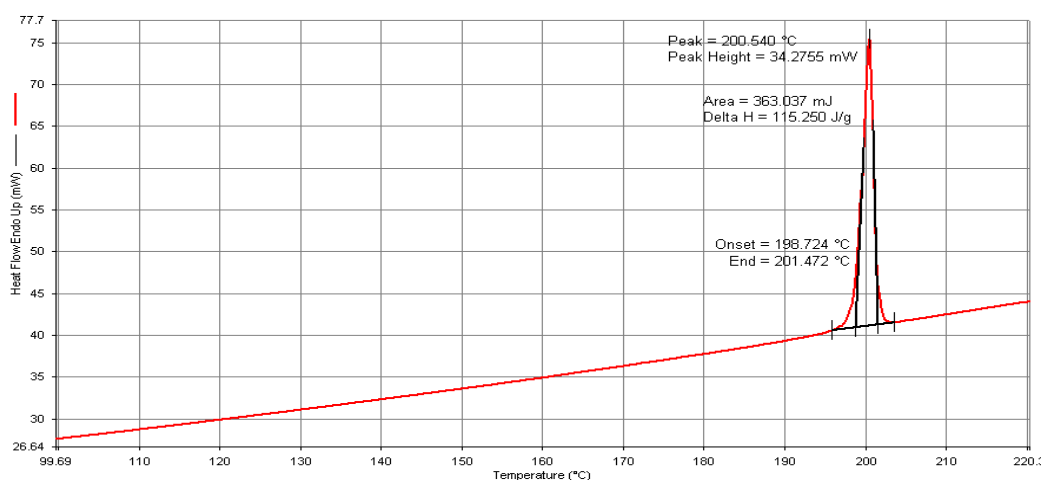
Figure 3.12   DSC scan at 10ºC/min of sulphathiazole sample, obtained by cooling from n-butanol

<table>
<tr><td>(a)</td><td>(b)</td></tr>
</table>
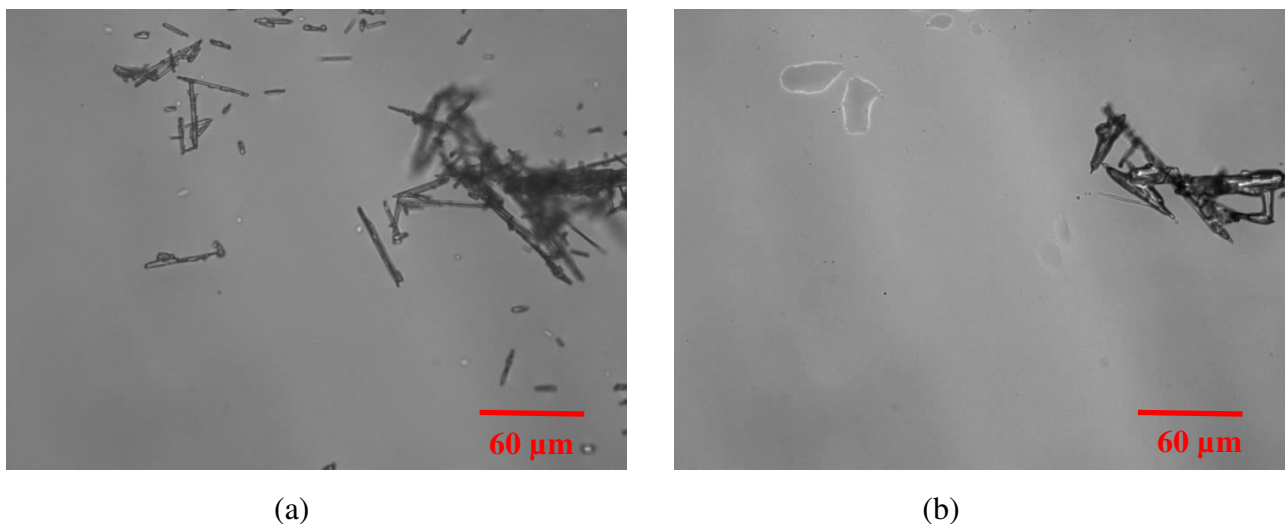
Figure 3.13   Sulphathiazole crystals, obtained by cooling from n-butanol, analysed under Hot Stage Microscope to observe the thermal events (a) Crystal sample before melting at 197 ºC (b) Crystal sample after melting at 204 ºC

As shown in Figures 3.10 and 3.12 both samples, obtained from 1-propanol and n-butanol, resulted in similar DSC scans with only a single melting event at 200-201 °C being observed. Also they do not show any transformation until melting at 201 °C. Pictures obtained from Hot Stage Microscopy (Figure 3.11a and 3.13a) also suggest that both samples maintained their needle like crystal morphology and did not show any changes/transformation in crystals prior to melting, which started at 199 °C. As shown in Figure 3.11b and 3.13b both samples showed complete melting of the crystals by 204 °C on HSM. The HSM results also support melting events seen in DSC. According to Anderson et al (2001), Kordikowski et al (2001), Anwar et al (1989), Lagas and Lerk (1981) and Kruger and Gafner(1972), Form I melts around 201-203 °C without any transformation. Therefore the above samples were undoubtedly confirmed as polymorph I. This result also confirms the results of IR and PXRD obtained in previous sections, which suggested samples obtained from 1-propanol and n-butanol to be the polymorph I of sulphathiazole.

The DSC result of sulphathiazole sample obtained by cooling crystallization from 2-propanol, is presented in Figure 3.14. To complement the results of DSC analysis, pictures from HSM for this sample are presented in Figures 3.15a to e.
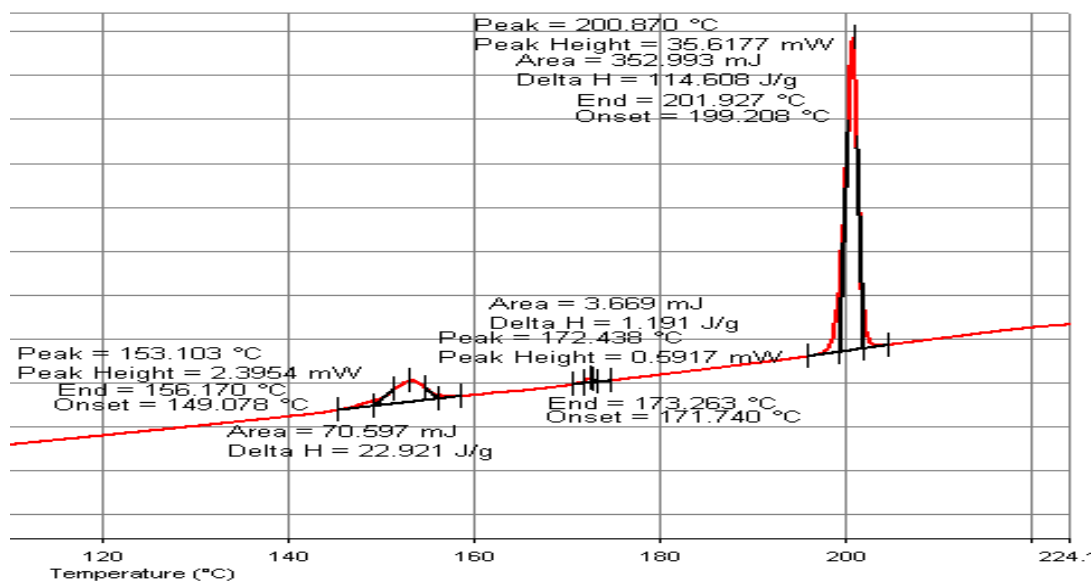
Figure 3.14   DSC scan at 10 ºC/min of sulphathiazole sample obtained by cooling from 2-propanol

(a)

(b)

(c)

(d)

<div align="center">(e)   (f)</div>
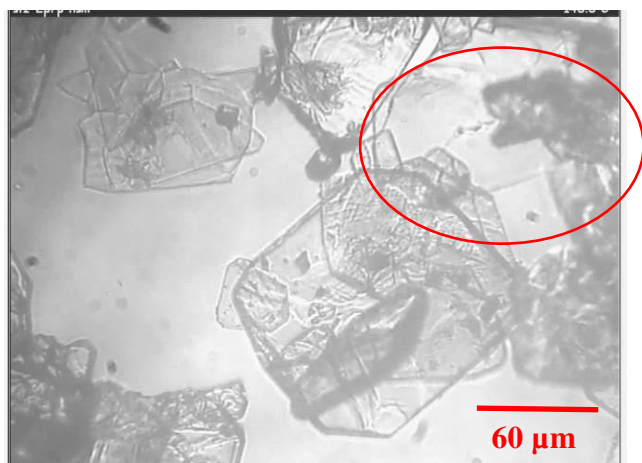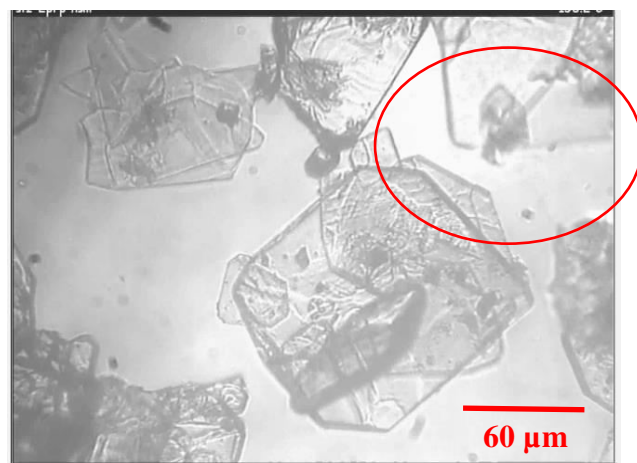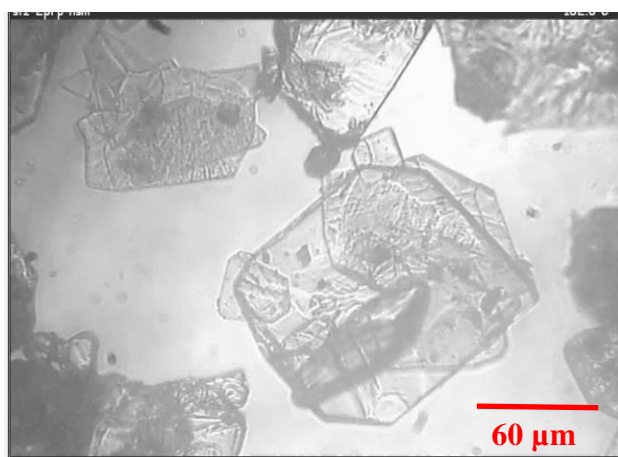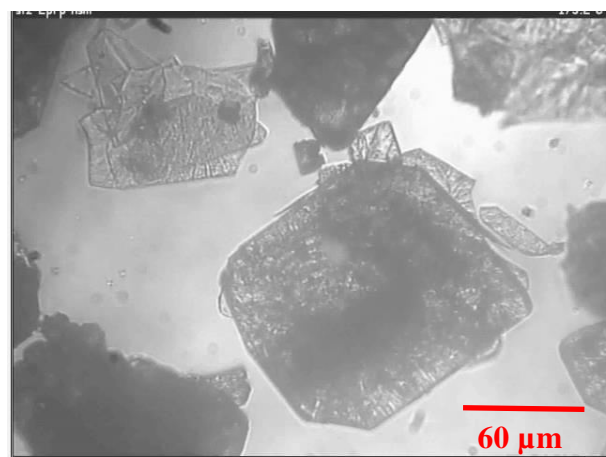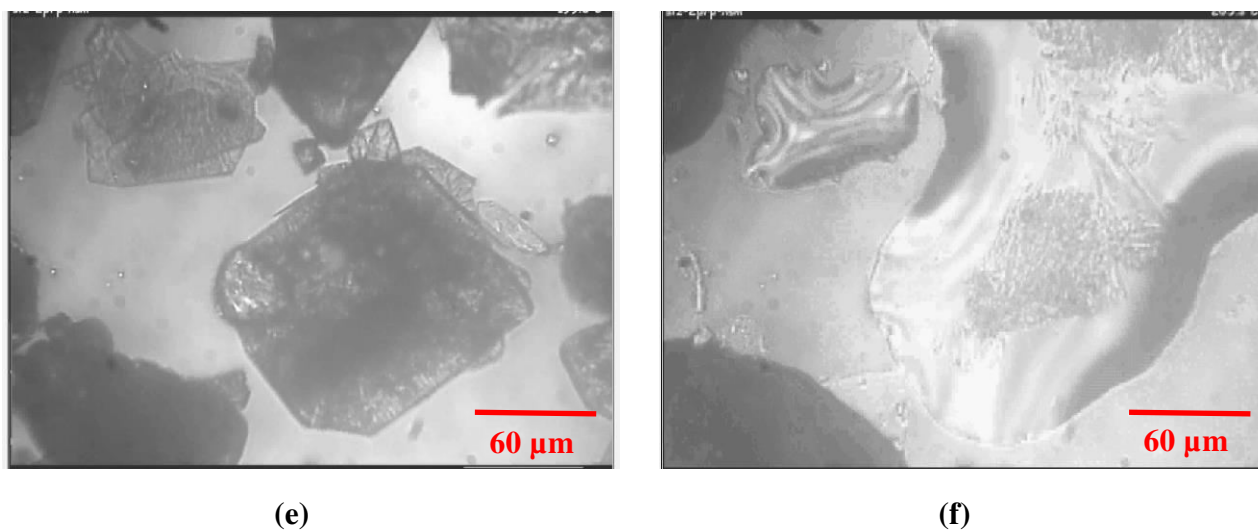
Figure 3.15   **Sulphathiazole crystal sample, obtained by cooling from 2-propanol, analysed under Hot Stage Microscopy to observe the thermal events (a) at 148°C (b) at 157°C (c) at 166°C (d) at 173°C (e) at 199°C (f) at 204°C**

In the above DSC results, the sample crystallized from 2-propanol showed two endotherms, one around 153°C and another around 172°C, prior to the final melting at 201°C. These events were also captured by HSM. As shown in Figures 3.15a and b, during the first transformation event some of the platey crystals shrank in size and showed movement when heated up to 157°C. In contrast, during the second transformation event most of the crystals become opaque when heated above 172°C (Figures 3.15c and d) without showing any changes in morphology. These opaque crystals finally melted completely above 201°C (Figure 3.15e and f).

According to Anwar et al (1989) polymorphs II to IV can transform to polymorph I anywhere between a temperature range of 140 – 177°C. Thus it is difficult to distinguish between them. However, other reports (Kordikowski et al, 2001; Melesly et al, 1971) observed the transformation of polymorph IV into I around 144-148°C and transformation of polymorph II and III into I around 166-172°C. The melting point for form V has been reported to be at 198°C (Anwar, 1989; Lagas & Lerk, 1981).

From the results and observations in Figures 3.14.and 3.15 (3.15 a to e), it could be said that the first endothermic peak shown at around 153°C shows the transformation of polymorph IV into polymorph I. The second small endotherm around 172°C could be assigned to the

transformation of the polymorph II or III into Form I. However, from HSM, it was observed that most of crystals in the sample become opaque and transformed around 172°C. This would suggest the predominant presence of either Form II or III in the sample. Finally all crystals show melting, as converted Form I, at ~201°C. From the DSC and HSM of the sample, obtained from 2-propanol, the sample may be either Form II or III with a small presence of Form IV.

The DSC of sulphathiazole obtained by cooling crystallization from ethanol is presented in Figure 3.16. The DSC scan is also supported by HSM of the sample (Figures 3.17a to e).
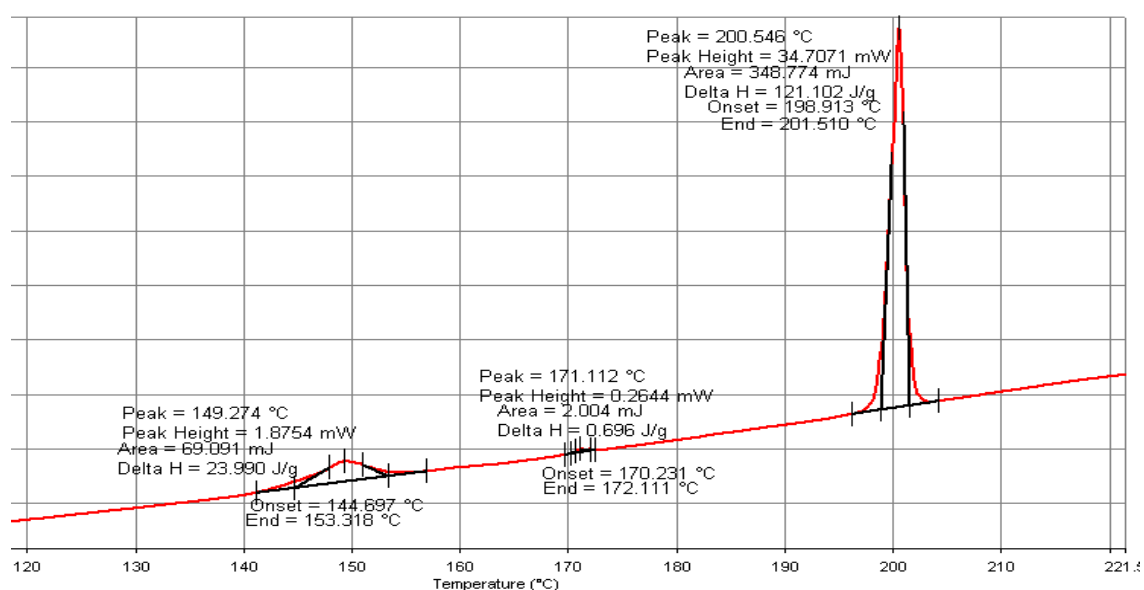
Figure 3.16   DSC scan at 10 °C/min of sulphathiazole sample, obtained by cooling from ethanol

In Figure 3.16, the sample crystallized from ethanol shows two transformation/melting peaks, one around 149°C and another around 171°C, prior to the final melting at 200.5°C. These transformations/melting events were also captured in HSM. As shown in Figures 3.17a and b, during the first transformation event most of crystals in the sample become opaque between 142° to 155°C without changing morphology. However, during the second transformation/melting event a few small crystals showed melting between 171° to 176°C as shown in Figure 3.17c and d. Finally all other crystals melted completely above 201°C (Figure 3.17e and f).
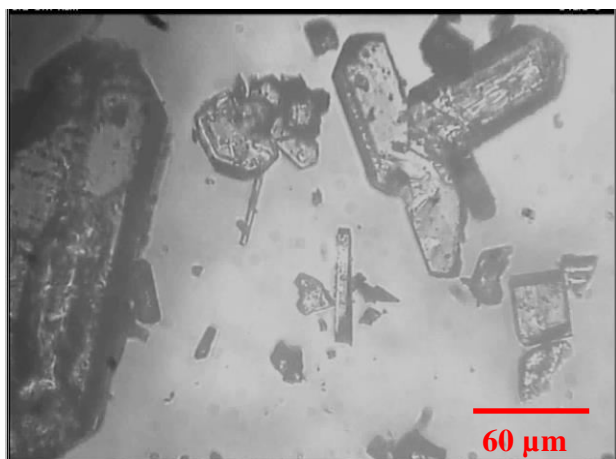
(a)

(b)

(c)

(d)

(e)

(f)

Figure 3.17   Sulphathiazole crystal sample, obtained by cooling from ethanol, analysedunder Hot Stage Microscopy to observe the thermal events (a) at 142 °C (b) at 155 °C (c) at 171 °C (d) at 176 °C (e) at 200 °C (f) at 205 °C

From previous studies (Kordikowski et al, 2001; Melesly et al, 1971), the first endotherm around 149 °C in Figure 3.16 could be assigned to the transformation of polymorph IV into Form I. The second small endotherm around 171 °C could be assigned to the transformation of the polymorph II or III into Form I. However, from HSM it was observed that most of crystals in a sample become opaque and showed transformation at around 149°C. This would suggest the predominant presence of Form IV in the sample. Finally all crystals show melting, as converted Form I, at 201°C. From the DSC and HSM analysis of the sample, obtained from ethanol, the sample could be Form IV with the presence of a small amount of Form II or III.

The DSC of sulphathiazole sample, obtained by cooling crystallization from methanol, is presented in Figure 3.18. The DSC scan is also supported by the HSM of the sample in Figures 3.19a to e.
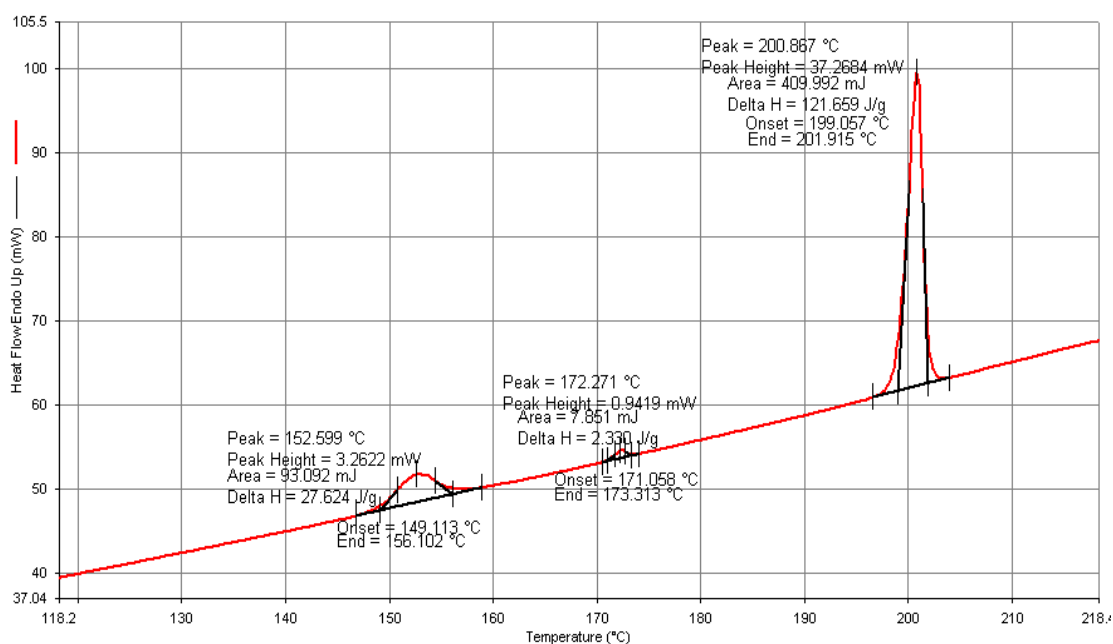
Figure 3.18   DSC scan at 10 ºC/min of sulphathiazole sample obtained by cooling from methanol
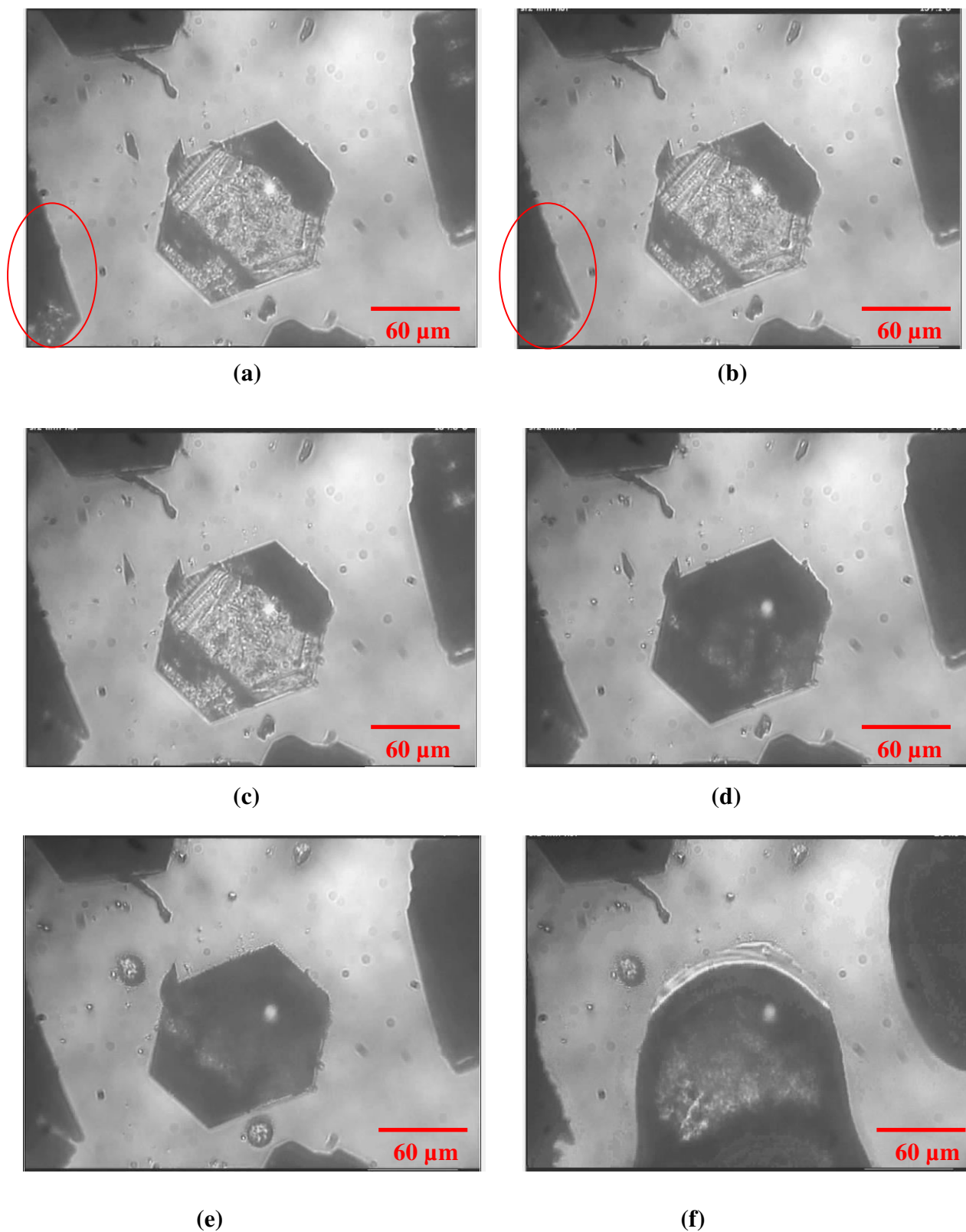
Figure 3.19 **Sulphathiazole crystal sample obtained by cooling from methanol, analysed under Hot Stage Microscopy to observe the thermal events (a) at 147 °C (b) at 155 °C (c) at 165 °C (d) at 175 °C (e) at 198 °C (f) at 204 °C**

In the DSC results (Figure 3.18), the sample crystallized from methanol showed two transformation/melting peaks, one around 152.5°C and another around 172°C, prior to final melting at 200.8°C. These transformations/melting events were also captured by HSM as shown in Figure 3.19a and b, during the first event a few crystals become opaque between 147° to 155°C. Most of the other crystals became opaque during the second transformation/melting event between 165° to 173°C as shown in Figure 3.19c and d. All opaque crystals finally melted above 201°C (Figure 3.19e and f).

From previous studies (Kordikowski et al, 2001; Melesly et al, 1971), the first endotherm around 152.5 °C in Figure 3.18 could be assigned to the transformation of polymorph IV into I. The second small endothermic peak around 172 °C could be assigned to the transformation of polymorph II or III into Form I. However, from HSM it was observed that most of crystals in the sample became opaque and showed transformation around 165-173 °C. This would suggest the predominant presence of either Form II or Form III in the sample. Finally, all crystals showed melting, as converted Form I, at 201 °C. From the DSC and HSM of the sample obtained from ethanol, it could be said that the sample was Form II or III with a small quantity of Form IV present.

3.3   Characterization of sulphathiazole crystals obtained by evaporation

Crystallization experiments of sulphathiazole by evaporation were also performed with the five different alcohol solvents as described in Section 2.2.2.2. The list of these experiments are given in Table 2.6

Samples, obtained from evaporative crystallization, were analyzed by optical microscopy, PXRD, and single crystal x-ray diffraction to determine their polymorphic identity.

3.3.1 Morphological analysis of crystallized samples

The evaporation experiments were regularly observed by optical microscopy to study the growth and changes in morphologies of the crystals. These time-resolved images of the morphologies of the crystals are shown in Figures 3.20 to 3.24.
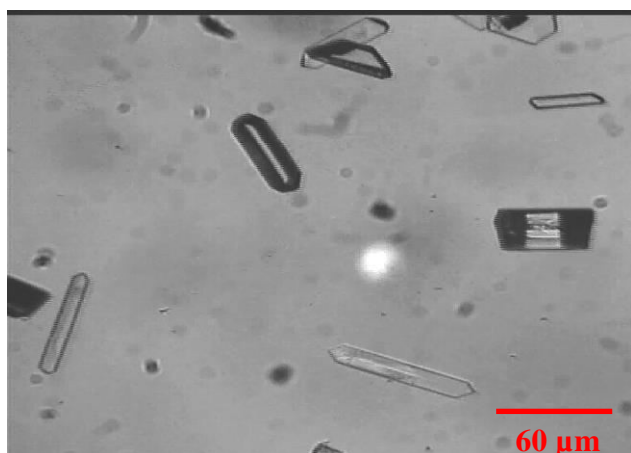
Figure 3.20 (a) Sample from methanol within 5 minutes of nucleation
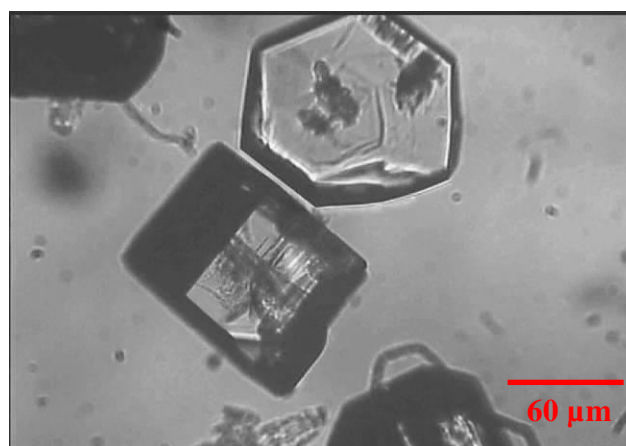
Figure 3.20 (b) Sample from methanol after complete evaporation

Figure 3.21 (a) Sample from ethanol within 5 minutes of nucleation

Figure 3.21 (b) Sample from ethanol after complete evaporation
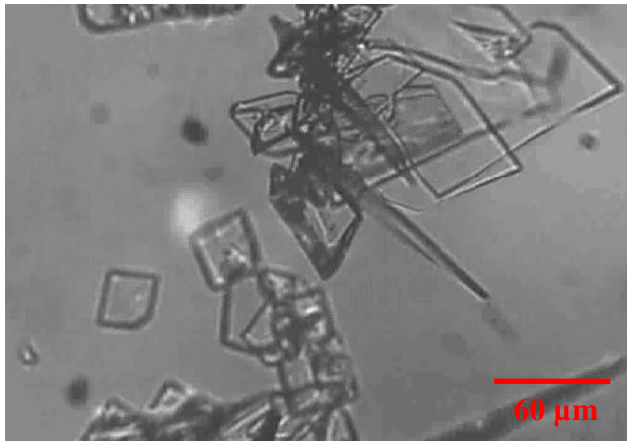
Figure 3.22 (a) Sample from 2-propanol within 5 minutes of nucleation
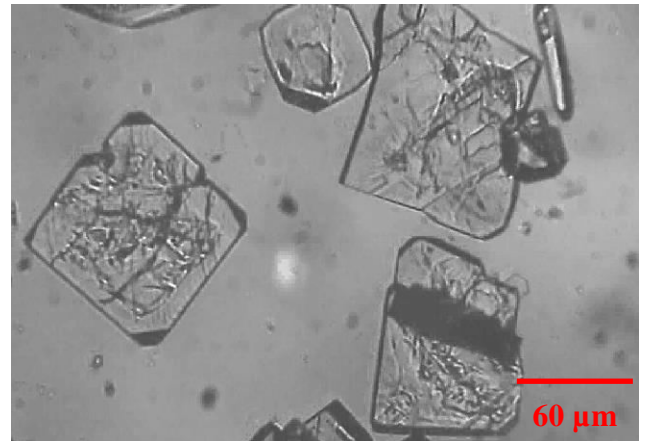
Figure 3.22 (b) Sample from 2-propanol after complete evaporation

Figure 3.23 (a) Sample from 1-propanol within 5 minutes of nucleation
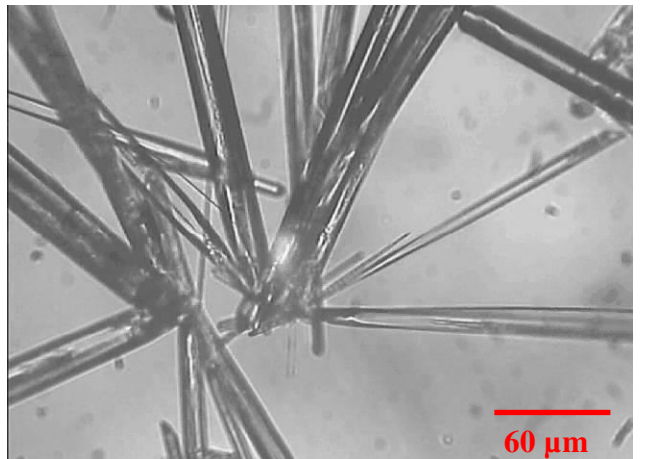
Figure 3.23 (b) Sample from 1-propanol after complete evaporation

Figure 3.24 (a) Sample from n-butanol within 5 minutes of nucleation
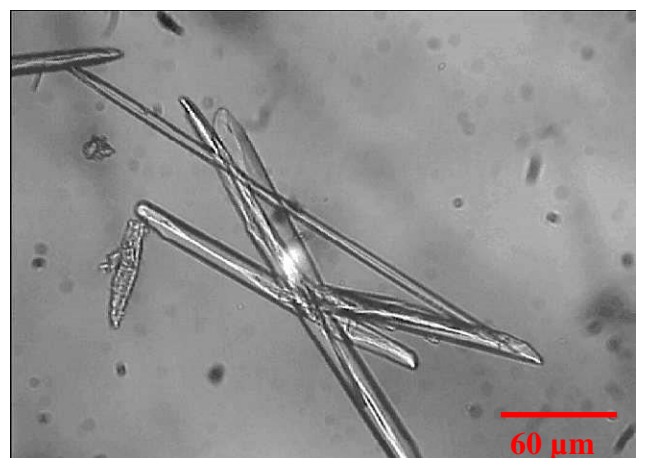
Figure 3.24 (b) Sample from n-butanol after complete evaporation

116

As shown in Figures 3.20 to 3.24, microscopic observation of the samples obtained from crystallization by evaporation displayed similar morphological behaviour to that observed during cooling crystallization experiments. However, crystals obtained by evaporation, were larger compared to crystals obtained from similar solvents by cooling crystallization as the evaporative crystallizations were slower in nature and proceeded without any agitation. All samples initially crystallised as elongated, or needle particles, which is established as the morphology of metastable form I (Anwar et al, 1989, Blagden el al, 1998).

When methanol or ethanol was used as the solvent, needles nucleated initially followed by small hexagonal plates within 2 minutes of nucleation (Figures 3.20a & 3.21a). The needles dissolved within a few minutes of nucleation; whereas, the hexagonal crystals grew in size and thickness, resulting in hexagonal prisms in the case of methanol (Figure 3.20b), and elongated thin hexagons in the case of ethanol (Figure 3.21b) with complete evaporation of solvent. Single crystal XRD identified that crystals grown from methanol were Form II, and from ethanol were Form IV (see Table 3.6).

In the case of 2-propanol as the solvent, sulphathiazole initially nucleated as needles and very small square plates (Figure 3.22a). Initially needle-shaped crystals predominated. However, with time, square plates grew slowly in size and numbers, and the needles disappeared from the slurry/solution when left overnight for complete evaporation as shown in Figure 3.22b. Square plates also converted into hexagonal plates by developing faces on the angles of square plates. The rate of growth was slower than for those crystals grown from the straight chain alcohols, with growth continuing for more than 4 hours after nucleation. Therefore, a few square plates were unable to develop faces on the angles before the complete evaporation of solvent (Figure 3.22b). Crystals were identified by single crystal X-ray diffraction as Form III.

As shown in Figures 3.23 and 3.24, 1-propanol and 1-butanol allowed nucleation of needle-shaped crystals. Once the evaporation of solvent started, nucleation of needles was prompt with maximum growth having occurred within 17-20 minutes of nucleation. No further growth was observed and the particles remained without transformation until the complete evaporation of the solvents. PXRD and single crystal XRD confirmed that each of these samples was Form I.

3.3.2 Powder x-ray diffraction analysis of Sulphathiazole samples

Sulphathiazole samples, crystallized immediately after nucleation (early samples) by evaporation of each of the solvents (Section 2.3.2.2), were isolated by filtration from the crystallising solution in order to check the early polymorphic identity during the crystallization process. The isolated sulphathiazole samples were dried and analysed by PXRD as described in Section 2.4.3. The PXRD patterns of these samples were compared with the PXRD of those isolated after complete evaporation of solvent (mature samples) to observe if any polymorphic transformation occurred during the crystallization process. The results are presented in Figures 3.25, 3.26, 3.27, 3.28, and 3.29.
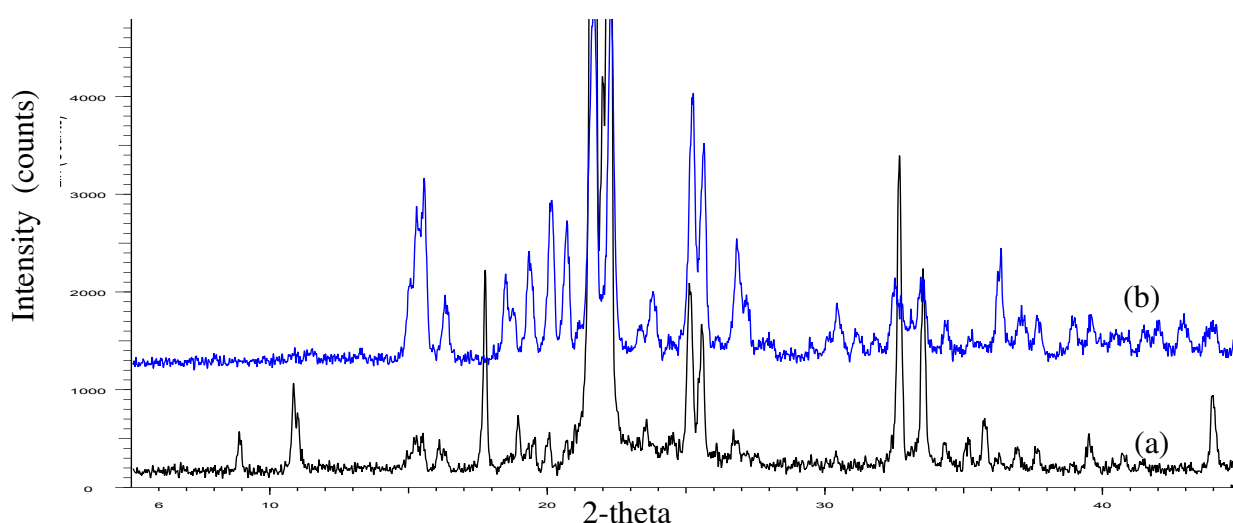
Figure 3.25   PXRD patterns of sulphathiazole crystal samples, (a) isolated within 5 minutes of nucleation and (b) isolated after complete evaporation of 2-propanol.
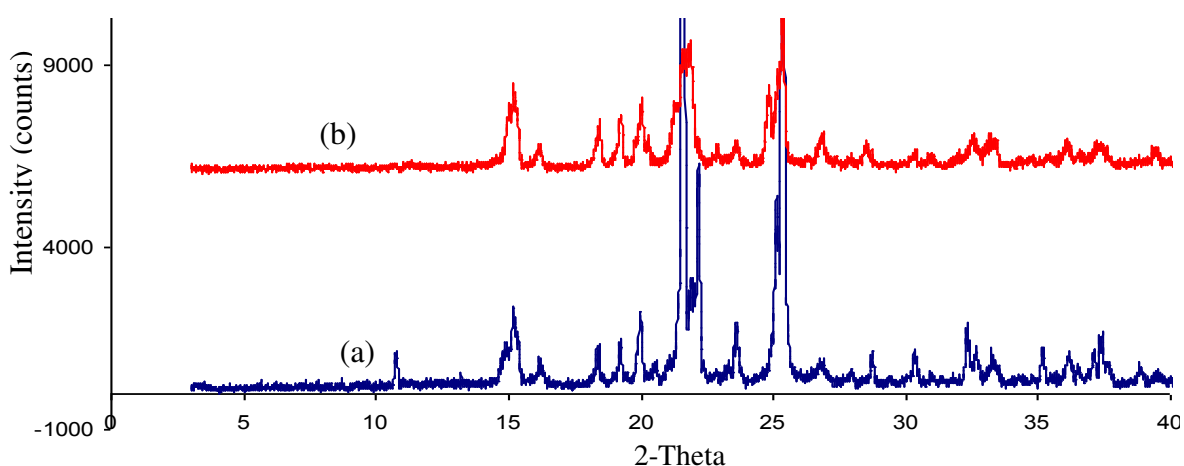
Figure 3.26   PXRD patterns of sulphathiazole samples, (a) isolated within 5 minutes of nucleation and (b) isolated after complete evaporation of ethanol.
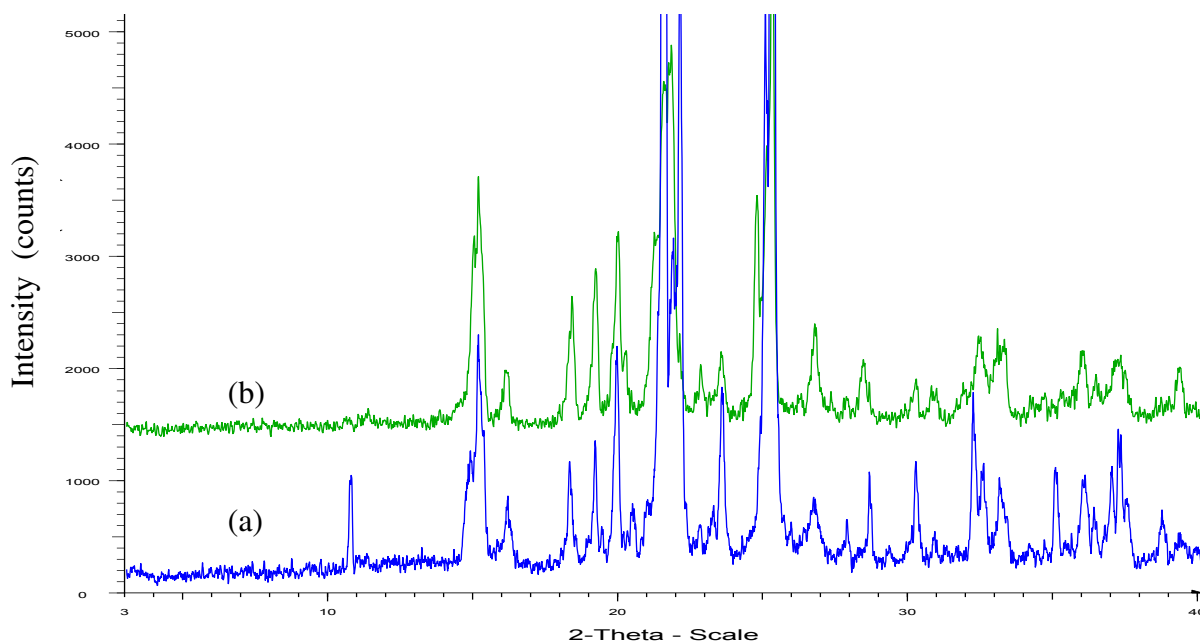
Figure 3.27   PXRD patterns of sulphathiazole samples, (a) isolated within 5 minutes of nucleation and (b) isolated after complete evaporation of methanol
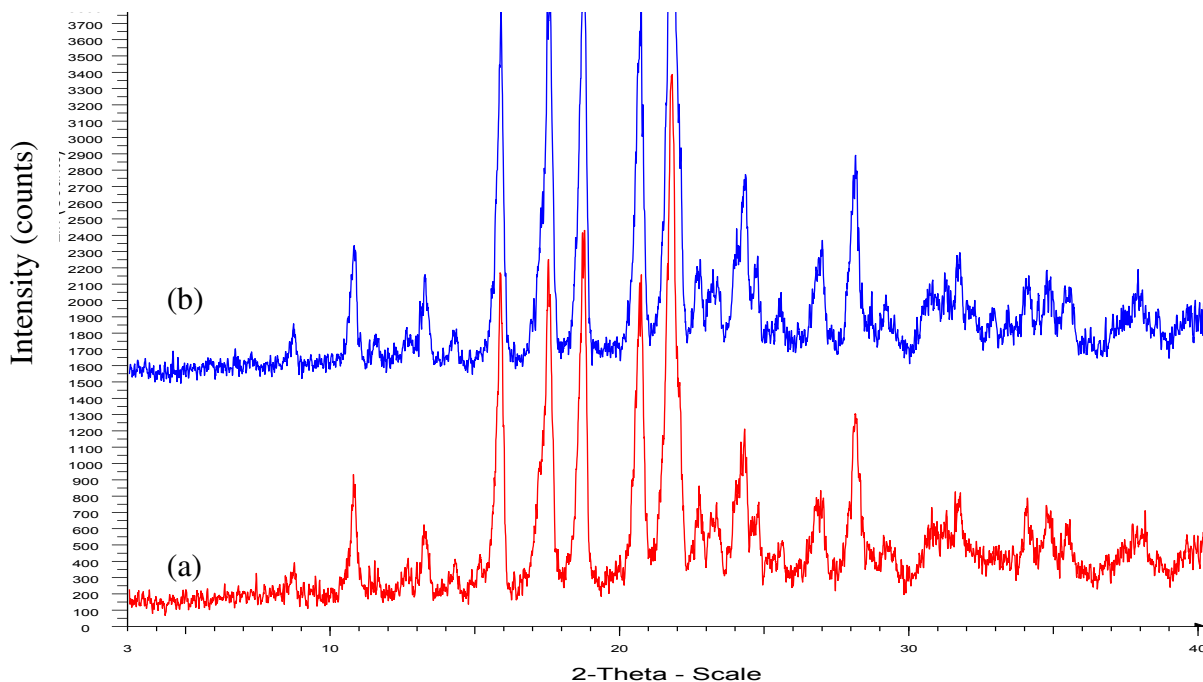
Figure 3.28   PXRD patterns of sulphathiazole samples, (a) isolated within 5 minutes of nucleation and (b) isolated after complete evaporation of 1-propanol
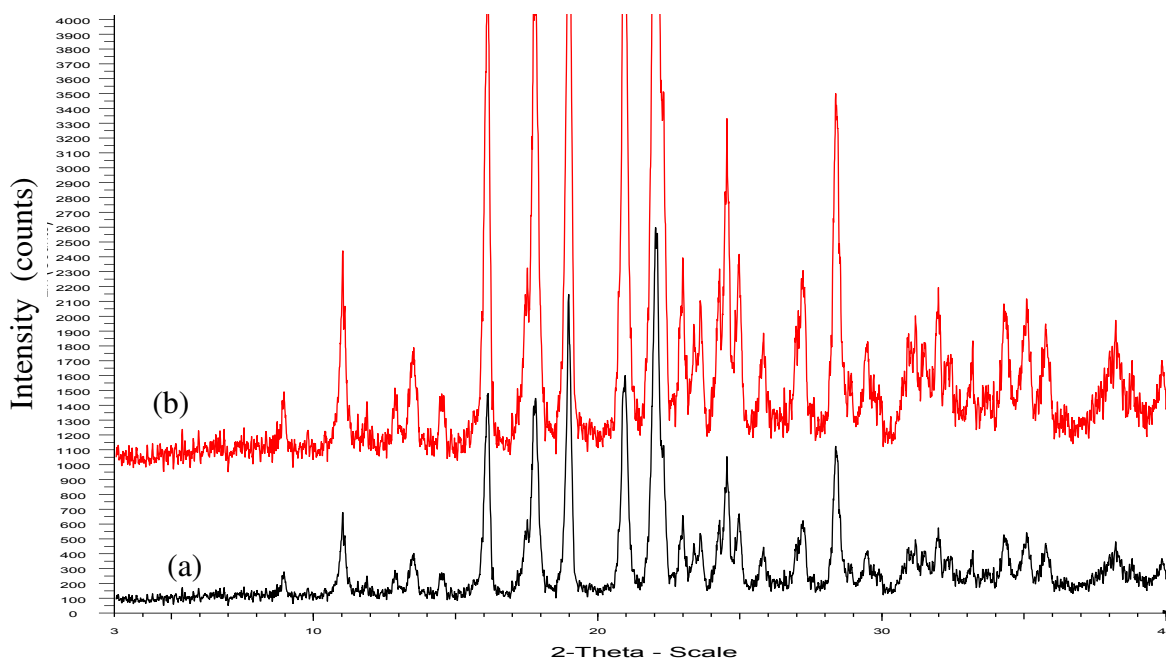
Figure 3.29   PXRD patterns of sulphathiazole samples, (a) isolated within 5 minutes of nucleation and (b) isolated after complete evaporation of n-butanol

As shown in Figures 3.25(a), 3.26(a), and 3.27(a), when methanol, ethanol or 2-propanol was used respectively as a solvent, PXRD patterns of early samples (isolated within 2 minutes of nucleation) indicated the presence of Form I by displaying characteristic peaks for Form I at 11° 2θ (see Section 3.2.2 for reference PXRD peaks reported previously for sulphathiazole polymorphs) but did not show a complete match with the reference PXRD spectra of Form I obtained from the CCDC (Section 3.2.2 - Figure 3.8). In addition to the identification peak for Form I at 11° 2θ, these samples also showed similarities/peaks with the CCDC patterns of Form II, III and IV, which suggests that apart from metastable Form I these early samples also contained Form II, III, or IV. These PXRD results also showed consistency with the time-resolved morphological studies of methanol, ethanol, and 2-propanol samples (Sections 3.3.1), where early samples showed the presence of needle-shaped Form I crystals in pictures with other small platey crystals. When mature samples were isolated, the peak at 11° 2θ was not present in any of the samples (Figure 2.25(b), 2.26(b), and 2.27(b)) and displayed a good match with the CCDC patterns of Forms II to IV (Figure 3.8), which indicate that any crystals of Form I had transformed into a more stable polymorph II, III, or IV. However, as explained in Section 3.2.2, due to similarities in the PXRD patterns of Forms II, III, and IV, it was not possible to positively distinguish them from their PXRD patterns. These results were also

consistent with the time resolved morphological studies of mature samples (Section 3.3.1), which showed the dissolution of needle-shaped Form I and growth of other stable crystals with time.

When 1-propanol or n-butanol was used as solvent, PXRD patterns of early samples and mature samples showed an exact match with each other (Figures 3.28 and 3.29). All samples displayed the identification peak for Form I at 11° 2θ and showed good similarity with the reference pattern of Form I obtained from the CCDC (Figure 3.8), which suggests the predominant presence of Form I in both early and mature samples, without any polymorphic transformation or changes with time. This was also consistent with the time-resolved morphological studies of samples obtained from 1-propanol and n-butanol (Section 3.3.1), which shows no change in needle-shaped Form I crystals with time.

3.3.3   Single crystal x-ray analysis of crystals obtained from evaporation

Powder x-ray diffraction can be used for fingerprint identification of various solid materials. However in some cases, PXRD patterns for the different polymorphs of the same substance are very similar to each other due to their structural similarities. This makes it very hard to distinguish the precise polymorph from the PXRD patterns. Also in the current study, sulphathiazole samples crystallized from methanol, ethanol and 2-propanol showed similar PXRD patterns, although clear morphological changes were observed under microscopy (Sections 3.2.1 and 3.3.1) that suggest the possibilities of different polymorphs. It is known that all solid crystalline compounds have their own particular unit cell, which should be unique in its dimensions. Even different polymorphs of the same compound sulphathiazole would differ from each other in their unit cell dimensions a, b, c and α, β, γ (see Section 1.1 for more details about unit cell dimensions). Therefore single crystal x-ray study was used to identify the unit cell and hence the polymorphic form of sulphathiazole crystallized from each solvent.

Sulphathiazole crystals were grown by evaporation from each solvent as described in Section 2.3.2.2. A single crystal was mounted on a glass fiber in a random orientation. Using a Stoe IPDS (Imaging Plate Diffraction System) area detector, unit cell constants were calculated by least squares refinement using the setting angles of 25 reflections and compared with reference unit cell data as shown in Table 3.4.

Table 3.4   Comparison of unit cell data, obtained from single crystal x-ray diffraction, with the data obtained from literature for polymorphic identification

Unit cells	Current study				Literature values			
	1-propanol and 1-butanol	methanol	2-propanol	ethanol	Form I[a]	Form II[b]	Form III[a]	Form IV[c]
a	10.45 Å	8.18 Å	17.40 Å	10.90 Å	10.55 Å	8.23 Å	17.57 Å	10.86 Å
b	13.27 Å	8.56 Å	8.5 Å	8.56 Å	13.22 Å	8.55 Å	8.57 Å	8.54 Å
c	17.20 Å	15.48 Å	15.9 Å	11.48 Å	17.05 Å	15.55 Å	15.58 Å	11.45 Å
β	107 °	94.18 °	112 °	89.6 °	108.06 °	93.67 °	112.93 °	88.13 °

Key for Literature values [a] Kruger and Gafner (1971)

[b] Kruger and Gafner (1972)

[c] Bablidev et al (1987)

From comparison with reference unit cell data, it was clear that sulphathiazole crystals crystallized from 1-propanol and n-butanol were Form I, whereas sulphathiazole crystallized from methanol, 2-propanol and ethanol showed good match with the reference unit cell data of Forms II, III and IV respectively, as shown in Table 3.4. Therefore samples crystallized from methanol, 2-propanol and ethanol were identified as polymorph II, III and IV respectively.

3.4   Effect of grinding on polymorphic stability

Grinding is one of the essential and routine operations for particle size reduction and tablet preparation. During the grinding process, the drug particle would be subject to high mechanical stress that could cause transformation of the solid drug compound. It is therefore desirable to check the stability of the metastable form of sulphathiazole against the mechanical stress of grinding.

The effects of grinding on sulphathiazole Form I crystal samples, obtained from crystallization by cooling 1-propanol (Section 2.2.2.1), were observed by comparing the PXRD patterns of extensively ground samples with gently ground samples. Sulphathiazole

Form I sample was ground manually using a mortar and pestle for 10 minutes (extensively ground sample). The PXRD pattern of this sample was compared with the PXRD patterns of Form I which was ground gently for 2 minutes using a mortar and pestle. The results are shown in Figure 3.30.
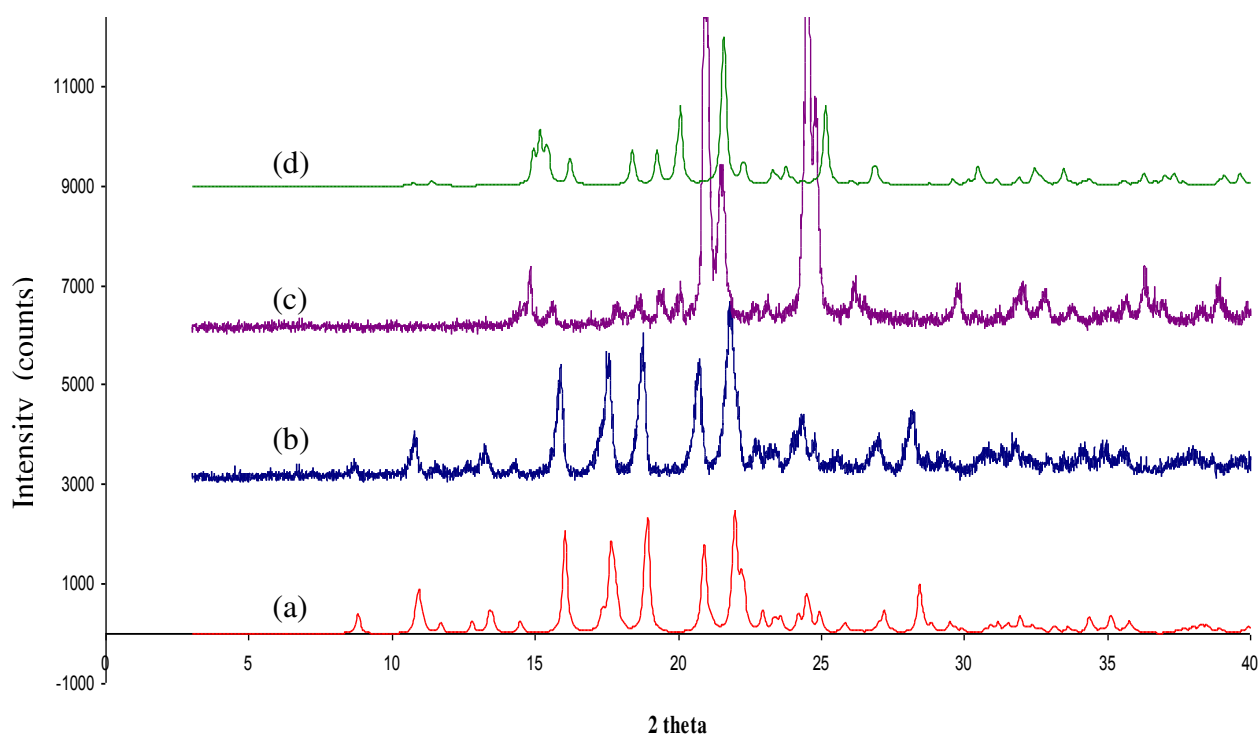
Figure 3.30   PXRD patterns of sulphathiazole samples, (a) reference pattern of Form I obtained from CCDC (b) Form I after grinding for 2 minutes (c) Form I after grinding for 10 minutes (d) reference pattern of Form II obtained from CCDC

From Figure 3.30, it is clear that crystals of Form I showed a significant effect of grinding on polymorphic stability. As shown in Figure 3.30 (b), the sample, ground for 2 minutes, showed the identification peak for Form I at 11° 2θ value and exactly matched with the reference PXRD pattern of Form I obtained from CCDC (Figure 3.30 a), which confirms that the sample was pure Form I. However, after grinding of the sample for 10 minutes, Form I lost its identity peak at 11° 2θ value as shown in Figure 3.30 (c). In addition, Form I after extensive grinding for 10 minutes showed a PXRD pattern, which showed similarity with the reference PXRD pattern of Form II (Figure 3.30 d), obtained from CCDC. This result indicates that extensive grinding of sample of Form I for a long time would cause a polymorphic transformation in to the more stable polymorph II, III or IV.

3.5 Effect of Seeding

According to Ostwald's rule of stages, the sulphathiazole polymorphs would transform from the least stable metastable state (Form I) to the thermodynamically more stable states (Form II, III, or IV). Also seeding of the more stable polymorph into the sulphathiazole solution should draw the nucleation or transformation of crystals into the more stable seeded polymorph.

In the current study, it is known from results (Sections 3.2 and 3.3) that Form I was stabilized when 1-propanol used as a solvent for the crystallization of sulphathiazole. The effects of seeding more stable Form II, III or IV on the crystallization of sulphathiazole was observed when 1-propanol used as a solvent. Form II, III and IV obtained from evaporative crystallization (Section 3.3.3) were used as seeds. The seeding experiments were performed as described in Section 2.2.2.1. Experiments are also listed in Table 2.3.

After crystallization, crystals were separated for powder X-ray diffraction analysis in order to check the polymorphic identity of the samples. Results of PXRD analysis are shown in Figure 3.31.
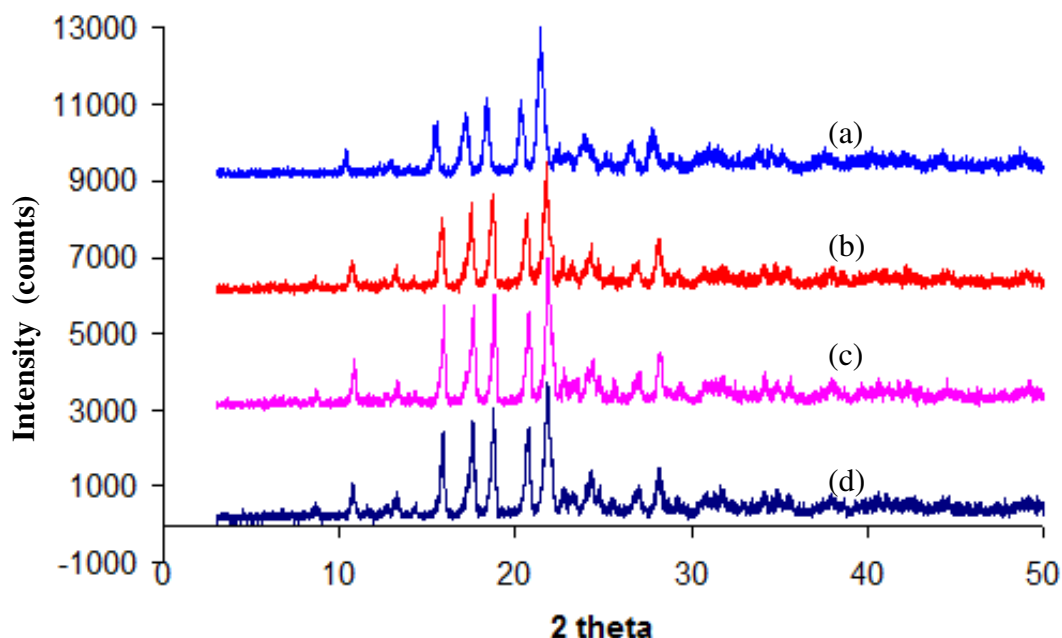
Figure 3.31 **PXRD patterns of sample obtained from crystallization using 1-propanol with (a) seeding with Form IV, (b) seeding with Form III, (c) seeding with Form II, and (d) without any seeding**

124

As shown in Figure 3.31, PXRD patterns of all samples showed the identification peak for form I at 11° 2θ and showed an exact match with the reference PXRD pattern of Form I (Figure 3.8), which confirms the identity of all the samples as Form I. From above PXRD results it is clear that even seeding of more stable forms (II, III and IV) into 1-propanol-sulphathiazole solution could not draw transformation of Form I into the more stable seeded forms. Even with seeding of a more stable form, 1-propanol stabilized metastable Form I only. PXRD patterns of the samples, crystallized from 1-propanol with or without seeding did not show any changes but showed identical behavior with each other. These results suggest that there was no effect of seeding with the more stable form on the stabilization of Form I from 1-propanol. This finding is consistent with the previous conclusion (section 3.2) that 1-propanol and n-butanol stabilized the growth of Form I.

3.6   Characterization of sulphathiazole solutions by solution NMR

It is possible that with the use of different solvents, the pre-nucleation clusters of solute molecules can arrange differently as the solvents are able to engineer the intermolecular interaction. Davey et al (2001) demonstrated, using 2, 6 dihydroxybenzoic acid as a model system, that when solute molecules in the solution arranged differently prior to the nucleation, different polymorphs would be formed (Davey et al, 2001). In current study, sulphathiazole showed the crystallization of different polymorphs with the use of different alcohols as solvent. Use of different alcohol solvents might engineer different pre-nucleation clusters of sulphathiazole molecules, which could impact on the polymorphic outcome of sulphathiazole crystallization. The pre-nucleation clusters would differ from each other in their hydrogen bonding arrangements. These differences in their hydrogen bonding can be observed using ^{1}H solution NMR by dissolving sulphathiazole in deuterated alcohol solvents. Here, sulphathiazole was dissolved in deutarated ethanol, methanol and n-butanol and samples were analysed in ^{1}H solution NMR as explained in section 2.4.7. The results are presented in Figure 3.32.
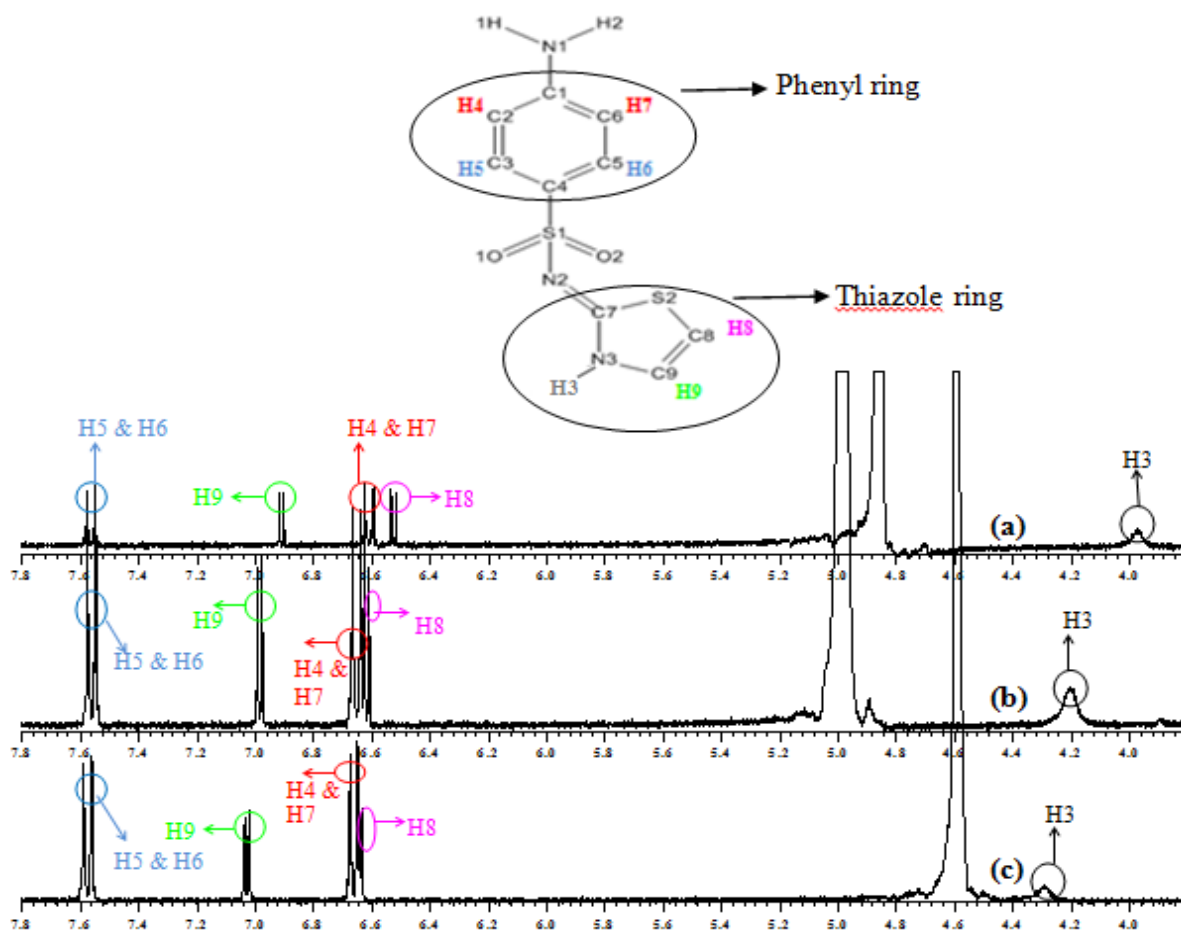
Figure 3.32 ¹H NMR analysis of commercial sulphathiazole in (a) 1-butanol, in (b) ethanol and in (c) methanol

Table 3.5 Chemical shifts of assigned hydrogen peaks in different solvents

Solvent used	H8	H4 & H7	H9	H5 & H6
1-butanol	**6.55**	6.60	**6.90**	7.56
Ethanol	6.61	6.62	7.00	7.56
Methanol	6.62	6.63	7.04	7.56

3.6.1 Phenyl ring hydrogens (H4, H7, H5, and H6)

As shown in Figure 3.32, H4 and H7 are nearer to the amino ($-NH_{2-}$) group, which is an electron donating group. Therefore, H4 and H7 experience more electron rich environments and require less energy to go to the higher energy state. In contrast, H5 and H6 are nearer to the sulphonamide (S=O) group, which is an electron withdrawing group. Therefore, H5 and H6 would experience an electron deficient environment compared to H4 and H7 and require more energy to reach the higher energy state. Hence H4 and H7 show a lower chemical shift (between 6.6 to 6.7) in all liquid NMR analysis; whereas H5 and H6 show higher chemical shifts (approximately at 7.6) in all the liquid NMR analyses. These hydrogens also show a

126

coupling effect (H4 with H5 and H7 with H6) and therefore they display doublets in their peaks. Also the consistent gap between the doublets in both peaks supports the peak assignments as hydrogens associated with an aromatic six carbon ring.

3.6.2 Thiazole ring hydrogens (H8 and H9)

In the thiazole ring, Sulphur (S2) is not connected to any other group (such as O or H), which makes it electron donating compared with the NH group (N3−H3). H8 is nearer to sulphur (S2) than H9 and therefore H8 would be more electron rich compared with H9 Hence, H8 results in a lower chemical shift of 6.5 to 6.7; whereas, H9 results in a higher chemical shift of 6.9 to 7.1. Again, both hydrogens show coupling effects with each other and therefore peaks for both hydrogens display as doublets.

As shown in Figure 3.32 and Table 3.5, ^{1}H NMR analyses with different alcohol solvents show changes in the chemical shift for the peaks associated with H8 and H9.

It is known from the experimental results (Section 3.3) that sulphathiazole crystallizes as Form I from 1-butanol; whereas, from methanol and ethanol it crystallized respectively as Form II and IV. Form I utilizes the thiazole ring H3 to make hydrogen bonds with N2 (N2−H3) for the unique α-dimer ring formation (Figure 1.9). In contrast, the Forms II, III, and IV use the thiazole ring H3 with the more electron negative N1 (N1−H3) for its unique β-dimer ring formation (Figure 1.10). Due to the electron negativity of N1, the N1−H3 bond in β-dimer would be stronger than N2−H3 bond in α-dimer. Hence, H8 and H9 would have a greater electron rich environment in the α-dimer compare to the β-dimer. Therefore, H8 and H9 in the α-dimer would require less energy to reach the higher energy state in the NMR magnetic field and show a lower chemical shift in the NMR spectra; whereas, H8 and H9 in the β-dimer would require more energy and hence show a higher chemical shift in the NMR spectra. In this analysis, the lower chemical shift for H8 and H9, when 1-butanol was used as the NMR solvent compared to methanol and ethanol, suggest that the formation of pre-nucleation cluster similar to the α-dimer (Form I) in 1-butanol and similar to the β-dimer (Form II-IV) in methanol and ethanol.

In this study all the liquid NMR samples were prepared with alcohol functionality solvents. Therefore, hydrogens associated with NH (H3) and NH$_2$ (H1 and H2) groups are more likely

to make many hydrogen bonds with solvent or solute molecules and due to that they are more likely to show very weak unpredictable broad peaks, which could even be merged with the base-line in Liquid NMR. However, all the NMR spectra in Figure 3.32 represent a very weak signal of broad peak between 3.9 and 4.2. This peak could be assigned to the hydrogen in the NH group (H3) as the NH group less likely to take part in hydrogen bonding compared with NH_2. Hence H3 would be more likely to appear on the NMR spectra compared with H1 and H2. As explained above, in the β-dimer H3 is involved in stronger hydrogen bonding compared with the α-dimer. Hence, pre-nucleation cluster formations similar to the α-dimer in 1-butanol show a lower chemical shift for H3 (3.9) compared to the chemical shift of H3 in methanol and ethanol.

These differences in hydrogen peaks also explain clustering formation and nucleation of different hydrogen arrangements related with particular polymorphs from a solvent and are consistent with other analytical and modelling results which explain the effect of solvents on the polymorph outcome.

Further ^{1}H NMR studies, as a titration of increasing sulphathiazole concentration in solvents, could provide more insight in to interactions between sulphathiazole and solvent molecules in saturated solutions. Since this work was conducted, the use of NMR to probe solution behaviour has been further developed. For example, in a similar study, Lohani et al (2011) used ^{1}H NMR to investigate the role of acetonitrile and ethanol in selection of Indomethacin polymorphs. From the results of ^{1}H NMR studies at different concentrations of Indomethacin in deuterated acetonitrile and ethanol, they suggested that acetonitrile favours the nucleation of stable γ-indomethacin as the critical supersaturation required to overcome the energy barrier for the nucleation is much lower in acetonitrile than in ethanol. Whereas, the nucleation of metastable α-indomethacin was favoured only at high supersaturation from ethanol solution as it required higher critical supersaturation to overcome the high energy barrier for nucleation. However, in this work, the current ^{1}H NMR studies were simple, preliminary investigations which successfully indicated differences in solution behaviour between those solvents that stabilize Form I containing the *α*-dimer and those that stabilize other forms containing the β-dimer (Figure 3.32).Further investigation of sulphathiazole interaction with solvent molecules and impact of that on polymorph selection is discussed in chapter 4 using molecular modelling.

3.7   Conclusion

The solvent dependence of polymorph generation is well-established for sulphathiazole (Blagden et al 1998; Anwar et al, 1989). This study examined the effect of a range of alcohols on polymorph selection of sulphathiazole and investigated the role of alcohol functional group in the polymorph selection process. Samples from all experiments were characterized using optical microscopy, PXRD, DSC, IR, and single crystal X-ray diffraction for their polymorphic identity. Results showed that solvent had a significant impact on polymorph selection. In common with 1-propanol, 1-butanol was found to stabilize the most metastable Form I, containing the α-dimer, without showing any nucleation or transformation to more stable polymorphs II, III and IV. Even the seeding of more stable polymorphs (II, III, and IV) in 1-propanol could not prompt the transformation of Form I in to any of the more stable forms. Whereas, methanol, 2-propanol, and ethanol did not stabilize Form I but stabilized Forms II, III, and IV, respectively, containing the β-dimer as their basic unit. It was observed by optical microscopy and PXRD that all samples initially crystallised as most metastable form I and then showed transformation to the more stable forms II, III, and IV when 2-propanol, methanol and ethanol were used as solvents.

The formation of the β-dimer is necessary for the transformation into the more stable forms II, III, and IV. Thus, for Form I to be kinetically stable, the formation of the α-dimer in solution must be favored and the formation of the *β*-dimer must be inhibited. In this study, where long chain alcohols (1-propanol and 1-butanol) stabilized α-dimer based Form I and shorter chain alcohols (methanol, ethanol and 2-propanol) stabilized β-dimer based Forms II, III, and IV suggest that it is not only the alcohol functionality but also the steric effects of the alkyl chain that contributed to the effect. The ^{1}H NMR studies (Figure 7) also indicate differences in solution behavior between those solvents that favor the stabilization of the form containing the *α*-dimer and those that favor the formation of forms containing the β-dimer. These results clearly indicate that solvents play an important role in the selection of metastable and stable polymorphs of sulphathiazole.

Also, the impact of grinding on the metastable Form I was investigated. It was observed that Form I was transformed into more stable Forms II to IV with grinding.

Chapter 4   Molecular modelling of sulphathiazole dimers

4.1   Introduction

The experimental results (chapter 3) indicated that 1-propanol and n-butanol stabilized Form I of sulphathiazole; whereas, methanol, ethanol, and 2-propanol resulted in the stabilisation of sulphathiazole Forms II, III and IV. It was also observed that initially Form I was nucleated and crystallised from all the solvents. However, Form I dissolved very quickly, within minutes of nucleation, with the crystallization of more stable Forms II to IV in the case of methanol, ethanol, and 2-propanol respectively. These polymorphic changes from the metastable to the stable form with time also indicated that sulphathiazole obeys Ostwald's rule of stages. As reported previously (Section 1.11.2), the Form I structure contains the α-dimer as its basic unit, whereas Forms II to IV contain the β-dimer as the basic unit. Hence, for the nucleation of Form I in solution, formation of the α- dimer would be required and for the nucleation of Forms II to IV in solution, formation of the β-dimer would be required. In the experimental results presented in Chapter 3, sulphathiazole crystallization from 1-propanol and n-butanol did not show nucleation of Forms II to IV, which requires the formation of the β-dimer. The 1H NMR studies also indicated differences in solution behaviour between those solvents that inhibit the formation of β-dimer and those that favor its formation (Parmar et al, 2007). These results may suggest unfavourable conditions for the formation of β-dimer in 1-propanol and n-butanol. Therefore the role of solvent was investigated thermodynamically using molecular modelling tools for the formation of dimers. In the current study, initial molecular modelling was performed using the Cerius2 and Mopac software packages and more detailed modelling was performed via the grid-based systematic search approach (Hammond et al, 2006).

4.2   Molecular modelling of pre-nucleation clusters using Cerius2 and Mopac

Solute molecules form clusters with solvent molecules prior to the nucleation, which are called pre-nucleation clusters (Blagden et al, 1998). For a particular polymorph to depend on solvent, these clusters may mimic the structural features of the polymorph. Hence pre-nucleation clusters of sulphathiazole with 1-propanol and 1-butanol may resemble α dimers, which is basic structural unit of Form I. Whereas, pre-nucleation clusters of sulphathiazole

with methanol, ethanol, and 2-propanol may resemble β dimers, which is basic structural unit of Forms II to IV. The energy of proposed pre-nucleation clusters of sulphathiazole, based on α and β dimers in the presence of each of the solvents, was investigated using Cerius2 and Mopac software packages. The details of Cerius2 and Mopac applications and calculations are described in Section 2.4.8.

The crystal structures of the polymorphs of sulphathiazole were adopted from the Cambridge Crystallographic Database (CCDC) and imported into the Cerius2 suite. The α- and β-dimers were selected from the crystal structure of sulphathiazole polymorphs I (CCDC reference – SUTHAZ01) and III (CCDC references SUTHAZ02) and loaded into Cerius2 visualiser windows separately. Thereafter the Dreiding force field was applied to both dimers, following which both dimers were energetically minimized (Figure 4.1 and 4.2).
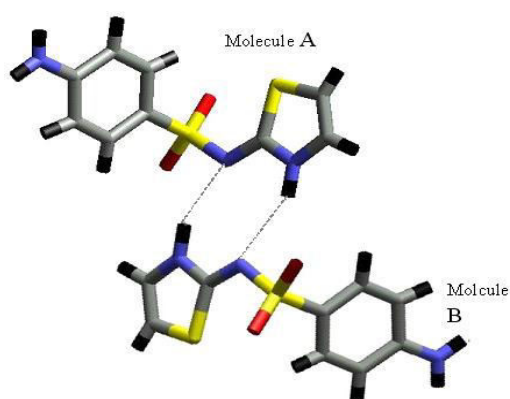
Figure 4.1 Energetically minimized α-dimer
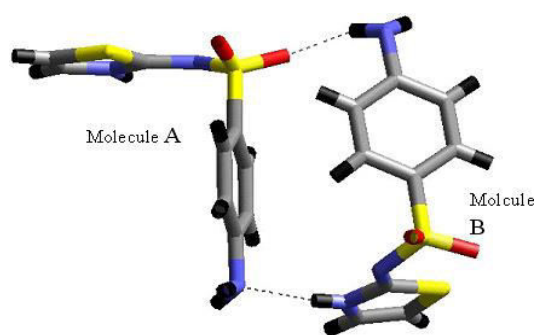
Figure 4.2 Energetically minimized β-dimer

As shown in Figures 4.1 and 4.2, the α- and β-dimers are formed by two hydrogen bonding interactions between molecules A and B. The energy released, when these bonds are created and form a dimer, is represented as the interaction energy, E_{int}. To calculate the interaction energies of α- or β-dimers, the energies of formation of the individual molecules (A and B) were subtracted from the energy of formation of the dimer (Equations 4.1). Here, the energies of formation for the individual molecules (A and B) were calculated at fixed position from dimers. The formation energies were calculated using the MOPAC module within Cerius2. MOPAC is a general purpose semiempirical molecular orbital package for the study of solid state and molecular structures and reactions (Dewar et al, 1985). MOPAC provides the selection to choose a task and a method. Task and methods are the most fundamental

131

parameters that define the characteristics for a MOPAC based calculation. In the current study, single point energy and PM3 (Parameterized Model number 3) were selected as task and method, respectively, for the calculation. The formation energy of α/β dimer, and individual energies of molecules A and B of the dimer are listed in Table 4.1. These values were used in equation 4.1 to calculate the interaction energies of α/β dimers.

$$E_{int} = \begin{pmatrix} Total\ energy \\ of\ cluster\ or\ dimer \end{pmatrix} - \begin{pmatrix} Energy\ of \\ formation \\ of\ molecule\ A \end{pmatrix} - \begin{pmatrix} Energy\ of \\ formation\ of \\ molecule\ B \end{pmatrix} \quad \text{(Equation 4.1)}$$

Table 4.1   Calculated energies of dimers and their individual molecules using MOPAC

Dimer	Total formation energy of dimer	Energy of formation for molecule A	Energy of formation for molecule B	Interaction Energy (Eint)
α	204.09 kcal/mol	109.36 kcal/mol	109.36 kcal/mol	-14 kcal/mol
β	292.48 kcal/mol	157.24 kcal/mol	157.24 kcal/mol	-22 kcal/mol

As shown in Table 4.1, the interaction energy for the α-dimer was calculated as -14 kcal/mol using Equation 4.1; whereas, the interaction energy for the β-dimer was observed to have a lower value (compared to the α-dimer) of -22 kcal/mol. This indicates that the β-dimer is thermodynamically more stable than the α-dimer. This is expected as it is known from the previous studies (Anwar et al, 1989; Blagden et al, 1998a) that structures containing β-dimer (Form II to IV) are thermodynamically more stable than Form I, which contains only the α-dimer.

4.2.1   Pre-nucleation clusters of α and β dimers with solvent molecule

To try to model the influence of the solvent on the tendency to form either α or β-dimers, and therefore to influence polymorph nucleation, clusters were generated based on either the α-structure or the β-structure with a solvent molecule inserted between the dimer pairs as shown in Figures 4.5 and 4.10. The clustering together of solute moleclues in the solution phase by interacting with each other and solvent can make a stable size cluster in solution which can nucleate as a crystal. This is called a pre-nucleation cluster (Section 1.4).

The possible location of the solvent molecule in such a cluster was determined from preliminary calculations where the lowest energy position from ten proposed positions was chosen as the preferred location of the solvent molecule. These ten proposed positions of the

solvent molecule were selected arbitrarily in three dimensional space such that a hydrogen bonding interaction could form with both sulphathiazole molecules involved in the α or β-dimer formation. (This group of molecules will be referred to as a "cluster"). These preliminary calculations at ten proposed positions were performed with methanol being selected as the solvent molecule.

4.2.1.1 Pre-nucleation cluster of α-dimer

In the case of the α-dimer, two molecules of sulphathiazole are connected to each other by N---H hydrogen bonds. Methanol, as a solvent molecule, was inserted into 10 different positions around N---H hydrogen bonds of the α-dimer so that methanol could hydrogen bond with both molecules of the α-dimer across N and H sites to make an α-solvated cluster (as illustrated in Figure 4.5 for position 5). The interaction energies of each of the α-solvated clusters, with a methanol molecule at 10 different positions, were calculated using Equation 4.2. In this equation total energy of this α-solvated cluster and individual energies of molecules were calculated at fixed positions.

$$E_{int}\begin{pmatrix} solvated \\ \alpha \\ cluster \end{pmatrix} = \begin{pmatrix} Total\ energy \\ of\ solvated \\ \alpha\ cluster \end{pmatrix} - \begin{pmatrix} Energy \\ of \\ formation \\ of\ \alpha\ dimer \\ molecule\ A \end{pmatrix} - \begin{pmatrix} Energy \\ of \\ formation \\ of\ \alpha\ dimer \\ molecule\ B \end{pmatrix} - \begin{pmatrix} Energy \\ of \\ formation \\ of\ solvent \\ (methanol) \\ molecule\ C \end{pmatrix}$$

(Equation 4.2)

The calculated energies of the ten positions of the methanol molecule, using Equation 4.2, are shown in Table 4.2 for the solvated α-cluster. Methanol was inserted in ten positions with fixed orientation (Table 4.2).

As shown in Table 4.2, from the above ten positions, position 5 displays the lowest energy, which would be the thermodynamically most preferred, from the ten positions, for a methanol molecule to interact with the α-dimer (Figure 4.3).

Table 4.2   Calculated interaction energy, E_{int}, of solvated α-cluster with a methanol molecule at 10 proposed positions (all the energies are kcal/mol)

Position	Total energy of cluster	Energy of formation for molecule A kcal /mol	Energy of formation for molecule B kcal /mol	Energy of formation for molecule C kcal /mol	Interaction Energy (E_{int}) kcal /mol
1	677.57	109.36	109.36	14.2	444.65
2	1756.98	109.36	109.36	14.2	1527.06
3	755.52	109.36	109.36	14.2	522.6
4	579.43	109.36	109.36	14.2	346.51
5	463.38	109.36	109.36	14.2	230.46
6	522.32	109.36	109.36	14.2	289.4
7	611.82	109.36	109.36	14.2	378.9
8	787.45	109.36	109.36	14.2	554.53
9	979.19	109.36	109.36	14.2	746.27
10	1211.87	109.36	109.36	14.2	978.95
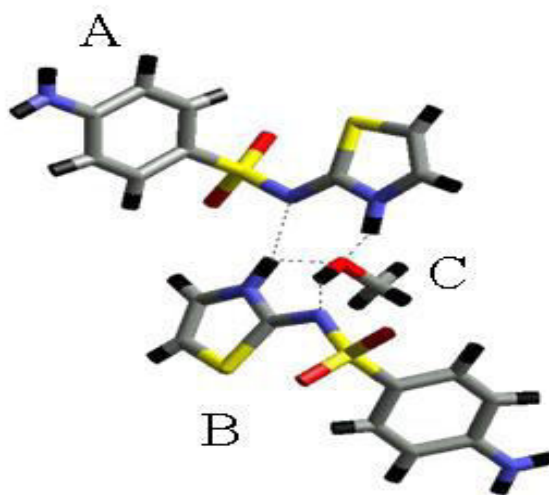
Figure 4.3   Solvated α-cluster with methanol being the solvent at lowest energy position 5

Hence, this position was selected as a thermodynamically preferred position and used as the preferred location for other solvent molecules (2-propanol, n-butanol, ethanol, and 1-propanol) to make solvated clusters with the α-dimer. The interaction energies of solvated α-clusters with 2-propanol, n-butanol, ethanol, and 1-propanol at the preferred location 5 were calculated in a similar manner using Equation 4.2 by replacing the methanol molecule with the respective solvent molecules as shown in Figure 4.4 to 4.7 and Table 4.3.
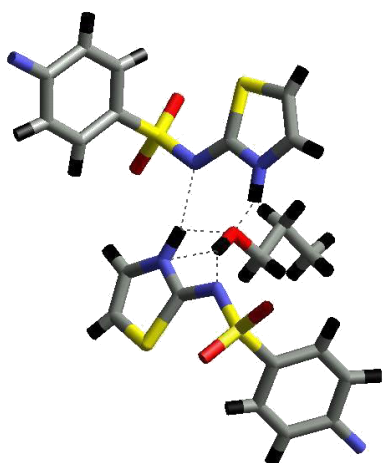
Figure 4.4 Solvated α-cluster with 1-propanol being the solvent at position 5
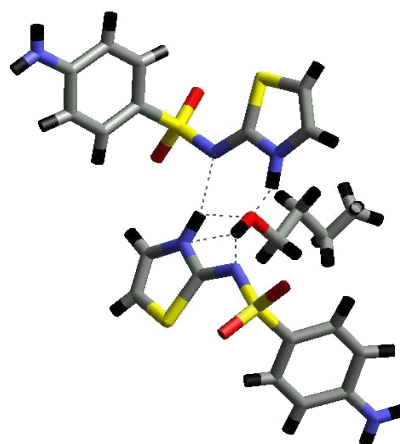
Figure 4.5 Solvated α-cluster with n-butanol being the solvent at position 5
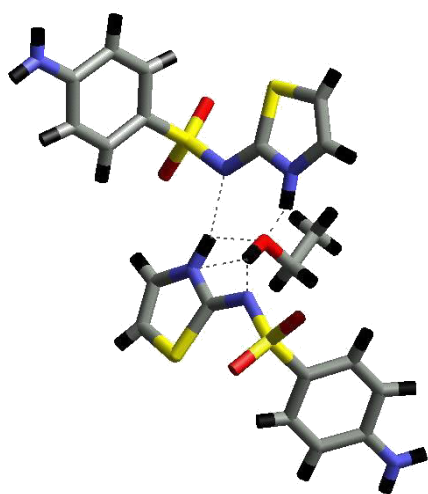
Figure 4.6 Solvated α-cluster with ethanol being the solvent at position 5
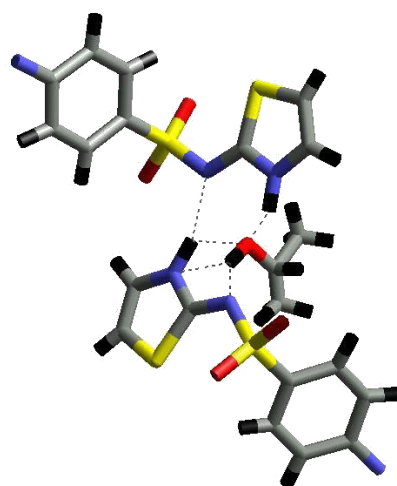
Figure 4.7 Solvated α-cluster with 2-propanol being the solvent at position 5

Table 4.3   Calculated E_{int} (Kcal/mol) of solvated α-clusters with n-butanol, 1-propanol, ethanol, 2-propanol and methanol at thermodynamically preferred position 5

Solvent molecule	Total energy of cluster kcal /mol	Energy of formation for molecule A kcal /mol	Energy of formation for molecule B kcal /mol	Energy of formation for molecule C kcal /mol	Interaction Energy (Eint)
1-propanol	486.05	109.36	109.36	15.6	236.13
n-butanol	425.86	109.36	109.36	16.2	190.94
ethanol	485.52	109.36	109.36	15.1	251.70
2-propanol	593.91	109.36	109.36	18.1	357.09
methanol	463.38	109.36	109.36	14.2	230.46

4.2.1.2 Pre-nucleation cluster of β-dimer

In the case of the β-dimer, two molecules of sulphathiazole are connected to each other by N1---H3 and O2---H1 hydrogen bonds. Out of these two hydrogen bonds, O2---H1, is presented in the crystal structure of all sulphathiazole Forms (I to IV), (Section 1.11.2); hence this bonding would not be the subject of solvent dependency. Therefore, methanol, as a solvent molecule, was inserted into 10 different positions around N1---H3 hydrogen bonds of the β-dimer so that the methanol molecule could hydrogen bond with both β-dimer molecules across N1 and H3 sites to make the β-solvated cluster (as illustrated in Figure 4.10 for position 8). The interaction energies of β-clusters, with methanol molecule at 10 different positions, were calculated in a similar manner using Equation 4.3. In this equation total energy of this β-solvated cluster and individual energies of molecules were calculated at fixed positions.

$$
E_{int}\begin{pmatrix} solvated \\ \beta \\ cluster \end{pmatrix} = \begin{pmatrix} Total\ energy \\ of\ solvated \\ \beta\ cluster \end{pmatrix} - \begin{pmatrix} Energy \\ of \\ formation \\ of\ \beta\ dimer \\ molecule\ A \end{pmatrix} - \begin{pmatrix} Energy \\ of \\ formation \\ of\ \beta\ dimer \\ molecule\ B \end{pmatrix} - \begin{pmatrix} Energy \\ of \\ formation \\ of\ solvent \\ (methanol) \\ molecule\ C \end{pmatrix}
$$

(Equation 4.3)

Calculated energies of interaction of solvated β-cluster with methanol at ten different positions using equation 4.3 are shown in Table 4.4.

Table 4.4   Calculated interaction energy (kcal/mol) of solvated β-clusters with methanol molecule at 10 proposed positions

Position	Total energy of cluster	Energy of formation for molecule A	Energy of formation for molecule B	Energy of formation for molecule C	Interaction Energy (Eint)
1	1439.98	157.24	157.24	19.4	1106.1
2	1019.54	157.24	157.24	19.4	685.66
3	1265.89	157.24	157.24	19.4	932.01
4	1338.88	157.24	157.24	19.4	1005
5	1085.18	157.24	157.24	19.4	751.3
6	755.58	157.24	157.24	19.4	421.7
7	640.91	157.24	157.24	19.4	307.03
8	558.00	157.24	157.24	19.4	224.12
9	666.04	157.24	157.24	19.4	332.16
10	985.71	157.24	157.24	19.4	651.83

As shown in Table 4.4, from the above ten positions position 8 displays the lowest energy, and would be the thermodynamically most preferred position, amongst all the ten positions, for a methanol molecule to interact with the β-dimer (Figure 4.8).
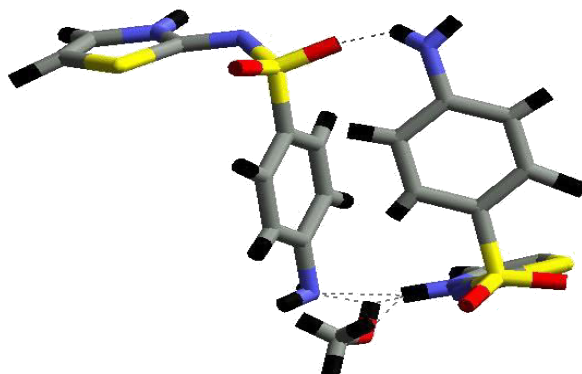
Figure 4.8 **Solvated β-cluster with methanol being the solvent at lowest energy position 8**

Hence, this position was selected as a thermodynamically preferred position and used as the preferred location for other solvent molecules (2-propanol, n-butanol, ethanol, and 1-propanol) to make solvated clusters with the β-dimer. The interaction energies of solvated β-clusters with 2-propanol, n-butanol, ethanol, and 1-propanol at the preferred location 8 were calculated using Equation 4.3 by replacing methanol molecule with the respective solvent molecule as shown in Figures 4.9 to 4.12 and Table 4.5.
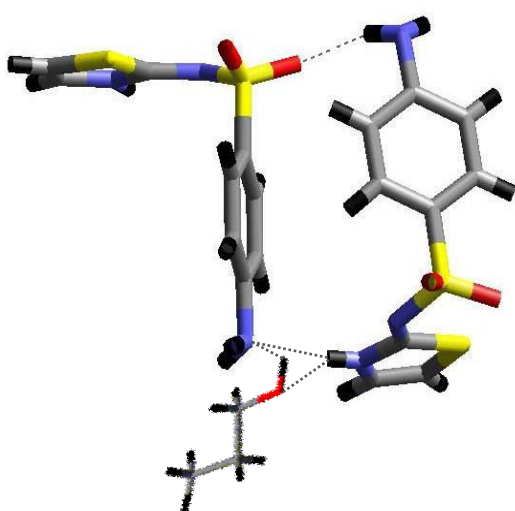
Figure 4.9 Solvated β-cluster with 1-propanol being the solvent at position 8
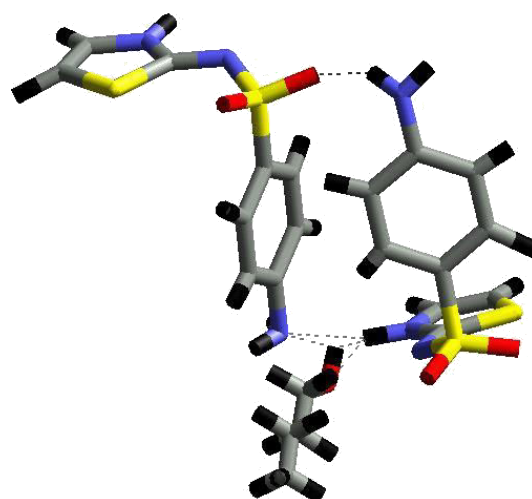
Figure 4.10 Solvated β-cluster with n-butanol being the solvent at position 8
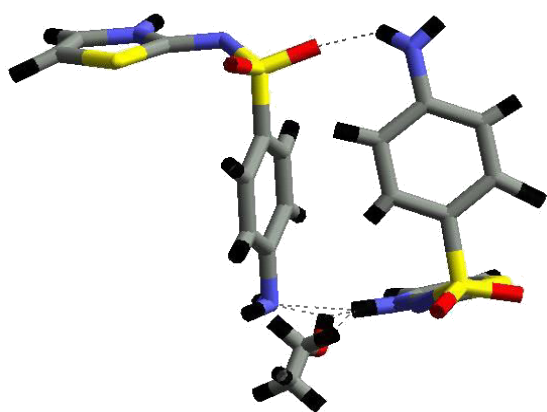
Figure 4.11 Solvated β-cluster with ethanol being the solvent at position 8
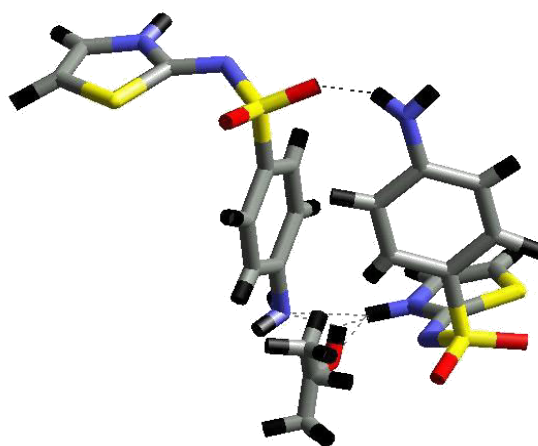
Figure 4.12 Solvated β-cluster with 2-propanol being the solvent at position 8

Table 4.5   Calculated E_{int} (Kcal/mol) of solvated β-clusters with n-butanol, 1-propanol, ethanol, 2-propanol, and 2- propanol at thermodynamically preferred position 8

Solvent molecule	Total energy of cluster kcal /mol	Energy of formation for molecule A kcal /mol	Energy of formation for molecule B kcal /mol	Energy of formation for molecule C kcal /mol	Interaction Energy (Eint) kcal /mol
1-propanol	759.29	157.24	157.24	24.90	419.91
n-butanol	704.99	157.24	157.24	28.70	361.81
ethanol	574.84	157.24	157.24	22.50	237.86
2-propanol	675.29	157.24	157.24	29.10	331.71
methanol	558.00	157.24	157.24	19.20	224.12

As shown in Tables 4.3 and 4.5, when the solvating molecule was chosen to be methanol, ethanol or 2-propanol, the β-cluster was calculated to have a lower energy of interaction compared to the α-cluster, indicating the β-cluster to be more thermodynamically stable than the α-cluster. This predicts that clustering similar to the β-dimer would be present in solution, and provide a route to the nucleation of polymorphs based on the β-dimer, namely Forms II, III, and IV. This is in agreement with the experimental observation that in these solvents, whilst Form I nucleates initially, one or more of the other forms nucleates, grows and is maintained in solution, as Form I dissolves.

The position is reversed for 1-propanol and 1-butanol. The interaction energy of the β-cluster has a much higher value than the α-cluster, suggesting that β-clusters would not form in

solution, and polymorphs containing the β-dimer would not be nucleated. Again this is in agreement with the experimental observation that Form I nucleates and remains stable in 1-propanol and 1-butanol solution, with no transformation or nucleation of any other polymorphs. The H[1] NMR studies (Section 3.6) also indicate differences in solution behaviour between those solvents that inhibit the formation of the β dimer, and those that favour its formation.

These preliminary calculations indicate that the ability of the solvent to inhibit transformation may be linked to the energies of substrate-solvent interactions, and show that clustering in solution may be thermodynamically controlled (Parmar et al, 2007). However these preliminary calculations for α/β dimers interactions with a solvent molecule were performed at 10 fixed positions. Therefore a more detailed systematic search approach was undertaken (section 4.3) that uses a grid based search system (Hammond et al, 2006; Hammond et al, 2003) of translations and rotations. This approach allowed us to access all the possible intermolecular packing arrangements between the sulphathiazole dimer and solvent molecule in direct space on the basis of atom-atom separation distance and intermolecular potential pair energy.

4.3   The systematic search approach for molecular modelling of the solvated structure

Following the results of preliminary calculations the molecular modeling study was expanded via the grid-based systematic search approach for the calculation of interaction energies of solvated clusters. The systematic search approach has been successfully applied to predict crystal structure of various materials from knowledge of unit cell parameters and space group alone, and to solve the crystal structure of various materials from the powder diffraction data (Kutzke et al, 2000; Smith et al 2001; Hammonds et al, 2003). The systematic search approach uses a grid based search system of translations and rotations to assess all the possible intermolecular packing arrangements or interactions in direct space. Hammond et al (2006) used the systematic search method to predict the host/counter ion binding for an organic salt of 3,4,6,7,8,9-Hexahydro-2H-pyrimido pyrimidinium (host molecule) with acetate (counter ion). In this study, dimer pairs between host and counter ion were identified by rotating and translating one molecule with the other at a fixed position. This grid-based

dimer search results in the generation of very large numbers of molecular pairs between host and counter ion. These pairs were further optimized and clustered to subsequently obtain the molecular pair with the lowest energy of formation, which was further analyzed and examined in the grid-based systematic search procedure (Hammond et al, 2003) to obtain the best match with the known salt structure from the CCDC database.

This study uses the principle of the systematic search method to identify all solvated pairs between a sulphathiazole dimer and a solvent molecule.

4.3.1 Method of GRID based systematic search

In this method, the sulphathiazole dimer (α or β) was fixed at one co-ordinate location (used as a fixed molecule), while the solvent molecule was chosen as the mobile molecule. Potential molecular clustering (molecular pairs) between the sulphathiazole dimer and the solvent molecule was studied by rotating and translating a mobile solvent molecule in space at each grid cell around a fixed sulphathiazole dimer. The solvent molecule was subjected to a grid based search, defined by three translational (x, y, and z) and three rotational degrees of freedom (θ_x, θ_y, and θ_z) as shown in Figure 4.13.
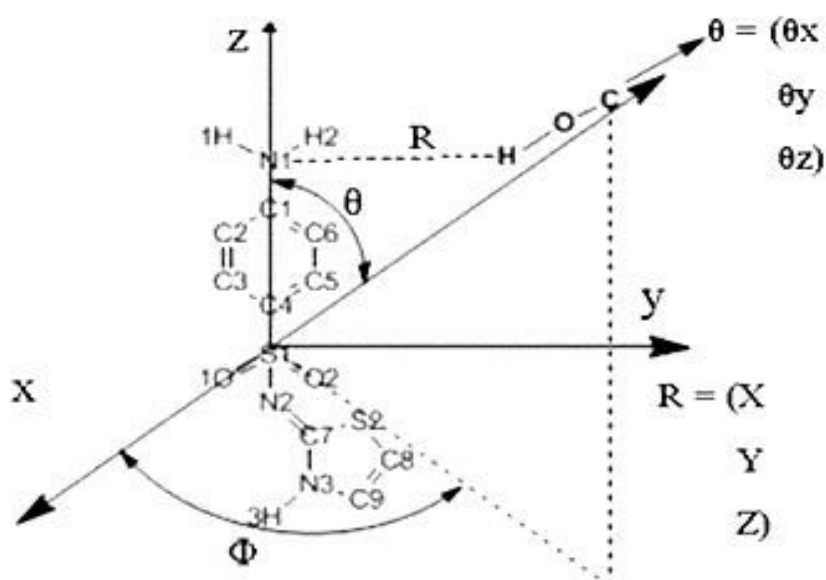
Figure 4.13   Sulphathiazole α-dimer (fixed molecule) and a methanol molecule (mobile molecule) in three dimensional space

Cartesian spherical polar coordinates were used with translation steps defined by a translation magnitude, λ, and a unit vector defined by two spherical polar angles (θ, ϕ) with $\Delta\theta$ and $\Delta\phi$ being the angular intervals defining distribution of similar sized grid cells on the spherical surface. The new atomic co-ordinates of the mobile molecule after translation and rotation were calculated using Equation 4.4.

$$\begin{pmatrix} x_i' \\ y_i' \\ z_i' \end{pmatrix} = M \begin{pmatrix} x_i \\ y_i \\ z_i \end{pmatrix} + \lambda R \qquad \text{(Equation 4.4)}$$

where, x_i, y_i, and z_i are the atomic co-ordinates of the mobile solvent molecule at its starting location, x_i', y_i', and z_i' are the coordinates upon transformation; M is a rotation matrix (a function of θ_x, θ_y, and θ_z); R is the position vector of the centre of coordinates of the mobile molecule, and λ is a translation magnitude that is minimized with respect to the intermolecular-pair potential energy. For each translation direction, defined by the mobile molecule, the minimum separation distance between the centres of the fixed and mobile molecules was determined by van der Waals radii. The separation distance was then used as the starting point for a one dimensional minimization of the pair potential energy to determine the final location of the mobile molecule for a given orientation and direction of translation.

The Dreiding force field (Mayo et al, 1990) and its parameters were used for the potential energy calculation. Atomic charges were calculated using the PM3 method within MOPAC (Dewar et al, 1985) function of Cerius2 for the single point energy task. The intermolecular potential energy was calculated from the Equation 4.5.

$$E = \sum_{i=1}^{M_i} \sum_{j=1}^{M_j} \left[\left(-\frac{A_{ij}}{r_{ij}^6} + \frac{B_{ij}}{r_{ij}^{12}} \right) + \left(-\frac{C_{ij}}{r_{ij}^{10}} + \frac{D_{ij}}{r_{ij}^{12}} \right) + \frac{g_i g_i}{D.r_{ij}} \right] \qquad \text{(Equation 4.5)}$$

Where A_{ij}, B_{ij}, C_{ij}, and D_{ij} are Dreiding force field parameters for atoms i and j in the first and second molecules; g_i and g_j are atomic point charges; D is the dielectric parameters, and r_{ij} is the central distance between atoms i and j.

In this study, the step size of the polar angle, θ, was selected as 30^0, and the step size of the corresponding polar angle, ϕ, was calculated from the relationship $\phi = \Delta\theta/(\pi\sin\theta)$, with $0\ ^{\circ} < \theta < 180\ ^{\circ 0}$, which divided the whole spherical surface into grid cells of the same size. The step size for the three rotational angles was set at 3^0C with range of variation from 0° to 360°. The energy cut off value was chosen as -3 kcal/mol so any pairs (cluster between sulphathiazole dimer and solvent molecule) resulting in an intermolecular energy greater than this value were removed from the calculation.

4.3.2 Evaluation of experimental method

The systematic search approach samples the potential energy surfaces at a set of equivalent points and with equivalent levels of intensity for a given solvent molecule. Hence, for a given solvent molecule it is reasonable to compare directly the distributions of pair energies for interactions with the different sulphathiazole dimers. An underlying assumption of the approach is that the configurations represented by grid-points in the search are, *a priori*, equally likely to be sampled by a given solvent molecule in a given solution environment. This seems a reasonable assumption given that we are modelling small, highly-mobile molecules. So if the grid points permit a representative sampling of possible interaction energies, then the systematic searches can indicate which dimer of sulphathiazole is solvated more effectively by a given solvent molecule.

A further factor which should be noted is that given the grid points are evaluated sequentially, two configurations that are favourable in energy may be mutually exclusive due to overlapping positions of the solvent molecule but, nevertheless, are both counted in compiling the histogram of pair energies. There are two approaches to this problem: firstly, the simple approach is to assume that the number of mutually exclusive pairs is on average the same. Secondly, systematic searches, taking as a starting point the most favourable pair configurations and then searching on a second solvent molecule, could be used to evaluate the validity of the simple hypothesis but at substantially increased computational expense. Another consideration is whether to include multiple conformations for the conformationally flexible solvent molecules. To do so adds a further degree of freedom in the systematic

search for every torsion angle considered. However, this is tractable given the use of multiple processors and modularisation of the searches.

4.3.3 Results

A total of 2300 molecular pair structures were identified for each calculation between the sulphathiazole dimer (α or β) and a solvent molecule. The energy distributions for each of these calculations are plotted in Figure 4.14.

The numbers of pairs between a fixed dimer (α or β) and a mobile solvent molecule decrease with decreasing pair potential energy. This overall energy distribution is also presented in Table 4.8.
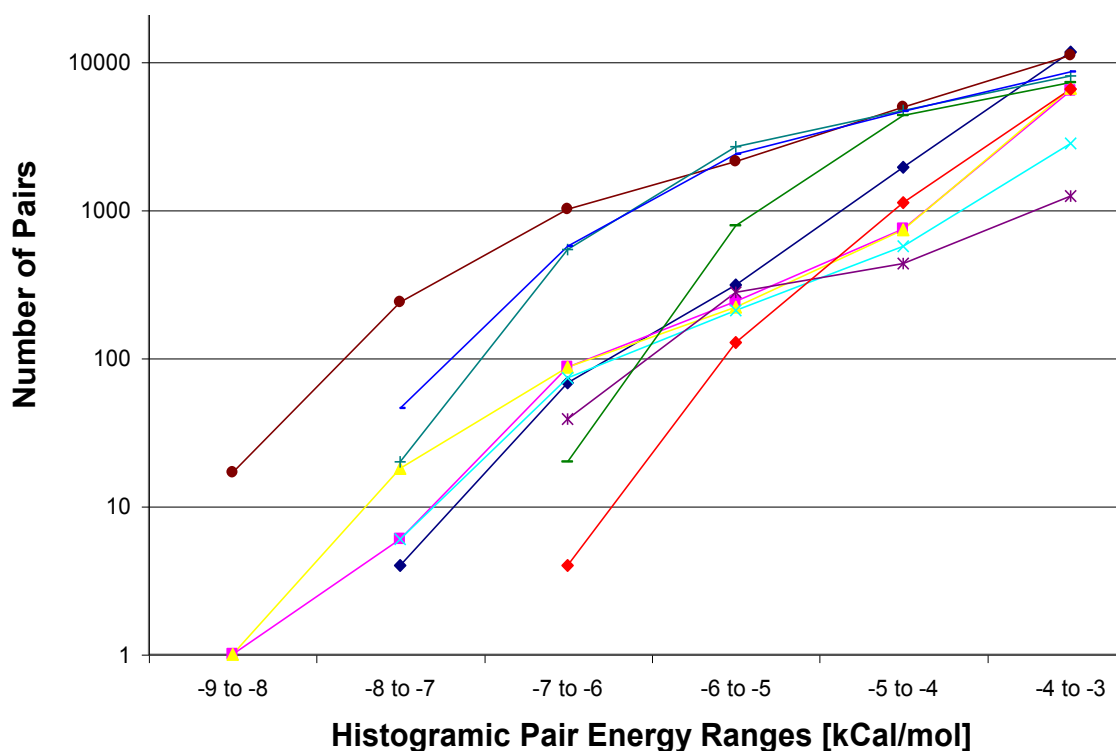
Figure 4.14 **Pair energy distributions for sulphathiazole dimers with alcohol molecules**

Key: energy distribution of α dimer with methanol, α dimer with ethanol, α dimer with 2-propanol, α dimer with 1-propanol, α dimer with 1-butanol, β dimer with methanol, β dimer with ethanol, β dimer with 2-propanol, β dimer with 1-propanol, β dimer with 1-butanol

The 23000 pairs, obtained from each calculation, were ranked in terms of their minimized lattice energy requirement for the formation of the solvated pair. The top 50 energetically favourable pairs (lowest energy pairs) or in other words the energetically most favourable 50 locations of a 1-butanol molecule to interact with the α dimer are shown in Figure 4.15.

Table 4.6   Energy distribution of all the α and β dimer pairs with solvent molecule obtained by Grid based systematic search method.

Energy Range [kCal/mol]	Number of Pairs (Evaluated Grid Points) with Energy in Histogramic Ranges at Intervals of 1 kcal/mol									
	Beta Dimer					Alpha Dimer				
	1-butanol	2-propanol	1-propanol	ethanol	methanol	1-butanol	2-propanol	1-propanol	ethanol	methanol
-9 to -8	0	1	0	0	0	17	0	1	0	0
-8 to -7	4	6	18	6	0	240	20	46	0	0
-7 to -6	68	87	87	74	39	1011	540	572	20	4
-6 to -5	311	241	220	210	277	2115	2688	2386	788	128
-5 to -4	1945	742	732	567	435	4959	4680	4617	4371	1129
-4 to -3	11729	6366	6637	2808	1236	11063	8090	8630	7220	6597
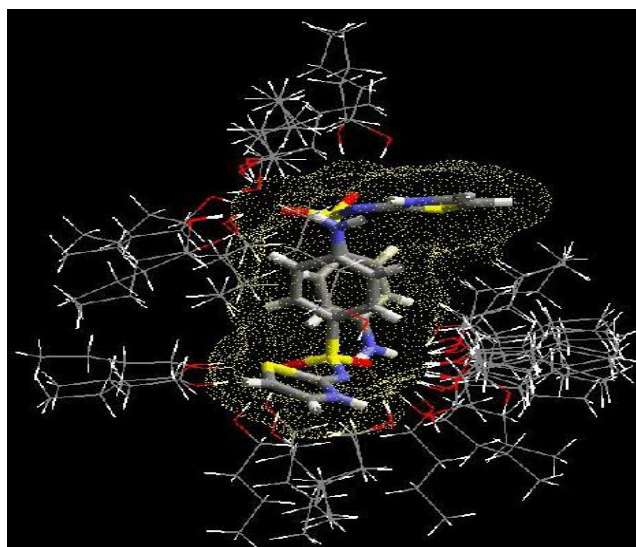
Figure 4.15   Thermodynamically favourable Top 50 pairs of interaction between α dimer and 1 butanol

Thermodynamically, the lower energy configurations of α and β-clusters are more favourable. Therefore all the pairs of sulphathiazole dimer with a given solvent molecule within the energy range of -9 to -6 Kcal/mol were considered as lower energy pairs (Table 4.6).

Within this lower energy range (-9 to -6 kcal/mol), a 1-butanol molecule made 1268 pairs of α-clusters with an α-dimer molecule; whereas, 1-butanol manifests only 72 pairs of the β-clusters with a β-dimer molecule. Similarly, 1-propanol made 618 pairs of α-clusters with the α-dimer molecule compared to 105 pairs of β-clusters with β-dimer within this lower energy range. This result indicates that 1-butanol and 1-propanol can more effectively solvate the α-cluster, which provides the route to the formation of α-dimer. This is consistent with the experimental observation that only metastable Form I, which is based on the packing of α-dimers, nucleates, grows and remains stable in 1-propanol and 1-butanol solution, with no transformation to or nucleation of any other polymorphs observed.

In the case of methanol, 39 pairs of β-clusters were observed between a β-dimer and a methanol molecule; whereas, only 4 pairs of α-clusters were observed between an α-dimer and a methanol molecule within the lower energy range of -9 to -6 kcal/mol. Similarly, for ethanol, 80 pairs of β clusters were observed compared to only 20 pairs of α-clusters between a dimer and ethanol molecule. This result indicates that methanol and ethanol can more effectively solvate the β-cluster, which provides the route to the formation of β-dimer. Again this is in agreement with the experimental observation that in these solvents, although the metastable Form I nucleates initially, one or more of the other Forms II to IV, which contain the β dimer as a basic unit, nucleates, grows, and is maintained in the solution, as Form I dissolves.

Interestingly, when 2-propanol was used as a mobile solvent molecule in a GRID search, it showed a great tendency to form α clusters with α-dimer (560 pairs) over the formation of β-clusters with β-dimer (94 pairs) within the overall lower energy range of -9 to -6 kcal/mol. However, as shown in table 4.8, between -9 to -8 kcal/mol, 2-propanol shows 1 pair of β-cluster compare to 0 pair of α-cluster, which also indicate the tendency of 2-propanol to solvate β-clusters. These results indicate that 2-propanol can effectively solvate the α-cluster and β-cluster, which provides the route to the formation of α-dimer and β-dimer. Experimentally, it was observed that the metastable Form I nucleates initially and stayed in

solution for more than 24 hours whilst Form III, which contains the β-dimer as a basic unit, nucleates, grows, and is maintained in the solution, as Form I dissolves. Metastable Form I shows slow rate of transformation to Form III when 2-propanol was used as a solvent. This is likely to be as a result of some other factor which inhibits nucleation of the β-dimer in comparison to ethanol and methanol.

Overall, in most of the cases, it could be said that the systematic search study was able to predict successfully and explain the solvent's ability to influence particular cluster formation (α or β) and hence the nucleation of a particular polymorph based on the chosen cluster within those solvents.

4.4   Conclusion

The thermodynamics of possible clustering of the solvent with the sulphathiazole molecules (dimers) prior to nucleation has been examined here in a molecular modelling study, which constituted a preliminary test using the Cerius2 suite and more detailed grid-based systematic search studies to determine whether there are thermodynamic differences in the interactions between the growth synthons that make up different structural patterns in the polymorphs. Both molecular modelling studies have successfully indicated that clustering between 1-propanol (or 1-butanol) and α-type dimers of sulphathiazole, which lead to the nucleation of Form I, are energetically favoured compared to clusters between 1-propanol (or 1-butanol) and β-type dimers, which promote the nucleation of other polymorphs.

Similarly, when short chain alcohols such as methanol, 2-propanol, and ethanol are modelled, the metastable α-dimer is not favoured thermodynamically, and thus consistent with the experimental observation that more stable polymorphs (Forms II, III, and IV) containing the β-dimer result from the crystallization. It was observed from experimental studies that methanol, ethanol, and 2-propanol also showed selection for a specific polymorph based on the β-dimer, i.e., Form II was crystallized from methanol, Form III was crystallized from 2-propanol, and Form IV was crystallized from ethanol solution. Each of these forms has the β-dimer as a basic unit; however, as explained in chapter 1, structural differences between them are subtle, relating to ring to ring contacts and contacts between the chains/sheets of β-dimers. It is possible that specific solvent interactions stabilise chain to chain contacts of

hydrogen bonding specific to each polymorph, and may have a similar energetic basis to those presented here.

Chapter 5 Controlling the morphology of sulphathiazole Form I

5.1 Introduction

Crystal morphology is defined as the external shape a crystal adopts, and is an important characteristic as many physical properties of crystals are implicitly dependent on their shape. Particularly, particle morphology can have a great affect on filterability, flowability, porosity, compactibility, and cohesiveness of powder. Adverse effects on any of these properties due to changes in particle morphology, can have a major impact on the manufacturing ability to formulate particles into finished products. For example, needle-shaped crystals display poor compaction behaviour and poor flowability compared to plate-shaped crystals. In addition, crystal morphology can also affect the performance characteristics of the drug product such as drug dissolution within the human body.

The different growth rates of crystal faces are responsible for the final morphology of a crystal (see Section 1.8). From previous literature (Section 1.8), it is known that a solvent, additive or impurity molecule has the ability to interact and bind preferentially to certain crystal faces. The use of solvent or additive can provide the route to control or engineer nucleation and crystal growth processes from the molecular level to design the crystal with desirable morphology (Weissbuch, and Lahav, 2001).

5.2   Control over the Morphology – Case of Sulphathiazole

Sulphathiazole Form I has been observed as a sharp, pointed needle-like morphology in the current studies as well as previous work. Examination of the fastest growing face (010) of form I (Blagden, 2001) indicates that this surface exposes the acceptor imine nitrogen (N2), sulfoxide oxygen (O2) groups and the donor amino hydrogen (H2). Molecules in a sulphathiazole Form I crystal are linked via α dimers and then extended into sheets and layers via amino hydrogen and sulfato oxygen bonding. Presumably this extended structure, linked through the α dimer in the (010) face, is responsible for the sharp, pointed morphology. It is known from experimental results described in Chapter 3

(page 73 to 79) that crystallization using 1-propanol and 1-butanol resulted in needle-like Form I crystals; whereas, using shorter chain alcohols (methanol and ethanol) resulted in plates of more stable Forms II to IV. Hence in this study, the effect of different ratios of 1-propanol with methanol (mixed solvent system) on crystal morphology and polymorph were investigated.

5.3 Characterization of sulphathiazole crystals obtained from cooling crystallization

Crystallization experiments of sulphathiazole by cooling were performed with different ratios of methanol and 1-propanol (mixed solvent system) as described in Section 2.2.2.1. Details of these experiments are listed in Table 2.4.

Samples, obtained from cooling crystallization, were analyzed by optical microscopy, Powder X-ray diffraction, and Differential Scanning Calorimetry for morphological and polymorphic analysis.

5.3.1 Morphological Analysis

Morphologies were observed periodically under a microscope throughout the experiment in order to observe the nucleation, growth and polymorphic transformation of the crystals. These time resolved morphologies of crystals are shown in Figures 5.1 to 5.8.
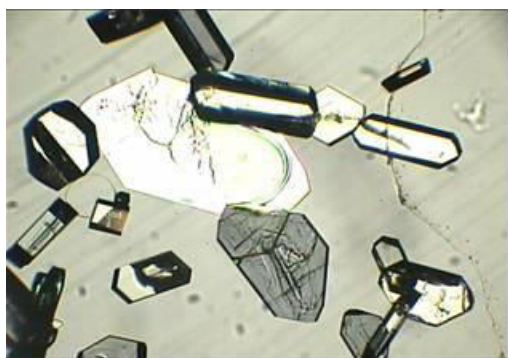
Figure 5.1   crystals obtained from crystallization in 100 % methanol
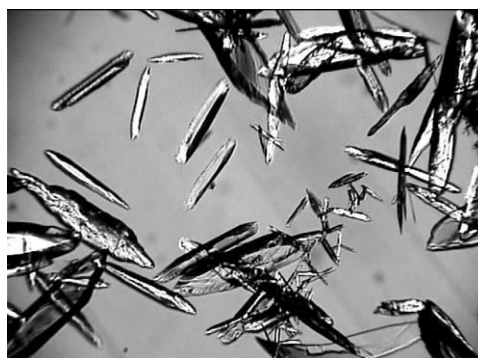
Figure 5.2   crystals obtained from crystallization in 100 % 1-propanol
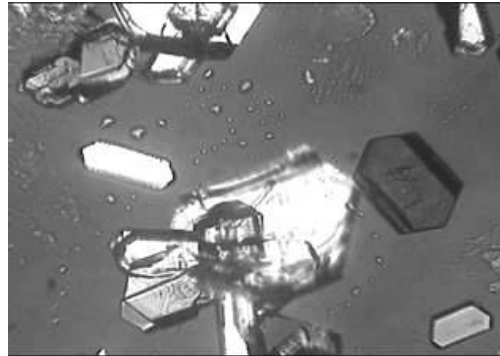
(a)   **(b)**

Figure 5.3 Crystals obtained from 80:20 ratios of methanol and 1-propanol solution; (a) within 10 minutes of nucleation, and, (b) 1 hour after nucleation
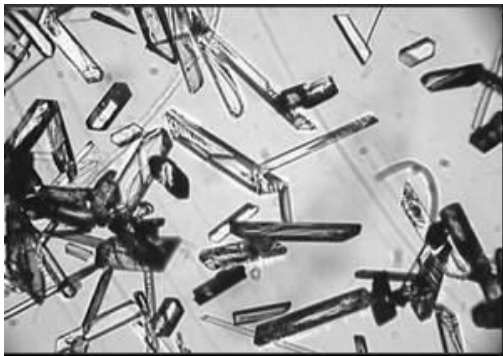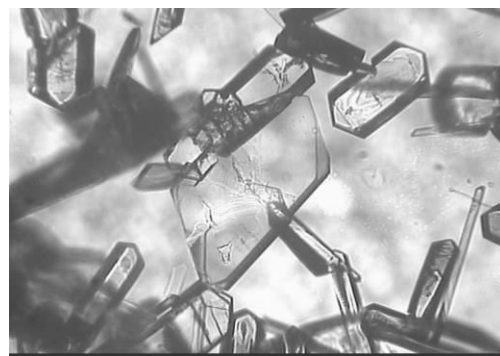
(a)   **(b)**

Figure 5.4 Crystals obtained from 60:40 ratios of methanol and 1-propanol solution; (a) within 10 minutes of nucleation, and, (b) 2 h after nucleation

(a)   **(b)**   **(c)**

Figure 5.5 Crystals obtained from 50:50 ratios of methanol and 1-propanol solution; (a) within 10 min of nucleation, (b) 1h after nulceation, and (c) 2 h after nucleation.
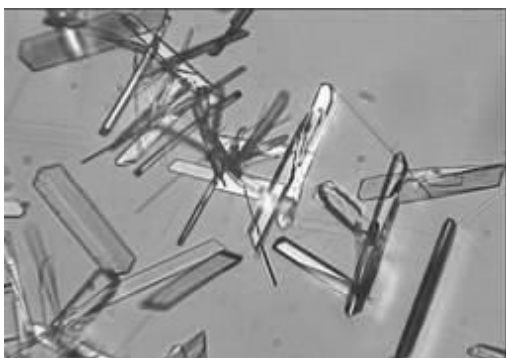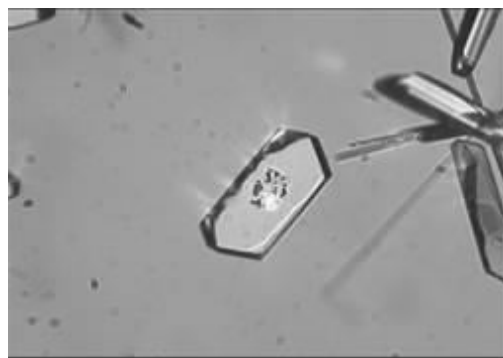
(a)   (b)

Figure 5.6 Crystals obtained from 40:60 ratios of methanol and 1-propanol solution; (a) within 10 min of nucleation, and (b) 1h after nucleation
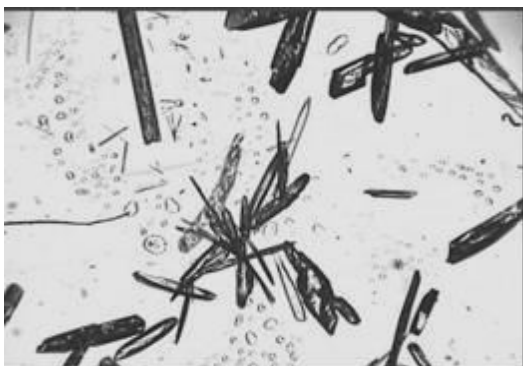
(a)   (b)

Figure 5.7 Crystals obtained from 20:80 ratios of methanol and 1-propanol solution; (a) within 10 min of nucleation, and (b) 1h after nucleation
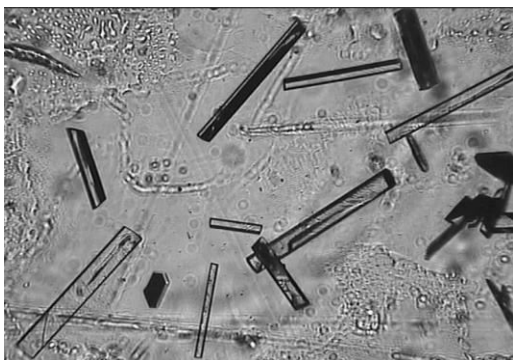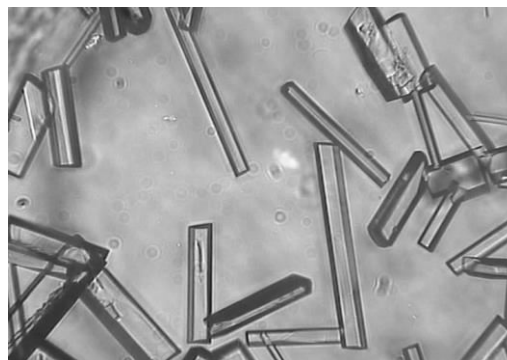
(a)   (b)

Figure 5.8 Crystals obtained from 10:90 ratios of methanol and 1-propanol solution; (a) within 10 min of nucleation, and (b) 1h after nucleation

It has already been established (See Chapter 3) that 1-propanol produces Form I crystals, which are the needle-like crystals as shown in Figure 1b and methanol produces hexagonal thick plates as shown in Figure 1a, which are identified as the more stable Form II (Section 3.3).

When 80:20, 60:40, 50:50, or 40:60 ratio of methanol: 1-propanol was used as the crystallization solvent, small hexagonal plates and needles were observed within 10 minutes of nucleation (Figure 5.3a, 5.4a, 5.5a, and 5.6a). The distribution of hexagonal plates and needles in these samples could be related to the percentage of methanol and 1-propanol used in the crystallization solvent. From previous experiments it is known that methanol favors the crystallization of thick hexagonal Form II crystals; whereas 1-propanol favors the crystallization of Form I needles. In case of 80:20 ratio (Figure 5.3a), the higher percentage of methanol (80 %) could be responsible for the dominant presence of hexagonal plates compared to a few needles due to the smaller percentage of 1-propanol. The numbers of needles, at 10 minutes after nucleation, were increased with the increased ratio of 1-propanol in the crystallisation solvent (Figure 5.4a, 5.5a, and 5.6a). All samples observed 1-2 h after nucleation showed the disappearance of needles and presence only of hexagonal plates. This suggests that even 60 % 1-propanol was not able to stabilize kinetically the most metastable Form I for a long period and Form I needles were seen to transform into the thermodynamically more stable hexagonal plates (in accordance with Ostwald's rule) due to the influence of methanol in the solution.

When 20:80 methanol: 1-propanol was used as a solvent, mainly small, sharp needles were observed as shown in Figure 5.7a. Eventually, after 1h, elongated hexagonal plates were also observed with needles as shown in Figure 5.7b. The dominant presence of 1-propanol in the solvent was able to stabilize many needles in the sample even after 1 h. However, 20 % methanol was also able to transform many of those needles, into elongated plates,. Hence the sample, even after one hour, showed the presence of both types of crystal and the conversion of needles into plates was slower compared to other samples.

When 1-propanol was doped with 10 % methanol, only small needles were observed and showed significant growth with time (Figure 5.8a and 5.8b). Form I needles were kinetically stable and the other forms (plates) were not observed over time (1 week). Additionally, the crystal habit of Form I needles was observed to be modified, being less elongated with well defined sides and end faces instead of the usual sharp needle-like morphology.

5.3.2 PXRD Analysis

Samples from cooling crystallisation (Table 2.4) were analysed by powder X-ray diffraction for polymorphic identification as described in Section 2.4.3. The PXRD patterns are shown in figures 5.9 to 5.16.
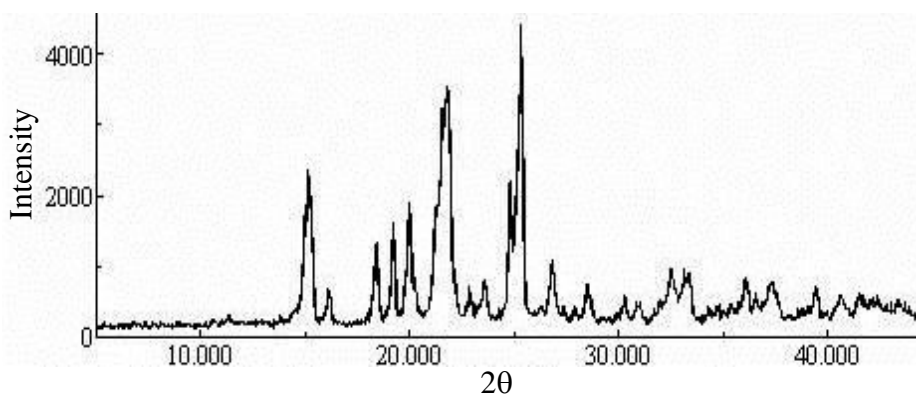
Figure 5.9 Powder –X-Ray pattern of sulphathiazole sample obtained from 100% methanol
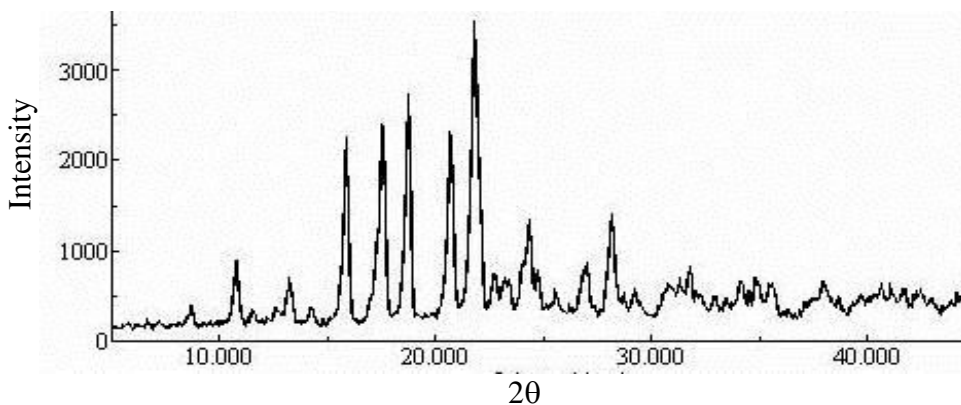
Figure 5.10   Powder –X-Ray pattern of sulphathiazole samples obtained from 100% 1-propanol
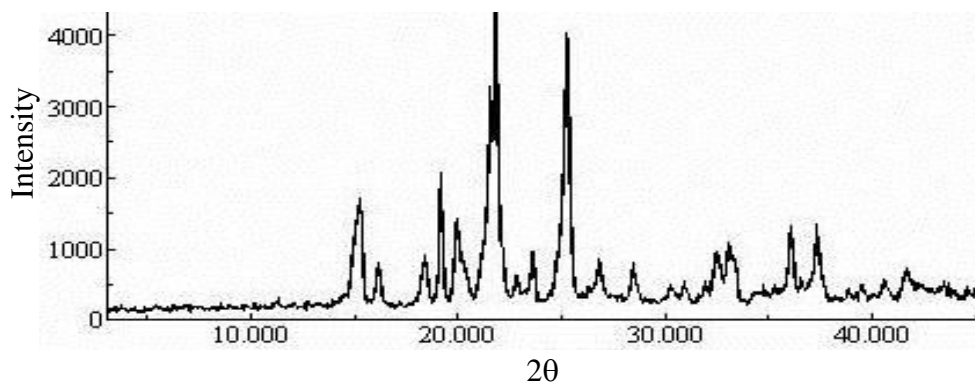
Figure 5.11   Powder –X-Ray pattern of sulphathiazole samples obtained from 80:20 ratios of methanol and 1-propanol
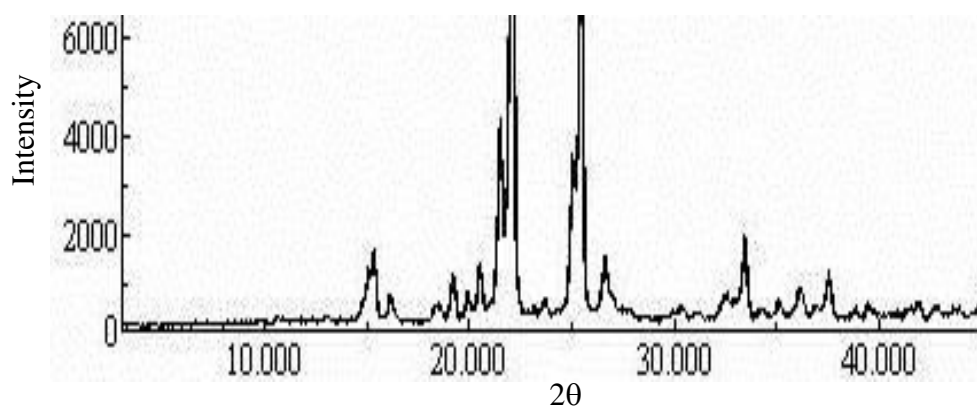
Figure 5.12   Powder –X-Ray pattern of sulphathiazole samples obtained from 60:40 ratios of methanol and 1-propanol
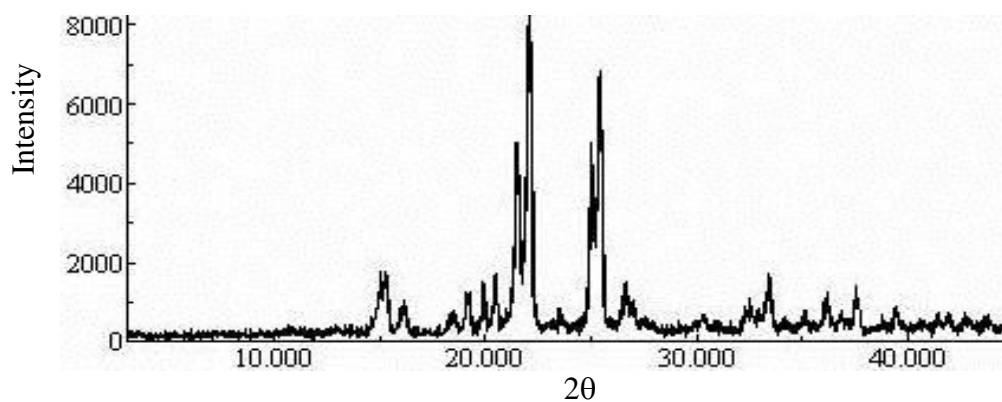
Figure 5.13   Powder –X-Ray pattern of sulphathiazole samples obtained from 50:50 ratios of methanol and 1-propanol
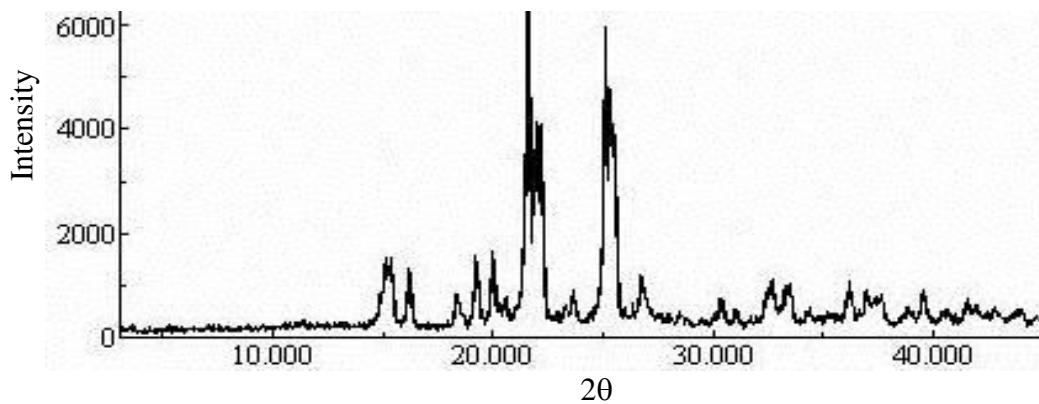
Figure 5.14   Powder –X-Ray pattern of sulphathiazole samples obtained from 40:60 ratios of methanol and 1-propanol
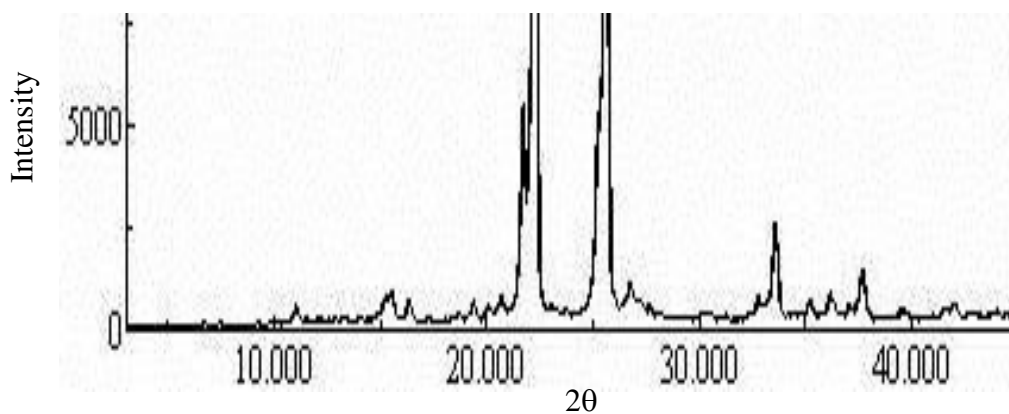
Figure 5.15   Powder –X-Ray pattern of sulphathiazole samples obtained from 20:80 ratios of methanol and 1-propanol
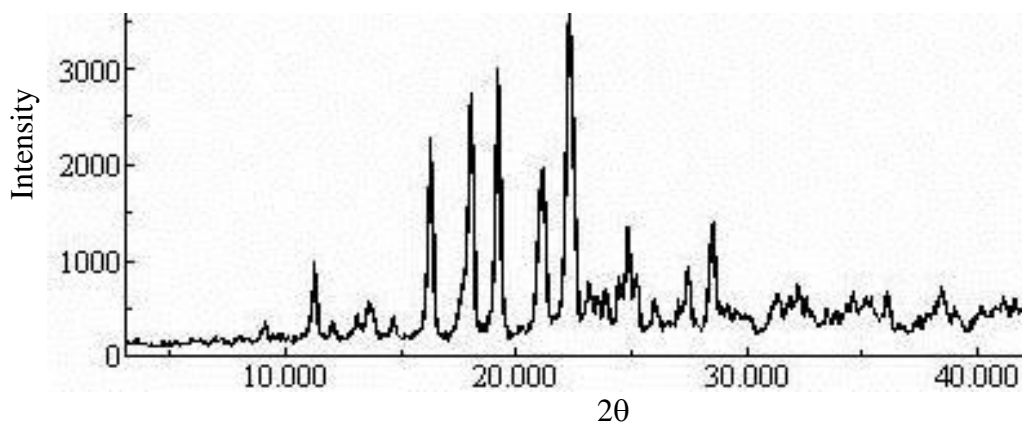
Figure 5.16   Powder –X-Ray pattern of sulphathiazole samples obtained from 10:90 ratios of methanol and 1-propanol

The sample obtained from 100 % 1-propanol solvent was identified as Form I by a peak at a 2θ value of 11, which is a characteristic peak for Form I (Blagden et al, 1998a & Appearly et al, 1999). In addition, an intense peak at 21.9 in this sample also stands as one of the identification peaks for Form I (Appearly et al, 1999). Furthermore, PXRD patterns of this sample also showed an exact match with the PXRD pattern of Form I obtained from CCDC (Chapter 3, Section 3.2.2).

Samples isolated from 100:00, 80:20, 60:40, 50:50 and 40:60 Methanol: 1-propanol did not show a peak at 2θ value of 11 (Figure 5.11 to 5.14), so the possibility of the presence of polymorph I in these samples could be eliminated. By comparing the PXRD patterns of these samples with the reference patterns in Section 3.2.2, it was clear that these patterns contained most of the peaks which are found in reference PXRD patterns of Form II, III and IV. Therefore it is likely that sulphathiazole samples crystallized by cooling from the above solvent ratios may contain Form II, III or IV, or a mixture of these polymorphs. However from single crystal X-ray Diffraction studies, described in Section 3.4, it is known that 100% methanol produces Form II crystals of sulphathiazole. It is likely, therefore that the samples contain Form II.

The sample isolated from a 20:80 ratio of methanol: 1-propanol solution showed a small peak at 2θ value of 11 (Figure 5.15), which confirms the presence of Form I in the sample. The PXRD pattern of this sample also contains many of the peaks which are found in Form II, III and IV PXRD patterns. This confirms that the sample contains only a small quantity of Form I as well as other forms.

The sample isolated from 10:90 ratio of methanol: 1-propanol solution showed an exact match with the PXRD pattern of Form I (Figure 5.16). The sample did not show any similarity with the PXRD patterns of Form II to IV, which suggests the absence of Forms II to IV in the sample. Hence, the sample was identified as pure Form I.

5.3.3 DSC Analysis

In DSC analysis, the endothermic melting behaviour and transformation of polymorphic forms were observed. All the samples, obtained from experiments listed in Table 2.4, were scanned in a closed pan at 10 ^{o}Cmin^{-1} as described in Section 2.4.3 (Chapter 2).
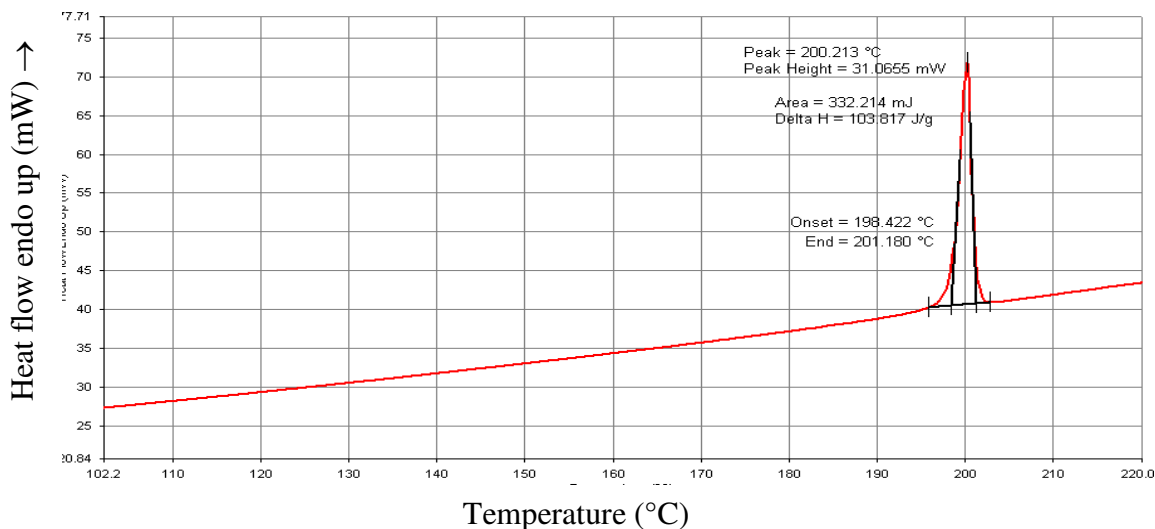
Figure 5.17   DSC thermograph of sulphathiazole samples obtained from 100 % 1-propanol (trace collected on a DSC7, Perkin Elmer, USA).
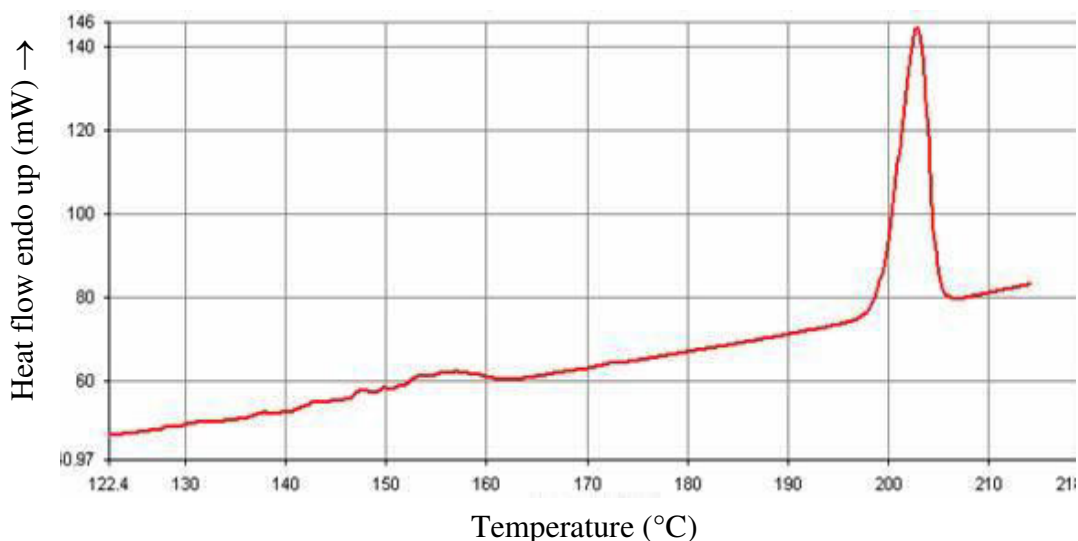
Figure 5.18   DSC thermograph of sulphathiazole samples obtained from 100 % methanol (trace collected on a DSC7, Perkin Elmer, USA).

157
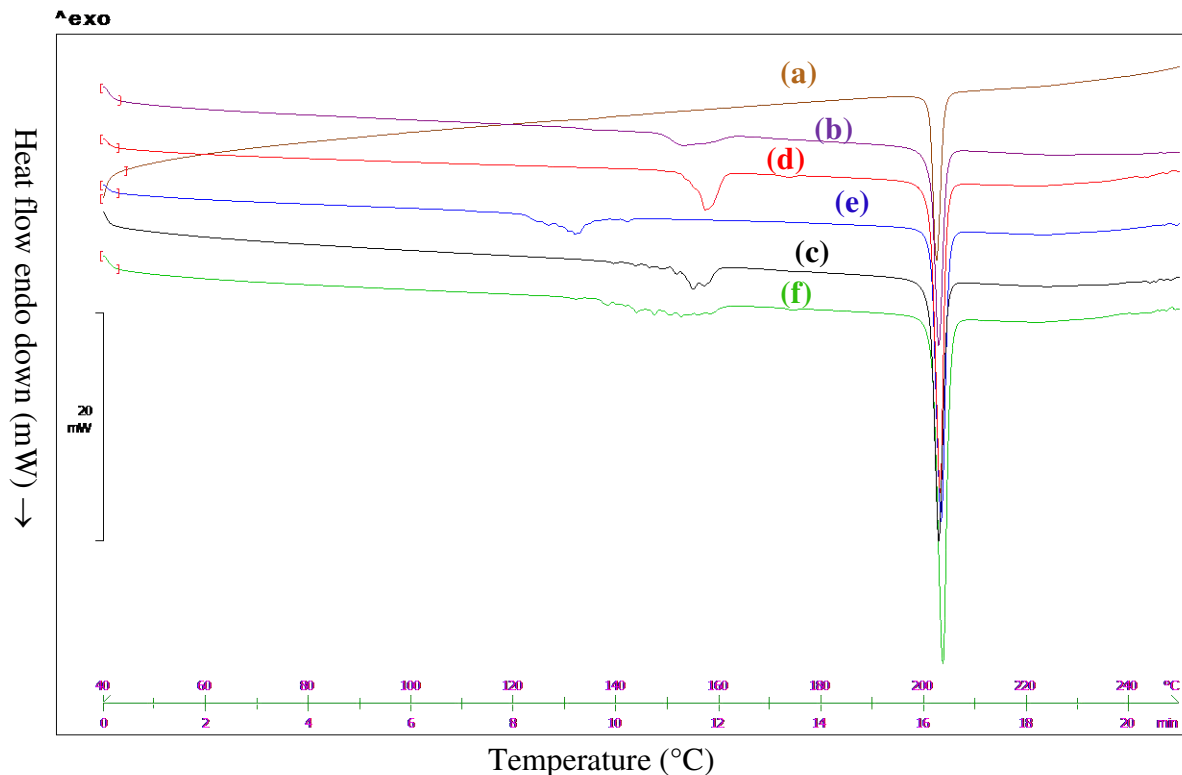
Figure 5.19 **(a) 10:90 methanol: 1-propanol, (b) 20:80 methanol:1-propanol, (c) 40:60 methanol:1-propanol, (d) 50:50 methanol:1-propanol, (e) 60:40 methanol: 1-propanol, (f) 80:20 methanol: 1-propanol (Trace collected on a DSC1, Metler Toledo, Switzerland).**

Figure 5.17 and 5.18 represent the DSC scan of samples obtained from 100% 1-propanol and 100% methanol, respectively. The sample obtained from 100 % 1-propanol solution did not show any transformation prior to melting at 201 °C. This result perfectly matches with the reference scan of Form I described in Section 3.2.4 and hence this sample was identified as Form I.The sample from 100% methanol showed broad peaks between 140 to 170 °C followed by final melting at 201 °C. The boiling point of methanol is 68 °C (Green and Perry, 2007) and hence this broad peak between 140 to 170 °C is unlikely to be a solvent loss peak. As reported in literature (Section 3.2.4), Forms II to IV show the transformation between 120 to 170 °C followed by final melting as Form I at 201 °C. However from single crystal X-ray Diffraction studies, described in Section 3.4, it is known that 100% methanol produces Form II crystals of sulphathiazole. It is likely, therefore that the samples contain Form II.

The sample crystallized from 90:10 1-propanol:methanol solution did not show any transformation or melting peak prior to the final melting of Form I at 201 °C (Figure 5.19a). This confirms that this sample is Form I only and does not contain any other forms. In comparison, the sample obtained from 20:80 methanol:1-propanol showed a small endothermic peak around 160 °C, likely to be due to transformation, prior to final melting at 201 °C (Figure 5.19b). This suggests that this sample contains a mixture of Forms II, III or IV with Form I.

As the percentage of methanol increased, the size of the transformation peak, prior to the final melting peak, increased (Figure 5.19 c to 5.19 f). These results coupled with PXRD results (Figures 5.11 to 5.14) suggest the predominance of Form II, III or IV, or a mixture of these forms in the samples.

5.4   Discussion

According to Cardew and Davey (1985) solvent mediated phase transformation goes through the dissolution of the metastable phase to form a solution supersaturated with more stable phase, followed by nucleation and subsequent growth of the more stable phase. Results from this study shows good agreement with Cardew and Davey's description (1985) for solvent mediated phase transformation. When more than 10% methanol is present in 1-propanol, Form I dissolves in the solution at a faster rate due to increased solubility of Form I in mixed solvents. As the Form I dissolves (section 5.3.1), the solution becomes supersaturated with the more stable Forms II to IV and eventually shows the nucleation and growth of β-type clusters and thus more stable Forms (II to IV) which then dominate the samples. Whereas, less than 10% methanol in 1-propanol may not influence the solubility of Form I significantly and hence the Form I in 10% methanol: 90% 1-propanol solution stays stable for a long time without showing dissolution. As described in the results (Section 5.3.1), it is found that 10 % methanol in 1-propanol worked as a habit modifying additive and tailored the sharp pointed needle face into a defined face (Figure 5.8), which is a more desirable shape. PXRD results also confirm that polymorph I has been maintained in both cases.

The observed end face in the modified crystals may arise from inhibition of growth at the fastest growing face [010] of Form I. Examination, using 'Mercury', CCDC molecular modelling software (Macrae et al, 2006), showed in Figure 5.20 that this surface exposes the acceptor imine nitrogen (N2), sulfoxide oxygen (O2) groups, and the donor amino hydrogen (H2). Sulphathiazole molecules are linked via α-dimers and then extended into sheets and layers via amino hydrogen and sulfato oxygen bonding.

The presence of methanol molecules in solution at low concentration, may lead to direct absorption of methanol at this surface, blocking H-bonding sites with subsequent inhibition of growth. Alternatively, β-dimer clusters with methanol (Figure 4.10) may be present in low concentration, which act as direct growth synthons, joining to available crystal surfaces, and inhibiting growth. We know that when the concentration of methanol is increased, Form II is nucleated, implying the presence of β-dimers. This modified habit clearly illustrates that the methanol interacts differently with the growing crystal than the main solvent, 1-propanol. Figures 5.20 and 5.21 show the growth in the [010] direction (needle axis) with available sites for H-bonding visible. The methanol molecule may dock into one of these sites, or facilitate β-type interaction with another sulphathiazole molecule.
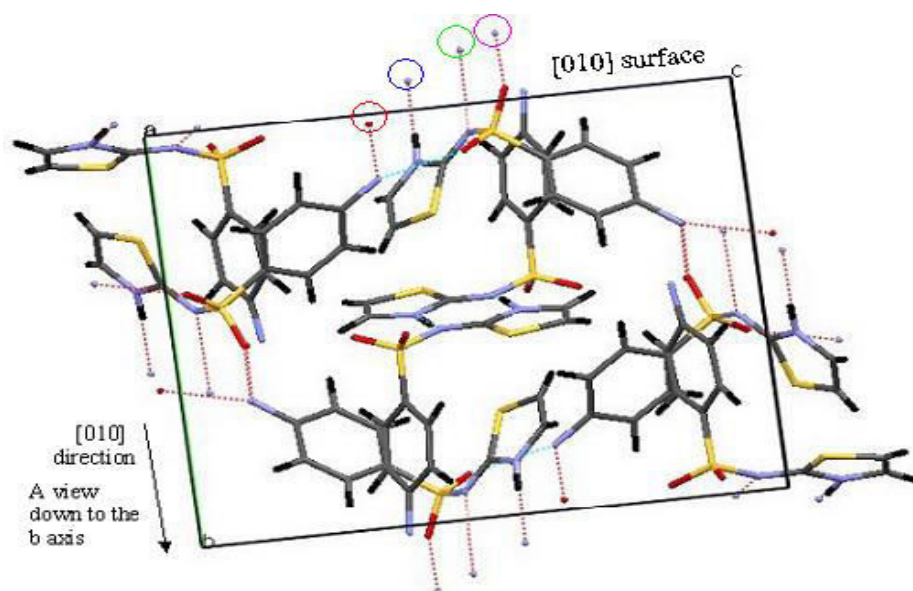
Figure 5.20 **Visualisation showing molecular interactions along [010] direction of sulphathiazole Form I.**

Keys: - O, amino hydrogen; O, thiazole hydrogen; O, imine nitrogen; O, sulfoxide oxygen.
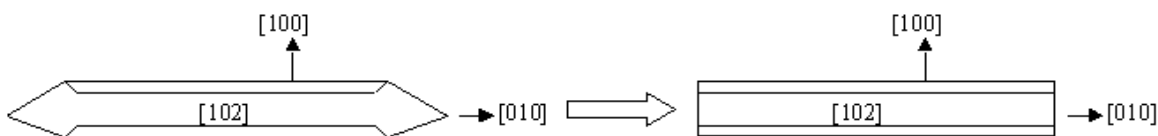
Figure 5.21 **Schematic showing habit modification (by growth inhibition) of [010] face of Form I**.

5.5 Conclusion

The different solvent interactions of solvents such as methanol, with the sulphathiazole molecule have been highlighted by the habit modifying effects of the additions of low concentrations of methanol to a 1-propanol crystallising solution. It is likely that the methanol molecules will form β- type clusters with the sulphathiazole. Since these are in very low concentration, Form I still nucleates and is kinetically stable. However, in the same way that structural additives (Weissbuch et al, 1994) modify habit by interacting at the substrate-solvent interface in a different way to the main solvent, the presence of methanol has shown a habit modifying effect, which improves the morphology. If the concentration of methanol becomes too high, then the β-clusters dominate and Form II results.

161

Chapter 6   Crystallisation of Indomethacin polymorphs in presence of additives

Crystallisation of materials with control over the size and morphology is an important aspect in the development of new materials in many fields including the pharmaceutical industry as they can affect both the production of effective and safe dosage form, and the biological behaviour of the finished form.

The crystallization of indomethacin polymorphs has been previously investigated (Section 1.12.1 and 1.12.5) and reported to exhibit an undesirable needle-like morphology. The work contained in this chapter focuses on morphological control of the α– Form of indomethacin using various organic solvents and additives. The effects of additives with a carboxylic acid group: adipic acid; myristic acid and oleic acid on the morphology of indomethacin have been investigated. The effect of a structurally related additive, 3-indoleacetic acid, on the morphology of indomethacin has also been investigated. Various organic solvents were selected for the crystallization of indomethacin. Crystal samples were characterised using optical microscopy and PXRD for morphological and polymorphic analysis. Details of experimental methods are described in Section 2.2 (Chapter 2).

6.1 Solubility of indomethacin

The solubility of indomethacin was determined at 60 °C in a range of organic solvents listed in Table 6.1. Amounts of indomethacin were added gradually into the solvent to determine its solubility, as described in Chapter 2. The solubility in various organic solvents are shown in Table 6.1.

Table 6.1 Solubility data of indomethacin in various organic solvents

Solvents	Solubility of Indomethacin at 60º C	Solubility of Indomethacin at 25º C
Ethanol	1.35 g/100 ml	0.67 g/100 ml
Acetonitrile	1.42 g/100 ml	0.79 g/100 ml
Ethyl acetate	1.44 g/100 ml	0.8 g/100 ml
Aqueous Acetic acid	1.05 g/100 ml	0.58 g/100 ml
Butanol	0.98g/100 ml	0.54 g/100 ml
Acetone	1.20g/ 100 ml	0.58 g/100 ml

Solubility obtained at 60 °C was used to determine the amount of indomethacin to be added to obtain a saturated solution at 60 °C in the crystallization experiments.

6.2 Crystallization of Indomethacin without additives

Indomethacin was crystallized without additives from each of the solvents listed in Table 2.5 by cooling crystallization as described in Section 2.2.2.1 (Chapter 2). In addition indomethacin was also crystallized without additives by liquid precipitation using ethanol as solvent and water as anti-solvent as described in Section 2.2.2.3. Samples, obtained from crystallization experiments, were analyzed using optical microscopy and powder X-ray diffraction to determine polymorphic identity.

6.2.1 Morphological analysis of crystallized samples

Samples were taken from each experiment and analysed under the optical microscope to observe the morphologies of crystals as shown in Figures 6.1 to 6.7.
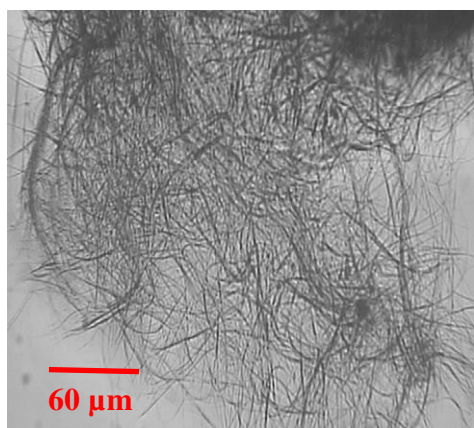
Figure 6.1 Sample obtained by cooling crystallization from ethanol
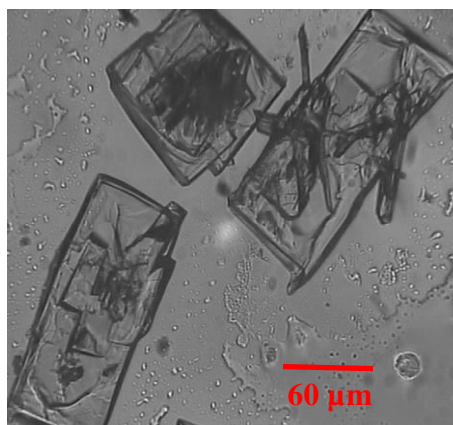
Figure 6.2 Sample obtained by cooling crystallization from acetonitrile

As shown in above figures 6.1, 6.4, and 6.5, sample crystallized by cooling using ethanol, aqueous acetic acid, and n-butanol resulted in a similar fibrous, thin, needle-like morphology. In all cases, these needles were aggregated. Sample crystallized from ethanol by liquid (water) precipitation also showed fibrous, thin, needle-like morphology with increased aggregation as shown in figure 6.7. Aggregated fibrous needles were precipitated as soon as water was added drop wise to the ethanol solution due to solubility difference of

indomethacin between water and ethanol. This kind of fibrous needle-like morphology is established in the literature as the morphology of α-Indomethacin (Section 1.12.5).
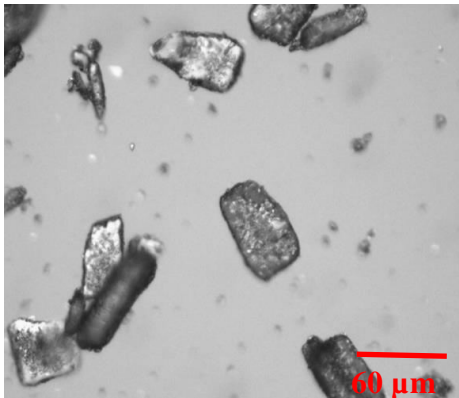
Figure 6.3 Sample obtained by cooling crystallization from Ethyl acetate
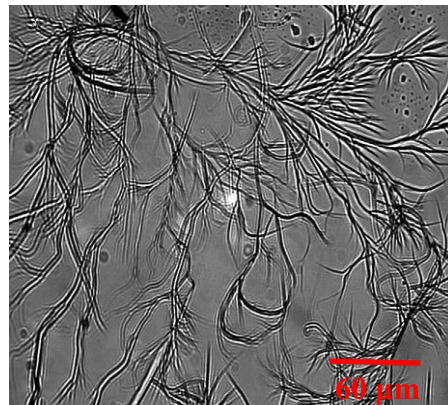
Figure 6.4 Sample obtained by cooling crystallization from aqueous acetic acid

Figure 6.5 Sample obtained by cooling crystallization from butanol
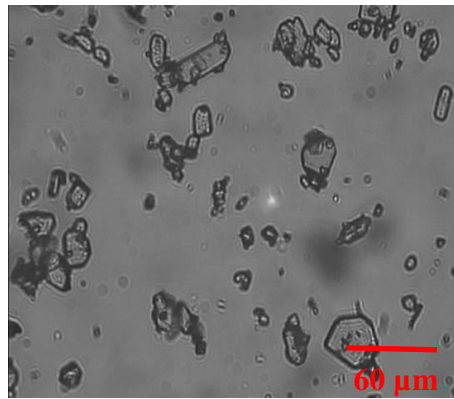
Figure 6.6 Sample obtained by cooling crystallization from acetone
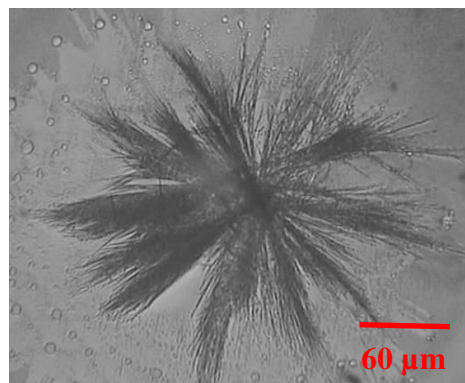
Figure 6.7 Sample obtained from crystallization by liquid precipitation from ethanol

As shown in Figure 6.2, the sample crystallized from acetonitrile exhibited a more defined rectangular morphology. Kistenmacher et al (1972), Borka et al (1974), and Slavin et al (2002) reported similar morphology when indomethacin was crystallized from acetonitrile. Cooling crystallization from ethyl acetate (Figure 6.3) and aqueous acetic acid (Figure 6.6) showed irregular plate like morphologies, which are in agreement with Pakula et al (1977) and Slavin et al (2002). These rectangular and irregular plate-like morphologies are established in the literature (Section 1.12.5) as the morphology of γ-Indomethacin.

6.2.3 PXRD analysis of crystallized samples

Powder X-ray diffraction studies were carried out for polymorphic identification of samples. The results of the PXRD patterns were compared with previous PXRD studies for the identification of Indomethacin polymorphs. Imaizumi et al (1980), Kaneniwa et al (1985), Otsuka et al (1986a & 2000), Lin et al (1992 &1999), Andronis et al (1997), Okumura et al (2006), Wu and Yu (2006) and Masuda et al (2006) reported PXRD patterns of Indomethacin polymorphs. They reported unique identification peaks for α-Indomethacin at 2θ value of 8.5 and for γ-Indomethacin at 2θ value of 11.6. In addition, PXRD patterns of Indomethacin polymorphs (CCDC reference codes: INDMTH, INDMTH1) were obtained from the Cambridge Crystallographic Database and used as reference for polymorphic identification of samples (Kistenmacher and Marsh, 197; Chen et al, 2002).

The powder diffraction data of each sample were collected using a Miniflex (Rigaku Corporation) laboratory powder x-ray diffractometer. The data were collected using a rotating flat plate sample holder over the 2θ range 5 – 34 °2θ in 5 ° steps at ambient conditions as described in Section 2.4.3. The PXRD patterns are shown in Figures 6.8 and 6.9.
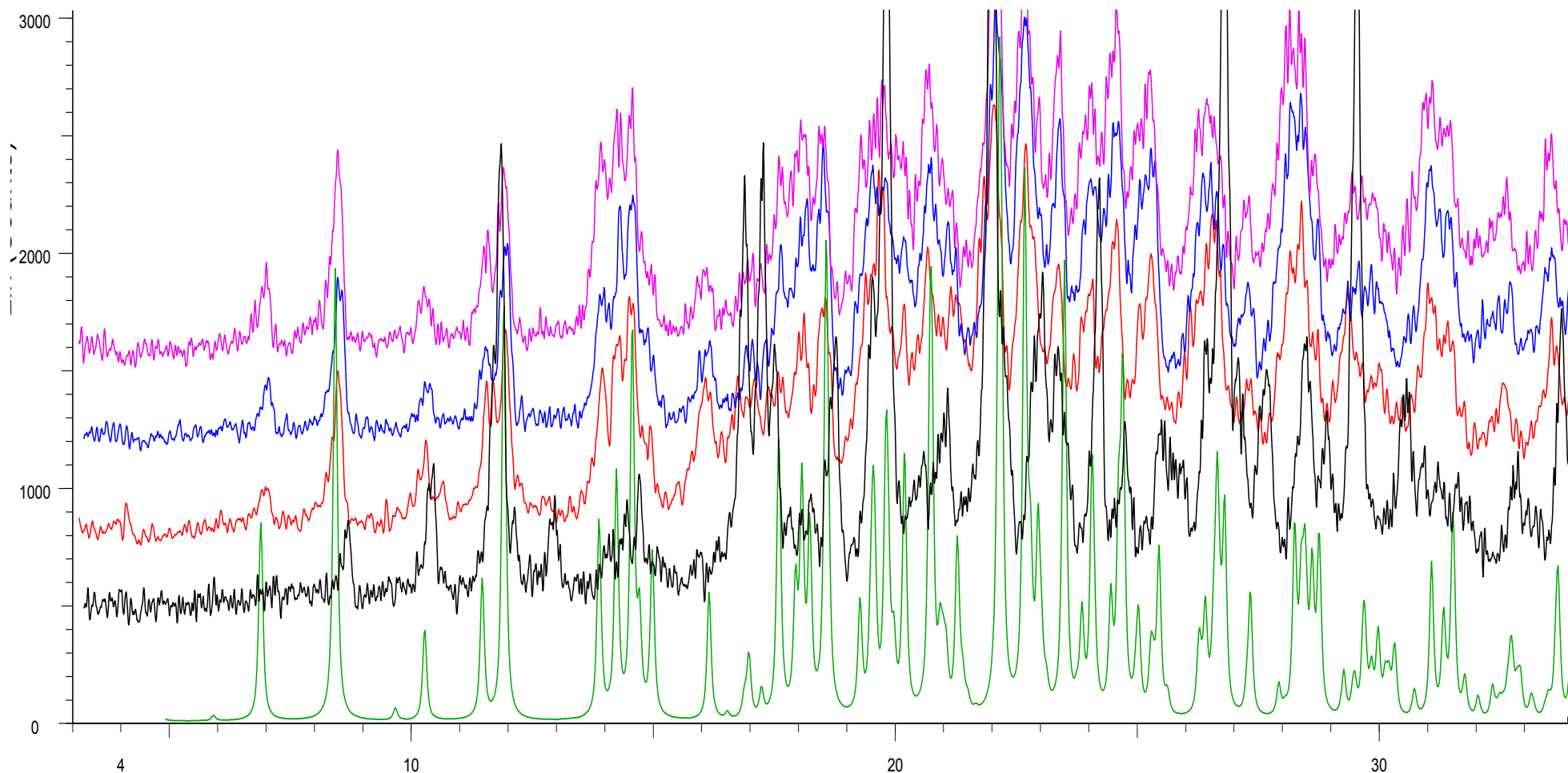
Figure 6.8   PXRD patterns obtained from recrystallized Indomethacin samples compared against reference pattern obtained from CCDC (Chen et al, 2002).

Key: samples obtained from cooling crystallisation using ethanol, aqueous acetic acid, n-butanol, and by water precipitation using ethanol as a solvent. PXRD pattern of α-Indomethacin obtained from CCDC (reference code INDMTH1).

166
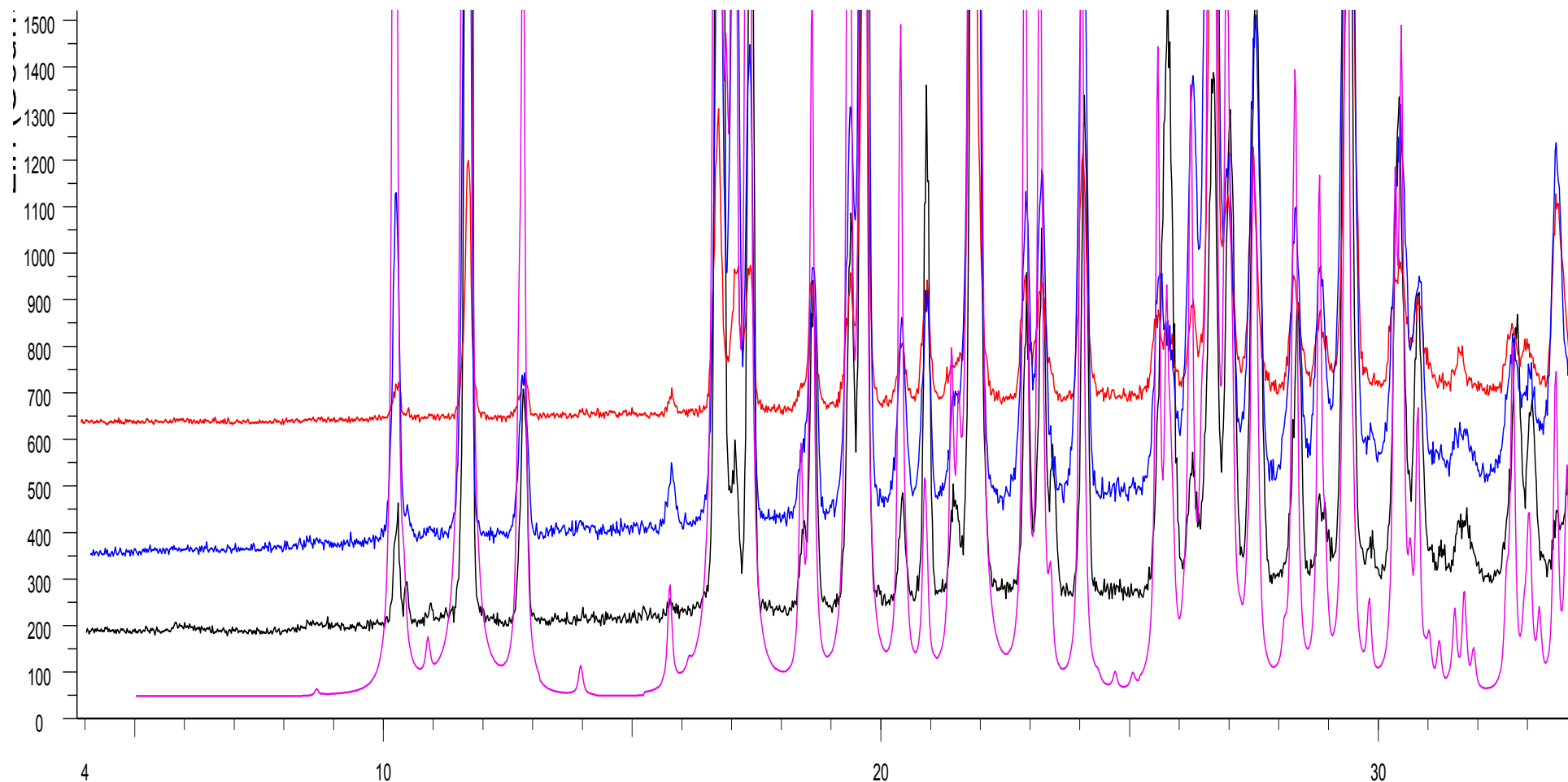
Figure 6.9 PXRD patterns obtained from recrystallized samples of Indomethacin compared against reference pattern obtained from CCDC (Kistenmacher and Marsh, 1972)

Key: samples obtained from cooling crystallisation using acetonitrile, ethyl acetate, and acetone. PXRD pattern of γ-Indomethacin obtained from CCDC (reference code INDMTH).

A detailed comparison between experimental pattern, literature data and reference pattern obtained from CCDC was carried out to investigate the polymorphic identity of the indomethacin samples obtained from crystallization experiments. From comparison, it was clear to identify samples crystallized from ethanol, aqueous acetic acid, and n-butanol as predominantly α-Indomethacin (Figure 6.8). These samples were identified by a unique peak with a 2θ value of 8.5, which is a characteristic peak for α-indomethacin (Lin et al, 1999; Kaneniwa et al, 1985; Andronis et al, 1997). Furthermore, PXRD patterns of these samples also showed an exact match with the PXRD pattern of α-indomethacin obtained from CCDC (Figure 6.8). Slavin et al (2002) and Chen et al (2002) identified sample as α-Indomethacin when crystallized by cooling or water precipitation using ethanol as a solvent. However, the sample crystallised from ethanol showed an additional small peak around 2θ value of 13 (Figure 6.8). This peak is present in the PXRD pattern of γ-indomethacin obtained from CCDC (Figure 6.9) and hence it suggests the small presence of γ-indomethacin in the sample. This evaluation of PXRD patterns leads to the conclusion that the sample crystallized from ethanol, aqueous acetic acid, and n-butanol were each predominantly α-indomethacin.

PXRD patterns of samples crystallized from acetonitrile, ethyl acetate, and acetone (Figure 6.9) displayed a peak at a 2θ value of 11.6, which is reported as a characteristic peak of γ (Lin et al, 1999; Kaneniwa et al, 1985; Andronis et al, 1997). In addition the PXRD pattern of these samples also showed an exact match with the PXRD pattern of γ-Indomethacin obtained from CCDC (CCDC reference code: INDMTH; Kistenmacher and Marsh, 1972) (Figure 6.9). Hence the samples crystallized from acetonitrile, ethyl acetate and acetone were identified as γ-idomethacin. Crystallization of γ-indomethacin from acetonitrile, ethyl acetate, and acetone is in agreement with Slavin et al (2002) and Pakula et al (1977).

6.3   Selection of additives for indomethacin crystallization

In the current project the focus is on controlling the fibrous needle-like morphology of α Indomethacin using additives. To understand the morphology it is necessary to study the crystal structure of α Indomethacin (Section 1.12.2). It is known from previous literature (Kistnemacher et al, 1972 and Chen et al, 2002) that the carboxylic acid functionality of the indomethacin molecule plays a significant role in the crystal structure of the α polymorph by forming a trimer in the asymmetric unit (Section 1.12.2).

The crystal structure of α-Indomethacin is reported in the CCDC (Cambridge Crystallographic Database) by Chen et al (2002). This crystal structure was viewed in Mercury (Macrae et al, 2006) and used to calculate morphology by BFDH (Bravais-Friedel Donnay-Harker) methodology (Bravais, 1866; Friedel, 1907; Donnay and Harker, 1937). This calculation predicted a needle-like morphology (Figure 6.10), which is a good match with morphology of α-indomethacin reported by Chen et al (2002) and the experimental morphology observed. Therefore this model was used to examine the crystal faces responsible for the long needle-like morphology.

Figure 6.10 Predicted morphology of α-indomethacin from the reported crystal structure (Chen et al, 2002) in CCDC using BFDH method of Mercury 2.1

In α Indomethacin as shown in Figure 6.10 the carboxylic groups are important for the stacking of indomethacin molecules in the (-1 0 0) and (1 0 0) directions by forming hydrogen bonds. Therefore it was considered that additives with a carboxylic acid group would be able to form bonds with the carboxylic acid group of indomethacin to prevent further addition of indomethacin molecule on these faces and thus inhibit the growth along the needle axis. Therefore, myristic acid, adipic acid, and oleic acid (Figure 6.11) were selected as additives. In addition, the Sigma Aldrich catalogue was searched for a structurally similar related additive. From this search, 3-Indoleacetic acid (Figure 6.11) looked structurally very similar to Indomethacin molecule and therefore it was also selected as an additive for this project.

Indomethacin

3-Indoleacetic acid

Adipic acid

Myristic acid

Oleic acid

Figure 6.11   Molecular structure of additive molecules selected for Indomethacin crystallisation.

The selected additive was used at 2 and 10%w/w concentration. Experimental methods for crystallisation of indomethacin with additive were performed according to method described in Section 2.2.2.1.

6.3.1   Microscopic analysis of indomethacin samples crystallized using additives.

Samples were taken from each experiment of indomethacin crystallisation with additives and analysed under the optical microscope to observe the morphologies of crystals as shown in Figures 6.12a to 6.15b.
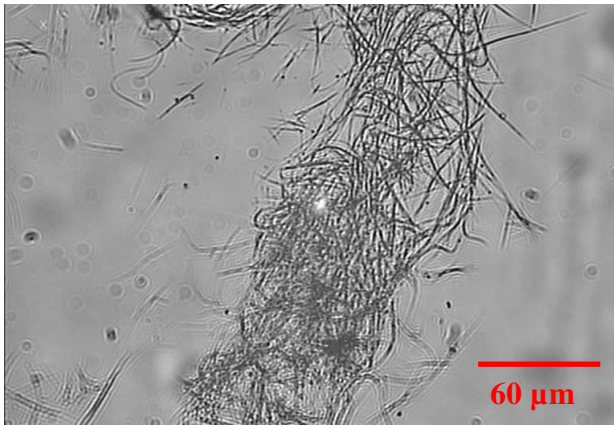
Figure 6.12a Sample from crystallisation using 2% myristic acid as additive
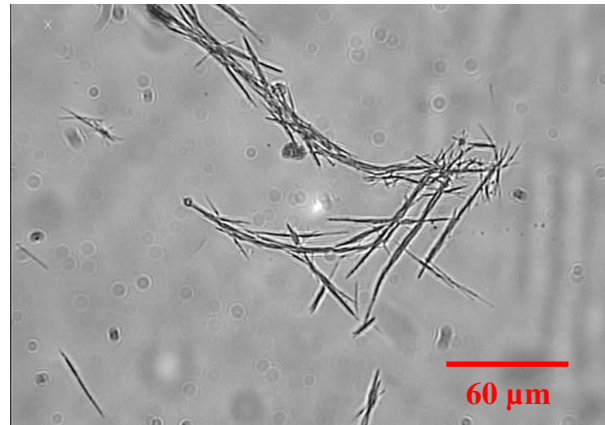
Figure 6.12b Sample from crystallisation using 10 % myristic acid as additive
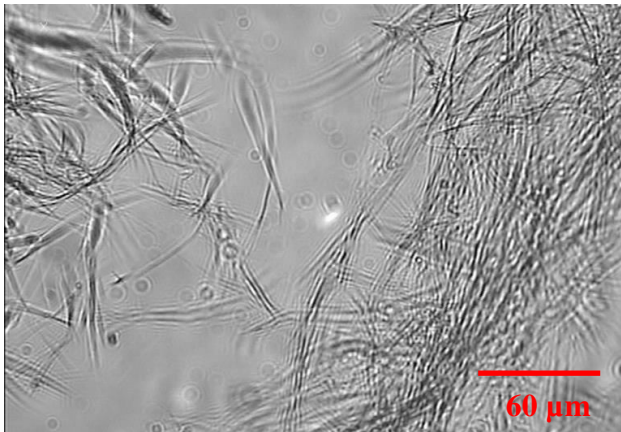
Figure 6.13a Sample from crystallisation using 2% adipic acid as additive
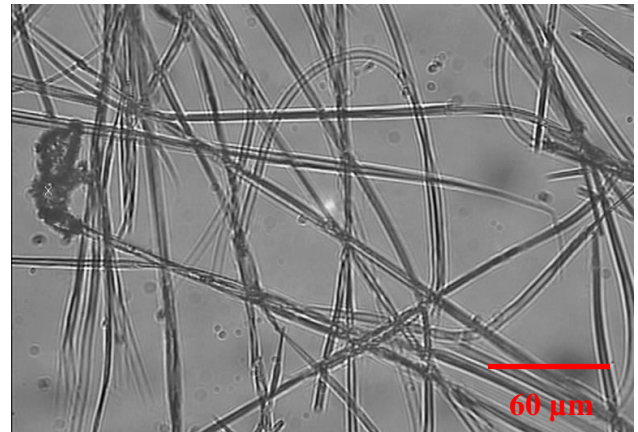
Figure 6.13b Sample from crystallisation using 10 % adipic acid as additive
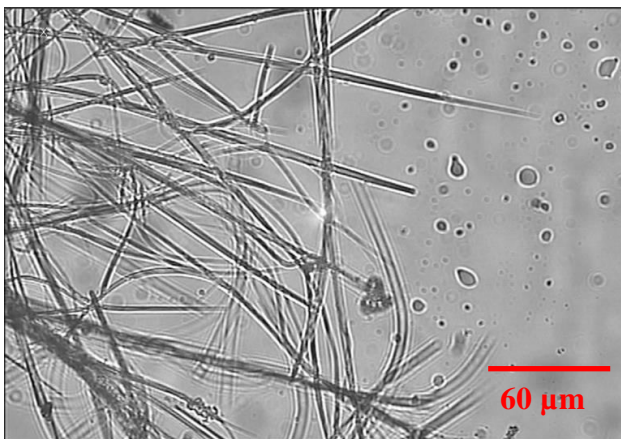
Figure 6.14a Sample from crystallisation using 2% oleic acid as additive
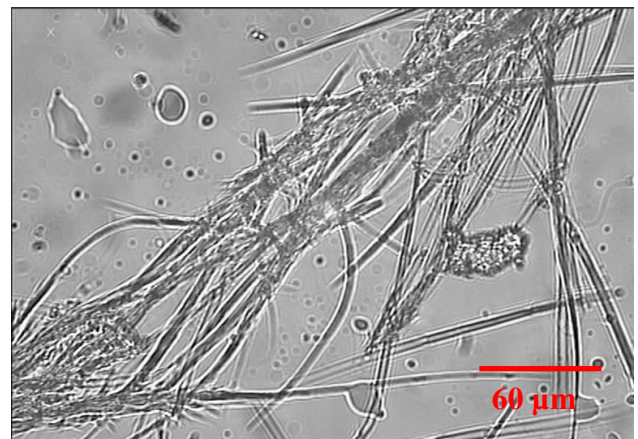
Figure 6.14b Sample from crystallisation using 10 % oleic acid as additive

171
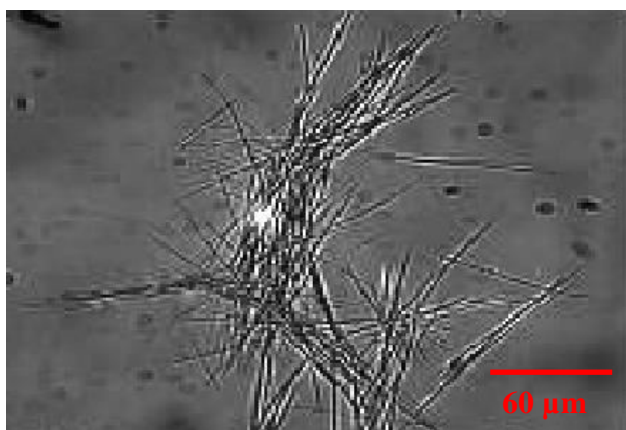
Figure 6.15a Sample from crystallisation using 2% 3-Indoleacetic acid as additive
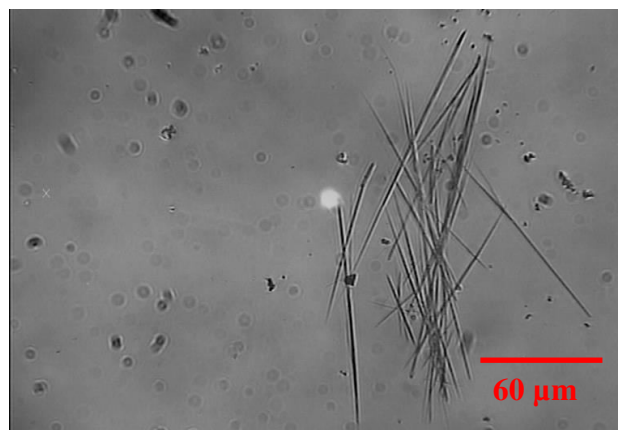
Figure 6.15b Sample from crystallisation using 10 % 3-Indoleacetic acid as additive

As shown in figures 6.12 to 6.15b samples crystallized by cooling using ethanol as a solvent in presence of selected additives resulted in needle-like morphology. However, differences were observed in the size and shape of needles with the use of additives. When 2% myristic acid, 10 % myristic acid, 2% adipic acid or 2% 3-indoleacetic acid used as additive, small and thin aggregated needles were produced (Figures 6.12a, 6.12b, 6.13a, and 6.15a). Whereas; in presence of 10% adipic acid, 2% oleic acid or 10% oleic acid as additives, bigger, thicker and less fibrous needles were observed (Figure 6.13b, 6.14a, and 6.14b). These needles were well defined but aggregations were still observed in all samples. When 10% 3-indoleacetetic acid used as additive; thin, less aggregated and well defined needles were produced (Figure 6.15b). No literatures have reported the use of additives in crystallization process of α-indomethacin.

From above results it is clear that presence of additive did not change the needle like morphology of α-indomethacin but less fibrous, well defined, and less aggregated needles were observed in presence of additives. These improvements in needle properties may improve the performance of downstream processes, such as, filtration, drying, and milling.

6.3.2 PXRD Characterization of indomethacin samples crystallized using additives

Powder X-ray diffraction studies were carried out for polymorphic identification of samples obtained from cooling crystallization with additives. The results of the PXRD patterns were compared with previous PXRD studies as before
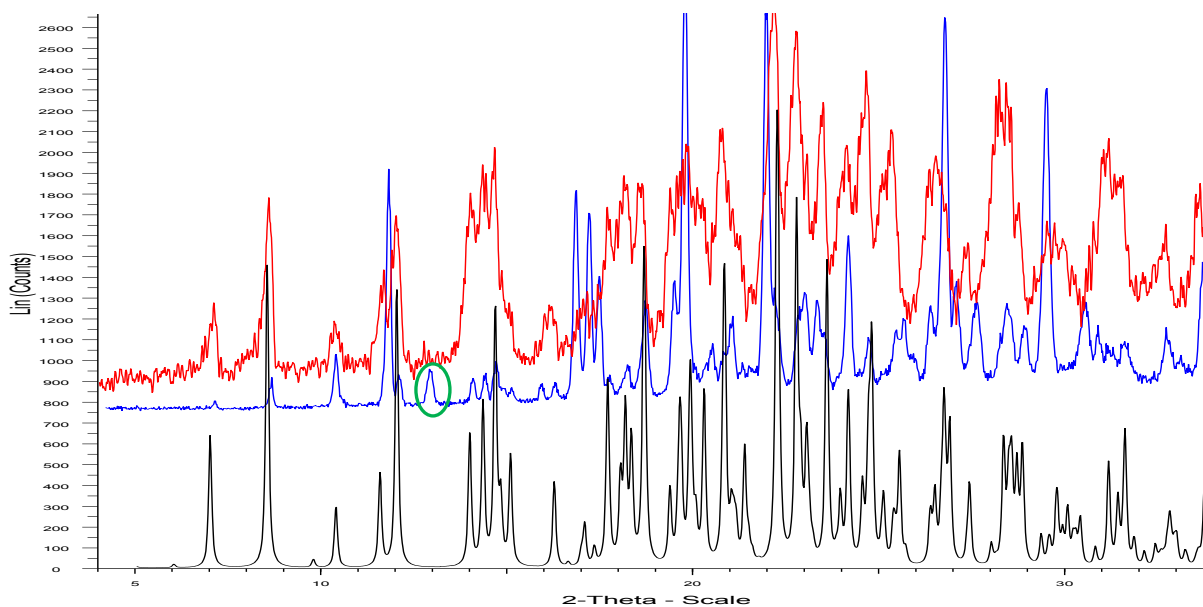
Figure 6.16 PXRD result of a sample crystallized with (a) 2% myristic acid as additive and (b) 10% myristic acid as additive (c) reference pattern of α-indomethacin obtained from CCDC
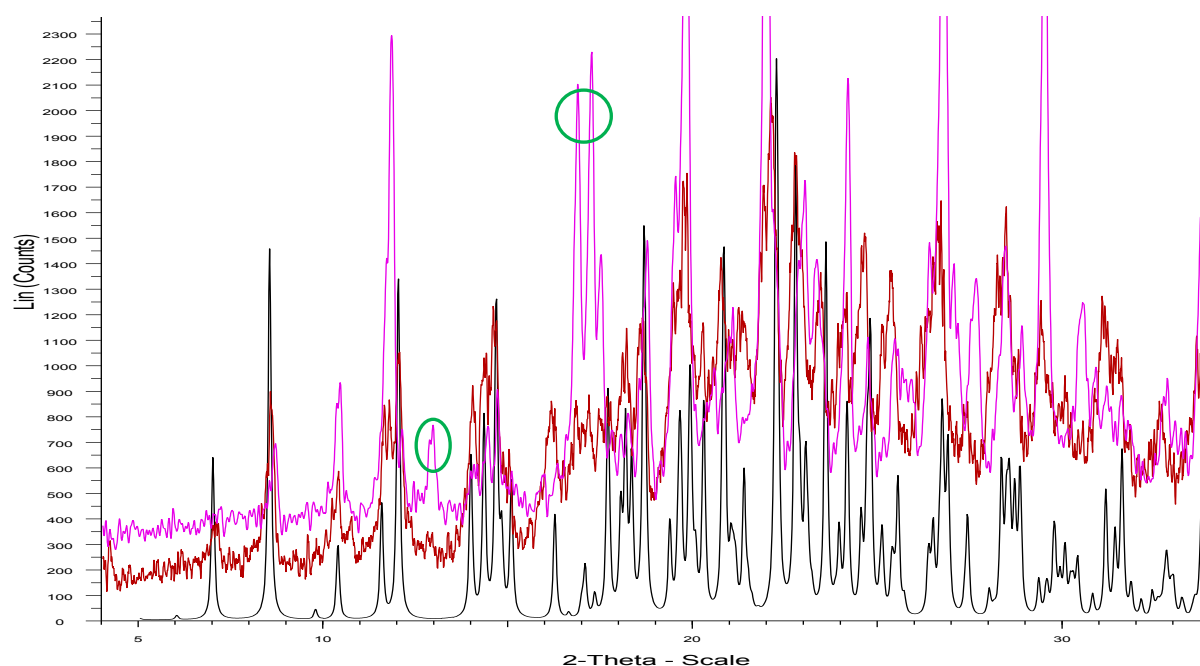
Figure 6.17 PXRD result of a sample crystallized with (a) 2% adipic acid as additive and (b) 10% adipic acid as additive (c) reference pattern of α-indomethacin obtained from CCDC
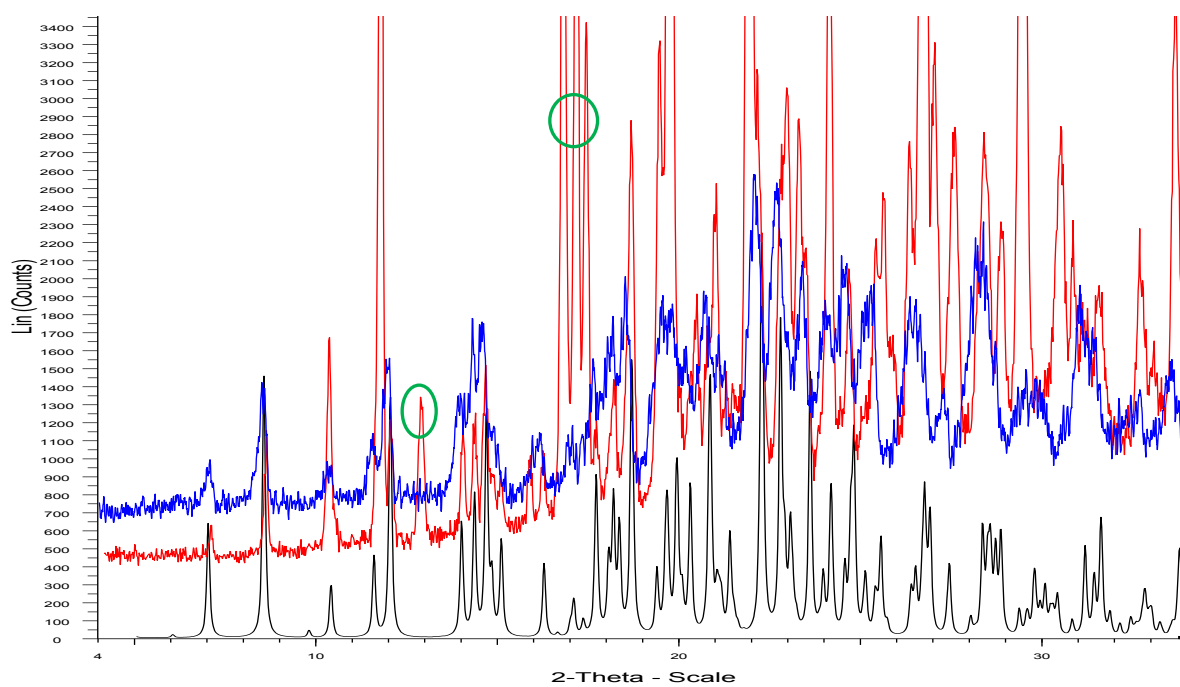
Figure 6.18   PXRD result of a sample crystallized with (a) 2% oleic acid as additive and (b) 10% oleic acid as additive (c) reference pattern of α-indomethacin obtained from CCDC
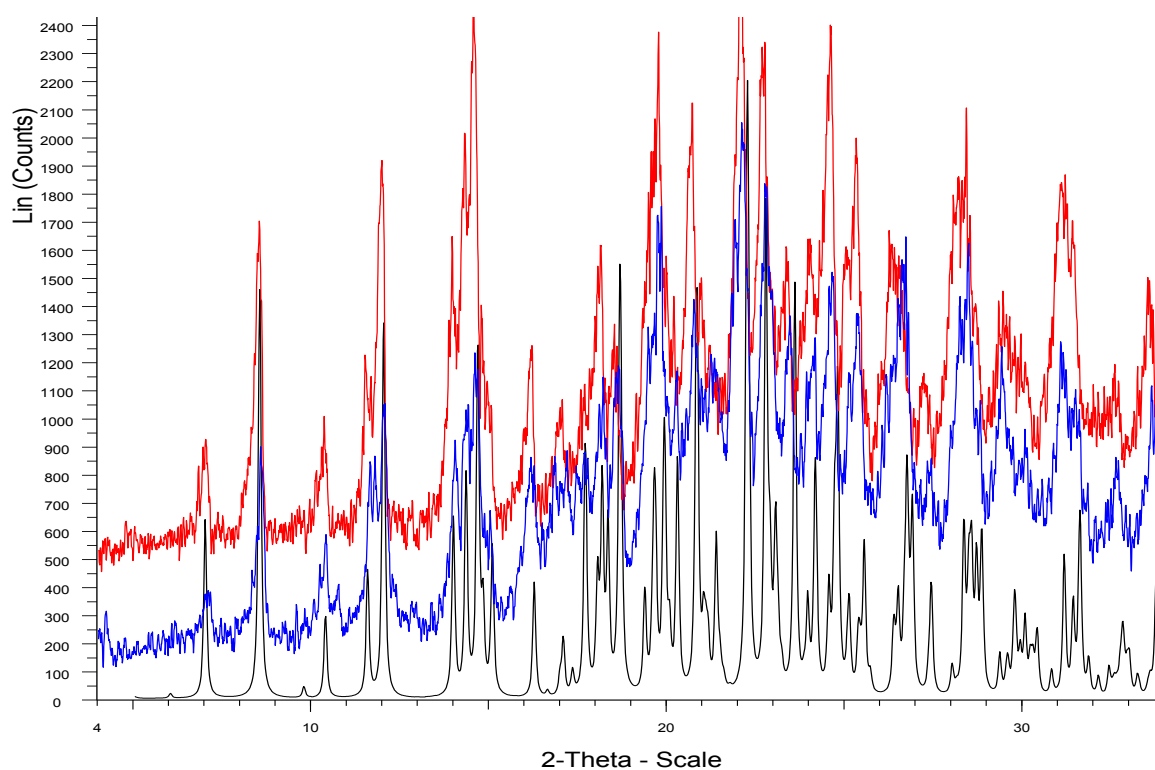
Figure 6.19   PXRD result of a sample crystallized with (a) 2% 3-Indoleacetic acid as additive and (b) 10% 3-Indole-3-acetic acid as additive (c) reference pattern of α-indomethacin obtained from CCDC

As shown in figure 6.16 to 6.19, PXRD patterns of all samples displayed a unique peak at a 2θ value of 8.5, which is a characteristic peak for α-indomethacin (Lin et al, 1999; Kaneniwa et al, 1985; Andronis et al, 1997). PXRD patterns of these samples also displayed good match with the reference PXRD pattern of the α-indomethacin obtained from CCDC. However, sample crystallised from ethanol using 10% myristic acid (Figure 6.16b), 2% adipic acid (Figure 6.17a), or 10% oleic acid (Figure 6.18a) as additive showed an additional peak around 2θ value of 13, which can be attributed to the presence of y-indomethacin (see Figure 6.9 for the reference PXRD pattern of γ-indomethacin). PXRD patterns of samples with 2% adipic acid, or 10% oleic acid also displayed increased intensity in peaks compare to peaks in pure α-indomethacin pattern between 2θ values of 16 to 17. This could be due to either preferred orientations of samples in x-ray diffraction or small presence of γ-indomethacin in samples as the γ-indomethacin display intense peaks between 2θ values of 16 to 17.

From above investigation, it was clear to identify all samples, crystallized from ethanol using myristic acid, adipic acid, oleic acid, or 3-Indole-3-acetic acid as additive, as predominantly α-indomethacin with small presence of y-indomethacin in some cases. It was also observed that low (2%) or high (10%) doping of additives did not change the outcome of Indomethacin polymorph crystallized using ethanol as a solvent.

6.4   Conclusion

As shown in microscopic analysis, each sample crystallized as α-indomethacin with needle-like morphology. The presence of any of the selected additives did not change the needle-like morphology of α-indomethacin when crystallized by cooling using ethanol as a solvent. However less fibrous, well defined, and/or less aggregated needles were observed in the presence of adipic acid, oleic acid, or 3-Indole-3-acetic acid. Whilst changing or improving the needle-like morphology of α-indomethacin using additives, the objective was also to maintain the polymorphic outcome of the crystallization process as α-indomethacin. PXRD results confirm that all samples, crystallized by cooing from ethanol with additives, were predominantly α-indomethacin.

After studying crystal structure and crystal faces of α-indomethacin, It was proposed that additives with carboxylic acid functionality would have more propensity to form hydrogen bond with growing crystal of α-indomethacin at (1 0 0) or (-1 0 0) faces and prevent further

addition of indomethacin molecule on these faces to inhibit long thin needle-like morphology. However, experimental results suggest that additive did not change the needle-like morphology of α-indomethacin and hence may have not displayed any association with the growing α-indomethacin crystal on (1 0 0) or (-1 0 0) faces.

A number of reasons can be discussed to explain why additives did not modify the needle like morphology of α-Indomethacin. Driving force for the growth of α-indomethacin needles could be very strong and it would have been difficult for additives to overcome this force. It is possible that the additives may have associated with the fastest growing face of needles but the effect was not sufficient to produce and equidimensional morphology. Results showed less fibrous crystals when adipic acid, oleic acid, or 3-Indole-3-acetic acid used as additives, which indicated some inhibition of growth in (1 0 0) or (-1 0 0) faces.

Also the interaction between one molecule of Indomethacin with another molecule of Indomethacin or interaction between one molecule of additive with another molecule of additive could be thermodynamically more favorable than the interaction between one molecule of Indomethacin with another molecule of a selected additive. If that is the case then interaction between Indomethacin and a selected additive is not preferred thermodynamically and hence both may crystallize independently as pure components.

The solubility of the additive in ethanol can be also important during crystallization. During the experiment, when additive is added to the solution, it was observed that additives were readily soluble in ethanol. In the current study crystallization of Indomethacin was performed by cooling ethanol solution up to 20 °C. If ethanol solution is undersaturated for additive during crystallization of indomethacin then additive may stay in solution phase and hence will not associate with crystals of α-indomethacin during crystal growth process.

For any future study detailed molecular modeling can be performed to investigate thermodynamically favorable interaction between Indomethacin and additive molecules. Also the solubility of additives should be checked at various temperatures to make sure that crystallization solvent does not stay undersaturated with additives.

Chapter 7   Discussion and future work

As described in section 1.13, the current study focuses on understanding the role of solvents and additives on the polymorph selection and morphology of crystals. Sulphathiazole and Indomethacin were used as model active ingredients.

7.1   Discussion: Sulphathiazole

For Sulphathiazole, the aim of the project was to examine the effect of a range of alcohols on the crystallisation of sulphathiazole and attempt to understand the mechanism of alcohols in the polymorph selection process. Experimental results (Chapter 3) clearly showed that long chain alcohols (1-propanol and 1-butanol) stabilized the α-dimer based, metastable Form I and did not show transformation to the β-dimer based, more stable Forms (II, III, and IV). Shorter chain alcohols methanol, ethanol and 2-propanol showed transformation of Form I into the more stable, β-dimer based Forms II, III, and IV, respectively. It was also observed that doping of 1-propanol with 10% methanol caused a habit modification of Form I (from needle to rod-shaped crystals) while maintaining the stabilization of Form I (Chapter 5). When 1-propanol was doped with more than 10% of methanol, Form I was transformed in to more stable, β-dimer based Forms II to IV. This habit modification of Form I may arise from the inhibition of growth at fastest growing surfaces, [010] (Blagden N, 2001). It is likely that methanol molecules will form β-type clusters with sulphathiazole at very low concentration and hence Form I will still nucleate and bekinetically stable. However, these β-cluster with methanol molecules may interact [010] face differently and block the H-binding sites with subsequent inhibition of growth, which resulted in improved morphology. This modified habit of Form I illustrates that methanol interacts differently with the growing crystal of sulphathiazole than the longer chain alcohol 1-propanol.

These results also indicate that it is not only the alcohol functionality but also the steric effects of the alkyl chain which impacts upon the selection of polymorph. To understand the role of solvent on the polymorph selection process, the energy of the proposed clusters (α- and β-dimer based pre-nucleation clusters in the presence of each of the solvents) was calculated using Cerius2 and

Mopac software packages, and more detailed calculations were performed via the grid-based systematic search approach (Chapter 4).

From the molecular modelling of proposed clusters, it was clear that clustering between a longer chain alcohol molecule (1-propanol or 1-butanol) and α-type dimers of sulphathiazole, which lead to the nucleation of Form I, are energetically favored compared to the clusters of long chain alcohol (1-propanol or 1-butanol) molecule with β-type dimer, which lead to the nucleation of stable Forms II to IV. Similarly, when short chain alcohols such as methanol, 2-propanol and ethanol were modeled, clustering with more stable β-dimer was favored thermodynamically. Thus the molecular modelling results were in agreement with the experimental observation that long chain alcohols stabilised Form I; whereas, crystallization using short chain alcohol solvents resulted in the more stable Forms II to IV. The ^{1}H NMR studies also indicated differences in the solution behavior between long chain alcohol solvent (1-butanol) that inhibit the formation of β-dimer based Forms (and favor the stabilization of α-dimer Form) and short chain alcohol solvents (methanol, ethanol) that favored β-dimer based Forms (Section 3.6).

These experimental and molecular modelling results clearly indicate that solvent plays an important role in the selection of polymorphs. Results also illustrate that the ability of the solvent to inhibit polymorphic transformation is linked to the energies of substrate-solvent interactions and shows that the clustering in the solution is thermodynamically controlled.

7.1.1   Future Work: Sulphathiazole

In this project, molecular modelling was limited to investigating thermodynamic differences between proposed α-dimer based clusters, which favored Form I, and proposed β-dimer based clusters, which favored Form II to IV.

It was observed from the experimental results that methanol, ethanol and 2-propanol select a specific polymorph, i.e., Form II from methanol, Form III from 2-propnaol, and Form IV from ethanol. Each of these forms has the β-dimer as a basic unit and structural differences between them are related to ring to ring contacts and contacts between the sheets of β-dimer rings

(Blagden et al, 1998). It is possible that specific solvent interactions may thermodynamically favor the ring structure specific to each polymorph and may have a similar energetic basis to those presented in this study. It will be interesting to perform further molecular modelling studies to calculate energies of pre-nucleation clusters, which are based on ring structures specific to Form II, III, and IV, in the presence of short chain alcohol solvent molecules. This work could help to understand the mechanism of polymorph selection for sulphathiazole when shorter chain alcohols are used as solvents.

As discussed above, doping of 10% methanol in 1-propanol modified the morphology of Form I crystals from needle-like to rod-like shape. It is believed that methanol or β-dimer clusters, favored by methanol, may have interacted on the fast growing faces [010] of Form I and resulted in improved rod-like morphology of Form I. These results also suggest that doping of a small concentration of a solvent can have a significant impact on the morphology of final crystals and may work like habit modifying additives. Further molecular modelling studies on sulphathiazole could be performed to understand this impact of solvent on the growing crystal. Future molecular modelling studies would include docking of each of the possible solvent molecules, sulphathiazole molecule, α-dimer and β-dimer on the fastest growing surfaces of sulphathiazole polymorphs. Interaction energies of each of these molecules or dimers with the fastest growing faces of sulphathiazole polymorph can be calculated and rationalized using molecular modelling via the grid based systemic search approach (Hammond et al, 2006). The results would help to evaluate the impact of thermodynamically favorable interactions on final morphology and polymorphism. It would be also valuable to plan an experimental study to validate the results from such modelling. This methodology could then be applied to other industrially relevant active ingredients to choose better solvent systems to achieve improved morphology with desired polymorph.

7.2   Discussion: Indomethacin

As mentioned in Chapter 1 (section 1.12.1), Indomethacin is known to exhibit at least five polymorphs but only the stable γ Form and metastable α Form are reported to be reliably produced by standard methods. The metastable α Form has an undesirable fibrous needle-like

morphology. The current study focused on producing crystals of α Indomethacin with a well-defined morphology using additives.

After studying the crystal structure and crystal faces of α-indomethacin in Mercury (section 6.3), it was believed that fastest growing faces [1 0 0] and [-1 0 0] are responsible for the thin, needle-like morphology and additives with carboxylic acid functionality were identified as suitable candidates to interact at these faces. Adipic acid, myristic acid, oleic acid and 3-indoleacetic acid were selected as additives and their impact on the morphology and polymorphism of indomethacin were investigated in this study.

However, experimental results from microscopy and PXRD suggest that additives did not significantly change the needle-like morphology of α-indomethacin but less fibrous and less aggregated needles were observed in presence of adipic acid, oleic acid and 3-indole-3-acetic acid.

7.2.2 Future Work: Indomethacin

As described above, additives selected in this study showed only limited success in modifying the morphology of α-indomethacin. Hence, in future a molecular modelling study it would be very helpful to investigate in more detail the action of the selected additives. For these additives to interact with indomethacin, interaction between additive molecules and indomethacin should be thermodynamically more favorable than the additive to additive and indomethacin to indomethacin interactions. Molecular modelling can be performed to calculate these interaction energies to provide explanation for the failure of additives used in current project.

Detailed molecular modelling studies using grid based systematic search or Absorption Locator module of Material Studio should be performed to identify more suitable additives with thermodynamically favorable interaction with the growing faces of α indomethacin. Interaction energies of these additives can be ranked to shortlist best additives for experimental studies. Thereafter experimental studies should be planned to validate results from molecular modelling.

Alternatively, co-crystals of indomethacin can be also investigated in future to obtain crystal with desired physical properties. Molecular modelling (Musumeci et al, 2011) based on electrostatic potential of molecule surfaces can be applied to select suitable co-formers for co-crystallisation. Experimental co-crystal screening work should be also performed to validate results from molecular modelling and investigate the physical properties of resulting co-crystals.

References

Aaltonen, J.; Rantanen, J.; Siiriä, S.; Karjalainen, M.; Jrgensen, A.; Laitinen, N.; Savolainen, M.; Seitavuopio, P.; Louhi-Kultanen, M.; Yliruus, J. Anal.Chem. 2003, 75, 5267–5273.

Andronis, V.; Yoshioka, M.; Zografi, G. J. Pharm. Sci. 1997, 86, 346-351

Andronis, V. & Zografi, G., J. Non-Cryst. Solids, 2000, 271, 236–248.

Allen, D. J. & Kwan, K. C. J. Pharm. Sci. 1969, 58, 1190

Allen, F. H. *Acta Crystallogr., Sect. B* 2002, *58*, 380-388.

Anderson, J. E.; Moore, S.; Tarczynski, F.; Walker, D. *Spectrochimica Acta A, 2001,* 57, 1793-1808

Anwar, J.; Tarling, S. E.; Barnes, P. *J. Pharm. Sci.* 1989, *78* (4), 337-342.

Appereley, D. C.; Fletton, R. A.; Harris, R. K.; Lancaster, R. W.; Tavener, S.; Threlfall, T. L. *J. Pharm. Sci.* 1999, *88,* 12, 1275-1280.

Aroyo, M. I.; Müller, U.; Wondratschek, H. International Tables for Crystallography (2006). Vol. A1, ch. 1.1, 2-5

Aulton, M. *Pharmaceutics: The Science of Dosage form Design*. 2nd edition. Churchill Livingstone; 2002, page 15.

Babilev, F. V.; Bel'ski, V. K.; Simnov, A.; Arzamastev, A. P. *Khim. Farm. Zh.* 1987, *21*, 1275-1280.

Bauer, J.; Morley, J.; Spanton, S.; Leusen, F. J. J.; Henry, R.; Hollis, S.; Heitmann, W.; Mannino, A.; Quick, J.; Dziki, W. J. Pharm. Sci. April 2006, 95, No. 4, 917-928.

Beckett, A. H. and Stenlake, J. B. Practical Pharmaceutical Chemistry: Part II Fourth Edition (Pt. 2), 2001

Berkovitch-Yellin, Z.; Addabi, L.; Idelson, M.; Lahav, M.; Leiserowitz, L. Angewandt Chemie Supplement, 1982, 1336-1345

Bernstein, J. Polymorphism in Molecular Crystals, Oxford University Press, 2002

Blagden, N. *Powder Tech.* 2001, *121*, 46-52.

Blagden, N.; Davey, R. J.; Lieberman, H. F.; Williams, L.; Payne, R.; Roberts, R.; Rowe, R.; Docherty, R. J. *Chem. Soc.*, *Faraday Trans.* 1998, *94* (8), 1035-1044.

Blagden, N.; Davey, R. J.; Rowe, R.; Roberts, R. Int. J. Pharm. 1998, 172, 169-177

Bogdanova, S.; Sidzhakova, D.; Karaivanova, V.; Georgieva, S. Int. J. Pharm. 1998, 163, 1-10

Boldyrev, V. V.; Shakhtshneider, T. P.; Chizhik, S. A. Int. J. Pharm. 2005, 295, 1–2, 177–182

Borka, L., 1974. Acta Pharm. Suecica 11, 295–303.

Bourne, J. R & Davey, R. J. Journal of Crystal Growth, 1977, 39, 267-274

Bragg W.L. *The Diffraction of Short Electromagnetic Waves by a Crystal*, *Proc. Cambridge Phil. Soc.*, 1913, 17, 43-57.

Bratu, I.; Grecu, R.; Borodi, G. H.; Gozman-Pop, F.; Bojita, M. STUDIA UNIVERSITATIS BABEŞ-BOLYAI, PHYSICA, 2001, SPECIAL ISSUE, 315-319

Bravais, A. *Etudes Cristallographiques*, Paris: Gauthier Villars, 1866

Burger, A.; Dialer, R. D. *Pharm. Acta Helv.* 1983, 56, 72-78

Burger, A.; Ramberger, R. Milkrochim. Acta, 1979, 2, 273

Burton, W. K,; Crabrera, N.; Frank, F. C. Philosophical Transactions, 1951, A243, 299-358

Buckton, G. 1995, Interfacial phenomena in drug delivery and targeting. Harwood Academic publishers, Switzerland.

Byrn, S. R.; Pfeiffer, R. R.; Stowell, J. G. Am. Pharm. Review, 2002, 5, 92-99

Cano, H.; Gabas, N.; Canselier, J. P. Journal of Crystal Growth, 2001, 224, 335-341.

Cardew, P. T.; Davey, R. J. Proceedings of the Royal Society of London. Series A, Mathematical and Physical Sciences, 1985, 398, 1815, 415-428

Carpentier, L.; Decressain, R.; Desprez, S.; Descamps, M. J. Phys. Chem. B, 2006, 110, 457-464.

CERIUS2, Molcular Modelling Software for Materials Research, version 4.2; Accelrys, Inc.: San Diego, CA, 2001.

Chan, C. F.; Anwar, J; Cernik, R.; Barnes, P; Wilson, R. M. *J. Appl. Cryst.* 1999, *32*, 436-441.

Chen, X.; Morris, K. R.; Griesser, U. J.; Byrn, S. R.; Stowell, J. G. J. Am. Chem. Soc, 2002, 124, 15012-15019

Chow, K. Y.; Go, M.; Mehdizadeh, M.; Grant, D. J. W. Int. J. Pharm. 1984, 20, 3-24.

Clayden, J.; Greeves, N.; Warren, S. Organic Chemistry, 2nd edition, 2001, Oxford University Press

Datta, S.; Grant, D. J. W. *Nat. Rev. Drug Discovery* 2004, *3*, 42-57.

Davey, R. J.; Black, S. N.; Logan, D.; Maginn, S. J.; Fairbrother, J. E.; Grant, D. J. W. *J. Chem. Soc., Faraday Trans.*, 1992, 88, 3461-3466

Davey, R. J.; Blagden, N; Quayle, M. Cryst. Growth Des. 2001; 1: 59-65

Davey, R. J. and Garside, J. From Molecules to Crystallizers: An Introduction to Crystallization, University Press, Oxford, 2000

DeCamp, W. H. The impact of polymorphism on drug development: A regulator's viewpoint, XVIII Congress of the International Union of Crystallography, 1999.

Deji, M. A.; Vissers, T.; Meekes, H.; Vlieg, E. Cryst. Growth Des. 2007, 7 (4), 778-786.

Desgranges, C.; Delhommelle, J. J. Am. Chem. Soc. 2006, 128 (47), 15104-15105.

Dewar, M. J. S.; Zoebisch, E. G.; Healy, E. F.; Stewart, J. J. P. *The Journal of the American Chemical Society* (ACS Publications), 1985, 107, 13, 3902–3909

Donnay, J. D. H. and Harker, D. *Am. Mineral.1937*, 22, 463

Fairbrother, J. E. and Grant, D. J. W. Journal of Pharmacy and Pharmacology, 1978, 30, S1, 19

Fawzi M.; Davison E.; Tute M. *J. Pharm. Sci.* 1980, 69, 104—105.

Ferrari, E. S.; Davey, R. J.; Cross, W. I.; Gillon, A. L.; Towler, C. S. *Cryst. Growth Des.* 2003, *3* (1), 53-60.

Ferrero, M. C.; Velasco, M. V.; Ford, J. L.; Rajabi-Siahboomi, A. R.; Munoz, A.; Jimenez-Castellanos, M. R. *Pharm. Res.* vol. 1999, 16, 9, 1464-1469.

Finnie, S. D.; Ristic, R. I.; Sherwood, J, N.; Zikic, A. M. Journal of Crystal Growth, 1999, 207, 4, 308-318

Frankenheim, M. L "System der Kristalle," Acta Acad. Nat. Curiosorum, 1842, 19, 471-660.

Friedel, G. *Bull. Soc. Franc. Mineral.* 1907, 30, 326

Fenimore, C. H. P. and Thrailkill, A. J. Am. Chem. Soc. 1949, 71, 2714

Galdecki, Z. & Glowka, M. L. Rocz. Chem., 1976, 50, 1139

Gardner, C. R.; Almarsson, O.; Chen, H. M.; Morissette, S.; Peterson, M.; Zhang, Z.; Wang, S.; Lemmo, A.; Gonzalez-Zugasti, J.; Monagle, J.; Marchionna, J.; Ellis, S.; McNulty, C.; Johnson, A.; Levinson, D.; Cima, M. *Comput. Chem. Eng.* 2004, *28,* 6-7, 943-953.

Garnier, S.; Petit, S.; Coquerel, G. J. Cryst. Growth, 2002, 234, 1, 207–219

Gibbs, J. W. *Collected Works*, Vol. I, Thermodynamics; Yale University Press: New Haven, 1948.

Giron, D. *J. Therm. Anal. Calorim.* 2001, *64*, 37-60.

Glaxo Inc. V Novapharm Ltd., 52F3d 1043, 34 U. S. P. Q. 2d (BNA) 1565 (fed. Cir. 1995)

Green, D. W. & Perry, R. H. *Perry's Chemical Engineers' Handbook, 8th Edition,* McGraw-Hill, *2007*

Grove, D. C. & Keenan, G. L. *J. Am. Chem. Soc.* 1941, *63*, 97-99.

Haleblian, J.; McCrone, W. J. Pharm. Sci. 1969, 58, 8, 911–929

Hammond, R. B.; Ma, C.; Roberts, K. J.; Ghi, P. Y.; Harris, R. K. *J. Phys. Chem. B* 2003, *107*, 11820-11826.

Hammond, R. B; Hashim, R. S.; Ma, C.; Roberts, K. *J. Pharm. Sci.* 2006, *95,* 11, 2361-2372.

Hamza Y.; Sammour O.; Abdel Latif, H. *Pharmazeutische Industrie*, 1994, 56, 286—291.

Hartman, P. & Perdock, W. G. Acta Crystallographica, 1955, 8, 49-52.

Hendriksen, B. A.; Grant, D. J. W.; Meenan, P.; Green, D. A. J. Cryst. Growth, 1998, 183, 4, 629–640

Higuchi, W. I.; Bernardo, P. D.; Mehta, S. C. J.Pharm.Sci. 1967, 56, 200–207.

Hilfiker, R. Polymorphism in the Pharmaceutical Industry, Wiley-VCH, 2006.

Hooton, J. C.; German, C. S.; Davies, M. C.; Roberts, C. J. European J. Pharm. Sci. 2006, 28, 315-324

Hughes, D.; Hursthouse, M.; Lancaster, B.; Tavener, S.; Threlfall, T.; Turner, P. *Acta Crystallogr., Sect. C* 1999, *55*, 1831-1834.

Imaizumi, H.; Nambu, N.; Nagai, T. Chem. Pharm. Bull. 1980, 28, 2565-2569

Jackson, K. A. Mechanism of growth in Liquid Metals and Solidification. Am. Soc. Metals, Cleveland. 1958.

Kala, H.; Moldenhauer, H.; Giese, R.; Kedvessy, G.; Selmeczi, B.; Pintye-Hódi, K. Pharmazie. 1982, 37, 2, 129-131.

Kaneniwa, N.; Otsuka, M.; Hayashi, T. Chem. Pharm. Bull. 1985, 33, 3447–3455

Kim, S. T.; Kwon, J.; Lee, J.; Kim C. Int J. Pharm. 2003, 263, 141-150

Kistenmacher, T. J.; Marsh, R. E.; J. Amer. Chem. Soc. 1972, 94, 1340

Kitamura, M. Journal of Crystal Growth, 2002, 237-239, 2205-2214.

Knapman, K. *Mod. Drug Discovery* 2000, *3,* 2, 53-54, 57.

Kordikowski, A.; Shekunov, T.; York, P. *Pharm. Res.* 2001, *18* (5), 682-688.

Kossel, W. Annalen der Physik, 1934, 457-480

Kruger, G. J. & Gafner, G. *Acta Crystallogr., Sect. B* 1971, *B27*, 326-333.

Kruger, G. J. & Gafner, G. *Acta Crystallogr., Sect. B* 1972, *28*, 272-283.

Kutzke, H.; Klapper, H.; Hammond, R. B.; Roberts, K. J. *Acta Cryst. 2000,* B56, 486–496

Lagas, M. & Lerk, C. F. *Int. J. Pharm.* 1981, *8*, 11-24.

Lancaster, R. W.; Karamertzanis, P. G.; Hulme, A. T.; Tocher, D. A.; Covey, D. F.; Price, S. L. *Chem. Commun.* 2006, *47*, 4921-4923.

Leitão, M. L. P.; Canotilho, J.; Cruz, M. S. C.; Pereira, J. C.; Sousa, A. T.; *Redinha, J. S. Journal of Thermal Analysis and Calorimetry, 2002, 68, 397-412*

Lin, S. Y. *Journal of Pharmaceutical Science*, 1992, 81, 572-576.

Lin, S. Y.; Chen, K. S.; Teng, H. H. J Microencapsul. 1999, 16, 6, 769-776

Liu, J.; Nicholson, C. E.; Cooper, S. J. *Langmuir,* 2007, 23, 13, 7286-7292.

Lohani, S.; Nesmelova, I. V.; Suryanarayanan, R.; Grant, D. J. W. Crystal Growth & Design. 2011, 11, 2368-2378.

Lu, Q. & Zografi, G. Pharm. Res. 1998, 15, 8, 1202-1206

Macrae, C. F.; Edgington, P. R.; McCabe, P.; Pidcock, E.; Shields, G. P.; Taylor, R.; Towler, M.; Van de Streek, J. *J. Appl. Cryst.*2006, 39, 453–457.

Masuda, K.; Tabata, S.; Kono, H.; Sakata, Y.; Hayase, T.; Yonemochi, E.; Terada, K. Int. J. Pharm. 2006, 318, 146-153.

Mayo, S. L.; Olafson, B. D.; Goddard, I. W. A. DREIDING: A Generic Force Field for Molecular Simulations. *J. Phys. Chem.* 1990, *94*, 8897-8909.

McCrone, W.C. Polymorphism. In Physics and Chemistry of the Organic Solid State, Vol. II, Wiley Interscience, New York, 1965, 725–767.

Mesley, R. J. *J. Pharm. Pharmac. 1971,* 23, 687-694

Miers, H. A. & Isaac, F. Journal of the Chemical Society, 1906, 89, 413-454.

Miers, H. A. & Isaac, F. Proceedings of the Royal Society,1907, A79, 322-351.

Miyazaki, H. 1947. Jpn. J. Pharm. Chem. 19,133–134.

Monissette, S. L.; Almarsson, O.; Peterson, M. L.; Remenar, J. F.; Read, M. J.; Lemmo, A. V.; Ellis, S.; Cima, M. J.; Gardner, C. R. *Ad*V. *Drug Deli*V*ery Re*V. 2004, *56,* 3, 275-300.

Monkhouse, D. C. & Lach, J. L. J. Pharm. Sci. 1972, 61, 1435

MOPAC Quantum Chemistry Program Exchange Program No. 455, version 6.0; Indiana University: Bloomington, IN, 1993.

Moustafa, M. A.; Carless, J. E. J.Pharm.Pharmacol. 1969, 21, 359–365.

Mullin, J. W. Crystallization, Fourth Edition, Butterworth-Heinemann , 2001.

Musumeci, D; Hunter, C. A.; Prohens, R.; Scuderi, s.; McCabe, J. F. Chem. Sci., 2011, 2, 883-890

Myerson, A. S. & Jang, S. M. J. Cryst. Growth, 1995, 156, 459-466.

Myerson, A. S. Handbook of Industrial Crystallization, Butterworth-Heinemann, 2001.

Myerson, A. S. Molecular Modelling Applications in Crystallization, Cambridge University Press, 2005.

Naciazek-wieniawska, A. & Wilczynska-Wojtulewicz, I. Pol. J. Pharmacol. Pharm. 1975, 27, 245-250

Niazi, S. J Pharm Sci. 1976, 65, 2, 302-4.

Neilsen, A. E. Kinetics of precipitation, Pergamon Press, New York, 1964

Okumura, T.; Ishida, M.; Takayama, K.; Otsuka, M. J. Pharm. Sci. 2006, 95, 3, 689-700

Ostwald, W. *Z. Phys. Chem. (Leipzig),* 1899.

Otsuka, M.; Kato, F.; Matsuda, Y. AAPS Pharmsci. 2000, 2, 1, article 9, 1-8

Otsuka, M.; Matsumoto, T. and Kaneniwa, K. Chem. Pharm. Bull. 1986a, 34, 1784-1793.

Pakula, R.; Pichnej, L.; Spychala, S.; Butkiewicz, K. Pol. J. Pharmacol. Pharm. 1977, 29, 2, 151-56

Park, K.; Evans, J. M. B.; Myerson, A. S. Crystal Growth & Design. 2003, 3, 6, 991-995

Parmar, M. M.; Khan, O.; Seaton, L.; Ford, J. L. Crystal Growth & Design. 2007, 7, 9, 1635-1642

Parsons, G. E.; Buckton, G.; Chatham, S. M. Int. J. Pharm. 1992, 83, 163-170

Pecharsky, V. K.; Zavalij, P. Y. Fundamentals of Powder Diffraction and Structural Characterization of Materials, Springer, 1st edition, 2003.

Pöllänen, K.; Häkkinen, A.; Reinikainen, S.-P.; Louhi-Kultanen, M.; Nyström, L. Chemical Engineering Research and Design, 2006, 84, 1, 47-59

Rio, D. Ars. Pharmaceutica. 2002, 43, 3-4, 113-120

Roberts, R. J. & Rowe, R. C. *Int. J. Pharm. 1996,* 129, 79-94

Roberts, R. J., Payne, R. S., Rowe, R. C., 2000. *Eur. J. Pharm. Sci.* 9, 277-283

Rowe, R. C. Int. J. Pharm. 1989a, 52, 149-154

Schutt, H. W. Eilhard Mitscherlich, Prince of Prussian Chemistry, Chemical Heritage Foundation, 1996

Shenouda, L. S. J. Pharm. Sci. 1970, 59, 785–787.

Sheth, A. R. PhD Thesis: Relationship Between Crystal Structure and Solid-state Properties of Pharmaceuticals, University of Minnesota, 2004

Silverstein, R. M.; Bassler, G. C.; Morrill, T. C. Spectrometric Identification of Organic Compounds, Wiley, New York. 1991

Singhal, D. & Curatolo, W. Advanced Drug Delivery Reviews, 2004, 56, 335– 347

Slavin, P. A.; Sheen, D. B.; Shepherd, E. E. A.; Sherwood, J. N.; Feeder, N.; Docherty, R.; Milojevic, S. J. Cryst. Growth, 2002, 237, 300–305.

Stuart, B. H. Infrared Spectroscopy: Fundamentals and Applications, John Wiley & Sons, 2004

Summers, M. P.; Enever, R. P.; Caxless, J. E. J. Pharm. Pharmacol. 1976, 28, 89-99.

Thompson, C.; Davies, M. C.; Roberts, C. J.; Tendler, S. J. B.; Wilkinson, M. J. Int. J. Pharm. 2004, 280, 1-2, *137-150*

Traini, D.; Rogueda, P.; Young, P.; Price, R. Pharm. Res. 2005, 22, 5, 816-825

Truelove J.; Bawarshi-Nassar R.; Chen N.; Hussain A. *Int. J. Pharm.* 1984, 19, 17—25

Uusi-Penttilä, M. S. & Berglund, K. J. Cryst. Growth, 1996, 166, 1-4, 1996, 967 -970.

Volmer M. *Kinetic der Phasenbildung*, Steinkoff: Dresden, 1939.

Weissbuch, I., Addadi, L.; Berkovitch-Yellin, Z.; Gati, E.; Weinstein, S.; Lahav, M.; Leiserowitz, L. *JACS. 1983, 105, 22,* 6615.

Weissbuch, I.; Popvitz-Biro, R.; Leiserowitz, L.; Lahav, M. *Lock and Key Principle* by Behr, J. P. Wiley, New York, 1994.

Weissbuch, I. & Lahav, M. Crystal morphology control with tailor-made additives; a stereochemical approach. In Advances in Crystal Growth Research (Sato, K. ed.), 1st edition, Elsevier, 2001, 381–400.

Wöhler, F. & Liebig, J. Ann. Pharm. 1832, 3, 249 – 282.

Wu, T. & Yu, L. *J. Phys. Chem. B*, 2006, *110*, 32, 15694–15699.

Yamamoto, H. Chem. Pharm. Bull. 1968, 16, 17–19.

Yokoyama, T.; Umeda, T.; Kuroda, K.; Nagafuku, T.; Yamamoto, T.; Asada, S. Yakugaku Zasshi, 1979, 99, 837–842.

Yu, L. & Ng, K. Journal of Pharmaceutical Sciences, 2002, 91, 11, 2367-2375

Zeitler, J. A.; Newnham, D. A.; Taday, P. F.; Threlfall, T. L.; Lancaster, R. W.; Berg, R. W.; Strachan, C. J.; Pepper, M.; Gordon, K. C.; Rades, T. *J. Pharm. Sci.* 2006, *95,* 11, 2486-2498.

Appendix

Polymorph Selection with Morphology Control Using Solvents

Manish M. Parmar,* Omar Khan, Linda Seton,* and James L. Ford

School of Pharmacy and Chemistry, Liverpool John Moores University, Byrom Street, Liverpool L3 3AF, United Kingdom

ABSTRACT: Sulfathiazole is a highly polymorphic model system exhibiting at least five polymorphic forms: I, II, III, IV, and V. Polymorph stability is known to be susceptible to solvent environment, and it is established that 1-propanol stabilizes the most metastable form I. This study examines the effect of a range of alcohols on polymorph selection and attempts to elucidate the mechanism. The role of the alcohol functional group in the polymorph selection process is thus investigated and evaluated. Crystals were characterized using optical microscopy, SEM, PXRD, DSC, IR, and single-crystal X-ray diffraction for their polymorphic identity. The role of solvent in the stabilization of polymorphs was investigated by visualizing and calculating energy requirements for the interaction of each solvent molecule with α- and β-dimers of sulfathiazole, using Cerius² modeling software. This study showed that solvent had a significant impact on polymorph selection. In common with 1-propanol, 1-butanol was found to stabilize form I by inhibiting the formation of the β-dimer, which is necessary for nucleation of and transformation to forms II−IV. Shorter chain alcohols and branched chain alcohols such as methanol, 2-propanol, and ethanol did not stabilize form I but stabilized forms II, III, and IV, respectively, showing that it is not only the alcohol functionality but also the steric effects of the alkyl chain that contributed to the effect. Sulfathiazole form I normally has a needlelike morphology. Form I with a modified rodlike morphology was produced by crystallization from 1-propanol with the addition of methanol in low concentration, showing that it is possible to control the morphology and selectively isolate polymorphs.

Introduction

Understanding the factors that control the nucleation of polymorphic materials, which have the ability to exist in two or more distinct crystalline phases,[1] has made advances in the past decade. The polymorph screening process now encompasses high throughput methods[2,3] and in silico prediction.[4] Understanding of the supramolecular processes that take place when polymorphic materials nucleate is expanding and can be applied to a variety of systems to control the polymorphic outcome of nucleation.[5] This is of scientific and commercial importance, as the well-known cases of Ritanovir[6,7] and Zantac[8] illustrate. Despite this, fundamental understanding remains incomplete and, in many cases, system specific. Polymorphs can exhibit different mechanical, thermal, and physical properties, such as compressibility, melting point, solubility, and crystal habit, which can have great influence on the bioavailability, filtration, and tableting properties of pharmaceuticals.[9]

Sulfathiazole is a highly polymorphic system, which is used to demonstrate the ability to isolate polymorphs with solvent. Already the subject of extensive study, the sensitivity of this material to solvent environment is well-established.[10,11] Sulfathiazole, see Figure 1 for molecular structure, is known to exhibit five polymorphic forms: I, II, III, IV, and V.[11−16] Relative thermodynamic stabilities are generally accepted to follow the order of the densities of the structure, i.e., III ≈ IV > II > I, with form I being the most metastable at room temperature.[10,15] At higher temperatures, when analyzed by DSC, form I does not show any transformation prior to melting at 201 °C. On the other hand, forms II−IV show transformation into form I at temperatures between 140 and 170 °C, prior to melting as transformed form I at 201 °C[17]. The nature of the structures has been described using a combination of graph set analysis and hydrogen-bonding motifs because the differences are subtle and require supramolecular treatment.[10] There has been some inconsistency in the literature regarding the naming
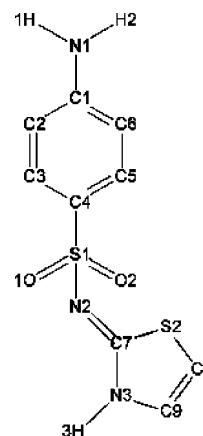
Figure 1. Molecular structure of sulfathiazole.

of the various forms; the numbering system used here follows that described by the work of Blagden et al.[10] (see Table 1). It has been established that the polymorphic outcome of crystallization of this material is influenced by the solvent[10] and that the most metastable polymorph, form I, can be selectively stabilized by 1-propanol.[10−12,18] In common with many metastable forms, the morphology is elongated, a shape generally considered to be undesirable. In this contribution, the mechanism of selection of the metastable form by solvent is probed by investigating the influence of a range of alcohols on the polymorphic outcome of crystallization. The importance of molecule−molecule interactions is evaluated by investigating a series of solvents with the same functionality. In addition, the nature of this mechanism is exploited to improve the particle morphology of the isolated, metastable crystal form.

Background: Polymorphism and Crystal Chemistry

The structure of sulfathiazole and its polymorphs has been the subject of investigation for almost 60 years.[19] The differences in the crystal chemistry, molecular arrangement, and structural

* Corresponding author. E-mail: m.parmar@2003.ljmu.ac.uk (M.M.P.); L.Seton@ljmu.ac.uk (L.S.).
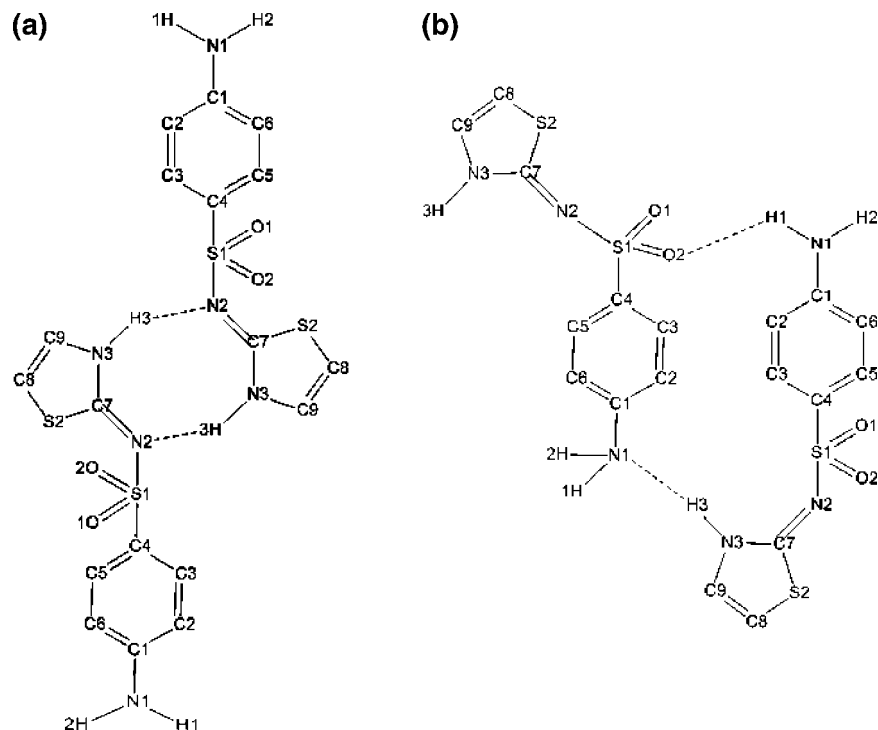
Figure 2. (a) α-Dimer, basic unit of form I; (b) β-dimer, basic unit of forms II−IV.

Table 1. Comparison of Unit-Cell Dimensions Obtained from Single-Crystal X-ray Diffraction with Literature Values

unit cells	current study				literature values			
	form I (1-propanol & 1-butanol)	form II (methanol)	form III (2-propanol)	form IV (water)	form I[10]	form II[11]	form III[10]	form IV[12]
a (Å)	10.45	8.18	17.40	10.90	10.55	8.23	17.57	10.86
b (Å)	13.27	8.56	8.5	8.56	13.22	8.55	8.57	8.54
c (Å)	17.20	15.48	15.9	11.48	17.05	15.55	15.58	11.45
β (deg)	107	94.18	112	89.6	108.06	93.67	112.93	88.13

motifs are responsible for the distinctiveness of the most metastable form I and the similarities found within forms II−IV[10,20]

Form I contains a unique dimer, defined by graph set analysis and referred to as α,[10] consisting of two molecules that are hydrogen-bonded via two imine nitrogen and amino hydrogen contacts N2−H3 (see Figure 2a for atom labeling). These dimers are linked in eight-member chains through the H1−O2 hydrogen bonding. However, forms II, III, and IV are all based on a common second level dimer, reported as β,[10] which in all three cases is constructed from a sulfato oxygen to aniline hydrogen (O2−H1) contact and aniline nitrogen to amino hydrogen (N1−H3) contact (see Figure 2b). According to Ostwald's Rule of Stages,[21] form I is likely to form initially in all cases. Each of the forms II, III, and IV contains the β-dimer and its presence is necessary for the transformation into the more stable forms II−IV. Thus, for form I to be kinetically stable, the formation of the α-dimer in solution must be favored and the formation of the β-dimer must be inhibited.

Experimental Section

Sulfathiazole was supplied by Sigma-Aldrich, UK. Five HPLC-grade alcohols, namely, methanol, ethanol, 1-propanol, 2-propanol, and 1-butanol, were selected as solvents. Batch crystallization experiments were conducted in thermostated, jacketed beakers. Samples were obtained by dissolving sulfathiazole between 1 and 1.5 g in 100 mL of solvent at 65 °C with stirring followed by cooling to 26 °C. Larger single crystals were obtained from each solvent by slow evaporation. In addition, sulfathiazole was crystallized from 1-propanol solutions doped with methanol. Batch crystallizations were performed by slow cooling from 1-propanol doped with 10, 20, and 40 v/v % methanol.

The morphology of the resulting samples was analyzed by optical microscopy; polymorph identification was conducted by powder X-ray diffraction (PXRD), infrared spectroscopy (IR), differential scanning calorimetry (DSC), and single-crystal X-ray diffraction. The powder diffraction data of each sample were collected using the Miniflex (Rigaku Corporation) laboratory powder X-ray diffractometer. The data were collected using a rotating flat-plate sample holder over the 2θ range 5−45° in 5° steps at ambient conditions. Previous studies[11,20] have reported that the spectra of forms II, III, and IV are similar and suggest that is due to the structural and molecular similarities within polymorphs II−IV. It is therefore not possible to differentiate between these forms by PXRD (Figure 3). However, the pattern of form I (Figure 3) is distinguished by a peak at a 2θ value of 11°, which is characteristic of form I,[11,22−23] so it was possible to identify those samples that contained form I. Similarly, it was possible to confirm the presence of form I by DSC and IR, but not to positively identify the other three polymorphs. To differentiate between the other forms, the unit cells of three individual single crystals grown from each of the solvents were collected by single-crystal X-ray diffraction. Using a Stoe IPDS area detector, we calculated unit-cell constants by least-square refinement using the setting angles of 25 reflections and compared them with reference unit cell-data.[10−16]

Additionally, to attempt to understand the solution behavior, ^{1}H nuclear magnetic resonance (NMR) was performed on a Bruker Avance 300 MHz spectrometer operating via XWIN-NMR, version 3.5, and locked using the deuterium signal from the deuterated methanol, ethanol, and 1-butanol.

Results

All samples initially crystallized as elongated or needle particles. This is established in the literature as the morphology of form I and is predicted by Ostwald's Rule to crystallize first.

Results
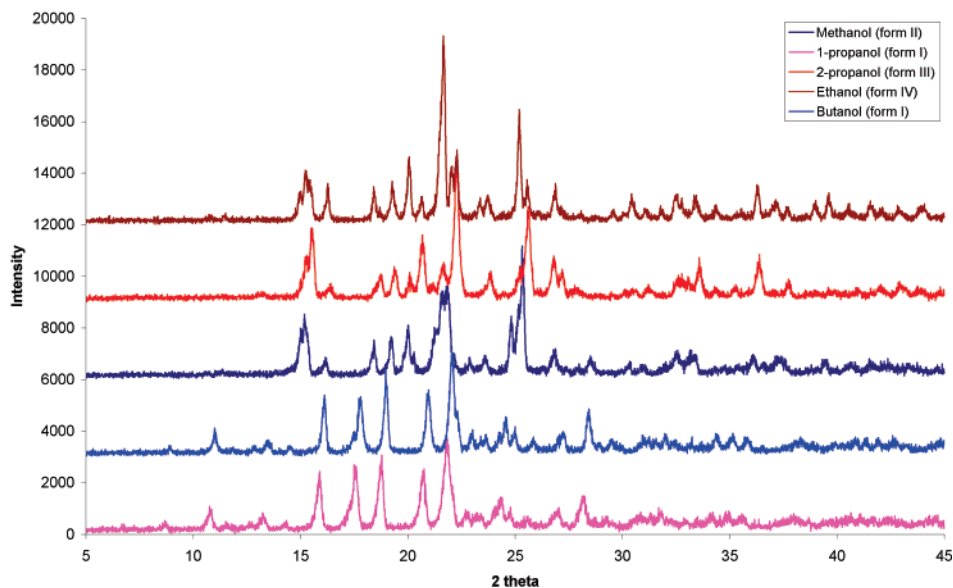
Figure 3. Powder X-ray patterns of sulfathiazole samples obtained from alcohols. Peak at 11° 2θ indicates the presence of form I.
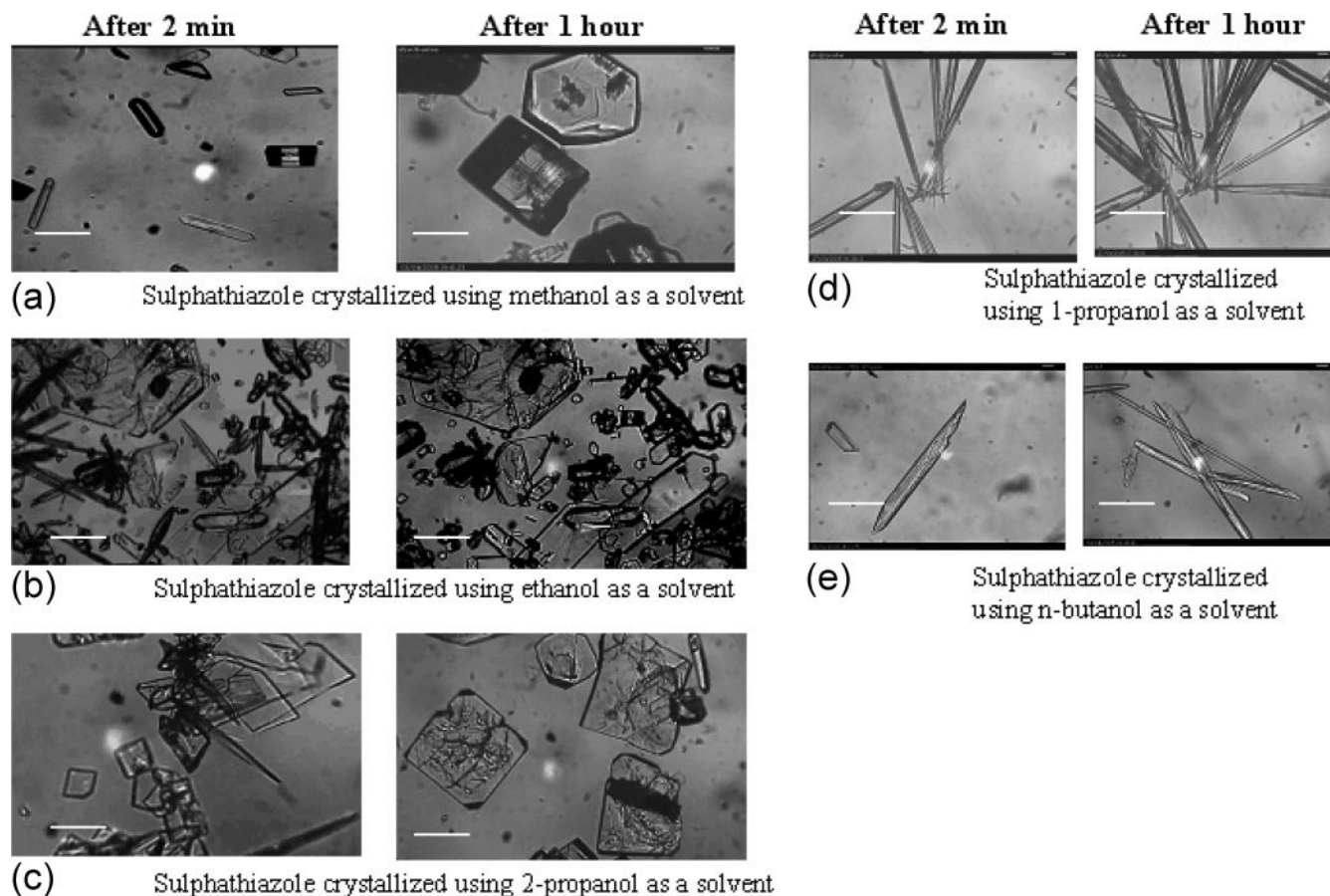
Figure 4. Microscopic results of sulfathiazole sample crystallized from each solvent. Scale bar is 60 μm.

When methanol or ethanol was the solvent, needles nucleated initially followed by small hexagonal plates, which appeared within 2 min of nucleation. The needle-shaped particles dissolved very quickly, within a few seconds of nucleation, and the hexagons grew in size and thickness, resulting in a hexagonal prism in the case of methanol (Figure 4a), and thin plates in the case of ethanol (Figure 4b). This change in aspect ratio as growth progressed could be a maturation effect or may indicate polymorphic change as growth progressed. Once mature crystals were obtained, there was no further change in the morphology. Single-crystal XRD identified that crystals grown from methanol were form II and those from ethanol were form IV (see Table
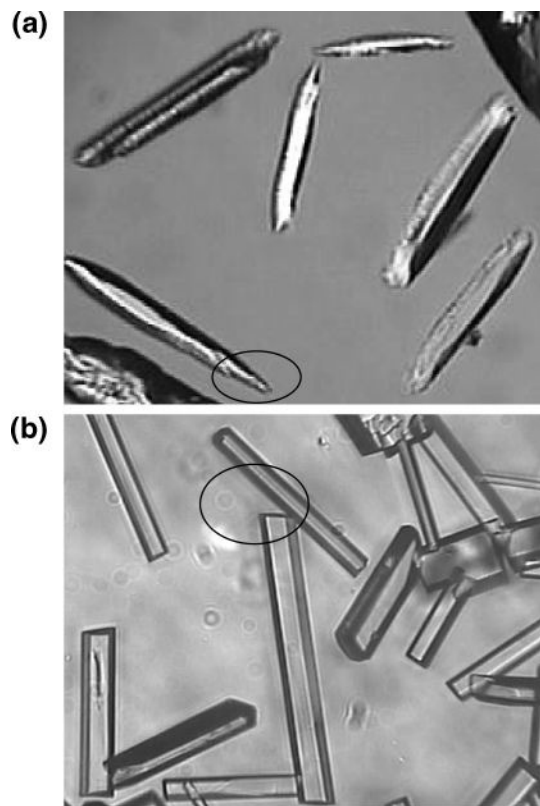
Figure 5. (a) Crystals growing in 100% 1-propanol; (b) modified crystals in 90:10 1-propanol:methanol.

1). PXRD of samples isolated immediately after nucleation indicated that form I was present in the sample by the presence of a peak at 11° 2θ. When mature samples were isolated, after the dissolution of the needle shapes, this peak was not present in the trace, indicating that any crystals of form I had transformed into a more stable polymorph.

When 2-propanol was the solvent, sulfathiazole initially nucleated as needles and very small square plates. The square plates grew in size and the needles disappeared as shown in Figure 4c. The rate of growth was slower than for those crystals grown from the straight chain alcohols, with growth continuing for 100 min after nucleation. There was no change to the morphology during growth. Crystals were identified by XRD as form III. As with samples grown from methanol and ethanol, PXRD of early samples indicated the presence of form I, whereas no form I peak was detected in mature samples.

For 1-propanol and 1-butanol, nucleation of needle-shaped crystals was very prompt, within a minute of reaching temperature, with maximum growth having occurred within 17–20 min of nucleation. No further growth was observed, and the particles remained without transformation for the length of the experiment (1 h) as shown in images d and e in Figure 4. No platey or prismatic crystals were observed. PXRD, DSC, IR, and single-crystal XRD confirmed that each of these samples was form I. When 1-propanol was doped with methanol, it was found that if there was 20% or more methanol in the solvent mix, form I was not kinetically stable, but transformed to form II. However, if the methanol was kept to 10%, then form I was kinetically stable and other forms were not observed. Additionally, the crystal habit was observed to be modified, being less elongated with well-defined side and end faces (Figure 5). PXRD confirmed that these modified crystals were the metastable form I (Figure 6).

All experiments were repeated at three different concentrations and temperatures to confirm that the selection of polymorphs is dependent on solvent composition rather than other experimental variables. Changes in temperature and concentration did not affect the polymorphic outcome. Polymorph V was not observed during this study.

The ^{1}H NMR spectra obtained of sulfathaizole dissolved in ethanol and methanol were similar (Figure 7). The peak attributed to the thiazole hydrogen, H3 (see Figure 1), can be seen at a chemical shift of 7.0, whereas in 1-butanol, this peak is shifted slightly to 6.9, indicating a slightly more shielded environment. This atom hydrogen bonds to N1 to form the β-dimer and N2 to form the α-dimer. This suggests that there are hydrogen-bonding differences in the solutions made from different solvents

Molecular Modeling of Prenucleation Clusters. It is clear from the results that 1-propanol and 1-butanol stabilized the metastable form I and inhibited the transformation of form I into more stable forms II−IV. To understand the polymorph selection process, it is necessary to study the different structural motifs present in the sulfathiazole forms. This has been done using a combination of graph set analysis and hydrogen-bonding motif.[10]

The form I structure contains the α-dimer only, and the other polymorphs contain a mixture of α and β. The energy of proposed clusters of sulfathiazole-based on α- and β-type dimers, in the presence of each of the solvents was investigated using Cerius2[24] and Mopac[25] software packages. The sulfathiazole structures of each of the polymorphs were taken from the Cambridge Crystallographic Database (CCD).[26] The α- and β-dimer pairs were taken from the structures of form I and form II, respectively, and minimized energetically with Dreiding force field,[27] such that the integrity of the bonding was maintained (structures a and b in Figure 8). Charges were generated using PM3 method within Mopac for a single point energy task. The α-dimer is formed by two hydrogen-bonding interactions between molecules A and B, shown in Figure 8. The interaction energy, E_{int} (α-dimer), represents the energy released when these bonds are formed. This energy was calculated using MOPAC as shown by eq 1 and found to be −14 kcal/mol. Similarly, the β-dimer is formed by two different hydrogen-bonding interactions; the H3−N1 interaction in particular is unique to the β-dimer pairing. E_{int} (β-dimer) was also calculated and found to have a lower value of −22 kcal/mol.

$$E_{int} (\alpha\text{-dimer}) = \text{total energy of cluster} -$$
$$\text{energies of formation of molecules A \& B} \quad (1)$$
$$E_{int} (\alpha\text{-dimer}) = 204.09 - 109.36 - 109.36 =$$
$$-14.87 \text{ kcal/mol}$$

Similarly

$$E_{int} (\beta\text{-dimer}) = -22 \text{ kcal/mol}$$

The value of E_{int} is lower for the β-dimer than for the α-dimer. This indicates that the β-dimer is thermodynamically more stable than the α-dimer, which is expected because we know that the structures containing the β-dimer are thermodynamically more stable than form I, which contains the α-dimer.

To try to model the influence of the solvent on the tendency to form either α- or β-dimers and therefore influence polymorph nucleation, we generated clusters based on either the α-structure or the β-structure, with a solvent molecule inserted between the dimer pairs (Figures 9 and 10). The location of the solvent
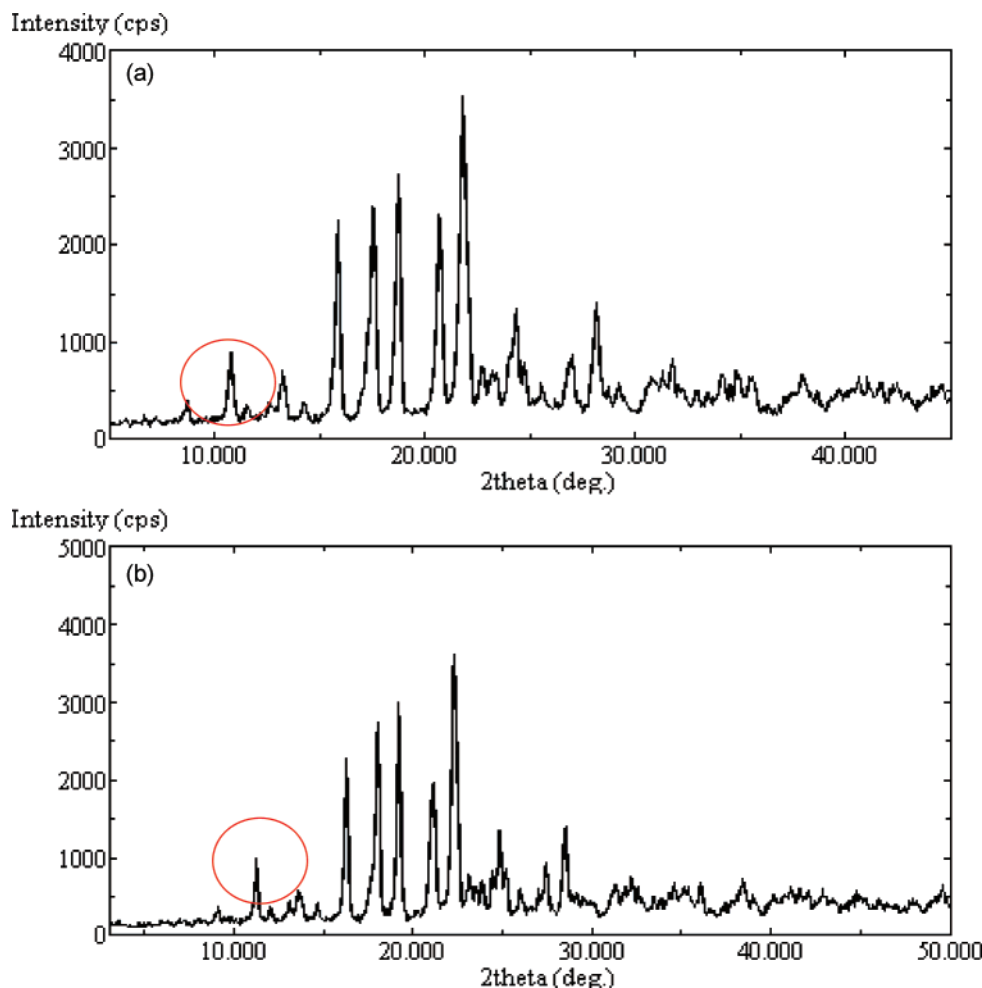
Figure 6. (a) PXRD (100% 1-propanol); (b) PXRD (90:10 1-propanol:methanol).
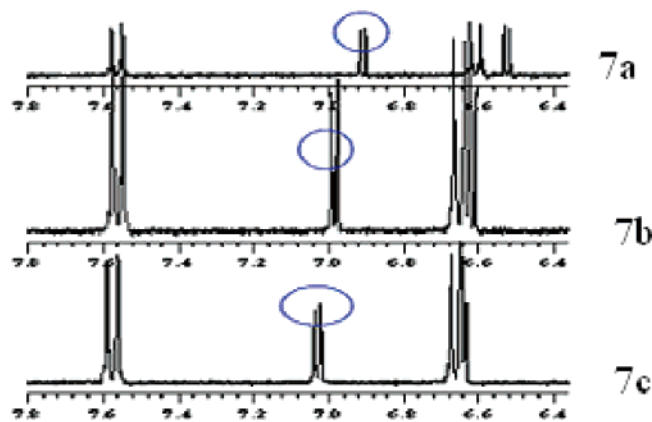
Figure 7. H^1 NMR of sulfathiazole (a) in 1-butanol, (b) in ethanol, and (c) in methanol.

Figure 8. (a) Energetically minimized α-dimer, $E_{int} = -14$ Kcal/mol; (b) energetically minimized β-dimer, $E_{int} = -22$ Kcal/mol.

For example, in the case of solvated α-cluster with methanol in the lowest energy position 5 (Table 2), eq 2 gives

E_{int} (methanol α-cluster) =

total energy of solvated cluster −
energies of formation of molecules A, B, & C (2)

E_{int} (methanol α-cluster) =

$463.38 - 109.36 - 109.36 - 14.2 = 230.46$ kcal mol^{-1}

In the same way, the energy of interaction was calculated for a β-cluster solvated with methanol and both calculations were repeated for each solvent, the results of which are shown in Table 3.

Discussion

When the solvating molecule was chosen to be methanol, ethanol, or 2-propanol, the β-cluster was calculated to have a

molecule was determined from preliminary calculations where the lowest energy position from ten proposed positions was chosen as the preferred location of the solvent molecule. The calculated energies of the ten positions are shown in Table 2, with position 5 having the lowest energy value for the α-type cluster, and position 8 for the β-type cluster. These were chosen for the energy calculations as illustrated in Figures 9 and 10 with methanol being the solvent.

The energy of interaction of the solvated α-type cluster was calculated in a similar manner using Mopac, according to eq 2.

Figure 9. Solvated α-cluster, based on α-dimer and incorporating a methanol molecule in the lowest energy position of those examined.

Figure 10. Solvated β-cluster, based on β-dimer and incorporating a methanol molecule in the lowest energy position of those examined.

Table 2. Calculated E_{int} at 10 Proposed Positions for Solvated α- and β-Clusters with Methanol as Solvent

position	E_{int} of solvated α-cluster (kcal mol^{-1})	E_{int} of solvated β-cluster (kcal mol^{-1})
1	436.15	1096.3
2	1506.7	681.36
3	512.4	923.01
4	340.61	996.2
5	230.46	743.8
6	286.8	417.6
7	367.4	305.23
8	548.93	224.12
9	732.87	331.76
10	963.65	648.53

Table 3. Lowest Calculated E_{int} of Solvated Clusters for α- and β-Dimers, Incorporating Each of the Solvents Examined

solvent	E_{int} of solvated α-cluster (kcal mol^{-1})	E_{int} of solvated β-cluster (kcal mol^{-1})
methanol	230.46	224.12
ethanol	251.70	237.86
2-propanol	357.09	331.71
1-propanol	236.13	419.91
1-butanol	190.94	361.81

lower energy of interaction, indicating it to be more thermodynamically stable than the α-cluster. This predicts that clustering similar to the β-dimer would be present in solution, and provide a route to the nucleation of polymorphs based on the β-dimer, namely II−IV. This is in agreement with the experimental observation that in these solvents, although form I nucleates initially, one or more of the other forms nucleates, grows, and is maintained in solution, as form I dissolves. The position is reversed for 1-propanol and 1-butanol. The interaction energy of the β-cluster has a much higher value than the α-cluster, suggesting that β-clusters would not form in solution, and polymorphs containing the β-dimer would not be nucleated.

Again, this is in agreement with the experimental observation that form I nucleates and remains stable in 1-propanol and 1-butanol solution, with no transformation or nucleation of any other polymorphs. The H^1 NMR studies (Figure 7) also indicate differences in solution behavior between those solvents that inhibit the formation of β-dimer and those that favor its formation. Further NMR studies may reveal more information.

These preliminary calculations indicate that the ability of the solvent to inhibit transformation may be linked to the energies of substrate−solvent interactions and show that that clustering in solution may be thermodynamically controlled. However, a more detailed systematic search approach is currently being undertaken that uses a grid-based search system[28,29] of translations and rotations. This will be able to assess all of the possible intermolecular packing arrangements between the sulfathiazole dimer (fixed position) and solvent molecule (mobile position)
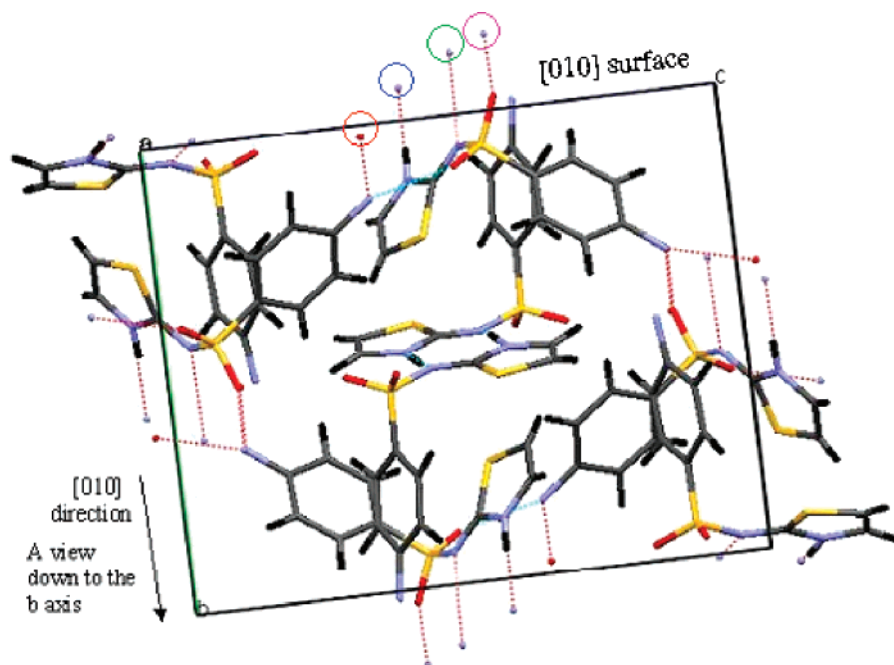
Figure 11. Visualization showing molecular interactions along the [010] direction of sulfathiazole form I. Keys: red O, amino hydrogen; blue O, thiazole hydrogen; green O, imine nitrogen; pink O, sulfoxide oxygen.

Figure 12. Proposed model for habit modification of form I.

in direct space on the basis of atom−atom separation distance and intermolecular potential pair energy.

It is observed that methanol, ethanol, and 2-propanol select a specific polymorph, i.e., form II was grown from methanol, form III from 2-propanol, and form IV from ethanol, and the solvent dependence of polymorph generation is well-established for sulfathiazole. Each of these forms has the β-dimer as a basic unit; structural differences between them are subtle, relating to ring-to-ring contacts and contacts between the sheets of β dimer rings. It is possible that specific solvent interactions stabilize other ring structures specific to each polymorph, as proposed by Blagden et al.,[10] and may have a similar energetic basis to those presented here.

Doping of 1-propanol with 10% methanol caused a habit modification while maintaining the stabilization of form I. The observed end face in the modified crystals may arise from inhibition of growth at the fastest growing face [010] of form I.[10,22] Examination showed that this surface exposes the acceptor imine nitrogen (N2), sulfoxide oxygen (O2) groups, and the donor amino hydrogen (H2). Sulfathiazole molecules are linked via α-dimers and then extended into sheets and layers via amino hydrogen and sulfato oxygen bonding.

The presence of methanol molecules in solution at low concentration may lead to direct absorption of methanol at this surface, blocking H-bonding sites with subsequent inhibition of growth. Alternatively, methanol β-clusters may be present in low concentration, which act as direct growth synthons, joining to available crystal surfaces and inhibiting growth. We know that when the concentration of methanol is increased, form II is nucleated, implying the presence of β-dimers. This modified habit clearly illustrates that the methanol interacts differently with the growing crystal than the main solvent, 1-propanol. Figure 11 shows the growth in the [010] direction (needle axis) with available sites for H-bonding visible. The methanol molecule may dock into one of these sites or facilitate β-type interaction with another sulfathiazole molecule.

Conclusion

The study has confirmed that the most metastable form, form I, is stabilized when crystals are grown from propanol and 1-butanol, whereas methanol, ethanol, and 2-propanol stabilized the more stable forms II, III, and IV, respectively. In common with many metastable forms, sulfathiazole form I displays an elongated, needlelike morphology. The thermodynamics of possible clustering of the solvent with the sulfathiazole molecule prior to nucleation has been examined in a modeling study, which constitutes a preliminary test to determine whether there are thermodynamic differences in the interactions between the growth synthons that make up the different structural patterns in the polymorphs. This study has indicated that clustering between 1-propanol (or 1-butanol) and α-type dimers of sulfathiazole, which lead to form 1, are energetically favored compared to clusters between propanol and β-type dimers, which promote the nucleation of the other polymorphs.

Similarly, when short chain alcohols such as methanol, 2-propanol, and ethanol are modeled, the metastable α-dimer

is not favored thermodynamically, and thus more stable polymorphs containing the β-dimer result from the crystallization.

The different solvent interactions of solvents such as methanol, with the sulfathiazole molecule have been highlighted by the habit modifying effects of the additions of low concentrations of methanol to a 1-propanol crystallizing solution. It is likely that the methanol molecules will form β-type clusters with the sulfathiazole. Because these are in very low concentration, form I still nucleates and is kinetically stable. However, in the same way that structural additives[30] modify habit by interacting at the substrate−solvent interface in a different way from the main solvent, the presence of methanol has shown a habit modifying effect, which improves the morphology. If the concentration of methanol becomes too high, then the β-clusters dominate and form II results.

References

(1) Giron, D. *J. Therm. Anal. Calorim.* **2001**, *64*, 37−60.

(2) Gardner, C. R.; Almarsson, O.; Chen, H. M.; Morissette, S.; Peterson, M.; Zhang, Z.; Wang, S.; Lemmo, A.; Gonzalez-Zugasti, J.; Monagle, J.; Marchionna, J.; Ellis, S.; McNulty, C.; Johnson, A.; Levinson, D.; Cima, M. *Comput. Chem. Eng.* **2004**, *28* (6−7), 943−953.

(3) Monissette, S. L.; Almarsson, O.; Peterson, M. L.; Remenar, J. F.; Read, M. J.; Lemmo, A. V.; Ellis, S.; Cima, M. J.; Gardner, C. R. *Adv. Drug Delivery Rev.* **2004**, *56* (3), 275−300.

(4) Lancaster, R. W.; Karamertzanis, P. G.; Hulme, A. T.; Tocher, D. A.; Covey, D. F.; Price, S. L. *Chem. Commun.* **2006**, *47*, 4921−4923.

(5) Desgranges, C.; Delhommelle, J. *J. Am. Chem. Soc.* **2006**, *128* (47), 15104−15105.

(6) Knapman, K. *Mod. Drug Discovery* **2000**, *3* (2) 53-54, 57.

(7) Datta, S.; Grant, D. J. W. *Nat. Rev. Drug Discovery* **2004**, *3*, 42−57.

(8) Glaxo Inc. V Novapharm Ltd., 52F3d 1043, 34 U. S. P. Q. 2d (BNA) 1565 (fed. Cir. 1995)

(9) Ferrari, E. S.; Davey, R. J.; Cross, W. I.; Gillon, A. L.; Towler, C. S. *Cryst. Growth Des.* **2003**, *3* (1), 53−60.

(10) Blagden, N.; Davey, R. J.; Lieberman, H. F.; Williams, L.; Payne, R.; Roberts, R.; Rowe, R.; Docherty, R. J. *Chem. Soc., Faraday Trans.* **1998**, *94* (8), 1035−1044.

(11) Anwar, J.; Tarling, S. E.; Barnes, P. *J. Pharm. Sci.* **1989**, *78* (4), 337−342.

(12) Kruger, G. J. & Gafner, G. *Acta Crystallogr., Sect. B* **1971**, *B27*, 326−333.

(13) Kruger, G. J. & Gafner, G. *Acta Crystallogr., Sect. B* **1972**, *28*, 272−283.

(14) Babilev, F. V.; Bel'ski, V. K.; Simnov, A.; Arzamastev, A. P. *Khim. Farm. Zh.* **1987**, *21*, 1275−1280.

(15) Chan, C. F.; Anwar, J; Cernik, R.; Barnes, P; Wilson, R. M. *J. Appl. Cryst.* **1999**, *32*, 436−441.

(16) Hughes, D.; Hursthouse, M.; Lancaster, B.; Tavener, S.; Threlfall, T.; Turner, P. *Acta Crystallogr., Sect. C* **1999**, *55*, 1831−1834.

(17) Zeitler, J. A.; Newnham, D. A.; Taday, P. F.; Threlfall, T. L.; Lancaster, R. W.; Berg, R. W.; Strachan, C. J.; Pepper, M.; Gordon, K. C.; Rades, T. *J. Pharm. Sci.* **2006**, *95* (11), 2486−2498.

(18) Lagas, M. & Lerk, C. F. *Int. J. Pharm.* **1981**, *8*, 11−24.

(19) Grove, D. C. & Keenan, G. L. *J. Am. Chem. Soc.* **1941**, *63*, 97−99.

(20) Appereley, D. C.; Fletton, R. A.; Harris, R. K.; Lancaster, R. W.; Tavener, S.; Threlfall, T. L. *J. Pharm. Sci.* **1999**, *88* (12), 1275−1280.

(21) Ostwald, W. *Z. Phys. Chem. (Leipzig)* **1899**.

(22) Blagden, N. *Powder Tech.* **2001**, *121*, 46−52.

(23) Kordikowski, A.; Shekunov, T.; York, P. *Pharm. Res.* **2001**, *18* (5), 682−688.

(24) *CERIUS2, Molcular Modelling Software for Materials Research*, version 4.2; Accelrys, Inc.: San Diego, CA, 2001.

(25) *MOPAC Quantum Chemistry Program Exchange Program No. 455*, version 6.0; Indiana University: Bloomington, IN, 1993.

(26) Allen, F. H. *Acta Crystallogr., Sect. B* **2002**, *58*, 380−388.

(27) Mayo, S. L.; Olafson, B. D.; & Goddard, I. W. A. DREIDING: A Generic Force Field for Molecular Simulations. *J. Phys. Chem.* **1990**, *94*, 8897−8909.

(28) Hammond, R. B; Hashim, R. S.; Ma, C.; Roberts, K. *J. Pharm. Sci.* **2006**, *95* (11), 2361−2372.

(29) Hammond, R. B.; Ma, C.; Roberts, K. J.; Ghi, P. Y.; Harris, R. K. *J. Phys. Chem. B* 2003, *107*, 11820−11826.

(30) Weissbuch, I.; Popvitz-Biro, R.; Leiserowitz, L.; Lahav, M. *Lock and Key Principle*; Behr, J. P. Ed.; Wiley: New York, 1994.